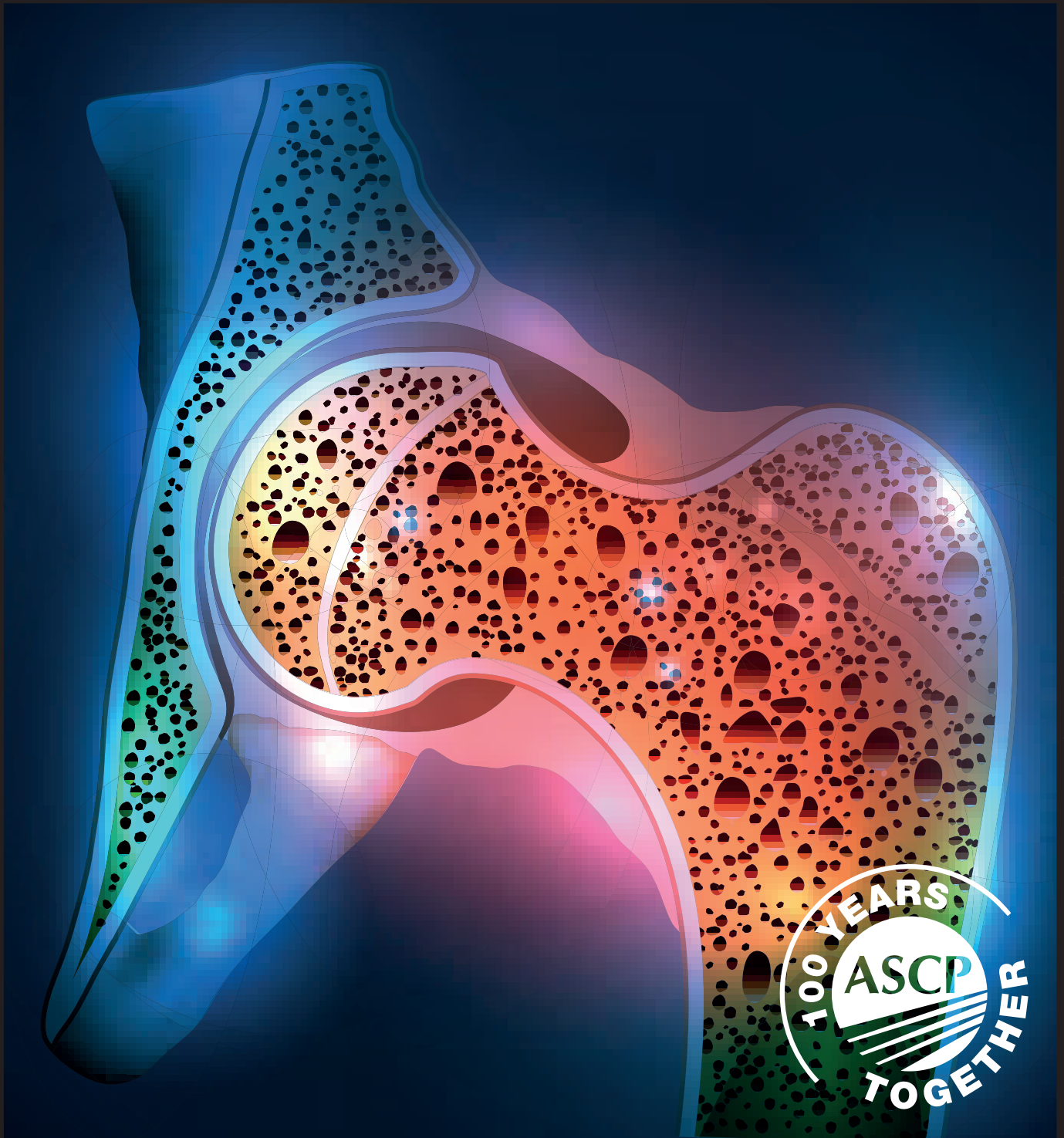


# Laboratory Medicine

September 2022 Vol 53 No 5 Pgs 437-542

labmedicine.com



## BOARD OF EDITORS

### Editor in Chief

**Roger L. Bertholf, PhD**  
Houston Methodist Hospital  
Weill Cornell Medicine

### Reviews

ASSOCIATE EDITOR

**Deniz Peker, MD**  
Emory University School of Medicine

ASSISTANT EDITOR

**Rahul Matnani, MD, PhD**  
Rutgers Robert Wood Johnson Medical School

### Clinical Chemistry

ASSOCIATE EDITOR

**Uttam Garg, PhD**  
University of Missouri Kansas City School of Medicine

ASSISTANT EDITORS

**David Alter, MD**  
Emory University School of Medicine

**Hong Kee Lee, PhD**  
NorthShore University HealthSystem

**Veronica Luzzi, PhD**  
Providence Regional Core Laboratory

**Alejandro R. Molinelli, PhD**  
St Jude Children's Research Hospital

### Cytology

ASSOCIATE EDITOR

**Antonio Cajigas, MD**  
Montefiore Medical Center

### Hematology

ASSOCIATE EDITOR

**Shiyong Li, MD, PhD**  
Emory University School of Medicine

ASSISTANT EDITORS

**Elizabeth Courville, MD**  
University of Virginia School of Medicine

**Alexandra E. Kovach, MD**  
Children's Hospital Los Angeles

### Histology

ASSOCIATE EDITOR

**Carol A. Gomes, MS**  
Stony Brook University Hospital

### Immunohematology

ASSOCIATE EDITOR

**Richard Gammon, MD**  
OneBlood

ASSISTANT EDITORS

**Phillip J. DeChristopher, MD, PhD**  
Loyola University Health System

**Gregory Denomme, PhD**  
Grifols Laboratory Solutions

**Amy E. Schmidt, MD, PhD**  
CSL Plasma

## STAFF

EXECUTIVE EDITOR FOR JOURNALS

**Kelly Swails, MT(ASCP)**

DIRECTOR OF SCIENTIFIC  
PUBLICATIONS

**Joshua Weikersheimer, PhD**

SENIOR EDITOR, JOURNALS

**Philip Rogers**

[www.labmedicine.com](http://www.labmedicine.com)

### Immunology

ASSOCIATE EDITOR

**Ruifeng Yang, MD, PhD**  
Nova Scotia Health

### Laboratory Management and Administration

ASSOCIATE EDITOR

**Lauren Pearson, DO, MPH**  
University of Utah Health

ASSISTANT EDITOR

**Joseph Rudolf, MD**  
University of Utah

### Microbiology

ASSOCIATE EDITOR

**Yvette S. McCarter, PhD**  
University of Florida College of Medicine

ASSISTANT EDITORS

**Alexander J. Fenwick, MD**  
University of Kentucky College of Medicine

**Allison R. McMullen, PhD**  
Augusta University—Medical College of Georgia

**Elitza S. Theel, PhD**  
Mayo Clinic

### Molecular Pathology

ASSOCIATE EDITOR

**Jude M. Abadie, PhD**  
Texas Tech University Health Science Center

ASSISTANT EDITORS

**Holli M. Drendel, PhD**  
Atrium Health Molecular Pathology Laboratory

**Rongjun Guo, MD, PhD**  
ProMedica Health System

**Shuko Harada, MD**  
University of Alabama at Birmingham

**Hongda Liu, MD, PhD**  
The First Affiliated Hospital of Nanjing Medical University

### Pathologists' Assistant

ASSOCIATE EDITOR

**Anne Walsh-Feeks, MS, PA(ASCP)**  
Stony Brook Medicine

*Laboratory Medicine* (ISSN 0007-5027), is published 6 times per year (bimonthly). Periodicals Postage paid at Chicago, IL and additional mailing offices. POSTMASTER: Send address changes to *Laboratory Medicine*, Journals Customer Service Department, Oxford University Press, 2001 Evans Road, Cary, NC 27513-2009.

**SUBSCRIPTION INFORMATION:** Annually for North America, \$173 (electronic) or \$225 (electronic and print); single issues for individuals are \$29 and for institutions \$64. Annually for Rest of World, £112/€159 (electronic) or £144/€206 (electronic and print); single issues for individuals are £19/€27 and for institutions £40/€57. All inquiries about subscriptions should be sent to Journals Customer Service Department, Oxford Journals, Great Clarendon Street, Oxford OX2 6DP, UK, Tel: +44 (0) 1865-35-3907, e-mail: [jnl.cust.serv@oup.com](mailto:jnl.cust.serv@oup.com). In the Americas, please contact Journals Customer Service Department, Oxford Journals, 2001 Evans Road, Cary, NC 27513. Tel: 800-852-7323 (toll-free in USA/Canada) or 919-677-0977, e-mail: [jnlorders@oup.com](mailto:jnlorders@oup.com).

**MEMBERSHIP INFORMATION:** The ASCP membership fees for pathologists are as follows: fellow membership is \$349; fellow membership plus 1-year unlimited online CE is \$519; 2-year fellow membership is \$675; and 2-year fellow membership plus 2-year unlimited online CE is \$1,015. The ASCP membership fees for laboratory professionals are as follows: newly certified membership is \$49; annual membership is \$99; annual membership plus 1-year unlimited online CE is \$129; 3-year membership is \$349. All inquiries about membership should be sent to American Society for Clinical Pathology, 33 West Monroe Street, Suite 1600, Chicago, IL 60603, Tel: 312-541-4999, e-mail: [ascp@ascp.org](mailto:ascp@ascp.org).

**CLAIMS:** Publisher must be notified of claims within four months of dispatch/ order date (whichever is later). Subscriptions in the EEC may be subject to European VAT. Claims should be made to Laboratory Medicine, Journals Customer Service Department, Oxford University Press, 2001 Evans Road, Cary, NC 27513, Tel: 800-852-7323 (toll-free in USA/Canada) or 919-677-0977, e-mail: [jnlorders@oup.com](mailto:jnlorders@oup.com).

*Laboratory Medicine* is published bimonthly by Oxford University Press (OUP), on behalf of the ASCP, a not-for-profit corporation organized exclusively for educational, scientific, and charitable purposes. Devoted to the continuing education of laboratory professionals, *Laboratory Medicine* features articles on the scientific, technical, managerial, and educational aspects of the clinical laboratory. Publication of an article, column, or other item does not constitute an endorsement by the ASCP of the thoughts expressed or the techniques, organizations, or products described therein. *Laboratory Medicine* is indexed in the following: MEDLINE/PubMed, Science Citation Index, Current Contents—Clinical Medicine, and the Cumulative Index to Nursing and Allied Health Literature.

*Laboratory Medicine* is a registered trademark. Authorization to photocopy items for internal and personal use, or the internal and personal use of specific clients, is granted by ASCP Press for libraries and other users registered with the Copyright Clearance Center (CCC) Transactional Reporting Service, provided that the base fee of USD 15.00 per copy is paid directly to the CCC, 222 Rosewood Drive, Danvers, MA 01923, 978.750.8400. In the United States prior to photocopying items for educational classroom use, please also contact the CCC at the address above.

**Printed in the USA**

© 2022 American Society for Clinical Pathology (ASCP)

### Advertising Sales Office Classified and Display Advertising

CORPORATE ADVERTISING

**Jane Liss**  
732-890-9812  
[jliss@americanmedicalcomm.com](mailto:jliss@americanmedicalcomm.com)

RECRUITMENT ADVERTISING

**Lauren Morgan**  
267-980-6087  
[lmorgan@americanmedicalcomm.com](mailto:lmorgan@americanmedicalcomm.com)

ASCP

**Laboratory Medicine**

33 West Monroe Street, Suite 1600  
Chicago, IL 60603

T: 312-541-4999

F: 312-541-4750

## OVERVIEW

- 439 **Quality Assessment and Clinical Utility of Plasma Obtained Via Apheresis vs That Obtained from Whole Blood**  
*Eiman Hussein, Azza Aboul Enein*

## SCIENCE

- 446 **Plasma LncRNA MALAT1 Expressions Are Negatively Associated with Disease Severity of Postmenopausal Osteoporosis**  
*Tie-Yong Qian, Hui Wan, Ci-You Huang, Xiao-Jing Hu, Wei-Feng Yao*
- 453 **Modified Proline Metabolism and Prolidase Enzyme in COVID-19**  
*Merve Ergin Tuncay, Salim Neselioglu, Emra Asfuroglu Kalkan, Osman Inan, Meryem Sena Akkus, Ihsan Ates, Ozcan Erel*
- 459 **Multiplex Microsphere PCR (mmPCR) Allows Simultaneous Gram Typing, Detection of Fungal DNA, and Antibiotic Resistance Genes**  
*Daniel J. Browne, Fang Liang, Kate H. Gartlan, Patrick N.A. Harris, Geoffrey R. Hill, Simon R. Corrie, Kate A. Markey*
- 465 **5-Amino-4-Imidazolecarboxamide Ribonucleotide Transformylase/IMP Cyclohydrolase Polymorphisms Affect the Susceptibility to Multiple Myeloma**  
*Yu Wang, Zhian Ling, Zuoqian Hu, Ying Gui, Chunni Huang, Yibin Yao, Ruolin Li*
- 475 **Cutoff Value of Qualitative HBsAg for Confirmatory HBsAg Using the Chemiluminescence Microparticle Immunoassay Method**  
*Merci Monica Pasaribu, Jessica Purwanti Wonohutomo, Suzanna Immanuel, July Kumalawati, Nuri Dyah Indrasari, Yusra Yusra*
- 479 **Elevated Lactate Dehydrogenase Concentrations in Plasma Compared to Serum**  
*Crystal Bockoven, Robert C. Benirschke, Hong-Kee Lee*
- 483 **Erythrocyte Sedimentation Rate in Patients with Renal Insufficiency and Renal Replacement Therapy**  
*Anna Buckenmayer, Lotte Dahmen, Joachim Hoyer, Sahana Kamalanabhaiah, Christian S. Haas*
- 488 **Usefulness of AFP, PIVKA-II, and Their Combination in Diagnosing Hepatocellular Carcinoma Based on Upconversion Luminescence Immunochromatography**  
*Song-gao Zhang, Yi Huang*
- 495 **Anticardiolipin IgA as a Potential Risk Factor for Pregnancy Morbidity in Patients with Antiphospholipid Syndrome**  
*Xiaodan Zhai, Shuo Yang, Liyan Cui*
- 500 **Topical Application of Methyl Nicotinate Solution Enhances Peripheral Blood Collection**  
*YuLi Zhu, Wei Xu, LiangLiang OuYang, Hong Wang, WeiWei Mao, HuiXiang Zhou, Chao Shen, ZhiJian Hu, YunChang Tan*
- 504 **Association of rs5742612 Polymorphism in the Promoter Region of IGF1 Gene with Nonalcoholic Fatty Liver Disease: A Case-Control Study**  
*Hossein Nobakht, Touraj Mahmoudi, Gholamreza Rezamand, Seidamir Pasha Tabaeian, Golnaz Jeddi, Asadollah Asadi, Hamid Farahani, Reza Dabiri, Fariborz Mansour-Ghanaei, Seyed Alireza Kaboli, Faramarz Derakhshan, Mohammad Reza Zali*
- 509 **The Viability of Hematopoietic Progenitor Cell Grafts after Cryopreservation Does Not Predict Delayed Engraftment in Allogeneic Hematopoietic Stem Cell Transplantation**  
*Emmanuel Fadeyi, Yafet T. Mamo, Amit K. Saha, Emily Wilson, Gregory Pomper*
- 514 **Reduced Immune Response and Neutralizing Antibody Activity to the SARS-CoV-2 Vaccination in Patients with a History of Solid Organ Transplant**  
*Deborah French, Chui Mei Ong, Paul Patel, Marisa Zuk, Alan H. B. Wu*

- 523 **Highly Sensitive Serum miRNA Panel for the Diagnosis of Hepatocellular Carcinoma in Egyptian Patients with HCV-Related HCC**  
*Ayman Yosry, Naglaa Zayed, Reham M. Dawood, Marwa K. Ibrahim, Marwa Elsharkawy, Sherif M. Ekladios, Ahmed Khairy, Aisha Elsharkawy, Marwa Khairy, Shereen Abdel Alem, Noha G. Bader El Din, Mostafa K. El Awady, Zeinab Abdellatif*
- 530 **Seasonal Variation of Ferritin among Swedish Blood Donors**  
*Johan Saldeen, Lena Carlsson, Anders Larsson*

## CASE STUDY

- 533 **EUS-FNA Diagnosis of a Metastatic Adult Granulosa Cell Tumor in the Stomach**  
*Ilias P. Nikas, Athanasia Sepsa, Evangelia Kleidaradaki, Charitini Salla*
- 537 **Macroprolactinoma-Induced Syndrome of Inappropriate Antidiuresis and Its Reversal with Dopamine Agonist Therapy**  
*Amnon Schlegel*
- 540 **Transient Pseudothrombocytopenia Detected 8 Months After COVID-19 Vaccination**  
*Takakazu Higuchi, Takao Hoshi, Astuko Nakajima, Kosuke Haruki*

## CORRECTION

- 542 **Correction to: Quality Assessment and Clinical Utility of Plasma Obtained Via Apheresis vs That Obtained from Whole Blood**

The following are online-only papers that are available as part of Issue 53(5) online.

- e101 **A Balanced Robertsonian Translocation in a Patient with a Janus Kinase 2-Positive Polycythemia Vera**  
*Bernhard Strasser, Christian Paar, David Kiesl, Josef Tomasits*
- e105 **Resolving Pseudohyponatremia: Validation of Plasma Sodium on Radiometer ABL800 Blood Gas Analyzers for Immediate Reflex Testing**  
*Michael A. Vera, Angela Sutphin, Lisa Hansen, Joe M. El-Khoury*
- e109 **A Simple and Applicable Method for Human Platelet Lysate Preparation Using Citrate Blood**  
*Narin Khongjaroensakun, Karan Paisooksantivatana, Suttikarn Santiwatana, Tulyapruet Tawonsawatruk, Kantarat Kusolthammarat, Praguynwan Kadegasem, Noppawan Tangbubpha, Juthamard Chantaraamporn, Ampaiwan Chuansumrit*
- e113 **Hospital and Laboratory Practice in an Integrated Medical System for HIV Infection Prevention Interventions at a Veteran Affairs Medical Center**  
*Jeffrey M. Petersen, Darshana N. Jhala*
- e117 **Chylomicronemia Due to the Rare Hyperlipoproteinemia Type 3 Complicated by a Circulating Monoclonal Protein**  
*Hiba Basheer, Beheshteh Nakhaee, Ishwarlal Jialal*
- e120 **Acquired FVII Deficiency and Acute Myeloid Leukemia: A Case Report and Literature Review**  
*Emna Hammami, Wijden El Borgi, Fatma Ben Lakhal, Sarra Fekih Salem, Hend Ben Neji, Emna Gouider*
- e123 **Multisite Pseudomonas aeruginosa Infections Detected by Metagenomic Next-Generation Sequencing in a Child with Aplastic Anemia: A Case Report**  
*Shu-yu Lai, Fang Liu, Li Chang, Guang-lu Che, Qiu-xia Yang, Yong-mei Jiang, Jie Teng*
- e126 **Acquired Factor VIII Inhibitors: A Case Study**  
*Eric A. Walradth*

**e129 Evaluation of RNA Isolation Methods in Human Adipose Tissue**  
*Bipasha Nandi Jui, Assel Sarsenbayeva, Henning Jernow, Susanne Hetty, Maria J. Pereira*

**e134 A Novel *USP25::PDGFRA* Gene Fusion in a 78 Year Old Patient with a Myeloid Neoplasm**  
*Joanna C. Dalland, Patrick R. Blackburn, Kaaren K. Reichard, Sarah H. Johnson, James B. Smadbeck, George Vasmatzis, Nicole L. Hoppman, Xinjie Xu, Patricia T. Greipp, Linda B. Baughn, Jess F. Peterson*

**e139 Corrigendum to: A Simple and Applicable Method for Human Platelet Lysate Preparation Using Citrate Blood**  
*Narin Khongjaroensakun, Karan Paisooksantivatana, Suttikarn Santiwatana, Tulyapruet Tawonsawatruk, Kantarat Kusolthammarat, Praguywan Kadegasem, Noppawan Tangbubpha, Juthamard Chantaraamporn, Ampaiwan Chuansumrit*



**ON THE COVER:** Derived from the Greek words for “bone” and “porous,” osteoporosis is one of the most common disorders associated with old age. The disease is about four times more common in women compared to men but still affects nearly 2 million men and 8 million women in the United States. In osteoporosis, the normal balance between bone formation and resorption is tilted in favor of the latter, resulting in brittle bones prone to fractures. Osteopenic bones develop pores in their matrix like those illustrated; normal bone has a denser and more homogenous appearance. The pathogenic mechanism underlying osteoporosis is complex but involves a combination of accelerated osteoclastic activity and reduced osteoblast formation. Regulation of osteoblastic and osteoclastic activity involves multiple molecular signaling pathways. In this issue of *Laboratory Medicine*, Qian and colleagues investigate one such signaling pathway involving a long-coding RNA and its potential influence on postmenopausal osteoporosis.

# Quality Assessment and Clinical Utility of Plasma Obtained Via Apheresis vs That Obtained from Whole Blood

Eiman Hussein, MD, PhD,\*<sup>✉</sup> and Azza About Enein, MD

Department of Clinical and Chemical Pathology, Division of Transfusion Medicine, Faculty of Medicine, Cairo University, Cairo, Egypt.\*To whom correspondence should be addressed. [eimanhussein@gmail.com](mailto:eimanhussein@gmail.com)

**Keywords:** transfusion medicine, hematology, coagulation, blood, banking/transfusion medicine, clinical pathology, hematopathology

**Abbreviations:** TP, thawed plasma; AP, apheresis prepared plasma; WBP, whole blood plasma; INR, international normalized ratio; aPTT, activated partial thromboplastin time; TTP, thrombotic thrombocytopenic purpura; FFP, fresh frozen plasma; PE, plasma exchange; AABB, Association for the Advancement of Blood and Biotherapies; WB, whole blood; CPDA-1, citrate-phosphate-dextrose adenine; ACD, acid citrate dextrose; PT/INR, prothrombin time/international normalized ratio; SD, standard deviation; RBC, red blood cell.

*Laboratory Medicine* 2022;53:439–445; <https://doi.org/10.1093/labmed/lmac029>

## ABSTRACT

**Objective:** We studied the impact of storage of thawed plasma (TP) on the in vitro coagulation quality and posttransfusion outcomes of apheresis plasma (AP) vs whole blood plasma (WBP).

**Methods:** One hundred units of each product were analyzed. In vitro assays were performed on TP on day 0, day 2, and after refreezing, evaluating international normalized ratio (INR), activated partial thromboplastin time (aPTT), fibrinogen, and factors V and VIII. Transfusion of TP on day 2 was studied in 70 patients with liver cirrhosis and 25 patients with thrombotic thrombocytopenic purpura (TTP).

**Results:** Refrozen specimens from both products showed a significant decline of all values, although AP had a considerably greater coagulation profile ( $P < .05$ ).

On day 0 and day 2, we observed significant decreases in coagulation values (except fibrinogen) with WBP, compared with AP ( $P < .05$ ). The WBP, however, provided similar INR for patients with liver cirrhosis and TTP, as compared with AP. The AP resulted in a significant correction of aPTT following plasma exchange in TTP ( $P < .05$ ).

**Conclusion:** AP demonstrated considerably greater factor activity. This would be beneficial when manufacturing clotting factor concentrates. Large scale clinical trials are needed to further address the hemostatic outcomes of both products in massively transfused patients.

Fresh frozen plasma (FFP) is indicated for the replacement of coagulation factors, coagulopathy of liver diseases, hemorrhagic complications associated with acquired coagulopathies, and massive blood transfusion. Other indications include warfarin reversal and plasma exchange (PE) in patients with thrombotic thrombocytopenic purpura (TTP).<sup>1</sup>

Earlier reports have supported the extensive and early use of plasma in massively transfused patients.<sup>2</sup> To meet the urgent demands of those patients, many centers are using thawed plasma (TP). According to the *AABB Standards for Blood Banks and Transfusion Services*, FFP thawed at 30°C–37°C and stored at 1°C–6°C has a shelf life of 24 hours. Unused FFP can be relabeled as TP and stored for an additional 4 days at 1°C–6°C.<sup>3</sup>

Plasma transfusion guidelines have been limited because of the lack of reliable data, with the last Association for the Advancement of Blood and Biotherapies (AABB) guidelines published in 2010.<sup>4</sup> Lately, the British Society for Haematology recommended that FFP be stored at 4°C, provided that transfusion is completed within 24 hours of thawing or within 4 hours without refrigeration. It also stated that prethawed standard FFP can be extended for 5 days only for patients with unexpected bleeding.<sup>5</sup>

Many studies have investigated the impact of different storage conditions on the coagulation profile of plasma.<sup>6–10</sup> Most of these studies lacked data, such as plasma collection procedure and clinical efficacy. Due to these limitations, and the small number of trials, definitive conclusions could not be drawn.

Plasma can be prepared from single donor via apheresis or from whole blood (WB). Limited data have been published comparing the coagulation profile of apheresis plasma (AP) with recovered plasma prepared from WB (WBP), and they reported the significant superiority of AP.<sup>11</sup>

None of the studies has addressed the clinical effectiveness following transfusion of both products.

To evaluate the impact of collection procedure on the in vitro quality of plasma, we studied AP obtained via 2 apheresis devices, the Trima Accel (Terumo BCT) and the Autopheresis-C (Fresenius Kabi Global) vs WBP collected in bags containing citrate-phosphate-dextrose adenine

(CPDA-1) anticoagulant. Thawed specimens of FFP were kept for 2 days at 4°C, and coagulation parameters were examined on day 0 and day 2. We also studied the impact of twice freezing and thawing of FFP on coagulation parameters.

Another objective of our study was to prospectively explore the posttransfusion effectiveness following transfusion of TP of both products, stored for 24–48 hours at 4°C, in a group of patients with chronic liver cirrhosis. All patients had an INR of 2–3 and received 10 mL/kg of TP prior to an invasive procedure.

We also investigated the coagulation profile of 25 patients with TTP, who were assigned to have PE sessions, using TP on day 2. Both AP and WBP were used alternatively as the replacement fluid. Plasma volumes exchanged were equivalent in paired sessions.

## Materials and Methods

We designed and performed the study according to the tenets of the Declaration of Helsinki; all human subjects signed informed consent paperwork. No investigational procedures were performed.

### Collection and Preparation of Plasma Units

We recruited donors from the Blood Bank and the Apheresis Center at Cairo University Hospital. All units were collected from donors, in compliance with the *AABB Standards for Blood Banks and Transfusion Services*.<sup>3</sup>

Plasma units prepared by 2 apheresis machines vs those obtained from WB were analyzed. Plasma units were classified into:

Group I: 50 AP units of 825 mL, prepared by the Autopheresis-C.

Group II: 50 AP units of 200 mL, prepared by the Trima.

Group III: WBP prepared from 50 WB units stored at 4°C for <3 hours.

Group IV: WBP prepared from 50 WB units stored at 4°C for 24 hours.

All WBP units were not leukoreduced.

### Collection and Preparation of WBP

A mean of 450 ± 20 mL of WB was collected in triple bags (JMS Singapore), containing 63 mL of anticoagulant solution (CPDA-1). Platelet-poor plasma was obtained by centrifugation for 10 minutes via Thermo Scientific centrifuge (Thermo Fisher Scientific), at 4200g. The blood to anticoagulant ratio in WBP was 7:1–8:1.

## Apheresis Machines

### Trima Accel Device

The Trima Accel Terumo machine is a highly automated continuous flow instrument operating on the centrifugation principle. The Trima system also has a white blood cell reduction system.

In our work, plasma was separated initially as a byproduct with platelets that were separated after plasma collection. A touch screen graphical monitor was used to configure and adjust collections. The target end points for our study were set at 200 mL of plasma, and it was collected along with  $9 \times 10^{11}$  platelets, based on donors' criteria.

At our center, family members and friends of patients are motivated to donate, particularly at times when platelet transfusions are needed. Donation priority is given to males who weigh >188 pounds (85 kg) with platelet counts >250 × 10.<sup>11</sup> This practice is seen as essential to recruit donors for apheresis. Further,

this protocol allows us to fully utilize and benefit the most from each apheresis kit.

The disposable tubing kit is loaded and a cassette is snapped into the top of the device. The WB is pumped into the system and mixed with an anticoagulant acid citrate dextrose (ACD), at an initial controlled ratio of 8:1 up to 12:1 over 15 minutes. The use of appropriate centrifugal force will separate the WB into various components according to its density and based on the blood donor volume and their complete blood count. Each component leaves the centrifuge via its own channel, and components that are not collected are returned to the donor via a return pump.

### Autopheresis-C

Autopheresis-C (Auto-C) (Fresenius Kabi Global) is an intermittent flow instrument operating on a unique spinning membrane combined with filtration technology. It is used for plasma collection. As the anticoagulated blood enters the separation chamber, the rotating filter rotates the blood, and the sweeping action of blood over the membrane surface keeps cells from collecting on the membrane surface and hence plugging the membrane pores. The separated plasma goes through the filter and drains by gravity into a container. The remaining packed cells are removed by a pump and sent to a reservoir. When the reservoir is full, the device moves automatically into a return cycle, and cells are returned to the donor, then the next cycle begins. Blood to ACD ratio in Auto-C was 16:1. Plasma collected by the Auto-C pheresis machine is also leukoreduced.<sup>12</sup>

### Sampling and In Vitro Plasma Analysis

Immediately after plasma collection, 3 aliquots were collected from the same plasma unit before freezing. Blood group A units were used for our analysis.

All aliquots were immediately stored for less than 1 month, under standard blood banking conditions at –20°C. Upon thawing at 37°C for batch analysis, the first aliquot was immediately analyzed (day 0); the second aliquot was stored at 4°C for 24–48 hours before analysis (day 2). To study the impact of a second freeze and thaw on coagulation parameters, a third aliquot was refrozen for further analysis. To maintain consistency of testing results between AP and WBP, aliquots were thawed, and assays were conducted for specimens concurrently at the same time after thawing.

In vitro assays were performed evaluating prothrombin time/international normalized ratio (PT/INR), activated partial thromboplastin time (aPTT), fibrinogen, and factors V and VIII.

### In Vitro Coagulation Assays

All samples were analyzed within 1 hour of thawing. We evaluated PT/INR, aPTT, fibrinogen, and factors V and VIII.

We performed our in vitro assays using standard procedures. All tests were performed via STA-R analyzer (Diagnostica Stago), using reagents from DiaMed GmbH (Switzerland). Factors V and VIII were determined via clotting assays, as described by the manufacturer, using reagents and corresponding human deficient plasmas from DiaMed. Fibrinogen was measured via the Claus method.

### In Vivo Evaluation of TP

#### Evaluation of Patients with Liver Disease

We prospectively evaluated 70 plasma transfusions in 70 patients, of whom 57 were males. Their mean age was 59 ± 8 years, and their

average weight was  $67 \pm 8$  kg. All patients were being treated for chronic liver cirrhosis and had a pretransfusion INR of 2–3 with a median of 2.5. None of the patients had bleeding or sepsis or received any hemostatic agents. All patients received a standard dose of 10 mL/kg of group-specific TP on day 2, of either AP prepared by the Trima (35 transfusions) or WBP prepared from WB stored <3 hours (35 transfusions) prior to an invasive procedure.

All plasma units were stored for less than 1 month. We drew peripheral blood samples immediately before plasma transfusion and within 4 hours after transfusion. We assessed their INR, via STA-R analyzer (Diagnostica Stago), using reagents of DiaMed.

### Evaluation of Patients with TTP

We studied 25 patients with TTP, with severely deficient ADAMTS13, who underwent PE sessions on the Optia platform (Terumo). TP of AB blood group that was stored at 4°C for 24–48 hours with a mean of  $41.5 \pm 3$  hours was used as the replacement fluid in all studied sessions. PE was conducted daily until normalization of both platelets and reticulocytes, then PE was tapered gradually. Typically, a plasma volume of 1.5 was exchanged in the first 3 sessions, followed by sessions of a single plasma volume.

Patients were assigned to receive 2 paired sessions using AP (prepared by Trima) and WBP (from WB stored <3 hours) alternatively, and the immediate coagulation changes were evaluated.

**FIGURE 1.** In vitro coagulation parameters of thawed apheresis plasma and whole blood plasma (WBP) on day 0, day 2, and after a second freeze. **A,** Activated partial thromboplastin time (aPTT). **B,** International normalized ratio (INR). **C,** Factor V. **D,** Factor VIII. **E,** Fibrinogen. Group I: Autopheresis-C device. Group II: Trima device. Group III: WBP collected <3 hours after whole blood donation. Group IV: WBP collected 24 hours after whole blood donation. Aliquot 1: Thawed plasma (TP) immediately analyzed. Aliquot 2: TP stored at 4°C for 24–48 hours before analysis. Aliquot 3: A second freeze and thaw preanalysis. \* $P < .05$  Aliquot 1 vs Aliquots 2 and 3. \*\* $P < .05$  groups I and II (AP) vs groups III and IV (WBP).

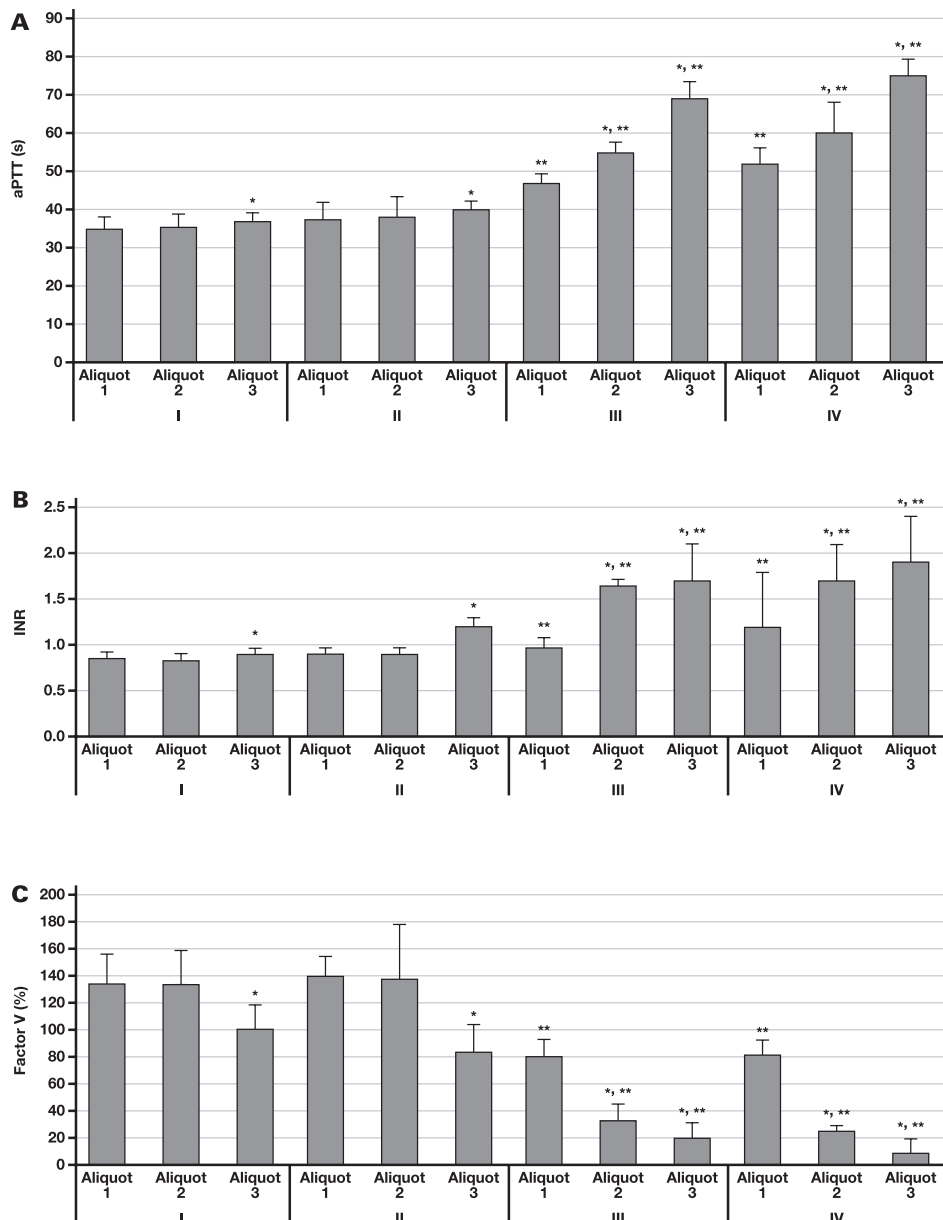
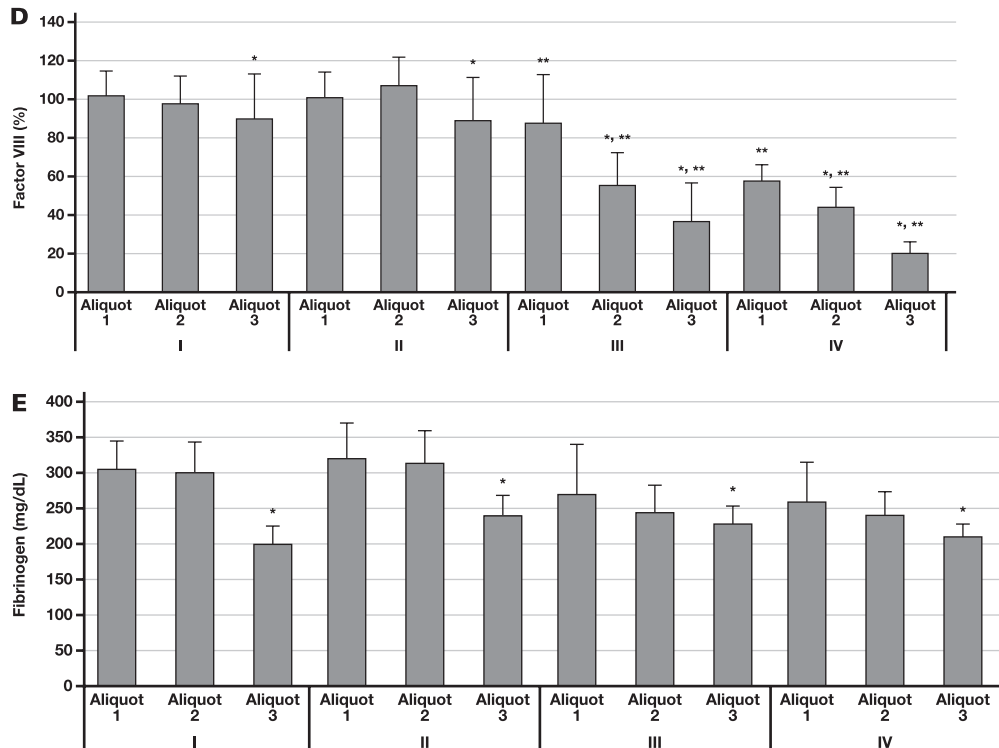
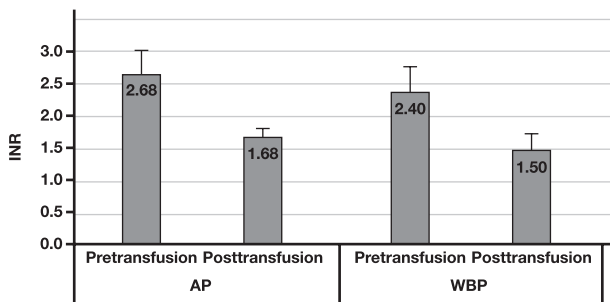


Figure 1. (cont)



**FIGURE 2.** Evaluation of the coagulation profile of patients with chronic liver cirrhosis pre and posttransfusion using thawed apheresis plasma (AP) and whole blood plasma (WBP) on day 2.



We drew peripheral blood samples immediately before and after sessions, and we assessed the INR and aPTT via STA-R analyzer (Diagnostica Stago), using reagents of DiaMed.

#### PE Protocol for Patients with TTP

We used a double lumen central venous access for all patients. The anticoagulant used for all sessions was citrate. The plasma volume exchanged was 1–1.5, and a fluid balance of 100% was used for all sessions. To ensure consistency of variables between sessions performed with AP and those with WBP, we removed the same volume of plasma for each paired study.

#### Statistical Analysis

Standard statistical analysis of test results was performed. Analysis included calculation of descriptive statistics, frequency distribution, median, mean, and standard deviation (SD). The Wilcoxon Rank-Sum

Test was used for comparative studies. A  $P$  value of less than .05 was considered to be significant.

## Results

### In Vitro Coagulation Parameters of Thawed AP vs WBP

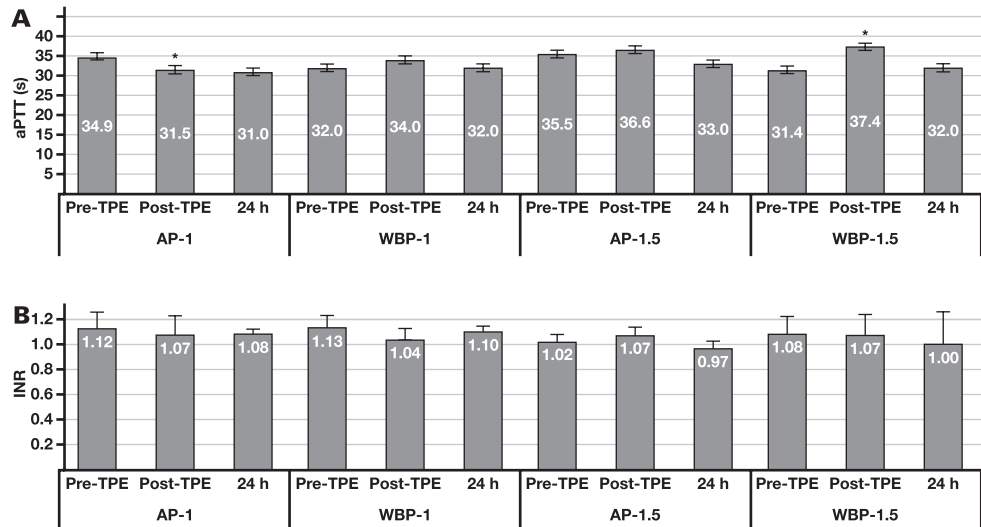
#### Analysis of Coagulation Parameters of Fresh Specimens of TP (Aliquot 1)

Immediately on thawing AP, no significant differences of coagulation values were noted between Trima and Autopheresis-C machines ( $P > .05$ ). Significant impairment of all coagulation parameters (except fibrinogen) was observed in WBP, compared with AP ( $P < .05$ ). WBP prepared 24 hours after donation showed a significant drop of factor VIII, compared to that prepared <3 hours ( $P < .05$ ). Normal levels of factor V and fibrinogen ( $81.2 \pm 11.7\%$  and  $260 \pm 55$  mg/dL, respectively) were retained in WBP prepared 24 hours after donation. Coagulation parameters of fresh immediately thawed plasma (Aliquot 1) separated by different procedures are presented in **FIGURE 1**.

#### Analysis of the Coagulation Profile of TP Stored for 24–48 Hours at 4°C (Aliquot 2)

Compared to immediately thawing values, values of thawed AP were not influenced by 24–48 hours storage at 4°C ( $P > .05$ ). A significant drop of factors V and VIII was noted with WBP ( $P < .05$ ), associated with a significant increase in the INR and aPTT ( $P < .05$ ). We observed significant increases of coagulation parameters in thawed AP of Aliquot 2, compared

**FIGURE 3.** Evaluation of the coagulation profile of patients with TTP pre and post sessions using thawed apheresis plasma (AP) and whole blood plasma (WBP) on day 2. AP-1: Plasma exchange of 1 plasma volume using apheresis plasma. WBP-1: Plasma exchange of one plasma volume using whole blood plasma. AP-1.5: Plasma exchange of 1.5 total plasma volume using apheresis plasma. A, Activated partial thromboplastin time (aPTT) of patients with thrombotic thrombocytopenic purpura (TTP) before and after sessions using thawed AP and WBP on day 2. B, International normalized ratio (INR) of patients with TTP before and after sessions using thawed AP and WBP on day 2. WBP-1.5, plasma exchange of 1.5 total plasma volume using whole blood plasma. TPE, therapeutic plasma exchange. \* $P < .05$ .



with those of WBP ( $P < .05$ ). Coagulation parameters of thawed plasma of Aliquot 2, separated by different procedures, are presented in **FIGURE 1**.

#### Analysis of the Coagulation Profile of Twice-Frozen Specimens of TP (Aliquot 3)

Compared to immediately thawing values, twice-frozen AP and WBP showed significant decreases in coagulation factors ( $P < .05$ ). However, the AP group had a considerably greater coagulation profile, when compared with the WBP group ( $P < .05$ ). A significant drop of factor V activity was noted with Trima with a mean of  $84 \pm 19.4$ , compared with the Auto-C with a mean of  $101 \pm 18$  ( $P = .04$ ). Coagulation profile of twice-frozen AP and WBP (Aliquot 3) is presented in **FIGURE 1**.

#### Clinical Evaluation of TP Stored for 24–48 Hours at 4°C Evaluation of INR After Transfusion of AP vs WBP in Patients with Chronic Liver Cirrhosis

The median correction of INR after transfusion of WBP was from 2.3 to 1.45 (37%). The median correction of INR after transfusion of AP was from 2.5 to 1.57 (37.2%). The difference was not statistically significant ( $P > .05$ ). See **FIGURE 2**. None of the patients had any bleeding events during or after the procedure.

#### Evaluation of INR and aPTT in Patients with TTP Undergoing Plasma Exchange with AP vs WBP

Percent decrease in INR following PE was comparable with both AP and WBP ( $P > .05$ ). Significant increases in values of aPTT were observed in patients with TTP who underwent PE using WBP, as compared with AP ( $P < .05$ ). Those values were significantly higher after the exchange of 1.5 total plasma volume, compared with those following sessions of 1 plasma volume ( $P < .05$ ). The aPTT recovered quickly 24 hours postprocedure.

Percent correction of aPTT was significantly higher with AP compared with WBP ( $P < .05$ ). See **FIGURE 3**. None of the 25 patients had any bleeding or clotting complications.

#### Discussion

With the extensive use of plasma therapy in the trauma settings nowadays, maintaining an inventory of prethawed plasma that provides the best hemostatic quality becomes paramount. In the current study, fibrinogen was not impacted by the plasma collection procedure.

Immediately on thawing our FFP specimens, WBP demonstrated significant decreases in all coagulation parameters (except fibrinogen), compared with the AP. We observed no differences between Trima and Autopheresis-C devices. A further drop of factor VIII was observed in WBP prepared 24 hours after donation. Normal levels of factor V and fibrinogen were retained in WBP regardless of time elapsed from donation. Our findings are consistent with data reported in the literature.<sup>11,13</sup>

The significantly higher coagulation profile of our specimens from AP compared with WBP can be attributed to their lower final citrate concentration, which can presumably be associated with greater levels of coagulation factors V and VIII.<sup>14</sup>

In our study, refrozen specimens from both products showed significant decreases of all values, compared with those from day 0, though AP had a considerably greater coagulation profile.

Such observation could be of particular significance during plasma manufacturing processes that require a second freeze in solvent/detergent treated plasma.

Our data on refrozen specimens are in agreement with previous observations in FFP units that were slowly frozen at  $-65^{\circ}\text{C}$  and rethawed at  $37^{\circ}\text{C}$ .<sup>15</sup>

A significant drop of factor V activity was demonstrated in our refrozen specimens from the Trima device, compared with those from Autopheresis-C, possibly due to the increased citrate concentration.<sup>14</sup>

Our values of thawed AP on day 2 were not significantly different when compared with day 0. Similar results were reported by Sidhu et al,<sup>10</sup> who suggested that thawed AP stored beyond 24 hours can be transfused into patients with deficiency of factors V or VIII without compromising clinical hemostatic outcomes. Our specimens from WBP, however, demonstrated a considerable drop in all coagulation values (except fibrinogen), as compared with the AP. This may indicate that the AP group was more standardized with consistent and stable coagulation activity and that processing and/or storage of WBP group were not optimized.

Another advantage of the AP is offering prestorage leukoreduction. Furthermore, large doses could be obtained reducing donor exposure.

Despite the significant decrease of coagulation parameters upon storage in the WBP group, as compared with the AP group, they provided similar INR to our cohort of patients with liver disease. This underscores the fact that normal clotting factor activity is not necessarily required to maintain appropriate coagulation. Residual coagulation factors V and VIII were considered sufficient to support an effective clinical coagulation at levels of 10%–30% and 30%, respectively.<sup>16</sup> However, whether the decreased quality of WBP over storage can adversely impact clinical outcomes in massively transfused patients with hemodilution and depleted factors remains in dispute and warrants further studies.

Most coagulation factors are typically temporarily depleted right after PE. It is well known that when plasma is being replaced with an equal volume of 5% albumin, significant increases in INR and aPTT are observed.<sup>17</sup> In the current study, both products provided comparable INR following PE in patients with TTP. The greater factor VIII activity in our AP group, however, provided a significant correction of aPTT values immediately after PE. We also observed further increases in aPTT with WBP following aggressive PE sessions of 1.5 total plasma volume. The aPTT for all patients was restored 24 hours postprocedure.

The significant increase in aPTT in this group of patients can also be caused by a possible decrease in factor IX in the WBP group,<sup>6</sup> which merits consideration and deserves further studies. Of note, coagulopathy in those patients may also be related to the potential citrate effect that can induce hypocalcemia for up to 6 hours post PE.<sup>18,19</sup> Further studies are warranted to address this finding.

In the past few years, transfusion specialists have investigated the use of thawed FFP beyond 24 hours. Smith and colleagues<sup>6</sup> reported significant decreases in activities of coagulation factors: VIII: C, V, IX, and von Willebrand factor antigen in specimens of thawed FFP kept at 1°C–6°C up to 24 hours.<sup>6</sup> Other studies, however, demonstrated stable coagulation factors beyond day 5.<sup>9,11,20–22</sup> The controversial results of factors V and VIII activities among various study groups could be attributed to interlaboratory procedure variability and to the significant variation of these factors among donors. Additionally, the collection method for plasma (AP vs WBP) and the ABO blood group were not mentioned in most previous studies. It is well known that the ABO blood group can influence factor VIII, with significantly lower levels in blood group O, as compared with other blood groups.<sup>23</sup> Plasma specimens of blood group A were used for our in vitro studies. We used plasma of AB blood group (universal plasma blood group donor) as the replacement fluid for all studied PE sessions.

Factor VIII can also be influenced by other factors, including genetics and endothelial stimulation.<sup>24</sup> Race, ethnicity, and gender can also impact factor VIII, with women and Blacks being associated with higher values.<sup>24,25</sup> The values that we report for factor VIII in AP were much higher (101 ± 14) than those reported in a previous study, using the Trima machine (60 ± 30).<sup>26</sup>

Earlier trials at trauma centers and in the military ER noted the significant benefit in survival rates when using plasma with red blood cells in a 1:1 ratio.<sup>2</sup> According to the *AABB Standards for Blood Banks and Transfusion Services*, TP is approved for transfusion up to 5 days after thawing at 30°C–37°C when stored at 1°C–6°C.<sup>3</sup> Currently, at our center in an attempt to maximize plasma utilization while meeting the urgent and extensive needs of trauma patients, thawed AP is extended for the standard 5 days. A more conservative approach is used for our thawed WBP, which is stored for only 48 hours.

In the present study, none of the WBP units were leukoreduced. Some studies have demonstrated a significant impact of inline filtration of WB on coagulation quality,<sup>27,28</sup> whereas others showed no significance.<sup>29,30</sup> Although leukoreduction may have caused estimates of coagulation for our AP to be skewed to lower than expected, it is unlikely that this would have had a significant impact on our results.

## Conclusion

Despite the considerable drop in coagulation factors upon storage, compared with the AP group, the WBP group provided similar INR to our group of patients with chronic liver cirrhosis and TTP. The significant reduction in factor VIII in the WBP group, however, resulted in a significant increase in aPTT following PE in patients with TTP.

Our analysis revealed that coagulation factors were well-preserved in thawed specimens from AP. This can ultimately provide effective utilization and management of plasma units while maintaining the greatest coagulation quality. This could be of particular importance when further manufacturing clotting factor concentrates.

Definitive conclusions, however, regarding the potential clinical utility of AP as compared with WBP cannot be drawn until large-scale prospective studies are conducted in massively transfused and hemostatically compromised patients.

## Acknowledgments

We acknowledge the nursing team at the Apheresis Unit, the technicians and technologists at the Blood Bank, the physicians at the Department of Internal Medicine, and the patients whom we serve.

## REFERENCES

- Hellstern P, Muntean W, Schramm W, et al. Practical guidelines for the clinical use of plasma. *Thromb Res*. 2002;107(1):S53–S57.
- Holcomb JB, Tilley BC, Baraniuk S, et al. Transfusion of plasma, platelets, and red blood cells in a 1:1:1 vs a 1:1:2 ratio and mortality in patients with severe trauma: the PROPPR randomized clinical trial. *JAMA*. 2015;313(5):471–482.
- Gammon RR, ed. *Standards for Blood Banks and Transfusion Services*. 32nd ed. Bethesda, MD: AABB Press; 2020.

4. Roback JD, Caldwell S, Carson J, et al. Evidence-based practice guidelines for plasma transfusion. *Transfusion*. 2010;50(6):1227–1239.
5. Green L, Bolton-Maggs P, Beattie C, et al. British Society of Haematology guidelines on the spectrum of fresh frozen plasma and cryoprecipitate products: their handling and use in various patient groups in the absence of major bleeding. *Br J Haematol*. 2018;181(1):54–67.
6. Smith JF, Ness PM, Moroff G, et al. Retention of coagulation factors in plasma frozen after extended holding at 1–6 degrees C. *Vox Sang*. 2000;78(1):28–30.
7. Ben-Tal O, Zwang E, Eichel R, et al. Vitamin K dependent coagulation factors and fibrinogen levels in FFP remain stable upon repeated freezing and thawing. *Transfusion*. 2003;43(7):873–877.
8. Buchta C, Felfernig M, Hocker P, et al. Stability of coagulation factors in thawed solvent/detergent-treated plasma during storage at 4 degrees C for 6 days. *Vox Sang*. 2004;87(3):182–186.
9. Monson J, Bracey A, Radovancevic R. Effect of thawing FFP at 37°C and 45°C and prolonged storage on the coagulation factors V, VII, and VIII. *Transfusion*. 2004;44:64A.
10. Sidhu RS, Le T, Brimhall B, Thompson H. Study of coagulation factor activities in apheresis thawed fresh frozen plasma at 1–6°C for 5 days. *J Clin Apher*. 2006;21(4):224–226.
11. Runkel S, Haubelt H, Hitzler W, et al. The quality of plasma collected by automated apheresis and of recovered plasma from leuko-depleted whole blood. *Transfusion*. 2005;45(3):427–432.
12. Fresenius Kabi. [https://www.fresenius-kabi.com/kr/documents/brochure\\_Autopheresis-C.pdf](https://www.fresenius-kabi.com/kr/documents/brochure_Autopheresis-C.pdf).
13. Cardigan R, Lawrie AS, Mackie IJ, et al. The quality of fresh frozen plasma produced from whole blood stored at 4 degrees C overnight. *Transfusion*. 2005;45(8):1342–1348.
14. Beeck H, Becker T, Kiessig ST, et al. The influence of citrate concentration on the quality of plasma obtained by automated plasmapheresis: a prospective study. *Transfusion*. 1999;39(11–12):1266–1270.
15. Dzik WH, Riibner MA, Linehan SK. Refreezing previously thawed fresh–frozen plasma: stability of coagulation factors V and VIII: C. *Transfusion*. 1989;29(7):600–604.
16. Acker JP, Marks DC, Sheffield WP. Quality assessment of established and emerging blood components for transfusion. *J Blood Transfus*. 2016. doi: 10.1155/2016/4860284.
17. Flaum MA, Cuneo RA, Appelbaum FR, et al. The hemostatic imbalance of plasma exchange transfusion. *Blood*. 1979;54(3):694–702.
18. Kaya E, Keklik M, Sencan M, et al. Therapeutic plasma exchange in patients with neurological diseases: multicenter retrospective analysis. *Transfus Apher Sci*. 2013;48(3):349–352.
19. Yamada C, Pipe SW, Zhao L., et al. Coagulation status after therapeutic plasma exchange using citrate in kidney transplant recipients. *Transfusion*. 2016;56(12):3073–3080.
20. Kakaiya RM, Morse EE, Panek S. Labile coagulation factors in thawed FFP prepared by two methods. *Vox Sang*. 1984;46(1):44–46.
21. Downes KA, Wilson E, Yomtovian R, Sarode R. Serial measurement of clotting factors in thawed plasma stored for 5 days. *Transfusion*. 2001;41(4):570.
22. Tholpady A, Monson J, Radovancevic R, et al. Analysis of prolonged storage on coagulation Factor (F)V, FVII, and FVIII in thawed plasma: is it time to extend the expiration date beyond 5 days? *Transfusion*. 2013;53(3):645–650.
23. Matijevic N, Kostousov V, Wang YW, et al. Multiple levels of degradation diminish hemostatic potential of thawed plasma. *J Trauma*. 2011;70(1):71–79.
24. Kamphuisen PW, Eikenboom JC, Bertina RM. Elevated factor VIII levels and the risk of thrombosis. *Arterioscler Thromb Vasc Biol*. 2001;21(5):731–738.
25. Keightley AM, Lam YM, Brady JN, et al. Variation at the von Willebrand factor (vWF) gene locus is associated with plasma vWF: Ag levels: identification of three novel single nucleotide polymorphisms in the vWF gene promoter. *Blood*. 1999;93(12):4277–4283.
26. Elfath MD, Whitley P, Jacobson MS, et al. Evaluation of an automated system for the collection of packed RBCs, platelets, and plasma. *Transfusion*. 2000;40(10):1214–1222.
27. Alhumaidan HS, Cheves TA, Holme S, et al. The effect of filtration on residual levels of coagulation factors in plasma. *Am J Clin Pathol*. 2013;139(1):110–116.
28. Chan KS, Sparrow RL. Microparticle profile and procoagulant activity of fresh frozen plasma is affected by whole blood-leukocyte depletion rather than 24-hour room temperature–hold. *Transfusion*. 2014;54(8):1935–1944.
29. Heiden M, Salge U, Henschler R, et al. Plasma quality after whole-blood filtration depends on storage temperature and filter type. *Transfus Med*. 2004;14(4):297–304.
30. Runkel S, Bach J, Haubelt H, et al. The impact of two whole blood inline filters on markers of coagulation, complement, and cell activation. *Vox Sang*. 2005;88(1):17–21.

# Plasma LncRNA MALAT1 Expressions Are Negatively Associated with Disease Severity of Postmenopausal Osteoporosis

Tie-Yong Qian, BS,<sup>1,✉</sup> Hui Wan, MS,<sup>1,1,✉</sup> Ci-You Huang, MS,<sup>1,✉</sup> Xiao-Jing Hu, BS,<sup>1,✉</sup> and Wei-Feng Yao, BS<sup>1,✉</sup>

<sup>1</sup>Department of Endocrinology, The Affiliated Wuxi No. 2 People's Hospital of Nanjing Medical University, Wuxi, China; \*To whom correspondence should be addressed. [wanhui071122@163.com](mailto:wanhui071122@163.com)

**Keywords:** LncRNA MALAT1, postmenopausal osteoporosis, disease severity, bone mineral density, bone turnover markers, vertebral fracture

**Abbreviations:** OP, osteoporosis; OBs, osteoblasts; OCs, osteoclasts; LncRNAs, long noncoding RNAs; BMSCs, bone-marrow mesenchymal stem cells; MALAT1, metastasis-associated lung adenocarcinoma transcript 1; PMOP, postmenopausal osteoporosis; DXA, dual-energy X-ray absorptiometry; EIA, enzyme immunoassay; BMD, bone mineral density; GSQ, Genant semiquantitative; VAS, Visual Analog Scale; ODI, Oswestry Disability Index; NA, nonapplicable

*Laboratory Medicine* 2022;53:446–452; <https://doi.org/10.1093/labmed/lmac009>

## ABSTRACT

**Background:** Long noncoding RNA metastasis-associated lung adenocarcinoma transcript 1 (LncRNA MALAT1) has been proven to promote osteogenesis in different health conditions. However, the role of plasma MALAT1 in postmenopausal osteoporosis (PMOP) has not been investigated.

**Objective:** To investigate whether plasma MALAT1 expressions are associated with severity of PMOP.

**Methods:** A total of 126 patients with PMOP and 126 healthy female control individuals were drafted into study participation. Plasma MALAT1 was detected using RT-PCR. Bone formation marker bone-specific alkaline phosphatase plasma concentration was determined using chemiluminescence immunoassay. Levels of bone absorption marker cross-linked N-telopeptidases of type I collagen were measured in duplicate using enzyme immunoassay. Bone mineral density (BMD) was examined in the total hips, femoral neck, and lumbar (L1–L4) spine using dual-energy x-ray absorptiometry. We used Genant semiquantitative (GSQ) criteria to assess the degree of vertebral deformity and fracture. Receiver operating characteristic

(ROC) curve analysis was performed to evaluate the potential diagnostic value of MALAT1 with regard to the GSQ grading. We used the Visual Analog Scale (VAS) and Oswestry Disability Index (ODI) to evaluate the symptomatic severity in and functional ability of the study participants.

**Results:** Plasma MALAT1 expressions were significantly lower in patients with PMOP, compared with healthy controls. Plasma MALAT1 expressions in patients with PMOP were positively associated with total hip, femoral neck, and lumbar (L1–L4) spine BMD. In total, 95 patients experienced vertebral deformity or fracture (VF), and 31 had no fractures. Plasma MALAT1 expressions were markedly decreased in patients with VF, compared with patients without fractures. Plasma MALAT1 expressions were negatively related to GSQ grading in patients with VF. ROC curve analysis demonstrated that decreased plasma MALAT1 expression exhibits decent diagnostic value with regard to GSQ grading. Finally, we discovered that plasma MALAT1 expression was also negatively associated with VAS and ODI.

**Conclusion:** Plasma MALAT1 expressions are negatively associated with severity of PMOP.

Osteoporosis (OP) is a chronic disease, defined as a skeletal disorder characterized by decreased bone strength, which predisposes affected individuals to fractures.<sup>1</sup> So far, OP has been regarded as 1 of the 3 main chronic diseases worldwide, along with diabetes and hypertension, that mostly occurs in individuals who have gone through menopause and among elderly individuals.<sup>2</sup> The pathogenesis of OP is mainly attributed to decreased estrogen and increased age.<sup>3</sup> Because of the reduction of estrogen after menopause, an imbalance occurs between osteoblasts (OBs) and osteoclasts (OCs), resulting in decreased bone volume and density, increased bone fragility, and increased risk of fractures.<sup>4</sup>

Currently, OP is diagnosed by decreased bone mineral density (BMD) and presence of clinical symptoms. However, the onset of OP is silent and insidious, with the diagnosis often only being made after there is irreversible damage resulting from a fragility-related fracture.<sup>5</sup> Therefore, it would be highly desirable to develop sensitive and reliable methods for the early diagnosis of and monitoring of treatment for this debilitating

disease. The effective monitoring of treatment efficacy might also help to improve long-term compliance with antiosteoporotic therapy.

Long noncoding RNAs (LncRNAs) are a subgroup of nonprotein coding RNAs with lengths longer than 200 nucleotides.<sup>6</sup> Research into this subgroup has become focused in recent years. These RNAs have been found to participate in regulating gene expression and to provide an epigenetic role in controlling phenotype.<sup>7</sup> It has been shown<sup>8</sup> that LncRNAs are not only present in human organs or tissues but also stably exist in human plasma, serum, and other body fluids.

The chief reason that OP occurs is the imbalance of bone metabolism, in which new bone formation activity is drastically weaker than bone absorption activity, therefore resulting in loss of bone mass and volume.<sup>4</sup> During the process of bone metabolism, OBs, OCs, and bone marrow mesenchymal stem cells (BMSCs) serve as the 3 most important cell types. The results of a study by Li et al<sup>9</sup> have shown that LncRNA is closely associated with the functions of these cells. For example, LncRNA HIF1 $\alpha$ -AS1 plays a key regulatory role in osteoblast differentiation by regulating HOXD10.<sup>10</sup> In the findings of another study, inhibition of LncRNA UCA1 promoted the proliferation and differentiation of osteoblasts.<sup>11</sup> However, upregulation of LncRNA-NONMMUT037835.2 inhibited osteoclastic differentiation.<sup>12</sup> LncRNA Neat1 stimulates osteoclastogenesis via absorbing miR-7.<sup>13</sup> Also, LncRNA HOTAIR inhibited osteogenic differentiation of BMSCs by regulating the Wnt/ $\beta$ -catenin pathway.<sup>14</sup> LncRNA HOTTIP enhances human osteogenic BMSC differentiation through interaction with WDR5.<sup>15</sup> These findings strongly suggest the potential role of LncRNA involved in normal bone metabolism and pathological bone remodeling.

Metastasis-associated lung adenocarcinoma transcript 1 (MALAT1) is a widely studied LncRNA that has been proven as a potential biomarker for lung cancer metastasis and has been correlated with the development of many other types of human tumors.<sup>16</sup> Also, MALAT1 has also been found to be implicated in cardiovascular disease,<sup>17</sup> rheumatoid arthritis, and diabetes.<sup>18</sup>

The findings of recent studies have also shown that MALAT1 yields positive effects on osteoblasts and inhibits osteoclastic activity through different types of signaling, which indicates that MALAT1 may be beneficial in OP. For example, MALAT1 could promote osteogenic differentiation of human periodontal ligament stem cells through inhibition of the miR-155-5p/ETS1 axis.<sup>19</sup> Similarly, MALAT1 can also facilitate the osteogenic differentiation of hBMSCs by regulating the miR-96/Osx axis.<sup>20</sup> In MALAT1-depleted osteoblasts, IL-1 $\beta$ -mediated PGE2 secretion was greater than in the control group.<sup>21</sup> In contrast, MALAT1 inhibits osteoclastic differentiation of macrophages in osteoporosis via absorbing the miR-124-3p.<sup>22</sup>

The aforementioned study findings indicate that MALAT1 may serve as an important protective factor during OP. However, there are no studies available, to our knowledge, that explore the potential relationship between plasma MALAT1 expressions and severity of OP. Therefore, the aim of the present study was to detect plasma expressions of MALAT1 in patients with postmenopausal OP (PMOP), to assess the potential utility of MALAT1 as a diagnostic biomarker for PMOP.

## Methods

### Study Patients

From May 2020 to May 2021, a total of 126 female patients with PMOP that had been admitted to Department of Endocrinology, the Affiliated Wuxi No. 2 People's Hospital of Nanjing Medical University, Wuxi,

China, were enrolled in our study. Meanwhile, 120 age-matched healthy women were enrolled as control individuals. The average (SD) age was 65.1 (5.1) years in the patient group and 64.8 (6.0) in the control group. All enrolled participants were ethnic Han Chinese.

Patients with OP were diagnosed via dual-energy X-ray absorptiometry (DXA) (T-score of < -2.5 SD). Plasma was extracted from collected patient blood using conventional methods. Inclusion criteria were as follows: having newly diagnosed OP, having complete medical records, and understanding the experimental procedure and being willing to participate. Exclusion criteria were as follows: having been treated for OP 3 months before current hospital admission; potentially having diseases including malignant tumors, diabetes, chronic kidney disease, liver diseases, or gut diseases; and not cooperating with researchers. None of the controls had osteoporosis or any other systemic disease that could influence bone mass, such as malignant tumors, diabetes, chronic kidney disease, liver diseases, or gut diseases. This study was approved by the Affiliated Wuxi No. 2 People's Hospital of Nanjing Medical University; signed consent forms were obtained from all the participants.

### Specimen Preparation and Laboratory Examination

From each participant, we collected 5 mL of venous blood in an EDTA anticoagulant gel tube; then, the specimens were centrifuged at 1000g for 10 minutes, followed by 13,000g for 10 additional minutes at 4°C. The supernatant plasma was then separated, split into 250- $\mu$ L aliquots, and frozen at -80°C until use. Total RNA was extracted from plasma using RNazol RT RNA Isolation Reagent (Sigma-Aldrich). A High-Capacity cDNA Reverse Transcription Kit (ThermoFisher Scientific) was used to perform reverse transcription. To detect the expression of LncRNA, a MALAT1 Kit (NEB) was used to prepare PCR systems. Primers of LncRNA MALAT1 and  $\beta$ -actin were designed and synthesized by GenePharma: MALAT1 sense, 5'-CTTCCCTAGGGGATTTCAGG-3' and antisense, and 5'-GCCACAGGAACAAGTCCTA-3'.  $\beta$ -actin was used as the internal reference, and the primers were as follows:  $\beta$ -actin sense, 5'-CTTAGTTGCGTTACACCCTTTCTTG-3' and antisense, and 5'-CTGTACCTTACCAGTTCCAGTTT-3'. Amplification was performed under the following conditions: 95°C for 30 seconds, followed by 40 cycles of 95°C for 5 seconds, 60°C for 30 seconds, and 72°C for 30 seconds. The expression of MALAT1 was normalized to  $\beta$ -actin via using the  $2^{-\Delta\Delta CT}$  method. Each specimen underwent PCR testing 3 times.

Plasma bone-specific alkaline phosphatase (BALP) was determined by chemiluminescence immunoassay (Access-Ostase immunoassay, Beckman-Coulter) on the ACCESS immunoassay system. ACCESS Ostase is a chemiluminescent immunoassay with paramagnetic particles for the quantitative determination of plasma BALP using the ACCESS Analyzer. N-telopeptidases of type I collagen (NTx) levels were measured in duplicate using enzyme immunoassay (EIA) kits. All replicates of quality control and participant specimens had a coefficient of variation <7.0%. The mean coefficient of variation percentage of internal controls was 5.7%.

### BMD Examination

We used the DXA system (Lunar Prodigy, GE Healthcare) to calculate BMD at the hips, femoral neck, and the first through the fourth lumbar vertebrae. BMD examination was conducted by an experienced physician (H.W.).

### Definition of Vertebral Deformity and Fracture

We used Genant semiquantitative (GSQ) criteria for evaluation of patients with OP who had experienced vertebral fracture.<sup>23</sup> The GSQ

criteria is currently the most-used approach in epidemiology studies and clinical trials for osteoporotic vertebral deformity and osteoporotic vertebral fracture evaluation using radiograph testing.<sup>22</sup> With this approach, each vertebra from T4 to L4 is assessed visually for height loss. Height loss of approximately 20%–25% is marked as grade 1 (mild), 25%–40% as grade 2 (moderate), and >40% as grade 3 (severe), compared with the heights of the same and/or neighboring vertebrae. Image findings were read by 2 experienced radiologists, and the  $\kappa$  value was used to examine the consistency of the results.

### Definition of Clinical Severity

The Visual Analog Scale (VAS) and Oswestry Disability Index (ODI) were used to evaluate symptomatic severity and functional ability. The VAS is the most frequently applied quantitative tool in clinical practice for evaluating the degree of pain. The detailed way to perform this test is to draw a 10-cm horizontal line on a piece of paper. One side is 0, indicating no pain, and the other side is 10, indicating extreme pain; the middle portion indicates different degrees of pain. The physician then asks the patient to point on the line to indicate the degree of pain they are feeling.<sup>24</sup> The ODI is currently the most widely used assessment method worldwide for lumbar or leg pain. The ODI questionnaire is composed of 10 questions, covering pain intensity, independent living, carrying, walking, sitting, standing, sleep, travel, sex, and social life. Every category includes 6 options, with the highest score for each question being 5 points. Thus, the first option is worth 0 points and the last option is worth 5 points; higher scores represent more-serious dysfunction.<sup>25</sup> The VAS and ODI are widely used for pain and function in different conditions, and are reliable and credible instruments.

### Statistical Analysis

We conducted statistical analyses using GraphPad Prism (version 8.0 for Windows; GraphPad Software). Normalized MALAT1 levels were demonstrated as  $\Delta Cq$ , with  $\Delta Cq = Cq(\text{MALAT1}) - Cq(\beta\text{-actin})$ . Data were expressed as mean (SD) or median. The differences between the 2 groups were analyzed via the Student *t*-test or Mann-Whitney test, whereas 1-way ANOVA or Kruskal-Wallis testing was used for 3 or more groups. The Kolmogorov-Smirnov test was used to examine whether data were normally distributed. Pearson or Spearman analysis was performed to explore the potential correlation between MALAT1 and other indices. ROC curves were drawn and the area under the curve (AUC) assessed to determine the diagnostic power of plasma MALAT1 in OP.  $P < .05$  was considered statistically significant.

## Results

### Demographic and Clinical Data

The basic clinical characteristics and BMD data of the patients with PMOP and the controls are depicted in **TABLE 1**. There were no statistically significant differences between patients with PMOP and controls regarding age, BMI, and age at menopause (**TABLE 1**). BMD values at the total hips, femoral neck, and lumbar (L1–L4) spine were all significantly lower in the PMOP group, compared with the control group (**TABLE 1**).

### Plasma MALAT1 Expressions in Patients with PMOP

Patients with PMOP showed significantly lower plasma MALAT1 relative expressions compared with healthy controls (mean [SD], 0.48 [0.15] vs

**TABLE 1. Baseline Clinical Characteristics**

Variable	Study Group, Mean (SD)		P Value
	PMOP	Control	
Age, y	65.1 (5.1)	64.8 (6.0)	.87
Age at menopause, y	52.1 (3.1)	51.7 (3.0)	.75
BMI, kg/m <sup>2</sup>	23.8 (3.3)	23.7 (3.5)	.56
Total hip BMD, g/cm <sup>2</sup>	0.84 (0.14)	1.12 (0.16)	<.001
Femoral neck BMD, g/cm <sup>2</sup>	0.81 (0.18)	1.04 (0.19)	<.001
L1-4 BMD, g/cm <sup>2</sup>	0.75 (0.20)	1.24 (0.21)	<.001
VAS	4.8 (1.8)	NA	NA
ODI	40.0 (6.7)	NA	NA

PMOP, postmenopausal osteoporosis; BMD, bone mineral density; VAS, Visual Analog Scale; ODI, Oswestry Disability Index; NA, nonapplicable.

1.00 [0.06];  $P < .001$ ; **FIGURE 1A**). Also, plasma MALAT1 expressions were positively associated with total hip BMD ( $r = 0.475$ ;  $P < .001$ ; **FIGURE 1B**), femoral neck BMD ( $r = 0.453$ ;  $P < .001$ ; **FIGURE 1C**), and L1-4 BMD ( $r = 0.462$ ;  $P < .001$ ; **FIGURE 1D**).

### Plasma MALAT1 Expressions with Genant Grade

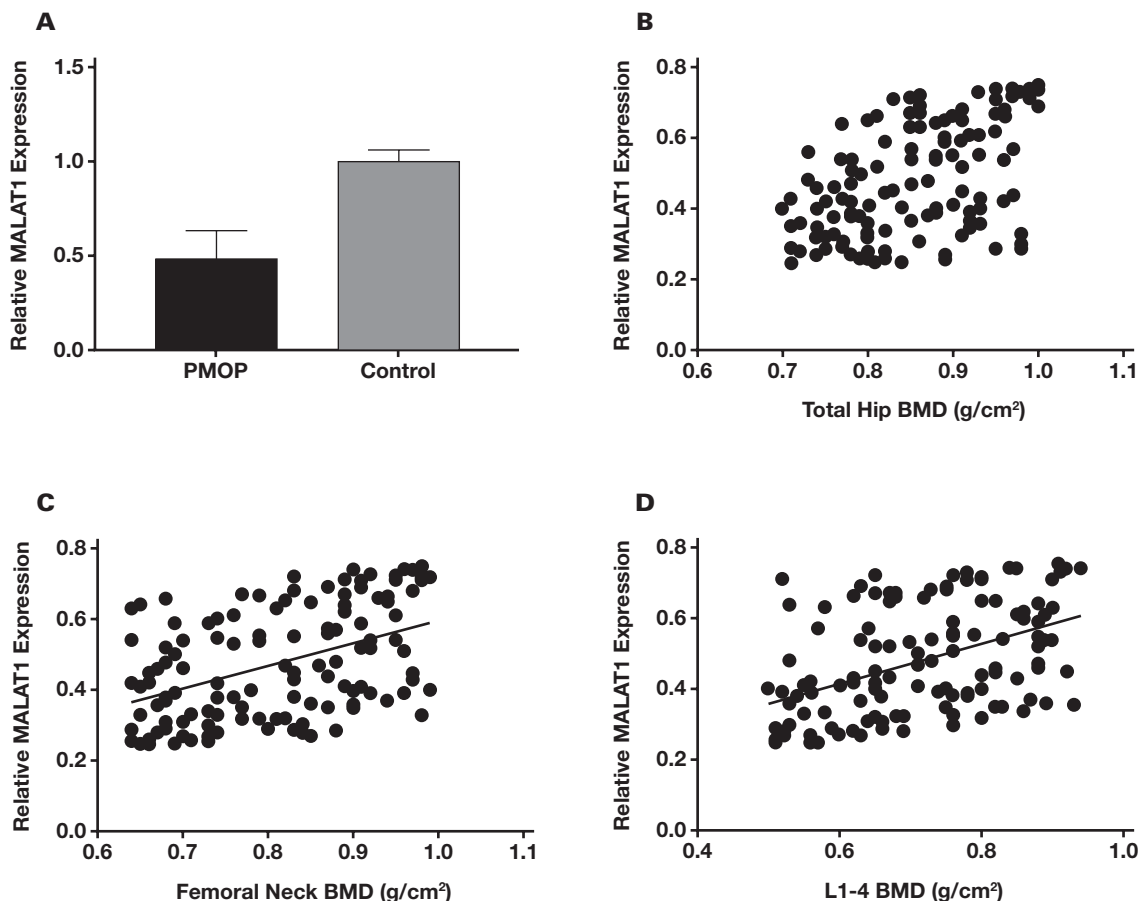
In patients with PMOP, 95 patients experienced vertebral deformity and fracture, and 31 had no fractures. Plasma MALAT1 expressions were significantly lower in patients with vertebral fractures, compared with patients with PMOP who did not have fractures (mean [SD], 0.43 [0.14] vs 0.61 [0.11];  $P < .001$ ; **FIGURE 2A**). According to the Genant grading, there were 34 patients with vertebral fracture and PMOP who had a Genant grade of 1, as well as 30 with grade 2 and 31 with grade 3, respectively. Patients with PMOP and Genant grade 3 vertebral fracture had significantly lower plasma-related MALAT1 expressions, compared with patients with a Genant grade of 2 (mean [SD], 0.36 [0.12] vs 0.42 [0.10];  $P = .02$ ; **FIGURE 2B**). Moreover, plasma-related MALAT1 expressions were significantly lower in patients with vertebral fracture, PMOP, and Genant grade 2, compared with those in the Genant grade 1 group (0.42 [0.10] vs 0.51 [0.15];  $P = .009$ ; **FIGURE 2B**). Plasma-related MALAT1 expressions were negatively associated with Genant grade ( $r = -0.457$ ;  $P < .001$ ; **FIGURE 2C**). The next ROC curve analysis demonstrated that decreased plasma MALAT1 exhibited diagnostic value regarding Genant grade 1 vs grade 2 (AUC = 0.667;  $P = .02$ ; **FIGURE 3A**) and Genant grade 2 vs grade 3 (AUC = 0.706;  $P = .008$ ; **FIGURE 3B**).

### Plasma MALAT1 Expressions with Clinical Severity and Biochemical Indices

To further analyze the potential correlation of MALAT1 with severity of PMOP, we recorded the VAS and ODI indices. We also discovered that plasma MALAT1 expressions were negatively associated with VAS ( $r = -0.466$ ;  $P < .001$ ) and ODI indices ( $r = -0.408$ ;  $P < .001$ ).

Finally, we explored the associations of plasma MALAT1 with bone-formation marker BALP and bone resorption marker NTx. We found that plasma MALAT1 expressions were significantly and positively related to plasma BALP levels ( $r = 0.581$ ;  $P < .001$ ; **FIGURE 4C**). However, plasma MALAT1 expressions were negatively associated with plasma NTx levels ( $r = -0.521$ ;  $P < .001$ ; **FIGURE 4D**).

**FIGURE 1.** Correlation of plasma metastasis-associated lung adenocarcinoma transcript 1 (MALAT1) expressions with bone mineral densities (BMDs). A, Comparison of plasma MALAT1 expressions among the postmenopausal osteoporosis (PMOP) and control groups ( $P < .001$ ). B, Correlation of plasma MALAT1 expressions with total hip BMD ( $r = -0.475$ ;  $P < .001$ ). C, Correlation of plasma MALAT1 expressions with femoral neck BMD ( $r = 0.453$ ;  $P < .001$ ) D, Correlation of plasma MALAT1 expressions with L1-4 BMD ( $r = 0.462$ ;  $P < .001$ ).



## Discussion

In this study, we found that MALAT1 expressions in plasma were significantly reduced in patients with PMOP, compared with healthy controls. Decreased plasma MALAT1 expressions in patients with PMOP were correlated with attenuated BMD, and lower MALAT1 expression was correlated with a greater possibility of vertebral fracture. Moreover, increased MALAT1 expression was inversely associated with pain and functional disability, as evaluated via the VAS and the ODI score. To our knowledge, this study is the first in the literature to demonstrate the association of plasma MALAT1 expressions and the severity of PMOP.

Development of potential biomarkers that are useful for evaluating early diagnosis and treatment response is urgently needed. Besides, gathering biomarkers is minimally invasive; the needed specimen material is easily accessible from patients. Hence, our focus in this study has been to identify potential noninvasive RNA-based circulating biomarkers, for more rapid and accurate diagnosis and monitoring of OP. Because OP is a complex, multifactorial disease, no singular molecular species will be enough to enable the diagnosis or prognosis of OP. Thus, an integrative approach based on several levels of RNA that form a potential biomarker signature, including mRNA and noncoding RNAs, is needed.

A growing number of study reports in the literature have shown that LncRNAs are key players in many physiological and pathological

processes, including osteoporosis. Several LncRNAs are implicated in the development of OP. For example, LncRNA TUG1 is more upregulated in patients with OP than in healthy controls, and overexpression of TUG1 facilitates the proliferation and inhibits the apoptosis of mice osteoclasts. In another study,<sup>26</sup> LncRNA GAS5 overexpression alleviates the development of OP via promoting osteogenic differentiation of MSCs. LncRNA MSC-AS1 promotes osteogenic differentiation and alleviates OP through absorbing miR-140-5p.<sup>27</sup>

As one of the most widely studied LncRNAs, MALAT1 has been implicated in various entities, including neural disorders, cardiovascular diseases, liver diseases, and diabetes. For example, MALAT1 induces inflammasome activation through epigenetic regulation of Nrf2 in Parkinson disease.<sup>28</sup> Abnormal expression of MALAT1 is expressed in endothelial cells or cardiomyocytes in response to hypoxia, high glucose, cytokine, and oxidative stress in cardiovascular diseases.<sup>17</sup> Wang et al<sup>29</sup> discovered that MALAT1 also promotes liver fibrosis by absorbing miR-181a and activating TLR4-NF- $\kappa$ B signaling. MALAT1 also acts as a potential regulator of inflammatory cytokines in diabetic complications.<sup>30</sup> Therefore, targeting MALAT1 in these diseases merits further research in the future.

In the current study, we found that MALAT1 expression in plasma was significantly reduced in patients with PMOP, compared with healthy

**FIGURE 2.** Comparison of plasma metastasis-associated lung adenocarcinoma transcript 1 (MALAT1) expressions among different Genant grades. A, Comparison of relative plasma MALAT1 expressions between vertebral fracture and nonfracture groups ( $P < .001$ ). B, Comparison of relative plasma MALAT1 expressions among different Genant grades. C, Correlation of relative plasma MALAT1 expressions with Genant grade ( $r = -0.457$ ;  $P < .001$ ).

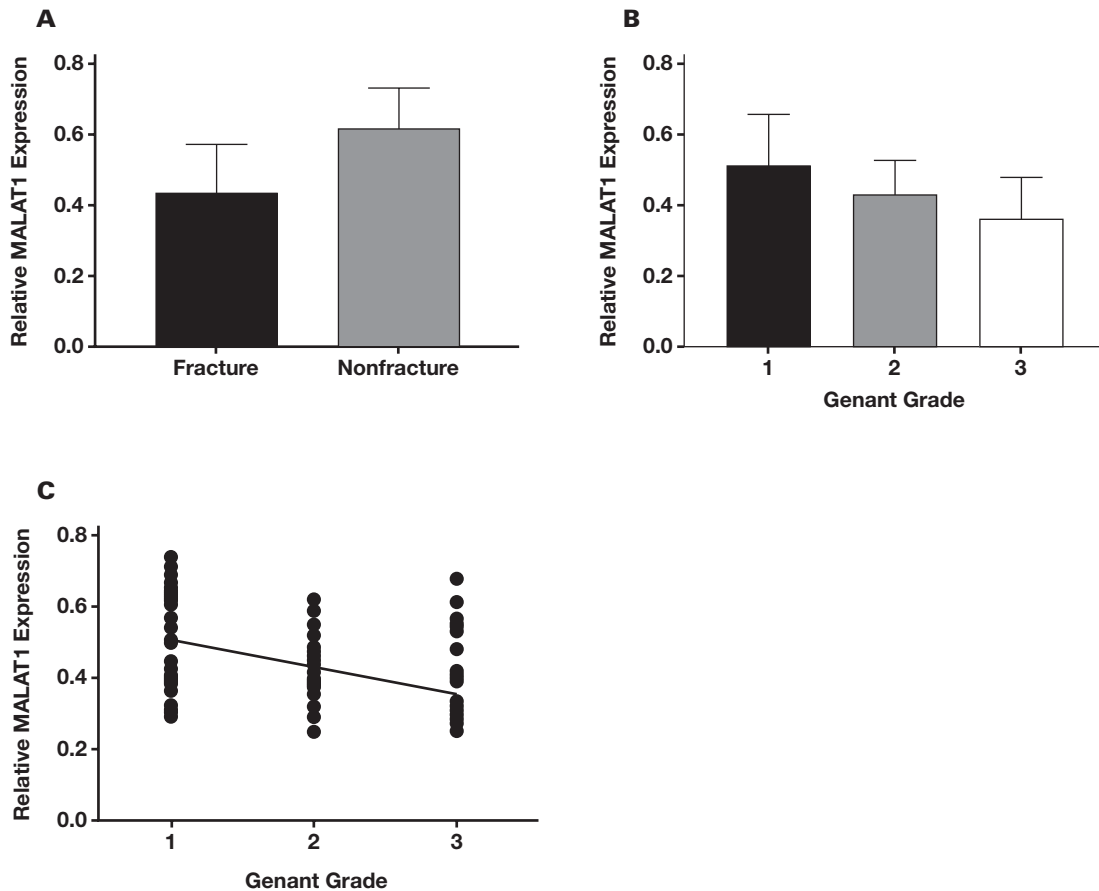
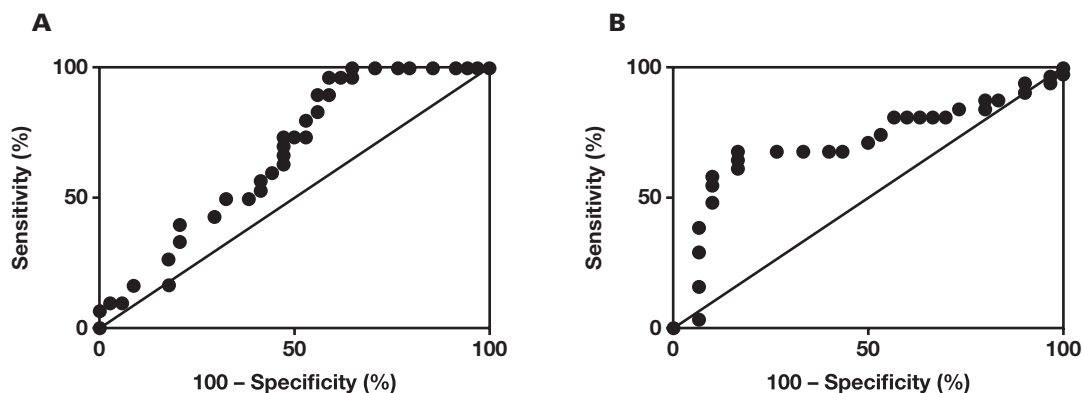


**FIGURE 3.** Diagnostic value of plasma MALAT1 expression by ROC curve analysis. A, Receiver operating characteristic curve analysis of plasma MALAT1 expression with regard to Genant grade 1 vs 2 (area under the curve [AUC] = 0.667;  $P = .02$ ). B, ROC curve analysis of plasma MALAT1 expression with regard to Genant grade 2 vs 3 (AUC = 0.706;  $P = .006$ ).

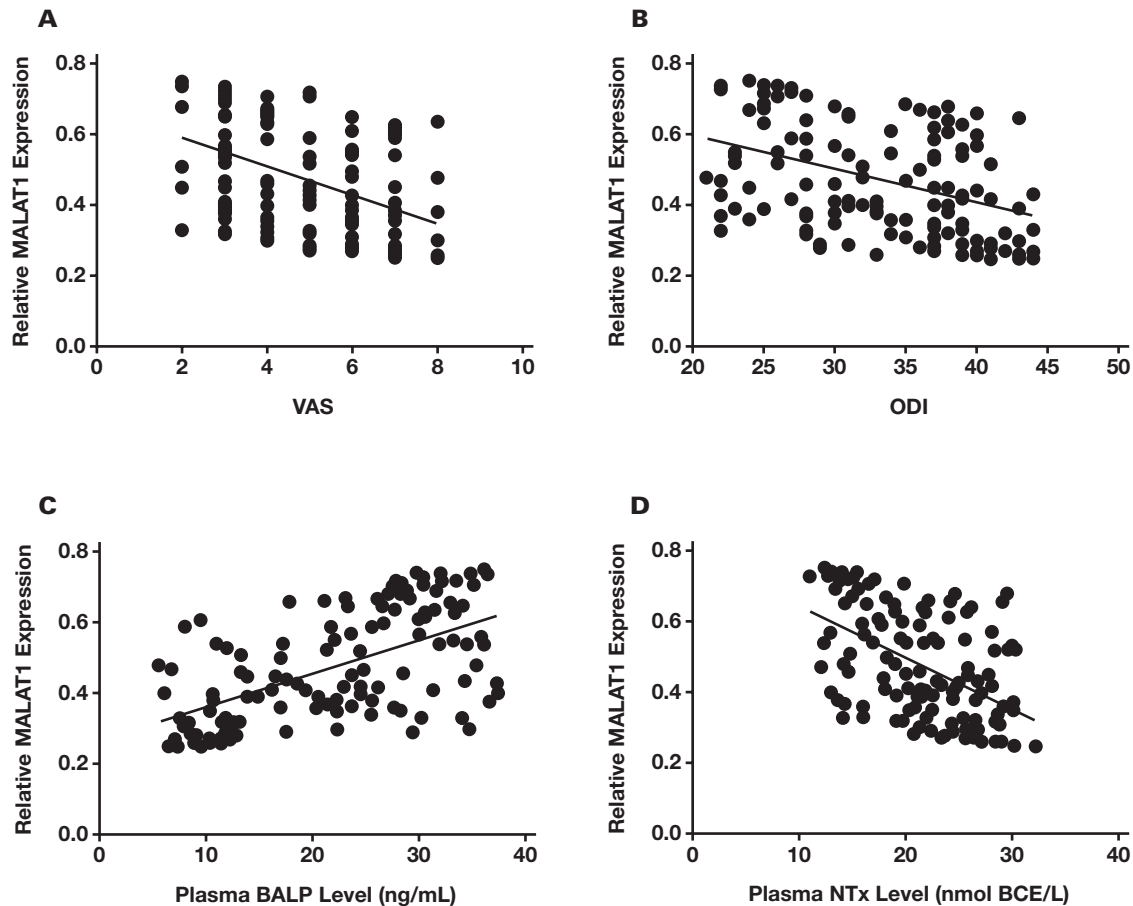


controls. Gao et al<sup>31</sup> found that the expression of MALAT1 was much lower in BMSCs from patients with OP, compared with healthy controls, and MALAT1 may act as a positive regulator in hBMSC osteogenic differentiation.<sup>31</sup> Yang et al<sup>32</sup> showed that BMSC-derived MALAT1 containing exosomes could alleviate OP through the microRNA-34c/SATB2 axis. Yi and colleagues<sup>33</sup> found that MALAT1 could absorb miR-30 to promote

osteoblast differentiation of adipose-derived MSCs by promotion of Runx2 expression.

Based on these aforementioned study reports, we speculate that MALAT1 may act as different types of miRNAs sponges to further regulate some key genes, including Runx2, or to activate different osteogenesis signal paths, such as Wnt/ $\beta$ -catenin and SMAD4 signaling. Mean-

**FIGURE 4.** Correlation of plasma metastasis-associated lung adenocarcinoma transcript 1 (MALAT1) expressions with clinical severity and bone turnover markers. **A.** Correlation of plasma relative MALAT1 expressions with Visual Analog Scale (VAS) score ( $r = -0.466$ ;  $P < .001$ ). **B.** Correlation of relative MALAT1 expressions with the Oswestry Disability Index (ODI;  $r = -0.408$ ;  $P < .001$ ). **C.** Correlation of plasma relative MALAT1 expression with plasma bone-specific alkaline phosphatase (BALP) levels ( $r = 0.581$ ;  $P < .001$ ). **D.** Correlation of relative MALAT1 expression with plasma cross-linked N-telopeptides of type I collagen (NTx) levels ( $r = -0.521$ ;  $P < .001$ ).



while, MALAT1 also targets miRNA-124 that controls osteoclastic activity in inhibiting macrophage differentiation to osteoclasts by regulating IGF2BP1/Wnt/ $\beta$ -catenin signaling, as mentioned previously.<sup>22</sup>

In the current study, we discovered that plasma lncRNA MALAT1 expressions were lower in patients with PMOP, compared with healthy controls. Also, decreased MALAT1 correlates with attenuated BMD, indicating that MALAT1 may serve as a positive regulator for bone volume in BMD. We further detected the relationship of plasma MALAT1 expression with vertebral fracture using Genant grade and performed ROC curve analysis to explore the potential diagnostic value of MALAT1. We found that lower MALAT1 expressions yielded more-severe vertebral deformity and fracture. Plasma MALAT1 expression had decent diagnostic value regarding Genant grade.

Osteoporotic fractures induce acute and chronic nociceptive and neuropathic pain.<sup>27</sup> Central sensitization seems to play a pivotal role in developing and maintaining chronicity of postfracture pain in osteoporosis.<sup>34</sup> Finally, we found that decreased MALAT1 was correlated with more pain and impaired functional ability. Similarly, the findings of a previous study<sup>35</sup> showed that reduced expression of MALAT1 in rat spinal cord tissue contributes to neuropathic pain by increasing neuron excitability, indicating that MALAT1 may participate in osteoporotic neuropathic pain.

Some limitations of this study should be taken into account. First, it was a cross-sectional study performed using a relatively small,

monoethnic sample size in a Chinese hospital. Therefore, a larger sample size and a greater number of ethnicities among cohort individuals are needed to verify our current findings. Second, the causal relationship between MALAT1 and severity of PMOP could not be illustrated. Third, only MALAT1 expression in plasma was detected; investigation of other biomarkers and/or RNAs may reveal more information.

Collectively, our findings demonstrated that plasma MALAT1 expressions are negatively associated with severity of PMOP. Further investigations are needed to study the deeper mechanisms of MALAT1 involvement in the development of PMOP.

### Personal and Professional Conflicts of Interest

None declared.

### REFERENCES

- Coughlan T, Dockery F. Osteoporosis and fracture risk in older people. *Clin Med.* 2014;14(2):187–191.
- Lane JM, Russell L, Khan SN. Osteoporosis. *Clin Orthop Relat Res.* 2000;372:139–150.
- Zhu S, He H, Zhang C, et al. Effects of pulsed electromagnetic fields on postmenopausal osteoporosis. *Bioelectromagnetics.* 2017;38(6):406–424.

4. Armas LAG, Recker RR. Pathophysiology of osteoporosis: new mechanistic insights. *Endocrinol Metab Clin North Am*. 2012;41(3):475–486.
5. Lane NE. Epidemiology, etiology, and diagnosis of osteoporosis. *Am J Obstet Gynecol*. 2006;194(2):S3–S11.
6. Quinn JJ, Chang HY. Unique features of long non-coding RNA biogenesis and function. *Nat Rev Genet*. 2016;17:47–62.
7. Wapinski O, Chang HY. Long noncoding RNAs and human disease. *Trends Cell Biol*. 2011;21(6):354–361.
8. Sarfi M, Abbastabar M, Khalili E. Long noncoding RNAs biomarker-based cancer assessment. *J Cell Physiol*. 2019;234(10):16971–16986.
9. Li Y, Li J, Chen L, Xu L. The roles of long non-coding RNA in osteoporosis. *Curr Stem Cell Res Ther*. 2020;15(7):639–645.
10. Xu Y, Wang S, Tang C, Chen W. Upregulation of long non-coding RNA HIF 1 alpha-antisense 1 induced by transforming growth factor-beta-mediated targeting of sirtuin 1 promotes osteoblastic differentiation of human bone marrow stromal cells. *Mol Med Rep*. 2015;12(5):7233–7238.
11. Zhang R-F, Liu J-W, Yu S-P, et al. LncRNA UCA1 affects osteoblast proliferation and differentiation by regulating BMP-2 expression. *Eur Rev Med Pharmacol Sci*. 2019;23(16):6774–6782.
12. Chang Y, Yu D, Chu W, et al. LncRNA expression profiles and the negative regulation of lncRNA-NOMMUT037835.2 in osteoclastogenesis. *Bone*. 2020;130:115072.
13. Zhang Y, Chen X-F, Li J, et al. lncRNA Neat1 stimulates osteoclastogenesis via sponging miR-7. *J Bone Miner Res*. 2020;35(9):1772–1781.
14. Shen J-J, Zhang C-H, Chen Z-W, et al. LncRNA HOTAIR inhibited osteogenic differentiation of BMSCs by regulating Wnt/ $\beta$ -catenin pathway. *Eur Rev Med Pharmacol Sci*. 2019;23(17):7232–7246.
15. Liu R, Li Z, Song E, et al. Share LncRNA HOTTIP enhances human osteogenic BMSCs differentiation via interaction with WDR5 and activation of Wnt/ $\beta$ -catenin signalling pathway. *Biochem Biophys Res Commun*. 2020;524(4):1037–1043.
16. Gutschner T, Hämmerle M, Diederichs S. MALAT1—a paradigm for long noncoding RNA function in cancer. *J Mol Med*. 2013;91(7):791–801.
17. Yan Y, Song D, Song X, Song C. The role of lncRNA MALAT1 in cardiovascular disease. *IUBMB Life*. 2020;72(3):334–342.
18. Abdulle LE, Hao J-L, Pant OP, et al. MALAT1 as a diagnostic and therapeutic target in diabetes-related complications: a promising long-noncoding RNA. *Int J Med Sci*. 2019;16(4):548–555.
19. Hua L, Zhang X. MALAT1 regulates osteogenic differentiation of human periodontal ligament stem cells through mediating miR-155-5p/ETS1 axis. *Tissue Cell*. 2021;73:101619.
20. Zang L-Y, Yang X-L, Li W-J, Liu G-L. Long noncoding RNA metastasis-associated lung adenocarcinoma transcript 1 promotes the osteoblast differentiation of human bone marrow-derived mesenchymal stem cells by targeting the microRNA-96/Osterix axis [pub ahead of print]. *J Craniofac Surg*. 2021; doi: [10.1097/SCS.0000000000008092](https://doi.org/10.1097/SCS.0000000000008092)
21. Alnajjar FA, Sharma-Oates A, Wijesinghe SN, et al. The expression and function of metastases associated lung adenocarcinoma transcript-1 long non-coding RNA in subchondral bone and osteoblasts from patients with osteoarthritis. *Cells*. 2021;10(4):786.
22. Li X. LncRNA metastasis-associated lung adenocarcinoma transcript-1 promotes osteogenic differentiation of BMSCs and inhibits osteoclastic differentiation of Mo in osteoporosis via the miR-124-3p/IGF2BP1/Wnt/ $\beta$ -catenin axis. *J Tissue Eng Regen Med*. 2021 Dec 27. doi: [10.1002/term.3279](https://doi.org/10.1002/term.3279)
23. Wáng YXJ, Diacinti D, Yu W, et al. Semi-quantitative grading and extended semi-quantitative grading for osteoporotic vertebral deformity: a radiographic image database for education and calibration. *Ann Transl Med*. 2020;8(6):398.
24. Heller GZ, Manuguerra M, Chow R. How to analyze the Visual Analogue Scale: myths, truths and clinical relevance. *Scand J Pain*. 2016;13(1):67–75.
25. Fairbank JCT, Pynsent PB. The Oswestry Disability Index. *Spine*. 2000;25(22):2940–2952.
26. Feng J, Wang J-X, Li C-H. LncRNA GAS5 overexpression alleviates the development of osteoporosis through promoting osteogenic differentiation of MSCs via targeting microRNA-498 to regulate RUNX2. *Eur Rev Med Pharmacol Sci*. 2019;23(18):7757–7765.
27. Zhang N, Hu X, He S, et al. LncRNA MSC-AS1 promotes osteogenic differentiation and alleviates osteoporosis through sponging microRNA-140–5p to upregulate BMP2. *Biochem Biophys Res Commun*. 2019;519(4):790–796.
28. Cai L-J, Tu L, Huang X-M, et al. LncRNA MALAT1 facilitates inflammasome activation via epigenetic suppression of Nrf2 in Parkinson's disease. *Mol Brain*. 2020;13(1):130.
29. Wang Y, Mou Q, Zhu Z, Zhao L, Zhu L. MALAT1 promotes liver fibrosis by sponging miR-181a and activating TLR4-NF- $\kappa$ B signaling. *Int J Mol Med*. 2021;48(6):215.
30. Gordon AD, Biswas S, Feng B, Chakrabarti S. MALAT1: a regulator of inflammatory cytokines in diabetic complications. *Endocrinol Diabetes Metab*. 2018;1(2):e00010.
31. Gao Y, Xiao F, Wang C, et al. Long noncoding RNA MALAT1 promotes osterix expression to regulate osteogenic differentiation by targeting miRNA-143 in human bone marrow-derived mesenchymal stem cells. *J Cell Biochem*. 2018;119(8):6986–6996.
32. Yang X, Yang J, Lei P, Wen T. LncRNA MALAT1 shuttled by bone marrow-derived mesenchymal stem cells-secreted exosomes alleviates osteoporosis through mediating microRNA-34c/SATB2 axis. *Aging*. 2019;11(20):8777–8791.
33. Yi J, Liu D, Xiao J. LncRNA MALAT1 sponges miR-30 to promote osteoblast differentiation of adipose-derived mesenchymal stem cells by promotion of Runx2 expression. *Cell Tissue Res*. 2019;376:113–121.
34. Vellucci R, Terenzi R, Kanis JA, et al. Understanding osteoporotic pain and its pharmacological treatment. *Osteoporos Int*. 2018;29:1477–1491.
35. Meng C, Yang X, Liu Y, et al. Decreased expression of lncRNA Malat1 in rat spinal cord contributes to neuropathic pain by increasing neuron excitability after brachial plexus avulsion. *J Pain Res*. 2019;12:1297–1310.

# Modified Proline Metabolism and Prolidase Enzyme in COVID-19

Merve Ergin Tuncay, MD, PhD,<sup>1,2,\*</sup> Salim Neselioglu, PhD,<sup>1,2</sup> Emra Asfuroglu Kalkan, MD, PhD,<sup>3</sup> Osman Inan, MD, PhD,<sup>3</sup> Meryem Sena Akkus, PhD,<sup>4</sup> Ihsan Ates, MD, PhD,<sup>3</sup> Ozcan Erel, MD, PhD<sup>1,2</sup>

<sup>1</sup>Department of Biochemistry, Yildirim Beyazit University Faculty of Medicine, Ankara, Turkey, <sup>2</sup>Central Biochemistry Laboratory, Ankara City Hospital, Ankara, Turkey, <sup>3</sup>Department of Internal Medicine, Ankara City Hospital, Ankara, Turkey, <sup>4</sup>Central Research Laboratory, Yildirim Beyazit University, Ankara, Turkey; \*To whom correspondence should be addressed. [erginmerve@hotmail.com](mailto:erginmerve@hotmail.com)

**Keywords:** copper, COVID-19, glutamic acid, prolidase, proline, zinc

**Abbreviations:** WHO, World Health Organization; EGFR, epidermal growth factor receptor; HER2, human epidermal growth factor receptor 2; NF- $\kappa$ B, nuclear factor  $\kappa$ B; RT-PCR, real-time polymerase chain reaction; AAS, atomic absorption spectrometer; HCL, hollow cathode lamp; ALB, albumin; TP, total protein; LDH, lactate dehydrogenase; CRP, C-reactive protein; PCT, procalcitonin; ESR, erythrocyte sedimentation rate; WBC, white blood cells; LYM, lymphocytes; ARDS, acute respiratory distress syndrome; CRS, cytokine release syndrome; IL, interleukin.

*Laboratory Medicine* 2022;53:453–458; <https://doi.org/10.1093/labmed/lmac017>

## ABSTRACT

**Objective:** The aim of the study was to evaluate proline metabolism in patients affected by COVID-19.

**Materials and Methods:** This case-control study consisted of 116 patients with COVID-19 and 46 healthy individuals. Tests related to proline metabolism (prolidase, proline, hydroxyproline, glutamic acid, manganese) and copper and zinc tests were analyzed.

**Results:** The levels of proline and hydroxyproline amino acids and the prolidase enzyme were found to be lower and glutamic acid was found to be higher in the COVID-19 group compared to the healthy group ( $P = .012$ ,  $P < .001$ ,  $P < .001$ , and  $P < .001$ , respectively). The copper/zinc ratio was higher in patients with COVID-19 than in healthy individuals ( $P < .001$ ). Significant correlations were found between proline metabolism tests and inflammatory and hemostatic markers commonly used in COVID-19.

**Conclusion:** The proline metabolic pathway was affected in COVID-19. Relationships between proline pathway-related tests and

inflammatory/hemostatic markers supported the roles of proline metabolism in proinflammatory and immune response processes.

The whole world continues to fight the SARS-CoV-2 infection, which causes COVID-19 according to the World Health Organization (WHO). Although many studies have been conducted on SARS-CoV-2 in a relatively short time, information about the pathogenesis of SARS-CoV-2 and the immune response against it in the host cell is still limited.<sup>1,2</sup>

COVID-19 displays a broad array of clinical features, from an asymptomatic infection to a severe lung illness and/or multiorgan failure.<sup>3</sup> The efficiency of the host's immune response has a considerable influence on the clinical presentation.<sup>3</sup> Throughout viral infection, the innate and adaptive immune systems are involved in the immune response.

In addition to their role as building blocks of proteins and polypeptides, some amino acids are substantial regulators of the fundamental metabolic pathways essential for maintenance, growth, reproduction, and immunity in organisms.<sup>4</sup> Proline and hydroxyproline are the most notable amino acids in the collagen structure. The proline metabolic pathway is strategically located in the metabolism. This pathway is connected to the Krebs cycle via glutamate and to the urea cycle via arginine.<sup>5,6</sup> Proline-containing peptides are involved in many biological processes such as proinflammatory response, immune response, and hemostasis.<sup>7</sup>

Prolidase (EC 3.4.13.9) is a dipeptidase that breaks down proline or hydroxyproline-containing aminopeptides and takes a crucial role in the remodeling of the collagen metabolism matrix and cell growth.<sup>8</sup> Prolidase is involved in numerous biological processes at the cellular level.<sup>7</sup> The catalytic function of prolidase provides for the delivery of proline or hydroxyproline, which modulates intracellular signaling. Prolidase is an epidermal growth factor receptor (EGFR) and human epidermal growth factor receptor 2 (HER2) ligand that regulates the signaling pathways depending on these receptors. Under physiological conditions, prolidase stimulates these pathways and can act as an interface in regeneration processes involved with inflammation or tissue damage.<sup>9</sup> Prolidase also participates in the immune response by stimulating the expression and maturation of the interferon  $\alpha/\beta$  receptor. It has also been observed that prolidase activity regulation modulates the biological effects of the nuclear factor  $\kappa$ B (NF- $\kappa$ B) transcription factor, which has a crucial position in the activation of the inflammatory

response.<sup>9,10</sup> Lung inflammation may trigger transcription factors such as NF- $\kappa$ B, which modulates the expression of proinflammatory genes.

Based on the role of proline-containing peptides in many biological processes such as proinflammatory and immune response and hemostasis, and the fact that prolylase enzyme activity is associated with inflammation and tissue damage, our study aimed to investigate proline metabolism in patients affected by COVID-19 and to evaluate molecules/tests related to this metabolism.

## Materials and Methods

### Study Design

The study was carried out with patients who had COVID-19 from March to May 2021 in Ankara City Hospital, which is one of the pandemic hospitals in Turkey. Clinical diagnoses were executed in accordance with WHO guidelines for COVID-19.<sup>11</sup> The study procedure was established in compliance with the Helsinki Declaration and confirmed by the local ethics board (number E1-20-1125). Patients with current clinical symptoms, signs of COVID-19 pneumonia on computed tomography, and/or positive real-time polymerase chain reaction (RT-PCR) test results of oro-nasopharyngeal swab specimens for SARS-CoV-2 were included in the study. All patients were hospitalized. Patients with negative RT-PCR results were not included in the study, nor were patients with an unverified diagnosis of SARS-CoV-2 infection. Healthy volunteers with a negative result from a RT-PCR test for SARS-CoV-2 infection constituted the control group. A detailed history was obtained from all patients. All participants underwent a comprehensive physical examination and routine clinical laboratory tests. In addition to the routine clinical examinations and blood tests, all participants had proline, hydroxyproline, and glutamic acid amino acid tests, along with prolylase enzyme, manganese, copper (Cu), and zinc (Zn) tests.

### Laboratory Analysis

Venous blood specimens were obtained from each participant by venipuncture immediately on admission to the hospital after being confirmed with SARS-CoV-2 infection. Afterward, serum was separated by centrifugation at 1500g for 10 minutes. Proline, hydroxyproline, and glutamic acid amino acid concentrations were analyzed using a liquid chromatography/mass spectrometry instrument (Sciex QTrap 4500, Foster City, CA). The specimens were studied using a ready-to-use commercial kit (Immuchrom, Heppenheim, Germany). Serum prolylase enzyme concentrations were determined with Chinard reagent according to the spectrophotometric assay defined by Myara et al.<sup>12</sup> Measurements were made using a Siemens Advia 1800 chemistry analyzer (Siemens Healthcare, Erlangen, Germany). Serum manganese levels were determined in a graphite furnace containing an atomic absorption spectrometer (AAS; Thermo Fisher Scientific ICE 3000 series, Waltham, MA) using the method proposed by Lisboa et al.<sup>13</sup> Serum Zn levels were measured using a Zn hollow cathode lamp (HCL) at a wavelength of 213.9 nm in an AAS-flame unit (Thermo Fisher Scientific ICE 3000 series).<sup>14</sup> Serum Cu levels were measured using a Cu HCL at a wavelength of 324.8 nm in an AAS-flame unit (Thermo Fisher Scientific ICE 3000 series).<sup>14</sup> Among the routine laboratory tests, albumin (ALB), total protein (TP), lactate dehydrogenase (LDH), iron, and C-reactive protein (CRP) levels were detected using Advia Chemistry-XPT systems (Siemens Healthcare Diagnostics Erlangen, Germany). Procalcitonin (PCT) and ferritin tests were analyzed

using the Atellica IM analyzer (Siemens Healthcare Diagnostics). Complete blood cell counts were measured using the Siemens Advia 2120 Hematology Analyzer (Siemens Healthcare Diagnostics). D-dimer tests were analyzed using the Sysmex CS-5100 coagulation analyzer. Erythrocyte sedimentation rates (ESRs) were analyzed using Vision c (YHLO Biotech, Shenzhen, China).

### Statistical Analysis

Visual (histograms) and statistical methods (Shapiro-Wilk test) were used to determine whether the data were normally distributed. Descriptive analyses were conducted using the mean and standard deviation for normally distributed variables. Because of the normal distribution of the data, independent-sample *t*-tests were performed to determine the significance levels of the investigated tests between the 2 groups. Correlation analyses were performed using Pearson correlation. In all comparative statistical analyses performed, the level of significance was accepted as <5% ( $P < .05$ ). The SPSS software program (version 26; IBM, Armonk, NY) was performed for statistical utilizations.

### Results

A total of 116 patients with confirmed COVID-19 were included in the study. Of these, 45 were female and 71 were male. The control group consisted of 46 healthy individuals (31 female, 15 male). Although the mean age of the patient group was 60.8 years, the mean age of the control group was 37.5 years. The most common symptoms seen in the patients were fever (67.2%), cough (56%), fatigue (46.5%), and shortness of breath (28.4%), respectively. Hypertension (33.6%) and diabetes (26.7%) were the most common comorbidities. The demographic characteristics of the study group are summarized in **TABLE 1**.

The test results regarding the proline metabolism of the participants and other laboratory findings are shown in **TABLE 2**. The prolylase enzyme level was found to be significantly lower in patients with COVID-19 compared to the control group ( $P < .001$ ). The levels of the proline and hydroxyproline amino acids were found to be lower in the COVID-19 group compared to the healthy group, whereas the glutamic acid amino acid was found to be higher in the COVID-19 group ( $P = .012$ ,  $P < .001$ , and  $P < .001$ , respectively). There was no significant difference between the groups in terms of manganese level ( $P = .299$ ). When the study groups were evaluated in terms of Cu and Zn, Cu was found to be significantly higher in patients with COVID-19 compared to the control group ( $P < .001$ ); Zn was significantly lower in the patient group than in healthy individuals ( $P < .001$ ). The Cu/Zn ratio was higher in patients with COVID-19 than in healthy individuals ( $P < .001$ ).

When the study groups were compared in terms of routine laboratory tests, we found that TP and ALB values were lower in the COVID-19 group than in the control group ( $P = .010$  and  $P = .034$ , respectively). Although the serum iron level was lower in the patient group than in healthy individuals ( $P < .001$ ), LDH enzyme activity was found to be higher in individuals with COVID-19 than in the healthy group ( $P < .001$ ). Furthermore, PCT, ferritin, ESR, and CRP levels were all significantly higher in patients with COVID-19 than in healthy control individuals ( $P < .001$  for all). When we considered the hemogram parameters white blood cell (WBC) and lymphocytes (LYM), we found that the WBC value

**TABLE 1. Demographic Characteristics of Patients with COVID-19 and Control Group<sup>a</sup>**

Characteristic	Patients with COVID-19 (n = 116)	Control Group (n = 46)	P Value <sup>b</sup>
Age (y, mean ± SD)	60.8 ± 10.8	37.5 ± 10.1	<.001
Sex (female/male)	45/71	31/15	.001
Signs and symptoms			
Fever	78 (67.2)	...	
Cough	65 (56)	...	
Dyspnea	33 (28.4)	...	
Fatigue	54 (46.5)	...	
Myalgia	17 (14.6)	...	
Nausea/vomiting	10 (8.6)	...	
Headache	6 (5.17)	...	
Diarrhea	5 (4.31)	...	
Comorbidities			
Diabetes	31 (26.7)	...	
Hypertension	39 (33.6)	...	
Coronary artery disease	18 (15.5)	...	
Chronic lung disease	16 (13.7)	...	
Malignancy	5 (4.31)	...	

SD, standard deviation.

<sup>a</sup>Data are expressed as numbers (%).

<sup>b</sup>P < .05, statistically significant.

was higher in patients with COVID-19 compared to those in the control group ( $P = .041$ ), whereas the LYM value was significantly lower in patients with COVID-19 compared to healthy individuals ( $P < .001$ ). D-dimer test results were more than 6 times higher in patients with COVID-19 than in patients in the control group ( $P < .001$ ).

The relationship between the tests related to the proline pathway and other laboratory tests in patients, as seen in **TABLE 3**, was examined. A significant correlation was observed between prolidase enzyme level and LYM ( $r = 0.56$ ,  $P = .001$ ) and Zn ( $r = 0.30$ ,  $P = .029$ ). Statistically significant negative correlations were obtained between prolidase enzyme and ferritin ( $r = -0.24$ ,  $P = .042$ ), D-dimer ( $r = -0.28$ ,  $P = .022$ ), CRP ( $r = -0.22$ ,  $P = .038$ ), Cu ( $r = -0.18$ ,  $P = .025$ ), and Cu/Zn ratio ( $r = -0.21$ ,  $P = .043$ ). Similarly, a significant correlation was observed between proline amino acid and LYM ( $r = 0.46$ ,  $P = .009$ ) and Zn ( $r = 0.28$ ,  $P = .025$ ). Negative correlations were found between proline amino acid and ferritin ( $r = -0.19$ ,  $P = .009$ ), D-dimer ( $r = -0.15$ ,  $P = .162$ ), CRP ( $r = -0.50$ ,  $P = .006$ ), Cu ( $r = -0.47$ ,  $P = .009$ ), and Cu/Zn ratio ( $r = -0.53$ ,  $P = .003$ ). While statistically significant negative correlations were observed between hydroxyproline amino acid and ferritin ( $r = -0.52$ ,  $P = .004$ ), D-dimer ( $r = -0.36$ ,  $P = .040$ ), CRP ( $r = -0.71$ ,  $P < .001$ ), Cu ( $r = -0.35$ ,  $P = .039$ ), and Cu/Zn ratio ( $r = -0.42$ ,  $P = .014$ ); a positive correlation was found between hydroxyproline amino acid and the LYM ( $r = 0.38$ ,  $P = .041$ ) and Zn ( $r = 0.28$ ,  $P = .041$ ). Unlike other amino acids, statistically significant negative correlations were observed between glutamic acid amino acid and LYM ( $r = -0.32$ ,  $P = .041$ ) and Zn ( $r = -0.36$ ,  $P = .012$ ); positive and significant correlations were found between glutamic acid and ferritin ( $r = 0.32$ ,  $P = .037$ ), D-dimer ( $r = 0.39$ ,  $P = .038$ ), CRP ( $r = 0.30$ ,  $P = .03$ ), Cu ( $r = 0.33$ ,  $P = .017$ ), and Cu/Zn ratio ( $r = .40$ ,  $P = .009$ ).

## Discussion

The results of our study not only provided information about the underlying causes of infection and inflammation in patients with COVID-19 whose proline metabolism was investigated but also revealed the relationships between inflammatory and prognostic markers, the prolidase enzyme, and the proline pathway for COVID-19. Our study has the feature of being the first research in this area to examine proline metabolism together with the prolidase enzyme in COVID-19.

SARS-CoV-2 is the cause of the ongoing COVID-19 pandemic. Unlike the majority of coronaviruses, SARS-CoV-2 multiplies in the lower respiratory tract and in severe cases causes the development of acute respiratory distress syndrome (ARDS) and progressive pneumonia, with fatal destruction of the human organism. The general step in the development of ARDS is the elevation of plasma proinflammatory cytokines and rapid lung infiltration by immune cells. Pulmonary fibrosis and cytokine release syndrome (CRS) are often present in the advanced stages of COVID-19. The widespread release of proinflammatory cytokines, combined with sepsis and major multiorgan damage, is responsible for at least 30% of fatal COVID-19 cases.<sup>15</sup> The molecular pathways responsible for the development of SARS-CoV-2-induced fibrosis, ARDS, and CRS are not yet understood.<sup>15,16</sup>

Proline and hydroxyproline are the most important amino acids in the collagen structure. The proline metabolic pathway is strategically located in the metabolism.<sup>17</sup> Proline-containing peptides are involved in many biological processes such as the proinflammatory response, immune response, and hemostasis.<sup>7</sup> Prolidase is a dipeptidase that breaks down proline or hydroxyproline-containing aminopeptides and plays an important role in the remodeling of the collagen metabolism matrix and cell growth.<sup>8</sup> It plays a regulatory role in the function of other biological molecules.<sup>8,9</sup> Prolidase is an EGFR and HER2 ligand that regulates signaling pathways dependent on these receptors such as PI3K/Akt/mTOR, ERK1/2, and JAK/STAT3. Under physiological conditions, prolidase stimulates these pathways and can act as an interface in regeneration processes involved with inflammation or tissue damage.<sup>9</sup> It has also been observed that the regulation of prolidase activity modulates the biological effects of the nuclear factor  $\kappa$ B (NF- $\kappa$ B) transcription factor.<sup>9</sup> The NF- $\kappa$ B is a transcription factor that plays an important role in the activation of the inflammatory response. Lung inflammation can stimulate transcription factors such as NF- $\kappa$ B, which regulate the expression of proinflammatory and antioxidant genes.<sup>18</sup>

The results of our study showed that the prolidase enzyme activity in patients with COVID-19 was statistically significantly lower than in healthy individuals. The role of prolidase in the modulation of NF- $\kappa$ B and its involvement in the signaling pathways in inflammation and tissue damage explain its low level in patients with COVID-19. When the amino acids in the proline pathway were examined, proline and hydroxyproline were found to be lower in patients with COVID-19 compared to the control group, whereas the glutamic acid level was found to be higher. Prolidase deficiency reduces circulating proline levels. The hydroxylation of proline is an important factor in regulating the stability of collagen. In addition, the hydroxylation of proline can prepare functional sites to interact with proteins and receptors. The low level of proline in the circulation may also have led to the decrease in hydroxyproline formed by the hydroxylation of proline.

The regulation of proline is critical to ensure tissue integrity. Mammals can synthesize proline from arginine, glutamine, and glutamate. It is known that glutamine plays a key role in protein metabolism.

**TABLE 2. Proline Metabolism Profile and Other Laboratory Results<sup>a</sup>**

Results	Patients with COVID-19 (n = 116)	Control Group (n = 46)	P Value <sup>b</sup>
Prolidase, U/L	788 ± 86.5	855 ± 52.3	<.001
Proline, μmol/L	196 ± 44.1	228 ± 46.2	.012
Hydroxyproline, μmol/L	4.93 ± 1.14	7.92 ± 1.43	<.001
Glutamic acid, μmol/L	219 ± 63.4	65 ± 13.7	<.001
Mn, mcg/L	2.52 ± 0.73	2.33 ± 1.01	.299
Cu, mcg/dL	138 ± 24.6	113 ± 21.3	<.001
Zn, mcg/dL	136 ± 19.4	159 ± 18.1	<.001
Cu/Zn ratio	1.01 ± 0.22	0.71 ± 0.17	<.001
TP, g/L	61 ± 5.81	68.3 ± 4.59	.010
ALB, g/L	36.4 ± 4.03	40.1 ± 3.6	.034
Iron, μg/dL	27.93 ± 7.89	69.2 ± 10.7	<.001
LDH, U/L	301.7 ± 42.63	198 ± 20.6	<.001
PCT, μg/L	0.066 ± 0.022	0.03 ± 0.01	<.001
Ferritin, μg/L	389 ± 41.55	48 ± 9.6	<.001
D-dimer, mg/L	1.38 ± 0.3	0.21 ± 0.07	<.001
WBC, ×10 <sup>9</sup> /L	7.01 ± 1.8	5.99 ± 1.23	.041
LYM, ×10 <sup>9</sup> /L	1.18 ± 0.25	1.93 ± 0.46	<.001
ESR, mm/h	43.09 ± 9.9	9.2 ± 2.8	<.001
CRP, g/L	0.042 ± 0.015	0.002 ± 0.0006	<.001

ALB, albumin; CRP, C-reactive protein; Cu, copper; ESR, erythrocyte sedimentation rate; LDH, lactate dehydrogenase; LYM, lymphocytes; Mn, manganese; PCT, procalcitonin; TP, total protein; WBC, white blood cells; Zn, zinc.

<sup>a</sup>Values are given as mean ± standard deviation.

<sup>b</sup>P < .05, statistically significant.

**TABLE 3. Relationship Between Proline Metabolism Tests and Other Laboratory Tests**

	LYM	Ferritin	D-dimer	CRP	Cu	Zn	Cu/Zn
Prolidase	r = 0.56 P = .001	r = -0.24 P = .042	r = -0.28 P = .022	r = -0.22 P = .038	r = -0.18 P = .25	r = 0.30 P = .029	r = -0.21 P = .043
Proline	r = 0.46 P = .009	r = -0.19 P = .009	r = -0.15 P = .162	r = -0.50 P = .006	r = -0.47 P = .009	r = 0.28 P = .025	r = -0.53 P = .003
Hydroxyproline	r = 0.38 P = .041	r = -0.52 P = .004	r = -0.36 P = .040	r = -0.71 P < .001	r = -0.35 P = .039	r = 0.28 P = .042	r = -0.42 P = .014
Glutamic acid	r = -0.32 P = .041	r = 0.32 P = .037	r = 0.39 P = .038	r = 0.30 P = .03	r = 0.33 P = .017	r = -0.36 P = .012	r = 0.40 P = .009

CRP, C-reactive protein; Cu, copper; LYM, lymphocyte; Zn, Zinc.

Therefore, glutamine is considered a regulatory amino acid of proline availability for collagen biosynthesis. Glutamic acid levels in patients with COVID-19 in our study may have been elevated to compensate for low proline levels and to provide a proline source. There was no difference between the patients with COVID-19 and the control group in terms of manganese levels. Manganese is located in the active site of prolidase. However, there are other divalent cations in the active site of prolidase. In this study, it was determined that manganese is not associated with low levels of the prolidase enzyme.

In our study, increased CRP, PCT, ESR, and ferritin, markers of inflammation, were found in patients with COVID-19 compared with healthy control individuals. Significant correlations were found between proline, hydroxyproline, glutamic acid amino acids, and the prolidase enzyme, which play a role in proline metabolism, with LYM, ferritin, D-dimer, and CRP parameters used in the diagnosis, treatment, and follow-up of the prognosis of COVID-19. The important role of prolidase in

the modulation of NF-κB and signaling pathways in inflammation and tissue damage explains the negative correlation between prolidase levels and inflammatory markers in patients with COVID-19. These data support the relationship of the proline pathway with inflammation, hemostasis, and immune response in COVID-19.

There are reports of the clinical relevance of prolidase in disorders of collagen metabolism,<sup>19-21</sup> metabolic disorders,<sup>22,23</sup> and oncological disorders.<sup>24,25</sup> In a study on the influenza A virus, it was shown that prolidase is a cellular factor required by the influenza virus for successful entry into target cells.<sup>26</sup> In addition, it has been shown that prolidase is required by the influenza virus in the early period of infection, and in the absence of prolidase, early viral events change, which leads to a decrease in the amount of virus in the early and late endosomes and fewer fusion events.<sup>26</sup>

In a metabolomics study in patients with COVID-19, in contrast to non-COVID-19 specimens, COVID-19 specimens showed reduced

proline in serum.<sup>27</sup> In this study, the researchers suggested that lactate and L-proline metabolites may help reduce the risk of SARS-CoV-2 infection because proteomic analysis of host cells infected with SARS-CoV-2 revealed that the inhibition of central carbon metabolism prevents viral replication.<sup>27</sup> Although the low proline levels in the earlier study are in line with the results of our study, the analysis of other metabolites in the proline pathway is an advantage of our study. In another metabolomics study, patients with COVID-19 were reported to exhibit low amino acid levels.<sup>28</sup> In addition, the study emphasized that arginine/proline/citrulline metabolism is an important pathway affected by COVID-19.<sup>28</sup> In the study, the low proline level in patients with COVID-19 was parallel to that reported in our study, whereas glutamine levels were found to be lower in patients with COVID-19 compared to the control group, unlike in our study.

Our results showed that iron levels were lower in patients with SARS-CoV-2 infection than in the control group. Because iron is a crucial factor in various processes involving DNA synthesis and adenosine triphosphate production, viruses principally count on iron to replicate in host cells.<sup>29</sup> The cytokines participating in the “cytokine storm” in COVID-19 are potent modulators of iron metabolism. For instance, interleukin (IL)-6 plays a role in many processes ranging from B-cell proliferation to hepcidin synthesis in the liver.<sup>30,31</sup> Hepcidin is the chief regulator of iron homeostasis. During infection or inflammatory conditions, hepcidin levels rise and limit the availability of iron in the plasma.<sup>32</sup> The emerging hypoferrremia is an indivisible part of the host defense system.<sup>32</sup> Moreover, certain cytokines such as IL-1 and tumor necrosis factor enhance the generation of ferritin, which is the iron storage protein. As a result, more iron is kept mostly in the reticuloendothelial system, which processes most of the iron recycled from deformed red blood cells. This hypoferrremia results in the impairment of iron uptake in many organs.<sup>30-33</sup>

Trace elements have an important place in maintaining a healthy body. For example, Zn is an essential trace element in the growth and maintenance of immune cells. It inhibits the RNA polymerase required to replicate RNA viruses such as those containing coronavirus.<sup>34</sup> Furthermore, Cu is an important micronutrient for viral infections for both pathogens and hosts. It has been shown to play an important role in immunity through its involvement in the production and differentiation of immune cells such as T-cell proliferation and natural killer activity in the host.<sup>34</sup> The Cu/Zn ratio is clinically more important than the concentration of these metals separately.<sup>35</sup> Previous studies have shown that Cu and Zn deficiencies predispose to infections, whereas systemic inflammation and infections result in a decreased serum Zn concentration during the acute-phase response because of the redistribution of serum Zn to the liver and other tissues.<sup>35-37</sup> In addition, acute infections cause an increased serum Cu concentration. Both responses end in an elevated serum Cu/Zn ratio.

The Cu/Zn ratio has been found to be high as an acute-phase response in several infectious diseases.<sup>35,37</sup> Researchers have extensively reviewed the relationship between the Cu/Zn ratio and health status.<sup>36</sup> Oxidative stress and inflammation impact the Cu/Zn ratio, and the Cu/Zn ratio modulates immune defense and stress response.<sup>36,37</sup> In our study, Cu levels and the Cu/Zn ratio were higher in patients with COVID-19 compared to the control group, and Zn levels were lower. In addition, we found significant correlations between tests of proline metabolism and Cu, Zn, and the Cu/Zn ratio. These results provide information that strengthens the relationship between proline metabolism and inflammation and immune response in COVID-19.

As in our study, Fromonot et al<sup>38</sup> found Zn levels lower in patients with COVID-19 than in patients without COVID-19. They also showed the association of low Zn with lymphopenia and inflammation in the early phase of COVID-19.<sup>38</sup> In another study, Skalny et al<sup>39</sup> found a high Cu level, low Zn level, and higher Cu/Zn ratio in patients with COVID-19 compared to healthy control individuals. In addition, as the severity of the disease increased, the Zn level gradually decreased and the Cu and Cu/Zn ratio gradually increased.<sup>39</sup> These data support the Cu, Zn, and Cu/Zn ratios we found in our study.

This study has some limitations. One of these is the age difference between the patient and control groups. The mean age of the patient group was higher than the mean age of the control group. When conducting a scientific study, it is often a challenge to create a control group of healthy individuals older than age 60 years. Another limitation is the sex distribution in the patient and control groups. We do not have any information on the effect of sex on amino acid levels.

## Conclusion

In conclusion, changes in proline metabolism have been observed in patients with COVID-19. Low levels of the proline and hydroxyproline amino acids and high glutamic acid amino acid levels suggest that they are associated with inflammation, the release of proinflammatory cytokines, and immune response in COVID-19. The relationship between proline metabolism tests and commonly used inflammatory and hemostatic markers in COVID-19 supports this hypothesis. In addition, proline pathway metabolites have associations with the Cu/Zn ratio, which is recognized to modulate immune response.

## Funding

This study was supported by the Yıldırım Beyazıt University Scientific Research Projects Coordination Unit (project number TKB-2020-2147).

## REFERENCES

1. Wu D, Wu T, Liu Q, et al. The SARS-CoV-2 outbreak: what we know. *Int J Infect Dis.* 2020;94:44–48.
2. Ergin Tuncay M, Gemcioglu E, Kayaaslan B, et al. A notable key for estimating the severity of COVID-19: 25-hydroxyvitamin D status. *Turk J Biochem.* 2021;46(2):167–172.
3. Tay MZ, Poh CM, Rénia L, et al. The trinity of COVID-19: immunity, inflammation, and intervention. *Nat Rev Immunol.* 2020;20:363–374.
4. Li P, Yin YL, Li D, et al. Amino acids and immune function. *Br J Nutr.* 2007;98(2):237–252.
5. Phang JM, Pandhare J, Liu Y. The metabolism of proline as microenvironmental stress substrate. *J Nutr.* 2008;138(10):2008S–2015S.
6. Malcolm W. Glutamine metabolism and function in relation to proline synthesis and the safety of glutamine and proline supplementation. *J Nutr.* 2008;138(10):2003S–2007S.
7. Misiura M, Miltky W. Proline-containing peptides—new insight and implications: a review. *Biofactors.* 2019;45(6):857–866.
8. Kitchener R, Grunden AM. Prolidase function in proline metabolism and its medical and biotechnological applications. *J Appl Microbiol.* 2012;113(2):233–247.

9. Misiura M, Miltyk W. Current understanding of the emerging role of prolidase in cellular metabolism. *Int J Mol Sci*. 2020;21(16):5906.
10. Surazynski A, Miltyk W, Palka J, et al. Prolidase-dependent regulation of collagen biosynthesis. *Amino Acids*. 2008;35:731–738.
11. World Health Organization. COVID-19 clinical management: living guidance, 25 January 2021. <https://apps.who.int/iris/handle/10665/338882>. Accessed February 28, 2022.
12. Myara I, Myara A, Mangeot M, et al. Plasma prolidase activity: a possible index of collagen catabolism in chronic liver disease. *Clin Chem*. 1984;30:211–215.
13. Lisboa TP, Flores LS, Correa CC, et al. Evaluation of chromium and manganese levels in sports supplements using graphite furnace atomic absorption spectrometry. *Rev Nutr*. 2020;33:e190141.
14. Parker MM, Humoller FL, Mahler DJ. Determination of copper and zinc in biological material. *Clin Chem*. 1967;13(1):40–48.
15. Petersen E, Koopmans M, Go U, et al. Comparing SARS-CoV-2 with SARS-CoV and influenza pandemics. *Lancet Infect Dis*. 2020;20:e238–e244.
16. Vagapova ER, Lebedev TD, Prassolov VS. Viral fibrotic scoring and drug screen based on MAPK activity uncovers EGFR as a key regulator of COVID-19 fibrosis. *Sci Rep*. 2021;11(1):11234.
17. Vettore LA, Westbrook RL, Tennant DA. Proline metabolism and redox; maintaining a balance in health and disease. *Amino Acids*. 2021;53(12):1779–1788.
18. Erel O, Neselioğlu S, Ergin Tuncay M, et al. A sensitive indicator for the severity of COVID-19: thiol. *Turk J Med Sci*. 2021;51(3):921–928.
19. Bhatnager R, Nanda S, Dang AS. Plasma prolidase levels as a biomarker for polycystic ovary syndrome. *Biomark Med*. 2018;12(6):597–606.
20. Rabus M, Demirbag R, Yildiz A, et al. Association of prolidase activity, oxidative parameters, and presence of atrial fibrillation in patients with mitral stenosis. *Arch Med Res*. 2008;39(5):519–524.
21. Ceylan MF, Tural Hesapcioglu S, Kasak M, et al. Increased prolidase activity and high blood monocyte counts in pediatric bipolar disorder. *Psychiatry Res*. 2019;271:360–364.
22. Dastani Z, Hivert MF, Timpson N, et al. Novel loci for adiponectin levels and their influence on type 2 diabetes and metabolic traits: a multi-ethnic meta-analysis of 45,891 individuals. *PLoS Genet*. 2012;8(3):e1002607.
23. Sabuncu T, Boduroglu O, Eren MA, et al. The value of serum prolidase activity in progression of microalbuminuria in patients with type 2 diabetes mellitus. *J Clin Lab Anal*. 2016;30(5):557–562.
24. Karna E, Surazynski A, Palka J. Collagen metabolism disturbances are accompanied by an increase in prolidase activity in lung carcinoma planoepitheliale. *Int J Exp Pathol*. 2000;81(5):341–347.
25. Ario DT, Camuzcuoglu H, Toy H, et al. Serum prolidase activity and oxidative status in patients with stage I endometrial cancer. *Int J Gynecol Cancer*. 2009;19(7):1244–1247.
26. Pohl MO, Edinger TO, Stertz S. Prolidase is required for early trafficking events during influenza A virus entry. *J Virol*. 2014;88(19):11271–11283.
27. Liu J, Liu S, Zhang Z, et al. Association between the nasopharyngeal microbiome and metabolome in patients with COVID-19. *Synth Syst Biotechnol*. 2021;6(3):135–143.
28. D'Alessandro A, Thomas T, Akpan I, et al. Biological and clinical factors contributing to the metabolic heterogeneity of hospitalized patients with and without COVID-19. *Cells*. 2021;10(9):2293.
29. Drakesmith H, Prentice A. Viral infection and iron metabolism. *Nat Rev Microbiol*. 2008;6(7):541–552.
30. Girelli S, Marchi G, Busti F, et al. Iron metabolism in infections: focus on COVID-19. *Semin Hematol*. 2021;58(3):182–187.
31. Hippchen T, Altamura S, Muckenthaler MU, et al. Hypoferremia is associated with increased hospitalization and oxygen demand in COVID-19 patients. 2020;4(6):e492.
32. Lee P, Peng H, Gelbart T, et al. Regulation of hepcidin transcription by interleukin-1 and interleukin-6. *Proc Natl Acad Sci USA*. 2005;102(6):1906–1910.
33. Yanling LV, Liangkai C, Xiaoling L, et al. Association between iron status and the risk of adverse outcomes in COVID-19. *Clin Nutr*. 2021;40(5):3462–3469.
34. Taheri S, Asadi S, Nilashi M, et al. A literature review on beneficial role of vitamins and trace elements: evidence from published clinical studies. *J Trace Elem Med Biol*. 2021;67:126789.
35. Laine JT, Tuomainen T-P, Salonen JT, et al. Serum copper-to-zinc-ratio and risk of incident infection in men: the Kuopio Ischaemic Heart Disease Risk Factor Study. *Eur J Epidemiol*. 2020;35(12):1149–1156.
36. Malavolta M, Piacenza F, Basso A, et al. Serum copper to zinc ratio: relationship with aging and health status. *Mech Ageing Dev*. 2015;151:93–100.
37. Chih-Hung G, Pei-Chung C, Maw-Sheng Y, et al. Cu/Zn ratios are associated with nutritional status, oxidative stress, inflammation, and immune abnormalities in patients on peritoneal dialysis. *Clin Biochem*. 2011;44(4):275–280.
38. Fromonot J, Gette M, Ben Lassoued A, et al. Hypozincemia in the early stage of COVID-19 is associated with an increased risk of severe COVID-19. *Clin Nutr*. Published online May 4, 2021. doi:10.1016/j.clnu.2021.04.042.
39. Skalny AV, Timashev PS, Aschner M, et al. Serum zinc, copper, and other biometals are associated with COVID-19 severity markers. *Metabolites*. 2021;11(4):244.

# Multiplex Microsphere PCR (mmPCR) Allows Simultaneous Gram Typing, Detection of Fungal DNA, and Antibiotic Resistance Genes

Daniel J. Browne, BSc,<sup>1,2,\*</sup> Fang Liang, PhD,<sup>1</sup> Kate H. Gartlan, PhD,<sup>1,3</sup> Patrick N.A. Harris, PhD,<sup>4,\*</sup> Geoffrey R. Hill, MD, FRACP, FRCPA,<sup>1,5</sup> Simon R. Corrie, PhD,<sup>6</sup> Kate A. Markey, MB, BS, MCLinRes, PhD, FRACP<sup>1,3,5,7,\*</sup>

<sup>1</sup>Division of Immunology, QIMR Berghofer Medical Research Institute, Brisbane, Australia, <sup>2</sup>Centre for Molecular Therapeutics, Australian Institute of Tropical Health and Medicine, James Cook University, Cairns, Australia, <sup>3</sup>School of Medicine, University of Queensland, Brisbane, Australia, <sup>4</sup>Faculty of Medicine, UQ Centre for Clinical Research, University of Queensland, Royal Brisbane and Women's Hospital, Brisbane, Australia, <sup>5</sup>Division of Hematopoietic Transplantation, Fred Hutchinson Cancer Research Center, Seattle, WA, USA, <sup>6</sup>Department of Chemical Engineering, ARC Centre of Excellence in Convergent Bio-Nano Science and Technology, Monash and QLD Nodes, Monash University, Clayton, Australia, <sup>7</sup>Memorial Sloan-Kettering Cancer Center, New York, NY, USA; \*To whom correspondence should be addressed. [kmarkey@fredhutch.org](mailto:kmarkey@fredhutch.org)

**Keywords:** multiplex PCR, flow cytometry, MagPlex-TAG microspheres, antibiotic resistance testing, Gram typing, fungi, analytical specificity

**Abbreviations:** mmPCR, multiplex microsphere polymerase chain reaction; PCR, polymerase chain reaction; NAAT, nucleic acid amplification test; GOI, genes of interest; gDNA, genomic DNA; qPCR, quantitative polymerase chain reaction; NTC, no-template negative control; Ct, cycle threshold; S/N, signal-to-noise ratio; PPV, positive predictive value; NPV, negative predictive value.

*Laboratory Medicine* 2022;53:459–464; <https://doi.org/10.1093/labmed/lmac023>

## ABSTRACT

**Objective:** To show the high analytical specificity of our multiplex microsphere polymerase chain reaction (mmPCR) method, which offers the simultaneous detection of both general (eg, Gram type) and specific (eg, *Pseudomonas* species) clinically relevant genetic targets in a single modular multiplex reaction.

**Materials and Methods:** Isolated gDNA of 16S/rRNA Sanger-sequenced and Basic Local Alignment Tool-identified bacterial and fungal isolates were selectively amplified in a custom 10-plex Luminex MagPlex-TAG microsphere-based mmPCR assay. The signal/noise ratio for each reaction was calculated from flow cytometry standard data collected on a BD LSR Fortessa II flow cytometer. Data were normalized to the no-template negative control and the signal

maximum. The analytical specificity of the assay was compared to single-plex SYBR chemistry quantitative PCR.

**Results:** Both general and specific primer sets were functional in the 10-plex mmPCR. The general Gram typing and pan-fungal primers correctly identified all bacterial and fungal isolates, respectively. The species-specific and antibiotic resistance-specific primers correctly identified the species- and resistance-carrying isolates, respectively. Low-level cross-reactive signals were present in some reactions with high signal/noise primer ratios.

**Conclusion:** We found that mmPCR can simultaneously detect specific and general clinically relevant genetic targets in multiplex. These results serve as a proof-of-concept advance that highlights the potential of high multiplex mmPCR diagnostics in clinical practice. Further development of specimen-specific DNA extraction techniques is required for sensitivity testing.

Accurate and timely diagnosis of pathogenic microorganisms can be challenging because a wide variety of pathogens can cause clinically indistinguishable pathologies.<sup>1</sup> Polymerase chain reaction (PCR)-based nucleic acid amplification tests (NAATs) offer rapid, minimally invasive, sensitive, and specific molecular diagnostics for infectious microorganisms.<sup>2</sup> However, these techniques can be limited by relatively long turnaround times, a reliance upon organism culture, predefined organism panels, a lack of parallel antimicrobial susceptibility testing, and limited capacity for modular addition of further genes of interest (GOI).<sup>1,3,4</sup> The ideal NAAT for use in clinical practice will have a high-multiplex capacity to identify established specific genotypes yet remain amenable to the incorporation of emerging resistance or species-specific genes in a flexible, modular fashion.

Multiplex microsphere PCR (mmPCR) is a technique that uses Cy3-labeled oligonucleotides as fluorescent reporters of primer consumption, which in turn allows the quantification of the number of copies of a given template in the specimen. When bound to carboxylated polystyrene Luminex MagPlex-TAG microspheres that are dyed into spectrally distinct sets, fluorescence intensity can be individually quantified using

© The Author(s) 2022. Published by Oxford University Press on behalf of American Society for Clinical Pathology.

This is an Open Access article distributed under the terms of the Creative Commons Attribution License (<https://creativecommons.org/licenses/by/4.0/>), which permits unrestricted reuse, distribution, and reproduction in any medium, provided the original work is properly cited.

flow cytometry.<sup>5</sup> Studies have shown that mmPCR advantageously allows high multiplex capacity (ie, theoretically capable of detecting up to 150 separate GOI in a single reaction) while maintaining the high specificity and sensitivity of PCR-based NAATs.<sup>6</sup> A previously published duplex-mmPCR assay has recently been developed for rapid (ie, <3 hours), culture-free, bacterial Gram typing.<sup>7</sup> In this study, we provide a significant extension to the functionality of this assay by broadening the polymicrobial detection capacity to include pan-fungal primers, specific primers targeting resistance-conferring GOIs, and species-specific primers (Supplemental Graphic Abstract). We show the high analytical specificity of our 10-plex mmPCR assay, which can simultaneously provide diagnostic information regarding Gram type, resistance genes, and specific clinically relevant pathogens.<sup>8</sup>

## Materials and Methods

### Oligonucleotide Design

Previously published primers were used to distinguish Gram type, fungi,  $\beta$ -lactamase resistance, and the specific species *Achromobacter xylosoxidans*, *Burkholderia cepacia*, and *Pseudomonas aeruginosa* (Supplemental Table 1). Primers targeting vancomycin type A, vancomycin type B, and methicillin resistance were designed to target the *Tn1546* genetic element, *vanB* mobile cluster, and *mecA* gene, respectively, utilizing the Primer3 software package as previously published.<sup>9</sup> To facilitate mmPCR, additional nucleotides were incorporated as previously described,<sup>5</sup> with MagPlex-TAG microspheres (Luminex) conjugated to DNA tags. Primers and labeled oligonucleotides were supplied as high-performance liquid chromatography grade (Integrated DNA Technologies).

### Bacterial and Fungal Genomic DNA

Thirteen bacterial and 3 fungal strains with characterized resistance phenotypes (Pathology Queensland) were provided from The University of Queensland and Pathology Queensland (FIGURE 1). Genomic DNA (gDNA) was extracted with a Prepito-D and Blood-600 extraction kit (Chemagen), from cultured viable cells homogenized with a Precellys 24-tissue homogenizer (Bertin Instruments) in L-type pathogen lysis tubes (Qiagen). The concentration of gDNA (genome copies/ $\mu$ L) was quantified with a Nanodrop ND-2000 spectrophotometer (Thermo Fisher Scientific). The identity of bacterial isolates was confirmed with Sanger sequencing (Australian Genomics Research Facility) and Basic Local Alignment Tool identification of PCR amplicons of the intervening variable 16S/rRNA regions, as previously published.<sup>10</sup> The presence of antibiotic resistance genes, Gram status, and fungal presence was confirmed via real-time quantitative PCR (qPCR) as previously described.<sup>7</sup> Briefly, SYBR Green (Applied Biosystems) qPCR was performed using a ViiA 7 quantitative thermocycler (Applied Biosystems), using standard cycling conditions (ie, 95°C for 10 minutes, followed by 40 cycles each of 95°C for 15 seconds and 60°C for 60 seconds, followed by a standard melt curve) with primers at 100 nmol/L. The template for amplification was 1  $\mu$ L gDNA ( $10^5$  genome copies/ $\mu$ L) or no-template negative control (NTC) RT-PCR Grade Water (Life Technologies). A cycle threshold (Ct) of 35 to 30 was considered weakly positive, and a Ct <30 was considered positive. In addition, for qPCR analytical specificity testing, we tested Ct <40 as positive. All reactions were followed by a melt curve specificity test.

Data were collected using QuantStudio V1.1 (Thermo Fisher Scientific) software.

### Microsphere Assay

The mmPCR assay was performed using a 2-step process as previously published,<sup>7</sup> with the addition of (8 $\times$ ) additional primers (Supplemental Table 1). Briefly, the TaqMan Universal Master Mix (Applied Biosystems) and all forward and reverse primers were employed to selectively amplify gDNA under standard conditions (50°C for 2 minutes, 95°C for 10 minutes, followed by 45 cycles of 95°C for 30 seconds, 60°C for 30 seconds, and 72°C for 60 seconds), with a final extension step at 72°C for 5 minutes on a T100 thermocycler (BioRad). The Gram-negative, fungi, and  $\beta$ -lactamase primers were at 80 nmol/L; the Gram-positive, species-specific, and vancomycin B and *mecA* resistance primers were at 40 nmol/L; and the vancomycin A resistance primers were at a 20 nmol/L concentration, respectively (Supplemental Table 1). An additional 4 mmol/L MgCl<sub>2</sub> and 275  $\mu$ mol/L deoxyribonucleotide triphosphate mix (Life Technologies) was added to the PCR, and the template for amplification was 1  $\mu$ L gDNA ( $10^5$  genome copies/ $\mu$ L) or NTC RT-PCR Grade Water (Life Technologies). After PCR, a second hybridization stage was performed. Microspheres at a ratio of 62.5 microspheres to 1 nmol/L primer pair and Cy3-labeled oligonucleotides at a ratio of 1 nmol/L to 1 nmol/L primer pair were added and then incubated at 37°C for 30 minutes. Microspheres were analyzed on a BD LSR Fortessa II (BD Biosciences) using BD FACSDiva Software (version 8.0.1, BD Biosciences).<sup>11</sup>

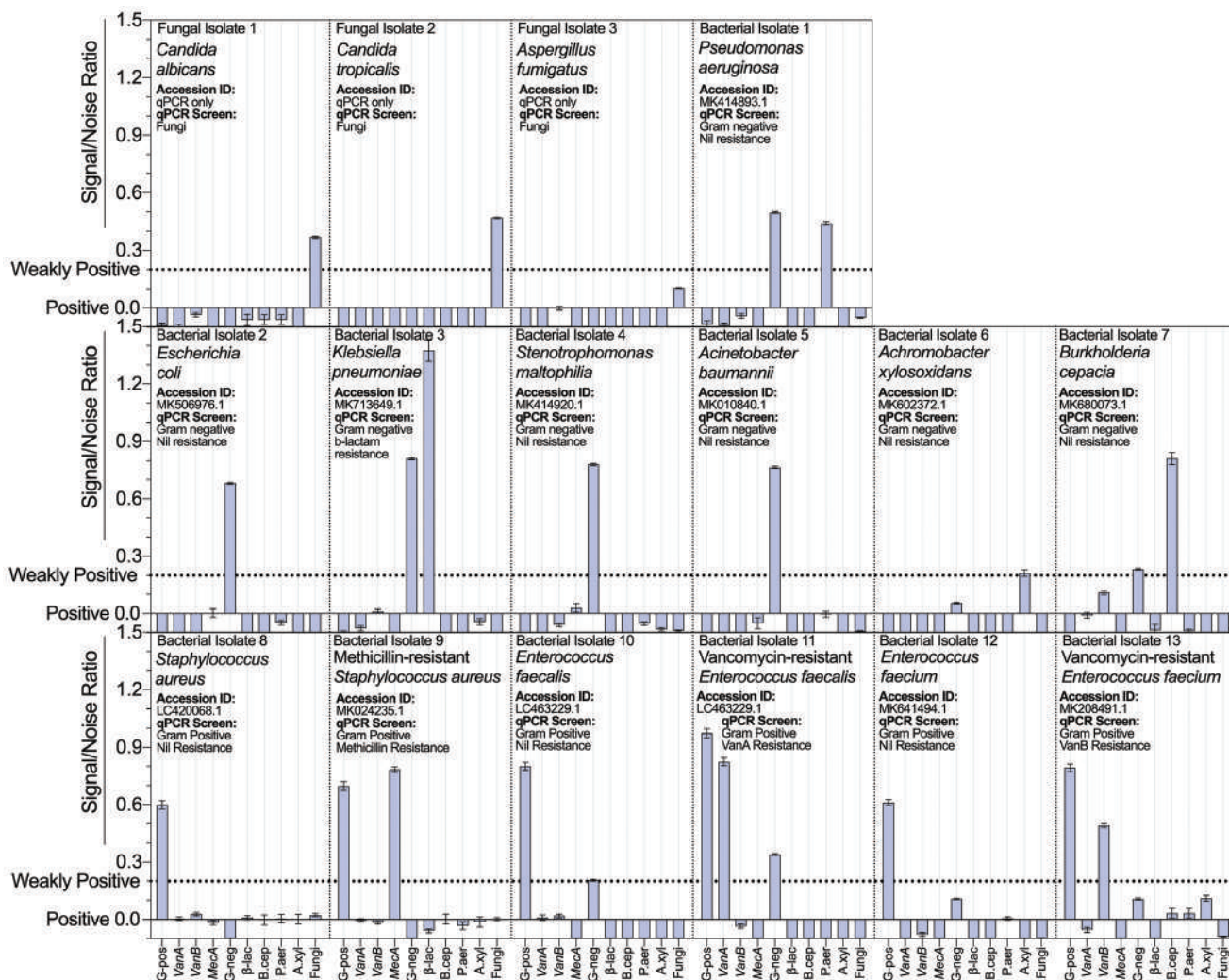
### Data Analysis

The raw data from the BD FACSDiva Software was analyzed as previously published.<sup>7</sup> Briefly, the signal/noise ratio (S/N) was calculated from data normalized to an NTC reaction (noise) and a “signal maximum” reaction that contained no template or forward and reverse primers (signal). A custom R Studio software package provided summary statistics directly from flow cytometry standard files via the bootstrap technique. An S/N >0.0 was considered positive and weakly positive when S/N values were between 0.0 and 0.2. An S/N less than -0.1 was omitted. For evaluating analytical specificity, the accuracy (%) was calculated by dividing the sum of the true positives and true negatives by the sum of all true and false positive and negatives. Positive predictive values (PPVs) and negative predictive values (NPVs) were determined using a chi-square test, and differences of accuracy between groups were assessed with a 1-way analysis of variance with Bonferroni-corrected multiple comparisons testing. In all cases,  $P < .05$  was considered significant. Data are representative of triplicate independent technical replicates. Figures were prepared using GraphPad Prism version 8.4.2 (GraphPad Software).

## Results

We first sequenced each bacterial isolate included in our study to confirm that the genotype was as expected (National Center for Biotechnology Information accession number [Accession ID]; FIGURE 1). We next tested the specificity of the selected primers (Supplemental Table 1) with single-plex SYBR chemistry qPCR. To confirm the specificity of the primers, we assessed the amplification Ct for each isolate. We confirmed that the Gram-positive, Gram-negative, and fungal primers correctly typed each isolate (Supplemental Figure 1A). The *P aeruginosa*,

**FIGURE 1.** Simultaneous detection of Gram type, fungi, antibiotic resistance genes, and species-specific genes with multiplex microsphere polymerase chain reaction (mmPCR). The signal-to-noise ratio (S/N) of (13x) 16S/rRNA Sanger-sequenced and Basic Local Alignment Tool-identified bacterial isolates and (3x) fungal isolates, selectively amplified in a custom 10-plex mmPCR assay. Each 10-plex mmPCR contained general Gram-positive (G-pos), Gram-negative (G-neg) and pan-fungal (Fungi) primers; specific primers targeting the resistance-conferring gene *mecA* (*MecA*), the type A vancomycin resistance-conferring *Tn1546 Transposon* (*VanA*), the *vanB* mobile cluster (*VanB*), and the  $\beta$ -lactamases expressing *bla*<sub>SHV-1</sub> gene ( $\beta$ -lac); and specific primers targeting the bacterial species *B cepacia* (*B.cep*), *P aeruginosa* (*P.aer*), and *A xylosoxidans* (*A.xyl*). The polymerase chain reaction was conducted using purified isolate genomic DNA at a concentration of  $10^5$  genomes/reaction. The S/N of each primer set for each isolate was calculated from data normalized to a no-template negative control reaction (noise) and a “signal maximum” reaction that contained no template or forward and reverse primers (signal). An S/N >0.0 was considered positive and weakly positive when between 0.0 and 0.2 (dotted line). An S/N less than -0.1 was omitted. Data are representative of triplicate independent technical replicates. The mean  $\pm$  standard error of the mean of technical triplicates is shown.



*B cepacia*, and *A xylosoxidans* isolates were only amplified weakly ( $C_t > 30$ ) using the Gram-negative primers. Therefore, we chose these species to show the modularity of mmPCR by incorporating these species-specific primers into the assay. When we tested them using single-plex qPCR, we found that the selected species-specific primers were specific for their target isolate (Supplemental Figure 1B). In addition, we observed that the resistance gene-specific primers correctly identified the expected resistance gene expression, based on laboratory-confirmed resistance phenotype (Supplemental Figure 1C). Taken together, these data indicate that the primers selected for this study are specific when tested using single-plex qPCR.

We next sought to show that the analytical specificity of these primers is maintained when incorporated into a combined 10-plex mmPCR assay and thus show that mmPCR allows the simultaneous detection of both general and specific clinically relevant genetic targets. Using our 10-plex mmPCR, we could correctly type and identify all bacterial and fungal isolates and their resistance genes where present (FIGURE 1). Consistent with previously published data,<sup>7</sup> low cross-reactive signals appeared alongside high S/N primer values. When considering the analytical sensitivity of the 10-plex mmPCR assay exclusive of weakly positive results, we found no statistically significant difference between the accuracy of qPCR and mmPCR ( $P > .9999$ ; qPCR [ $C_t < 30$ ] vs

mmPCR [S/N >0.2]; **TABLE 1**). False-positive measurements increased in frequency for both mmPCR and qPCR as the threshold of positivity was lowered (NPV = 0.9854 vs 0.8321 and NPV = 1.000 vs 0.6449 for mmPCR [S/N >0.2 vs >0.0] and qPCR [Ct <30 vs Ct <40], respectively; **TABLE 1**). Taken together, these data indicate that mmPCR can simultaneously detect a number of clinically relevant genetic targets and that our 10-plex mmPCR has a similar analytical specificity to single-plex SYBR chemistry qPCR.

## Discussion

Herein, we present an mmPCR assay that can successfully detect 10 clinically relevant specific and general targets in parallel, and as proof of principle, we show its accuracy across multiple pathogens. By allowing Gram typing and establishing resistance genotypes, high-multiplex mmPCR may guide initial treatment options and minimize

the use of empiric broad-spectrum antibiotics.<sup>12</sup> We acknowledge that functional assays will remain critical components of resistance testing, as resistance genotype and phenotype are not always perfectly matched.<sup>13</sup> However, an assessment of the likelihood of resistant organisms within ~3.5 hours is likely to be both clinically meaningful and cost-effective.<sup>7</sup>

By integrating species-specific primers, we have shown that this technology has the capacity for the modular addition of novel GOI targets. This capacity may facilitate the monitoring of rapidly emerging resistance or species-specific genotypes during an outbreak of a previously uncommon organism.<sup>12</sup> Indeed, we suggest that the modular multiplex capacity of this mmPCR assay can be used to generate assays fit for specific patient populations in specific health care facilities, where local microbiological patterns can vary considerably. The Luminex platform allows up to 150 beads to be simultaneously detected in a single tube, although we speculate that there may be technical limitations that would

**TABLE 1. Analytical Sensitivity of mmPCR and qPCR**

Pathogen or Target	Analytical Specificity					Analytical Specificity				
	Exclusive of Weakly Positive Results				Inclusive of Weakly Positive Results					
	qPCR Ct <30		mmPCR S/N >0.2		qPCR Ct <35		mmPCR S/N >0.0		qPCR Ct <40	
	TP (TN) FP (FN)	Acc (%)	TP (TN) FP (FN)	Acc (%)	TP (TN) FP (FN)	Acc (%)	TP (TN) FP (FN)	Acc (%)	TP (TN) FP (FN)	Acc (%)
General primers										
Gram-positive	6 (10) 0 (0)	100	6 (10) 0 (0)	100	6 (9) 1 (0)	93.8	6 (10) 0 (0)	100	6 (6) 4 (0)	75.0
Gram-negative	4 (9) 3 (3)	81.3	6 (7) 2 (1)	81.3	7 (9) 0 (0)	100	7 (5) 4 (0)	75.0	7 (6) 3 (0)	81.3
Fungi	3 (13) 0 (0)	100	2 (13) 0 (1)	93.8	3 (11) 2 (0)	100	3 (11) 2 (0)	87.5	3 (13) 0 (0)	100
Species-specific primers										
<i>B cepacia</i>	1 (9) 0 (0)	100	1 (15) 0 (0)	100	1 (9) 0 (0)	100	1 (13) 2 (0)	87.5	1 (1) 8 (0)	20.0
<i>P aeruginosa</i>	1 (9) 0 (0)	100	1 (15) 0 (0)	100	1 (0) 0 (0)	100	1 (12) 3 (0)	81.3	1 (2) 7 (0)	30.0
<i>A xylosoxidans</i>	1 (9) 0 (0)	100	1 (15) 0 (0)	100	1 (7) 2 (0)	80.0	1 (13) 2 (0)	87.5	1 (1) 8 (0)	20.0
Resistance-specific primers										
VanA	1 (12) 0 (0)	100	1 (15) 0 (0)	100	1 (12) 0 (0)	100	1 (12) 3 (0)	81.3	1 (12) 0 (0)	100
VanB	1 (12) 0 (0)	100	1 (15) 0 (0)	100	1 (12) 0 (0)	100	1 (11) 4 (0)	75.0	1 (6) 6 (0)	53.8
MecA	1 (12) 0 (0)	100	1 (15) 0 (0)	100	1 (12) 0 (0)	100	1 (13) 2 (0)	87.5	1 (11) 1 (0)	92.3
SHV	1(12) 0(0)	100	1 (15) 0 (0)	100	1 (12) 0 (0)	100	1 (14) 1 (0)	93.8	1 (11) 1 (0)	92.3
Chi-square test	PPV	0.8696		0.9130		1.000		1.000		1.000
	NPV	0.9727		0.9854		0.9720		0.8321		0.6449
1-way ANOVA	Dunn's multiple comparisons testing						Adjusted <i>P</i> value			
	qPCR (Ct <30) vs mmPCR (S/N >0.2)						<i>P</i> > .9999			
	qPCR (Ct <30) vs qPCR (Ct <35)						<i>P</i> > .9999			
	qPCR (Ct <30) vs mmPCR (S/N >0.0)						<i>P</i> = .0233			
qPCR (Ct <30) vs qPCR (Ct <40)						<i>P</i> = .0150				

Acc, accuracy quantified as (TP + TN)/(TP + TN + FP + FN); ANOVA, analysis of variance; Ct, cycle threshold (qPCR); FN, false negative; FP, false positive; MecA, methicillin resistance; mmPCR, multiplex microsphere polymerase chain reaction; NPV, negative predictive value; PPV, positive predictive value; qPCR, quantitative polymerase chain reaction; SHV,  $\beta$ -lactamase resistance; S/N, signal-to-noise ratio (mmPCR); TN, true negative; TP, true positive; VanA, vancomycin resistance type A; VanB, vancomycin resistance type B.

prevent 150-gene detection with mmPCR. Nevertheless, our data show that high multiplexing capacity, with both specific and general primers, is possible with this platform.

This study was conducted on isolates grown from culture, with purified gDNA at a concentration of  $10^5$  genome copies/reaction (ie, 0.5–0.4 ng gDNA/reaction). When considering analytical specificity, we observed low cross-reactive signals in reactions with high S/N primer values, in agreement with the previously reported Gram-typing duplex-mmPCR.<sup>7</sup> Although we were able to distinguish both Gram type and resistance profile, we do accept that this finding suggests possible challenges in detecting microbial GOIs in low-biomass polymicrobial biological specimens.

When considering sensitivity, in agreement with others in the literature when testing both specific and general microbial diagnostic primers,<sup>14</sup> we found that the PPV of purified and concentrated specimens was very high (0.80–1.00). We expect that this value will decrease significantly when testing clinical specimens.<sup>15</sup> Indeed, the analytical and diagnostic sensitivity of a NAAT is largely dependent on the nucleic acid extraction and purification method performed, and further development of specimen-specific DNA extraction methods is required for sensitivity testing.<sup>16</sup> For example, current nucleic acid isolation technologies can reproducibly isolate nucleic acids from single mammalian cells.<sup>17</sup> However, no current-generation nucleic acid isolation strategy is capable of reproducibly extracting enough gDNA for analysis from the low bacterial cell numbers (ie, 0.1- to 10-colony-forming units/mL) that would be required for these methods to supersede traditional blood culture.<sup>12</sup> These circumstances are despite considerable effort being devoted to the development of nucleic acid extraction technologies using combined mechanical, chemical, thermal, and enzymatic lysis strategies<sup>18</sup> or increasing specimen volume.<sup>19</sup>

## Conclusion

We have shown a significant extension to the functionality of a previously published duplex mmPCR Gram-typing molecular diagnostic by adding clinically relevant specific and general genetic targets to generate a 10-plex mmPCR. This assay may guide treatment options via establishing Gram status, the presence of fungal DNA, and the prediction of phenotypic resistance. Furthermore, it provides a modular flexible platform that can be adapted swiftly to changes in local epidemiology.

## Supplementary Material

Supplemental figures and tables can be found in the online version of this article at [www.labmedicine.com](http://www.labmedicine.com).

## Acknowledgments

The authors thank Professor Rob Capon (University of Queensland), Professor Graeme Nimmo (Pathology Queensland), and Professor James Fraser (University of Queensland) for gifts of microbial isolates and Emeritus Professor Ross Barnard (University of Queensland) for his helpful suggestions. The graphic abstract was created with BioRender.com software.

## Funding

K.A.M. was supported by a Queensland Health Junior Clinical Research Fellowship. D.J.B. was supported by Prestige Research Training Program Stipend (RTPS).

## Conflict of Interest Statement

The authors declare that the research was conducted in the absence of any commercial or financial relationships that could be construed as a potential conflict of interest.

## REFERENCES

1. Simmer PJ, Miller S, Carroll KC. Understanding the promises and hurdles of metagenomic next-generation sequencing as a diagnostic tool for infectious diseases. *Clin Infect Dis*. 2018;66(5):778–788.
2. Zhang Y, Hu A, Andini N, Yang S. A “culture” shift: application of molecular techniques for diagnosing polymicrobial infections. *Biotechnol Adv*. 2019;37(3):476–490.
3. van Belkum A, Burnham CD, Rossen JWA, Mallard F, Rochas O, Dunne WM Jr. Innovative and rapid antimicrobial susceptibility testing systems. *Nat Rev Microbiol*. 2020;18(5):299–311.
4. Bravo D, Blanquer J, Tormo M, et al. Diagnostic accuracy and potential clinical value of the LightCycler SeptiFast assay in the management of bloodstream infections occurring in neutropenic and critically ill patients. *Int J Infect Dis*. 2011;15(5):e326–e331.
5. Liang F, Lai R, Arora N, et al. Multiplex-microsphere-quantitative polymerase chain reaction: nucleic acid amplification and detection on microspheres. *Anal Biochem*. 2013;432(1):23–30.
6. Lai R, Liang F, Pearson D, et al. PrimRglo: a multiplexable quantitative real-time polymerase chain reaction system for nucleic acid detection. *Anal Biochem*. 2012;422(2):89–95.
7. Liang F, Browne DJ, Gray MJ, et al. Development of a multiplexed microsphere PCR for culture-free detection and Gram-typing of bacteria in human blood samples. *ACS Infect Dis*. 2018;4(5):837–844.
8. Saah AJ, Hoover DR. “Sensitivity” and “specificity” reconsidered: the meaning of these terms in analytical and diagnostic settings. *Ann Intern Med*. 1997;126(1):91–94.
9. Thornton B, Basu C. Real-time PCR (qPCR) primer design using free online software. *Biochem Mol Biol Educ*. 2011;39(2):145–154.
10. James G. Universal bacterial identification by PCR and DNA sequencing of 16S rRNA gene. In: Schuller M, Sloots TP, James GS, Halliday CL, Carter IWJ, eds. *PCR for Clinical Microbiology: An Australian and International Perspective*. Dordrecht, The Netherlands: Springer Netherlands; 2010: 209–214.
11. Corrie SR, Feng Q, Blair T, Hawes SE, Kiviat NB, Trau M. Multiplatform comparison of multiplexed bead arrays using HPV genotyping as a test case. *Cytometry A*. 2011;79(9):713–719.
12. Sinha M, Jupe J, Mack H, Coleman TP, Lawrence SM, Fraley SI. Emerging technologies for molecular diagnosis of sepsis. *Clin Microbiol Rev*. 2018;31(2):e00089-17.
13. Dantas G, Sommer MO. Context matters—the complex interplay between resistome genotypes and resistance phenotypes. *Curr Opin Microbiol*. 2012;15(5):577–582.
14. Loonen AJ, Bos MP, van Meerbergen B, et al. Comparison of pathogen DNA isolation methods from large volumes of whole blood to improve molecular diagnosis of bloodstream infections. *PLoS One*. 2013;8(8):e72349.
15. van de Groep K, Bos MP, Varkila MRJ, et al. Moderate positive predictive value of a multiplex real-time PCR on whole blood for pathogen detection in critically ill patients with sepsis. *Eur J Clin Microbiol Infect Dis*. 2019;38(10):1829–1836.

16. Stone M, Lanteri MC, Bakkour S, et al. Relative analytical sensitivity of donor nucleic acid amplification technology screening and diagnostic real-time polymerase chain reaction assays for detection of Zika virus RNA. *Transfusion*. 2017;57(3pt2):734–747.
17. Browne DJ, Brady JL, Waardenberg AJ, Loiseau C, Doolan DL. An analytically and diagnostically sensitive RNA extraction and RT-qPCR protocol for peripheral blood mononuclear cells. *Front Immunol*. 2020;11:402.
18. Gosiewski T, Szała L, Pietrzyk A, Brzychczy-Włoch M, Heczko PB, Bulanda M. Comparison of methods for isolation of bacterial and fungal DNA from human blood. *Curr Microbiol*. 2014;68(2):149–155.
19. van de Groep K, Bos MP, Savelkoul PHM, et al. Development and first evaluation of a novel multiplex real-time PCR on whole blood samples for rapid pathogen identification in critically ill patients with sepsis. *Eur J Clin Microbiol Infect Dis*. 2018;37(7):1333–1344.

# 5-Amino-4-Imidazolecarboxamide Ribonucleotide Transformylase/IMP Cyclohydrolase Polymorphisms Affect the Susceptibility to Multiple Myeloma

Yu Wang, MM,<sup>1,a,\*</sup> Zhian Ling, PhD,<sup>2,a</sup> Zuojian Hu, PhD,<sup>1</sup> Ying Gui, MM,<sup>3</sup> Chunni Huang, PhD,<sup>1</sup> Yibin Yao, PhD,<sup>4</sup> Ruolin Li, PhD<sup>1,\*</sup>

<sup>1</sup>Department of Laboratory Medicine, First Affiliated Hospital of Guangxi Medical University, Nanning, China, <sup>2</sup>Department of Orthopedics, First Affiliated Hospital of Guangxi Medical University, Nanning, China, <sup>3</sup>Department of Scientific Research, First Affiliated Hospital of Guangxi Medical University, Nanning, China, <sup>4</sup>Department of Hematology, First Affiliated Hospital of Guangxi Medical University, Nanning, China; \*To whom correspondence should be addressed. [ruolin8297@163.com](mailto:ruolin8297@163.com); <sup>a</sup>Contributed as first authors.

**Keywords:** ATIC, multiple myeloma, polymorphism, lactate dehydrogenase, linkage disequilibrium, haplotypes

**Abbreviations:** ATIC, 5-amino-4-imidazolecarboxamide ribonucleotide transformylase/IMP cyclohydrolase; MM, multiple myeloma; LD, linkage disequilibrium; MTX, methotrexate; LDH, lactate dehydrogenase; ISS, International Staging System; DS, Durie-Salmon staging; Ca, calcium; Cr, creatinine; Alb, albumin;  $\beta$ 2-MG,  $\beta$ 2-microglobulin; ESR, erythrocyte sedimentation rate; OR, odds ratio; CI, confidence interval.

*Laboratory Medicine* 2022;53:465–474; <https://doi.org/10.1093/labmed/lmac022>

## ABSTRACT

**Objective:** The upregulation of 5-amino-4-imidazolecarboxamide ribonucleotide transformylase/IMP cyclohydrolase (ATIC) may affect tumorigenesis and multiple myeloma (MM) development.

**Materials and Methods:** A total of 97 patients with MM and 102 healthy control patients were included in the study. The SNaPshot technique was used to detect the ATIC gene polymorphisms. Linkage disequilibrium (LD) and haplotype analyses were conducted using SHEsis software.

**Results:** The genotype distribution or allele frequency of rs3772078 and rs16853834 was significantly different between the patients with MM and the healthy control patients (all  $P < .05$ ). The rs16853834 A allele, rs3772078 CT genotype, and C allele were associated with a decreased risk of MM (all  $P < .05$ ). Five single-nucleotide polymorphism combinations showed strong LD. Three haplotypes were associated with MM risk (all  $P < .05$ ). We found that ATIC rs7604984

was significantly associated with serum lactate dehydrogenase levels ( $P = .050$ ).

**Conclusion:** We determined that the rs3772078 and rs16853834 polymorphisms are associated with a decreased risk of MM.

Multiple myeloma (MM) is a plasma cell dyscrasia characterized by clonal plasma cell proliferation in the bone marrow and monoclonal immunoglobulin in serum and/or urine.<sup>1</sup> It is the second most common hematologic malignancy in the United States; approximately >30,000 new patients were diagnosed and >10,000 deaths occurred in 2020.<sup>2</sup> The clinical features in most patients with MM include hypercalcemia, renal insufficiency, anemia, and susceptibility to infections. Some viral infections and genetic, biochemical, and environmental factors may be involved in the etiology and pathogenesis of MM.<sup>3</sup> Numerous clinical reports have indicated that patients with MM often have abnormal serum indicators; thus, the disease can be detected early and evaluated through laboratory testing.<sup>4</sup>

5-amino-4-imidazolecarboxamide ribonucleotide transformylase/IMP cyclohydrolase (ATIC) is a bifunctional protein with 2 enzymatic activities. It encodes a bifunctional protein and catalyzes the last 2 steps of the de novo purine biosynthetic pathway.<sup>5</sup> Its N-terminal domain possesses a phosphoribosylaminoimide-azolecarboxamide formyltransferase function, and the C-terminal domain exhibits IMP cyclohydrolase activity.<sup>6,7</sup> Therefore, ATIC may influence carcinogenesis. Many studies have shown that ATIC polymorphisms play an important role in many diseases. For example, meta-analysis showed a significant association between the ATIC 347 GG + GC genotype and a nonresponse to MTX therapy in 1056 rheumatoid arthritis (RA) patients, so ATIC 347 C/G polymorphism may affect MTX efficacy.<sup>8</sup> Another study revealed that ATIC 347C > G polymorphism may influence the treatment outcome of MTX in pediatric osteosarcoma.<sup>9</sup> A previous study found that increased congenital heart disease susceptibility was associated with ATIC polymorphisms for de novo nucleotide biosynthesis in the northern Chinese population.<sup>10</sup> The purpose of this study was to investigate the relationship between ATIC polymorphism and the risk of MM.

Autophagy regulates cancer formation, metastasis, proliferation, and energy metabolism and plays an essential role in plasma cell development and MM pathogenesis.<sup>11-13</sup> One study noted that ATIC is one of the 16 autophagy-related genes (ARGs) with prognostic value in MM.<sup>13</sup> Other previous research found that compared with ATIC mRNA and protein levels in normal bone marrow control specimens, those in MM specimens were significantly increased.<sup>14</sup> This ATIC upregulation indicates that it may play an important role in the tumorigenesis of MM and may be an independent indicator for predicting survival in MM.<sup>13,14</sup>

Several serum markers of MM have also been studied recently. Barlogie et al<sup>15</sup> suggested that high serum lactate dehydrogenase (LDH) levels reduce the early survival of patients with MM. Chen et al<sup>16</sup> reported that a high serum LDH level is a poor prognostic factor for early mortality. Furthermore, LDH is a crucial unfavorable predictor of MM in older adult Chinese patients.<sup>17</sup> Therefore, detecting the serum LDH level is of great value in MM diagnosis.

However, no studies to date have analyzed the role of ATIC polymorphisms in MM. In this study, we have evaluated the relationship between 5 ATIC gene loci (rs7604984, rs2372536, rs4673993, rs3772078, and rs16853834) and susceptibility to MM, and analyzed the correlation between the genotype of these single nucleotide polymorphisms (SNPs) and clinical features in the population of the Guangxi region in China.

## Materials and Methods

### Study Population

This was a case-control study of 199 patients, including 97 patients with MM and 102 healthy control patients. Blood specimens were collected from patients with MM who visited the hematology department of the First Affiliated Hospital of Guangxi Medical University from January 2019 to January 2020. For the MM group, the enrolled patients fulfilled the guidelines of the National Comprehensive Cancer Network. Patients with MM who had any of the following were excluded: (1) hepatitis B virus, hepatitis C virus, HIV, or other viral infections; (2) neoplastic disease; and (3) other hematological diseases. The MM staging was based on the International Staging System (ISS) and the Durie-Salmon staging system (DS). Based on a physical examination conducted at our hospital, 102 matched healthy control patients were identified. The clinical characteristics of all patients are presented in **TABLE 1**.

The study was approved by the ethics committee of the First Affiliated Hospital of Guangxi Medical University (number 2017KY-E-100). Each participant provided written informed consent.

### Methods

A Beckman Coulter LH780 blood analyzer (Beckman Coulter, Brea, CA) was used to measure the levels of hemoglobin. A Hitachi 7600 automatic biochemical analyzer (Hitachi, Tokyo, Japan) was used to detect the serum biochemical indices. The following pretreatment parameters were analyzed: calcium (Ca), serum, creatinine (Cr), albumin (Alb), LDH, and  $\beta$ 2-microglobulin ( $\beta$ 2-MG). Automated erythrocyte sedimentation (Sysmex, Kobe, Japan) was used to measure the erythrocyte sedimentation rate (ESR). The Abbott AxSYM System (Abbott Laboratories, Chicago, IL) was used to identify the immunoglobulin subtype. Bone marrow smears were stained with Wright stain solution (Baso, Zhuhai, China), and the ratio of plasma cells was calculated.

**TABLE 1. Clinical Characteristics of Patients with MM and Healthy Control Patients**

Clinical Features	MM (n = 97)	Healthy Control Patients (n = 102)	P Value
Sex (male/female), No. (%)	54 (55.7)/43 (44.3)	60 (58.8)/42 (41.2)	.653
Age, y, mean $\pm$ SD	58.25 $\pm$ 9.91	56.19 $\pm$ 11.28	.173
Laboratory indices, mean $\pm$ SD			
Hb (g/dL)	8.55 $\pm$ 2.25		
Ca (mg/dL)	9.30 $\pm$ 1.17		
Cr (mg/dL)	1.87 $\pm$ 2.38		
Alb (mg/dL)	3.44 $\pm$ 0.82		
$\beta$ 2-MG (mg/L)	7.62 $\pm$ 4.96		
LDH (U/L)	200.11 $\pm$ 94.50		
ESR (mm/60 min)	79.97 $\pm$ 45.28		
Plasma cells, No. (%)			
<30%	58 (59.8)		
$\geq$ 30%	39 (40.2)		
Durie-Salmon stage, No. (%)			
I	3 (3.1)		
II	7 (7.2)		
III	87 (89.7)		
ISS stage, No. (%)			
I	9 (9.3)		
II	25 (25.8)		
III	63 (64.9)		
Immunoglobulin subtype, No. (%)			
IgG	46 (47.4)		
IgA	22 (22.7)		
IgM	2 (2.1)		
IgD	1 (1.0)		
Light chain only	23 (23.7)		
Nonsecretory	3 (3.1)		

Alb, albumin;  $\beta$ 2-MG,  $\beta$ 2-microglobulin; Ca, calcium; Cr, creatinine; ESR, erythrocyte sedimentation rate; Hb, hemoglobin; ISS, International Staging System; LDH, lactate dehydrogenase; MM, multiple myeloma; SD, standard deviation.

### DNA Extraction and Genotyping

According to the manufacturer's instructions, we used an AxyPrep Blood Genomic DNA Kit (Axygen Biosciences, Hangzhou, China) to collect genomic DNA from peripheral blood specimens. **TABLE 2** summarizes the primer sequences for the ATIC gene loci (rs7604984, rs2372536, rs4673993, rs3772078, and rs16853834). The SNaPshot polymerase chain reaction was consistent with that of previous work.<sup>18</sup>

### Statistical Analysis

All statistical analyses were performed using the IBM SPSS software package version 26 (IBM, Armonk, NY). The distribution type of the data was determined using the Kolmogorov-Smirnov test. We used the mean and standard deviation to describe normally distributed data and the median and interquartile range to describe skewed distributed data. The clinical features of patients with MM are represented by numbers and proportions. Genotype and allele frequencies of rs7604984, rs2372536, rs4673993, rs3772078, and rs16853834 were calculated by direct counting.

**TABLE 2. Primer Sequences Used for Detecting ATIC SNPs**

SNP ID	PCR Primers	Single-Base Extension Primer Sequences
rs7604984	F: 5'-ATTTTGGTCTCATAGTCCCACG-3'	Sep:5'-TAGTCCCACGTGC TGGGCTGTGCCCTTGCATT CTGTGATGTC-3'
	R: 5'-ACTACGGCTATCAATGTGTAAGAAAG-3'	
rs2372536	F: 5'-ACAGCCAGATTCTGCTTTTGTTTA-3'	Sep:5'-TTTTATAGATTGTTG CCTGCAATCTCTATCCCTT TGTAAGACAGTGGCTTCTCC AGGTGTA-3'
	R: 5'-ACTTACCAATGTCAATTTGCTCCA-3'	
rs4673993	F: 5'-GGCTGCTAATCAATACTAGATGGTC-3'	Sep:5'-GGTCTTCTGAAGAC CAATTGACTACCCTCAGTT TTTTA-3'
	R: 5'-CAGCCTCACTCTTCAATGACACTT-3'	
rs3772078	F: 5'-CCTGCTGACTAAATACCTCTGCTC-3'	Sep: 5'-AAAACAAGTCAGTACT ATTAACGTAACAAAAGC CATAGAGAACTAATA-3'
	R: 5'-AAGCCACTGTCTTTACAAGGGATA-3'	
rs16853834	F: 5'-CCAACATTTCTCACTGTGTGACG-3'	Sep: 5'-AAGAAAAGGCTAGCA GAGACCTCAGAGATGAAC CAGCTCCATCTTGATTCTGA GGCTC-3'
	R: 5'-GTTTGTACTACAGAGACTGGCAATC-3'	

ATIC, 5-amino-4-imidazolecarboxamide ribonucleotide transformylase/IMP cyclohydrolase; F, forward; R, reverse; SNP, single-nucleotide polymorphism.

The Hardy-Weinberg equilibrium was tested using the goodness-of-fit chi-square test in the control group. Genotype and allele frequencies of rs7604984, rs2372536, rs4673993, rs3772078, and rs16853834 were compared between the MM and control groups using a chi-square test or Fisher's exact probability method, as appropriate. Similarly, the clinical parameters of patients with MM were compared with ATIC polymorphisms using the chi-square test for categorical variables. The independent *t*-test for continuous variables was used to compare the serum LDH levels in patients with MM with their clinical features. The correlation between serum LDH levels and  $\beta$ 2-MG and Alb levels was analyzed using Pearson correlation. To evaluate the relative risks of specific alleles and genotypes, binary logistic regression was used to calculate the odds ratios (ORs) and 95% confidence intervals (CIs) after adjusting for age and sex status. The linked disequilibrium (LD) and haplotype analyses were performed using the SHEsis online software ([analysis.bio-x.cn](http://analysis.bio-x.cn)).<sup>19</sup> The *D'* and *r*<sup>2</sup> were calculated for LD analysis. Statistical significance was set at *P* < .05.

## Results

### Basic Characteristics of Patients with MM

The clinical characteristics of patients with MM are shown in **TABLE 1**. Among the 97 MM patients, 54 were male (55.7%) and 43 were female (44.3%). The average age of patients with MM was 58.25 ± 9.91 years.

The immunoglobulin subtype in 46 patients was IgG (47.4%), 22 patients had IgA (22.7%), 2 patients had IgM (2.1%), 1 patient had IgD (1.0%), 23 patients were light chain only (23.7%), and 3 patients were nonsecretory (3.1%). According to the ISS, 9 (9.3%), 25 (25.8%), and 63 (64.9%) patients were classified as stage I, II, and III, respectively. In the DS staging system, 3 (3.1%), 7 (7.2%), and 87 (89.7%) patients were classified as stage I, II, and III, respectively. Moreover, the plasma cell ratio in the bone marrow of 39 patients (40.2%) was >30%. There was no difference in sex or age between the MM group and the healthy control patients.

### Correlation Between 5 Polymorphisms and Risk of MM

**TABLE 3** describes the genotypes and allele frequencies of the rs7604984, rs2372536, rs4673993, rs3772078, and rs16853834 polymorphisms of the ATIC gene in patients with MM and healthy control patients. The genotype distributions of rs7604984, rs2372536, rs4673993, rs3772078, and rs16853834 in the control group were consistent with the Hardy-Weinberg equilibrium hypothesis (all *P* > .05). The genotype distribution or allele frequency of rs3772078 and rs16853834 was significantly different between patients with MM and healthy control patients (all *P* < .05). However, the genotype distribution or allele frequency of rs7604984, rs2372536, and rs4673993 was not significantly different between patients with MM and healthy control patients. After we adjusted for age and sex, a binary logistic regression analysis showed that the ATIC rs7604984, rs2372536, and rs4673993 polymorphisms were not associated with MM risk (all *P* > .05). Analysis of the ATIC rs3772078 polymorphism indicated that compared with that in patients carrying the TT genotype, MM risk was decreased in those carrying the CT genotype, with an adjusted OR of 0.315 (95% CI, 0.135–0.733; *P* = .007). Similarly, MM risk was found to be less in patients carrying the rs3772078 C allele (OR, 0.511; 95% CI, 0.340–0.770; *P* = .001) relative to those carrying the T allele. In addition, the rs16853834 A allele was associated with a decreased MM risk (OR, 0.522; 95% CI, 0.321–0.850; *P* = .009).

### Association of ATIC Polymorphisms and Serum LDH Levels with Clinical Variables

The associations of ATIC polymorphisms with the clinical variables of patients with MM are summarized in **TABLES 4** and **5**. The ATIC rs7604984 polymorphism was significantly associated with serum LDH levels (*P* = .050). However, the ATIC rs2372536, rs4673993, rs3772078, and rs16853834 polymorphisms were not. The serum LDH levels were not significantly different in the stratification of age, hemoglobin, Cr, Ca, ESR, plasma cell ratio, Durie-Salmon (DS) stage, and immunoglobulin subtype. As shown in **TABLE 6**, the serum LDH levels of female Alb ≥3.5 mg/dL,  $\beta$ 2-MG ≥5.5 mg/L, and ISS stage III were significantly higher than that of male (*P* = .036), Alb <3.5 mg/dL (*P* = .017),  $\beta$ 2-MG <5.5 mg/L (*P* = .032), and ISS stages I and II (*P* = .009). Moreover, there was no difference in LDH levels between patients in ISS stages I, II, and III (**FIGURE 1**). There was a significant difference in serum LDH levels between male and female patients (*P* = .036; **FIGURE 2**). The serum LDH levels were not correlated with  $\beta$ 2-MG levels (**FIGURE 3**). However, serum LDH and Alb levels were found to be correlated (*P* = .002; **FIGURE 4**).

### LD Analysis

The LD analysis was performed to study the relationships between these 5 SNPs and MM. For patients with MM, rs3772078 and rs2372536,

**TABLE 3. Genotype and Allele Frequencies of ATIC rs7604984, rs2372536, rs4673993, rs3772078, and rs16853834 Polymorphisms for MM and Healthy Control Groups**

Polymorphisms	Healthy Control Patients No. (%)	MM No. (%)	OR (95% CI)	P Value <sup>a</sup>
<b>rs7604984</b>				
GG	28 (27.7)	22 (22.7)	1.0 <sup>Ref</sup>	
GA	49 (48.5)	44 (45.4)	0.606 (0.278–1.323)	.209
AA	24 (23.8)	31 (31.9)	0.676 (0.344–1.330)	.257
G	105 (52.0)	88 (45.4)	1.0 <sup>Ref</sup>	
A	97 (48.0)	106 (54.6)	1.307 (0.877–1.947)	.188
P <sup>HWE</sup>	.777	.403	...	
<b>rs2372536</b>				
CC	42 (41.6)	42 (43.3)	1.0 <sup>Ref</sup>	
GC	45 (44.6)	45 (46.4)	1.337 (0.529–3.379)	.539
GG	14 (13.8)	10 (10.3)	1.319 (0.523–3.330)	.558
C	129 (63.9)	129 (66.5)	1.0 <sup>Ref</sup>	
G	73 (36.1)	65 (33.5)	0.901 (0.594–1.367)	.625
P <sup>HWE</sup>	.411	.965	...	
<b>rs4673993</b>				
TT	39 (38.2)	38 (39.2)	1.0 <sup>Ref</sup>	
CT	53 (52.0)	50 (51.5)	0.978 (0.354–2.700)	.965
CC	10 (9.8)	9 (9.3)	1.021 (0.378–2.753)	.968
T	131 (64.2)	126 (64.9)	1.0 <sup>Ref</sup>	
C	73 (35.8)	68 (35.1)	0.980 (0.648–1.483)	.925
P <sup>HWE</sup>	.187	.193	...	
<b>rs3772078</b>				
TT	22 (21.6)	45 (46.4)	1.0 <sup>Ref</sup>	
CT	58 (56.8)	36 (37.1)	0.315 (0.135–0.733)	.007 <sup>b</sup>
CC	22 (21.6)	16 (16.5)	1.156 (0.527–2.533)	.718
T	102 (50.0)	126 (64.9)	1.0 <sup>Ref</sup>	
C	102 (50.0)	68 (35.1)	0.511 (0.340–0.770)	.001 <sup>b</sup>
P <sup>HWE</sup>	.166	.069	...	
<b>rs16853834</b>				
GG	53 (52.0)	68 (70.1)	1.0 <sup>Ref</sup>	
GA	41 (40.2)	25 (25.8)	0.338 (0.092–1.242)	.102
AA	8 (7.8)	4 (4.1)	0.678 (0.174–2.647)	.577
G	147 (72.1)	161 (83.0)	1.0 <sup>Ref</sup>	
A	57 (27.9)	33 (17.0)	0.522 (0.321–0.850)	.009 <sup>b</sup>
P <sup>HWE</sup>	.986	.391	...	

ATIC, 5-amino-4-imidazolecarboxamide ribonucleotide transformylase/IMP cyclohydrolase; CI, confidence interval; HWE, Hardy-Weinberg equilibrium; MM, multiple myeloma; OR, odds ratio.

<sup>a</sup>P values appear for heterogeneity.

<sup>b</sup>P < .05.

rs3772078 and rs4673993, rs2372536 and rs4673993, rs2372536 and rs7604984, and rs4673993 and rs7604984 showed strong LD. However, other relationships did not show LD (TABLE 7).

### Haplotype Analysis

Haplotype analyses were performed for all patient groups and healthy control patients using the SHEsis software, and the 5 possible haplotype frequencies of the 5 SNPs are shown in TABLE 8. We did not analyze frequencies < .03. The CCGTG haplotype was more frequent in the control patients and was found to have a protective effect against disease

development (OR, 0.428; 95% CI, 0.191–0.960; P = .034965). The TCATA (OR, 3.073; 95% CI, 1.458–6.477; P = .002161) and TGGCG (OR, 1.587; 95% CI, 1.008–2.498; P = .045260) haplotypes were found to be linked with a significant increased risk of MM. The CCGTA and TCGTA haplotypes were not correlated with MM (all P > .05).

### Discussion

Abnormal autophagy has been related to the pathogenesis of various diseases, including malignant tumors.<sup>20</sup> Previous studies have

**TABLE 4. Associations of ATIC Polymorphisms with Clinical Variables of Patients with MM**

Genotype	rs7604984			P Value	rs2372536			P Value	rs4673993			P Value
	GG (n = 22)	GA (n = 44)	AA (n = 31)		CC (n = 42)	GC (n = 45)	GG (n = 10)		TT (n = 38)	CT (n = 50)	CC (n = 9)	
Sex, No. (%)												
Male	8 (36.4)	25 (56.8)	21 (67.7)	.075	28 (66.7)	21 (46.7)	5 (50.0)	.153	26 (68.4)	24 (48.0)	4 (44.4)	.145
Female	14 (63.6)	19 (43.2)	10 (32.3)		14 (33.3)	24 (53.3)	5 (50.0)		12 (31.6)	26 (52.0)	5 (55.6)	
Age, No. (%)												
<60 y	11 (50.0)	21 (47.7)	20 (64.5)	.331	24 (57.1)	23 (51.1)	5 (50.0)	.837	20 (52.6)	27 (54.0)	5 (55.6)	1.000
≥60 y	11 (50.0)	23 (52.3)	11 (35.5)		18 (42.9)	22 (48.9)	5 (50.0)		18 (47.4)	23 (46.0)	4 (44.4)	
Hb, No. (%)												
<10 g/dL	20 (90.9)	33 (75.0)	22 (71.0)	.196	29 (69.0)	37 (82.2)	9 (90.0)	.260	27 (71.1)	40 (80.0)	8 (88.9)	.512
≥10 g/dL	2 (9.1)	11 (25.0)	9 (29.0)		13 (31.0)	8 (17.8)	1 (10.0)		11 (28.9)	10 (20.0)	1 (11.1)	
Cr, No. (%)												
<2 mg/dL	17 (77.3)	35 (79.5)	24 (77.4)	1.000	34 (81.0)	35 (77.8)	7 (70.0)	.683	31 (81.6)	39 (78.0)	6 (66.7)	.541
≥2 mg/dL	5 (22.7)	9 (20.5)	7 (22.6)		8 (19.0)	10 (22.2)	3 (30.0)		7 (18.4)	11 (22.0)	3 (33.3)	
Alb, No. (%)												
<3.5 mg/dL	16 (72.7)	21 (47.7)	14 (45.2)	.096	20 (47.6)	24 (53.3)	7 (70.0)	.469	16 (42.1)	28 (56.0)	7 (77.8)	.136
≥3.5 mg/dL	6 (27.3)	23 (52.3)	17 (54.8)		22 (52.4)	21 (46.7)	3 (30.0)		22 (57.9)	22 (44.0)	2 (22.2)	
Ca, No. (%)												
<11.5 mg/dL	21 (95.5)	43 (97.7)	28 (90.3)	.436	39 (92.9)	44 (97.8)	9 (90.0)	.312	36 (94.7)	48 (96.0)	8 (88.9)	.490
≥11.5 mg/dL	1 (4.5)	1 (2.3)	3 (9.7)		3 (7.1)	1 (2.2)	1 (10.0)		2 (5.3)	2 (4.0)	1 (11.1)	
β2-MG, No. (%)												
<5.5 mg/L	7 (31.8)	17 (38.6)	12 (38.7)	.843	16 (38.1)	18 (40.0)	2 (20.0)	.542	16 (42.1)	19 (38.0)	1 (11.1)	.245
≥5.5 mg/L	15 (68.2)	27 (61.4)	19 (61.3)		26 (61.9)	27 (60.0)	8 (80.0)		22 (57.9)	31 (62.0)	8 (88.9)	
LDH, No. (%)												
<220 U/L	16 (72.7)	27 (61.4)	27 (87.1)	.050 <sup>a</sup>	35 (83.3)	28 (62.2)	7 (70.0)	.083	31 (81.6)	33 (66.0)	6 (66.7)	.239
≥220 U/L	6 (27.3)	17 (38.6)	4 (12.9)		7 (16.7)	17 (37.8)	3 (30.0)		7 (18.4)	17 (34.0)	3 (33.3)	
ESR, No. (%)												
<15 mm/60 min	1 (4.5)	4 (9.1)	5 (16.1)	.427	7 (16.7)	3 (6.7)	0 (0)	.214	6 (15.8)	4 (8.0)	0 (0)	.413
≥15 mm/60 min	21 (95.5)	40 (90.9)	26 (83.9)		35 (83.3)	42 (93.3)	10 (100.0)		32 (84.2)	46 (92.0)	9 (100.0)	
Plasma cells, No. (%)												
<30%	15 (68.2)	25 (56.8)	18 (58.1)	.656	25 (59.5)	25 (55.6)	8 (80.0)	.383	22 (57.9)	28 (56.0)	8 (88.9)	.181
≥30%	7 (31.8)	19 (43.2)	13 (41.9)		17 (40.5)	20 (44.4)	2 (20.0)		16 (42.1)	22 (44.0)	1 (11.1)	
DS stage, No. (%)												
I and II	2 (9.1)	6 (13.6)	2 (6.5)	.695	5 (11.9)	4 (8.9)	1 (10.0)	.891	5 (13.2)	4 (8.0)	1 (11.1)	.614
III	20 (90.9)	38 (86.4)	29 (93.5)		37 (88.1)	41 (91.1)	9 (90.0)		33 (86.8)	46 (92.0)	8 (88.9)	
ISS stage, No. (%)												
I and II	7 (31.8)	16 (36.4)	11 (35.5)	.934	15 (35.7)	17 (37.8)	2 (20.0)	.647	14 (36.8)	19 (38.0)	2 (22.2)	.742
III	15 (68.2)	28 (63.6)	20 (64.5)		27 (64.3)	28 (62.2)	8 (80.0)		24 (63.2)	31 (62.0)	7 (77.8)	
Immunoglobulin subtype, No. (%)												
IgG	14 (63.6)	18 (40.9)	14 (45.2)	.209	21 (50.0)	20 (44.4)	5 (50.0)	.895	17 (44.8)	25 (50.0)	4 (44.4)	.772
IgA	5 (22.7)	9 (20.5)	8 (25.8)		9 (21.4)	9 (20.0)	4 (40.0)		9 (23.7)	9 (18.0)	4 (44.4)	
IgM	1 (4.6)	0 (0)	1 (3.2)		1 (2.4)	1 (2.2)	0 (0)		0 (0)	2 (4.0)	0 (0)	
IgD	0 (0)	0 (0)	1 (3.2)		1 (2.4)	0 (0)	0 (0)		1 (2.6)	0 (0)	0 (0)	
Light chain only	2 (9.1)	14 (31.8)	7 (22.6)		9 (21.4)	13 (28.9)	1 (10.0)		10 (26.3)	12 (24.0)	1 (11.2)	
Nonsecretory	0 (0)	3 (6.8)	0 (0)		1 (2.4)	2 (4.5)	0 (0)		1 (2.6)	2 (4.0)	0 (0)	

Alb, albumin; ATIC, 5-amino-4-imidazolecarboxamide ribonucleotide transformylase/IMP cyclohydrolase; β2-MG, β2-microglobulin; Ca, calcium; Cr, creatinine; DS, Durie-Salmon staging; ESR, erythrocyte sedimentation rate; Hb, hemoglobin; ISS, International Staging System; LDH, lactate dehydrogenase; MM, multiple myeloma.

<sup>a</sup>P < .05.

**TABLE 5. Associations of ATIC Polymorphisms with Clinical Variables of Patients with MM**

Genotype	rs3772078			P Value	rs16853834			P Value
	TT (n = 45)	CT (n = 36)	CC (n = 16)		GG (n = 68)	GA (n = 25)	AA (n = 4)	
Sex, No. (%)								
Male	25 (55.6)	18 (50.0)	11 (68.8)	.454	38 (55.9)	13 (52.0)	3 (75.0)	.750
Female	20 (44.4)	18 (50.0)	5 (31.2)		30 (44.1)	12 (48.0)	1 (25.0)	
Age, No. (%)								
<60 y	28 (62.2)	16 (44.4)	8 (50.0)	.267	34 (50.0)	16 (64.0)	2 (50.0)	.454
≥60 y	17 (37.8)	20 (55.6)	8 (50.0)		34 (50.0)	9 (36.0)	2 (50.0)	
Hb, No. (%)								
<10 g/dL	32 (71.1)	31 (86.1)	12 (75.0)	.287	54 (79.4)	18 (72.0)	3 (75.0)	.674
≥10 g/dL	13 (28.9)	5 (13.9)	4 (25.0)		14 (20.6)	7 (28.0)	1 (25.0)	
Cr, No. (%)								
<2 mg/dL	35 (77.8)	29 (80.6)	12 (75.0)	.897	51 (75.0)	22 (88.0)	3 (75.0)	.410
≥2 mg/dL	10 (22.2)	7 (19.4)	4 (25.0)		17 (25.0)	3 (12.0)	1 (25.0)	
Alb, No. (%)								
<3.5 mg/dL	25 (55.6)	18 (50.0)	8 (50.0)	.861	35 (51.5)	15 (60.0)	1 (25.0)	.421
≥3.5 mg/dL	20 (44.4)	18 (50.0)	8 (50.0)		33 (48.5)	10 (40.0)	3 (75.0)	
Ca, No. (%)								
<11.5 mg/dL	42 (93.3)	35 (97.2)	15 (93.8)	.706	63 (92.6)	25 (100.0)	4 (100.0)	.451
≥11.5 mg/dL	3 (6.7)	1 (2.8)	1 (6.2)		5 (7.4)	0 (0)	0 (0)	
β2-MG, No. (%)								
<5.5 mg/L	17 (37.8)	13 (36.1)	6 (37.5)	.988	26 (38.2)	8 (32.0)	2 (50.0)	.682
≥5.5 mg/L	28 (62.2)	23 (63.9)	10 (62.5)		42 (61.8)	17 (68.0)	2 (50.0)	
LDH, No. (%)								
<220 U/L	33 (73.3)	25 (69.4)	12 (75.0)	.911	49 (72.1)	17 (68.0)	4 (100.0)	.552
≥220 U/L	12 (26.7)	11 (30.6)	4 (25.0)		19 (27.9)	8 (32.0)	0 (0)	
ESR, No. (%)								
<15 mm/60 min	5 (11.1)	3 (8.3)	2 (12.5)	.825	5 (7.4)	4 (16.0)	1 (25.0)	.163
≥15 mm/60 min	40 (88.9)	33 (91.7)	14 (87.5)		63 (92.6)	21 (84.0)	3 (75.0)	
Plasma cells, No. (%)								
<30%	29 (64.4)	21 (58.3)	8 (50.0)	.584	43 (63.2)	15 (60.0)	0 (0)	.051
≥30%	16 (35.6)	15 (41.7)	8 (50.0)		25 (36.8)	10 (40.0)	4 (100.0)	
DS stage, No. (%)								
I and II	5 (11.1)	4 (11.1)	1 (6.2)	1.000	8 (11.8)	2 (8.0)	0 (0)	.823
III	40 (88.9)	32 (88.9)	15 (93.8)		60 (88.2)	23 (92.0)	4 (100.0)	
ISS stage, No. (%)								
I and II	16 (35.6)	12 (33.3)	6 (37.5)	.954	25 (36.8)	6 (24.0)	3 (75.0)	.110
III	29 (64.4)	24 (66.7)	10 (62.5)		43 (63.2)	19 (76.0)	1 (25.0)	
Immunoglobulin subtype, No. (%)								
IgG	26 (57.8)	14 (38.9)	6 (37.5)	.397	30 (44.1)	14 (56.0)	2 (50.0)	.854
IgA	10 (22.2)	9 (25.0)	3 (18.8)		16 (23.6)	4 (16.0)	2 (50.0)	
IgM	1 (2.2)	1 (2.8)	0 (0)		2 (2.9)	0 (0)	0 (0)	
IgD	0 (0)	0 (0)	1 (6.2)		1 (1.5)	0 (0)	0 (0)	
Light chain only	7 (15.6)	11 (30.5)	5 (31.3)		17 (25.0)	6 (24.0)	0 (0)	
Nonsecretory	1 (2.2)	1 (2.8)	1 (6.2)		2 (2.9)	1 (4.0)	0 (0)	

Alb, albumin; ATIC, 5-amino-4-imidazolecarboxamide ribonucleotide transformylase/IMP cyclohydrolase; β2-MG, β2-microglobulin; Ca, calcium; Cr, creatinine; DS, Durie-Salmon staging; ESR, erythrocyte sedimentation rate; Hb, hemoglobin; ISS, International Staging System; LDH, lactate dehydrogenase; MM, multiple myeloma.

identified ATIC as an ARG.<sup>21</sup> Studies have shown that ATIC depletion or its transformylase activity suppression observably decreases the survival rate of cells, indicating that ATIC may promote can-

cer cell line proliferation and migration.<sup>6</sup> Therefore, ATIC may play an important role in carcinogenesis and the survival of cancer cells. Park and Shin<sup>9</sup> reported that the ATIC 347C > G (rs2372536)

**TABLE 6. Association of Serum LDH Levels with Clinical Variables**

Clinical Features	LDH (U/L)	t	P Value
Sex			
Male	180.76 ± 56.44	-2.143	.036 <sup>a</sup>
Female	224.42 ± 123.72		
Age			
<60 y	204.04 ± 112.47	0.438	.662
≥60 y	195.58 ± 69.17		
Hb			
<10 g/dL	201.57 ± 102.99	0.280	.780
≥10 g/dL	195.14 ± 58.44		
Cr			
<2 mg/dL	195.57 ± 98.00	-0.901	.370
≥2 mg/dL	216.57 ± 80.56		
Alb			
<3.5 mg/dL	178.53 ± 66.36	-2.428	.017 <sup>a</sup>
≥3.5 mg/dL	224.04 ± 114.22		
Ca			
<11.5 mg/dL	201.40 ± 9.87	0.574	.567
≥11.5 mg/dL	176.40 ± 67.09		
β2-MG			
<5.5 mg/L	177.58 ± 49.81	-2.174	.032 <sup>a</sup>
≥5.5 mg/L	213.41 ± 111.17		
ESR			
<15 mm/60 min	209.40 ± 51.34	0.327	.745
≥15 mm/60 min	199.05 ± 98.40		
Plasma cells			
<30%	190.55 ± 62.88	-1.079	.286
≥30%	214.33 ± 127.61		
DS stage			
I and II	200.40 ± 47.46	0.010	.992
III	200.08 ± 98.66		
ISS stage			
I and II	172.62 ± 46.64	-2.651	.009 <sup>a</sup>
III	214.95 ± 109.69		
Immunoglobulin subtype			
IgG	184.35 ± 48.65	0.885	.384
IgA	168.09 ± 79.34		

Alb, albumin; β2-MG, β2-microglobulin; Ca, calcium; Cr, creatinine; DS, Durie-Salmon staging; ESR, erythrocyte sedimentation rate; Hb, hemoglobin; ISS, International Staging System; LDH, lactate dehydrogenase.

<sup>a</sup>P < .05.

polymorphism may influence adenosine levels after MTX treatment, which may affect the histologic response of osteosarcoma. However, the rs2372536 polymorphism is not associated with MTX treatment outcomes.<sup>22</sup>

No previous studies have examined the relationship between ATIC rs7604984, rs2372536, rs4673993, rs3772078, and rs16853834 polymorphisms and MM. In this study, the genotype distribution or allele frequency of rs7604984, rs2372536, and rs4673993 was not markedly different between patients with MM and healthy control

**FIGURE 1. The association of serum lactate dehydrogenase (LDH) levels with different International Staging System (ISS) stages in multiple myeloma.**

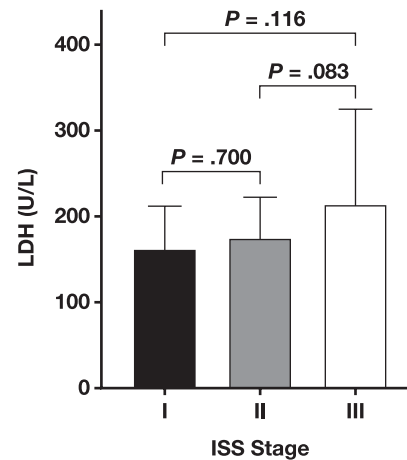


**FIGURE 2. The association of serum lactate dehydrogenase (LDH) levels with different sex in multiple myeloma.**

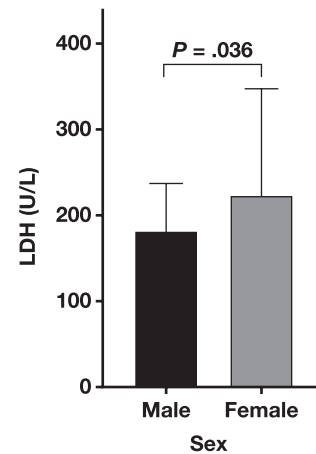
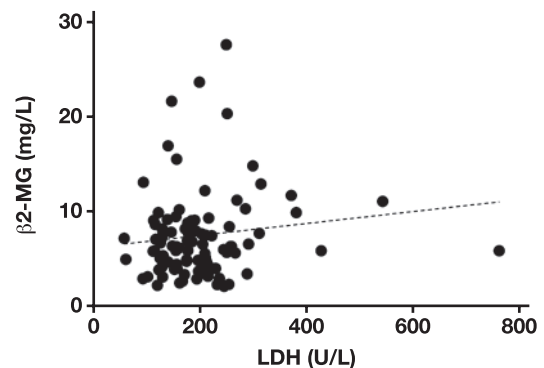


**FIGURE 3. Correlation between serum lactate dehydrogenase (LDH) levels and β2-microglobulin (β2-MG) in multiple myeloma.  $y = 0.006281x + 6.362$ .**



patients. However, ATIC rs3772078 and rs16853834 polymorphisms were associated with MM. Therefore, our results suggest that ATIC rs3772078 and rs16853834 polymorphisms are involved with susceptibility to MM in the Guangxi population.

In other studies, ATIC rs16853834 polymorphisms were associated with thiopurine metabolism in patients with Crohn's disease.<sup>23</sup> Owen et al<sup>24</sup> reported that the ATIC rs16853834 polymorphism was significantly associated with MTX efficacy. In our study, the results of binary logistic regression statistical analysis showed that ATIC rs7604984, rs2372536, and rs4673993 polymorphisms were not associated with MM risk after adjustments for age and sex (all  $P > .05$ ). However, the presence of the ATIC rs3772078 CT genotype significantly decreased MM risk. A similar association was observed for the C allele. Simulta-

neously, MM risk was decreased in patients carrying the rs16853834 A allele.

In addition, we performed LD analysis for all 5 SNPs in this study and determined that the rs3772078 and rs2372536, rs3772078 and rs4673993, rs2372536 and rs4673993, rs2372536 and rs7604984, and rs4673993 and rs7604984 SNP combinations had strong LD. One ATIC haplotype, CCGTG, was found to be correlated with MM in the Guangxi population and has a protective effect for MM. The TCATA and TGGCG haplotypes were found to be linked with a significant increased risk of MM. However, LD analysis and haplotype analysis require larger patient samples to further verify the association with MM.

We also investigated the relationship between ATIC polymorphisms and serum LDH levels using clinical variables. The results suggested that 4 ATIC loci polymorphisms (rs4673993, rs2372536, rs3772078, and rs16853834) were not associated with the clinical variables in patients with MM. We observed that the LDH level of patients in ISS stage III was significantly higher than that of patients in ISS stages I and II (TABLE 6). As noted in TABLE 4, more minor allele genotypes of rs7604984 were in patients in ISS stage III. These findings may indicate that ATIC rs7604984 was significantly associated with serum LDH levels in our results. In the future, we need to collect more clinical specimens from patients with MM for further confirmation.

Furthermore, the serum LDH levels in female patients with Alb  $\geq 3.5$  mg/dL and  $\beta 2$ -MG  $\geq 5.5$  mg/L were significantly higher than those of male patients with Alb  $< 3.5$  mg/dL and  $\beta 2$ -MG  $< 5.5$  mg/L. The serum LDH levels were significantly associated with the Alb levels. These results suggest that the serum LDH level can reflect disease severity in patients with MM and may predict prognosis. Studies have shown that LDH, a cellular enzyme widely distributed in many tissues, particularly the heart, liver, kidneys, and muscles, is the key enzyme that catalyzes the conversion of lactic acid to pyruvate, which can be significantly elevated in tissue hypoxia, malignant tumor diseases, and anemia.<sup>25,26</sup> Previous studies have shown that serum LDH levels are correlated with prognosis in patients with MM.<sup>27-31</sup> An abnormal serum LDH level is an independent prognostic factor for overall survival and progression-free survival.<sup>29</sup>

In summary, ATIC gene polymorphisms are correlated with MM. This study has several limitations in terms of the analysis and discussion processes. First, the number of specimens collected in this experiment was small, and a larger patient sample size was required to verify the results. Second, we collected blood specimens only from patients in the Guangxi region, which does not represent the entire Chinese population. Therefore, multicenter studies are necessary. Third, we studied only 5 gene loci polymorphisms. Thus, the results may not accurately reflect the relationship between ATIC polymorphisms and MM. Hence,

**FIGURE 4. Correlation between serum lactate dehydrogenase (LDH) levels and albumin in multiple myeloma.  $y = 0.002691x + 2.899$ .**

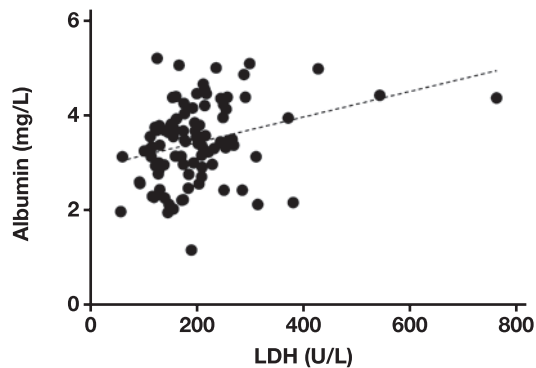


**TABLE 7. LD Analysis Among rs3772078, rs2372536, rs16853834, rs4673993, and rs7604984<sup>a</sup>**

SNPs	$D'$	$r^2$
rs3772078, rs2372536	0.928	0.339
rs3772078, rs16853834	0.366	0.029
rs3772078, rs4673993	0.905	0.335
rs2372536, rs4673993	0.883	0.754
rs2372536, rs7604984	1.000	0.563
rs16853834, rs4673993	0.215	0.007
rs4673993, rs7604984	0.902	0.473
rs2372536, rs16853834	0.314	0.016
rs16853834, rs7604984	0.272	0.021
rs3772078, rs7604984	0.405	0.115

LD, linkage disequilibrium; SNP, single-nucleotide polymorphism.

<sup>a</sup> $D'$  and  $r^2$  represent LD.  $D' = 0$ ,  $r^2 = 0$ : no LD;  $D' = 1$ ,  $r^2 = 1$ : complete LD;  $0.5 \leq D' < 0.8$ : moderate LD;  $D' > 0.8$ : strong LD.

**TABLE 8. Major Haplotype Frequencies of ATIC Gene in Patients with MM and Control Patients**

Haplotype	Frequency		$\chi^2$ P Value OR (95% CI)		
	Patients with MM	Control Patients			
CCGTA	54.48 (0.281)	53.40 (0.264)	0.067	.795739	1.061 (0.677–1.663)
CCGTG	9.17 (0.047)	20.51 (0.102)	4.449	.034965 <sup>a</sup>	0.428 (0.191–0.960)
TCATA	27.89 (0.144)	10.35 (0.051)	9.417	.002161 <sup>a</sup>	3.073 (1.458–6.477)
TCGTA	19.27 (0.099)	13.47 (0.067)	1.269	.259954	1.516 (0.732–3.141)
TGGCG	61.91 (0.319)	45.61 (0.226)	4.011	.045260 <sup>a</sup>	1.587 (1.008–2.498)

CI, confidence interval; MM, multiple myeloma; OR, odds ratio.

<sup>a</sup> $P < .05$ .

we need to explore the relationship between other ATIC loci and MM. Furthermore, we were unable to complete the survival analysis and follow-up of patients with MM because of the number of patients, time constraints, and patient death. Therefore, we will further expand the number of patients and invest more time and energy to collect survival information and follow up with patients in our future studies. Finally, there is still a need to explore the involvement of serum LDH levels in the prognosis of patients with MM.

## Conclusion

Our results indicate that the ATIC rs3772078 and rs16853834 polymorphisms contribute to a decreased MM risk. The ATIC rs7604984 polymorphism affects the clinical features of patients with MM. However, other SNPs do not affect these features. We also found that 5 SNP combinations in the ATIC gene showed strong LD and that the CCGTG haplotype has a protective effect for MM in the Guangxi population. However, the TCATA and TGGCG haplotypes were found to be linked with significant increased risk of MM. The serum LDH level reflects disease severity in patients with MM, and its level may predict patient prognosis. Because of the relatively small sample size (97 patients with MM), there were limitations to the interpretation of the results obtained in our analyses. Therefore, further investigations with larger patient sample sizes are needed to confirm our results.

## Acknowledgments

Ruolin Li drafted the overall design of this article. Zuojian Hu, Chunni Huang, and Yibin Yao collected resources for the blood specimens. Yu Wang, Zhian Ling, and Ying Gui conducted the experiments. Yu Wang, Zhian Ling, Zuojian Hu, and Ruolin Li conducted data curation and analyzed the data using software. Yu Wang wrote the original draft article. Ruolin Li and Zhian Ling reviewed and edited the original draft.

## Funding

This study was supported by grants from Guangxi Natural Science Foundation (2020JJA140382), Guangxi Province Health Technology Development and Application Project (number S2018076), the Research Foundation of Guangxi Education Department (No. 2019KY0107), Science and technology plan project of Qingxiu region of Guangxi, Nanning (No. 2019027), and Innovation Project of Guangxi Graduate Education (No. YCSW2022224).

## REFERENCES

- Röllig C, Knop S, Bornhäuser M. Multiple myeloma. *The Lancet* 2015;385:2197–2208.
- Siegel RL, Miller KD, Jemal A. Cancer statistics, 2020. *CA Cancer J Clin*. 2020;70:7–30.
- Corre J, Munshi N, Avet-Loiseau H. Genetics of multiple myeloma: another heterogeneity level? *Blood*. 2015;125:1870–1876.
- Morrison T, Booth RA, Hauff K, et al. Laboratory assessment of multiple myeloma. *Adv Clin Chem*. 2019;89:1–58.
- Beardsley GP, Rayl EA, Gunn K, et al. Structure and functional relationships in human pur H. *Adv Exp Med Biol*. 1988;431:221–226.

- Liu X, Paila UD, Teraoka SN, et al. Identification of ATIC as a novel target for chemoradiosensitization. *Int J Radiat Oncol Biol Phys*. 2018;100:162–173.
- Verma P, Kar B, Varshney R, et al. Characterization of AICAR transformylase/IMP cyclohydrolase (ATIC) from *Staphylococcus lugdunensis*. *FEBS J*. 2017;284:4233–4261.
- Lee YH, Bae SC. Association of the ATIC 347 C/G polymorphism with responsiveness to and toxicity of methotrexate in rheumatoid arthritis: a meta-analysis. *Rheumatol Int*. 2016;36:1591–1599.
- Park JA, Shin HY. ATIC gene polymorphism and histologic response to chemotherapy in pediatric osteosarcoma. *J Pediatr Hematol Oncol*. 2017;39:e270–e274.
- Jiang YC, Kuang LL, Sun SN, et al. Association of genetic polymorphisms of de novo nucleotide biosynthesis with increased CHD susceptibility in the northern Chinese population. *Clin Genet*. 2017;91:748–755.
- Kenific CM, Debnath J. Cellular and metabolic functions for autophagy in cancer cells. *Trends Cell Biol*. 2015;25:37–45.
- Kenific CM, Thorburn A, Debnath J. Autophagy and metastasis: another double-edged sword. *Curr Opin Cell Biol*. 2010;22:241–245.
- Zhu FX, Wang XT, Zeng HQ, et al. A predicted risk score based on the expression of 16 autophagy-related genes for multiple myeloma survival. *Oncol Lett*. 2019;18:5310–5324.
- Li R, Chen G, Dang Y, et al. Upregulation of ATIC in multiple myeloma tissues based on tissue microarray and gene microarrays. *Int J Lab Hematol*. 2020;43:1–9.
- Barlogie B, Bolejack V, Schell M, et al. Prognostic factor analyses of myeloma survival with intergroup trial S9321 (INT 0141): examining whether different variables govern different time segments of survival. *Ann Hematol*. 2011;90:423–428.
- Chen YK, Han SM, Yang Y, et al. Early mortality in multiple myeloma: experiences from a single institution. *Hematology*. 2016;21:392–398.
- Gu Y, Yuan YH, Xu J, et al. High serum lactate dehydrogenase predicts an unfavorable outcome in Chinese elderly patients with multiple myeloma. *Oncotarget*. 2017;8:48350–48361.
- Li R, Hu Z, Chen H, et al. Association of growth differentiation factor-15 polymorphisms and growth differentiation factor-15 serum levels with susceptibility to multiple myeloma in a Chinese population. *Clin Lab*. 2021;67. doi: 10/7754/Clin. Lab.2020.200341.
- Shi YY, He L. SHEsis, a powerful software platform for analyses of linkage disequilibrium, haplotype construction, and genetic association at polymorphism loci. *Cell Res*. 2005;15:97–98.
- Amaravadi RK, Kimmelman AC, Debnath J. Targeting autophagy in cancer: recent advances and future directions. *Cancer Discov*. 2019;9:1167–1181.
- Moussay E, Kaoma T, Baginska J, et al. The acquisition of resistance to TNF $\alpha$  in breast cancer cells is associated with constitutive activation of autophagy as revealed by a transcriptome analysis using a custom microarray. *Autophagy*. 2011;7:760–770.
- Qiu Q, Huang J, Shu X, et al. Polymorphisms and pharmacogenomics for the clinical efficacy of methotrexate in patients with rheumatoid arthritis: a systematic review and meta-analysis. *Sci Rep*. 2017;7:44015.
- Choi R, Lee MN, Kim K, et al. Effects of various genetic polymorphisms on thiopurine treatment-associated outcomes for Korean patients with Crohn's disease. *Br J Clin Pharmacol*. 2020;86:2302–2313.
- Owen SA, Hider SL, Martin P, et al. Genetic polymorphisms in key methotrexate pathway genes are associated with response to treatment in rheumatoid arthritis patients. *Pharmacogenomics J*. 2013;13:227–234.
- Fujiwara S, Kawano Y, Yuki H, et al. PDK1 inhibition is a novel therapeutic target in multiple myeloma. *Br J Cancer*. 2013;108:170–178.

26. Teke HU, Basak M, Teke D, et al. Serum level of lactate dehydrogenase is a useful clinical marker to monitor progressive multiple myeloma diseases: a case report. *Turk J Haematol*. 2014;31:84–87.
27. Chim CS, Sim J, Tam S, et al. LDH is an adverse prognostic factor independent of ISS in transplant-eligible myeloma patients receiving bortezomib-based induction regimens. *Eur J Haematol*. 2015;94:330–335.
28. Gkatzamanidou M, Kastritis E, Gavriatopoulou MR, et al. Increased serum lactate dehydrogenase should be included among the variables that define very-high-risk multiple myeloma. *Clin Lymphoma Myeloma Leuk*. 2011;11:409–413.
29. Jimenez-Zepeda VH, Duggan P, Neri P, et al. Revised International Staging System applied to real world multiple myeloma patients. *Clin Lymphoma Myeloma Leuk*. 2016;16:511–518.
30. Palumbo A, Avet-Loiseau H, Oliva S, et al. Revised International Staging System for multiple myeloma: a report from International Myeloma Working Group. *J Clin Oncol*. 2015;33:2863–2869.
31. Terpos E, Katodritou E, Roussou M, et al. High serum lactate dehydrogenase adds prognostic value to the international myeloma staging system even in the era of novel agents. *Eur J Haematol*. 2010;85:114–119.

# Cutoff Value of Qualitative HBsAg for Confirmatory HBsAg Using the Chemiluminescence Microparticle Immunoassay Method

Merci Monica Pasaribu, MD, PhD,<sup>1,\*</sup> Jessica Purwanti Wonohutomo, MD,<sup>1</sup> Suzanna Immanuel, MD,<sup>1</sup> July Kumalawati, MD,<sup>1</sup> Nuri Dyah Indrasari, MD,<sup>1</sup> and Yusra Yusra, MD, PhD<sup>1</sup>

<sup>1</sup>Department of Clinical Pathology, Faculty of Medicine University of Indonesia/National General Hospital Dr Cipto Mangunkusumo, Jakarta, Indonesia  
\*To whom correspondence should be addressed. [mercipasaribu@gmail.com](mailto:mercipasaribu@gmail.com)

**Keywords:** CMIA; HBsAg Qualitative II; HBsAg Qualitative II Confirmatory; hepatitis B, S/CO value, false positive

**Abbreviations:** HBV, hepatitis B virus; WHO, World Health Organization; HBsAg, hepatitis B surface antigen; RSUPNCM, Central Laboratory of the National Central General Hospital Dr Cipto Mangunkusumo; CMIA, chemiluminescence microparticle immunoassay; ECLIA, electrochemiluminescence immunoassay; ELFA, enzyme-linked fluorescent assay

*Laboratory Medicine* 2022;53:475–478; <https://doi.org/10.1093/labmed/lmac021>

## ABSTRACT

**Background:** Confirmatory hepatitis B surface antigen (HBsAg) is an assay used to distinguish weakly reactive from false-positive HBsAg results.

**Objective:** To determine the signal to cutoff (S/CO) value of chemiluminescence microparticle immunoassay (CMIA) HBsAg assay that should trigger follow-up confirmatory HBsAg testing.

**Methods:** All specimens with an initial S/CO value of 0.90–100.00 were subjected to repeat HBsAg testing after high-speed centrifugation. The specimens with an initial S/CO value in that range remained in the same range and were then followed up with confirmatory HBsAg testing.

**Result:** In total, 132 specimens had an S/CO value between 0.90 and 100.00 after high-speed centrifugation, followed by confirmatory HBsAg retesting. The S/CO value of HBsAg specimens for which the results required verification with confirmatory HBsAg was 0.98 (100% sensitivity, 3.3% specificity) through 9.32 (47.1% sensitivity, 100% specificity).

**Conclusion:** The HBsAg S/CO values (as determined by the chemiluminescent microparticle immunoassay [CMIA] method) that should trigger confirmatory HBsAg testing are 0.98–9.32.

Hepatitis B virus (HBV) infection has, until recently, remained one of the most prevalent diseases around the world. A report by the World Health Organization (WHO) in 2017 states that approximately 257 million people worldwide were infected with HBV.<sup>1</sup> The international prevalence of HBV infection in 2015 was approximately 3.5%, with the highest prevalence in the Pacific region, Africa, and Southeast Asia.<sup>1,2</sup> Data obtained by Indonesian Basic Health Research in 2017 showed that the prevalence of HBV infection in the Indonesian population was 7.1%, and 2.7% of pregnant women have reactive hepatitis B surface antigen (HBsAg) test results.<sup>3</sup> Approximately 90% of perinatal infections will progress to chronic HBV, which is the most prevalent cause of liver cirrhosis and hepatocellular carcinoma.<sup>2,4</sup>

HBsAg is a serological marker widely utilized in screening and diagnostic testing for HBV infection.<sup>5</sup> The WHO guideline recommends routine use of the HBsAg marker for antenatal screening in countries with a high prevalence of HBV infection ( $\geq 2\%$ ).<sup>6</sup> Improvement in the analytical sensitivity of the HBsAg assay increased the detection rate and allowed earlier diagnosis. However, the risks of having weakly reactive and false-positive results were also increased. Use of confirmatory HBsAg assay aids clinicians in differentiating weakly reactive from false-positive results. In wealthy countries in Europe and North America, all reactive HBsAg results, particularly borderline-reactive results, must be followed up with a repeated HBsAg test and confirmatory HBsAg testing, to ensure the accuracy of the laboratory results and to prevent unnecessary treatment.<sup>7</sup> However, if all HBsAg tests are followed up with confirmatory assays, patient management may be delayed, and the cost of laboratory testing may increase.

The HBsAg assay at the Central Laboratory of the National Central General Hospital Dr Cipto Mangunkusumo (RSUPNCM) in Jakarta, Indonesia, currently uses the chemiluminescence microparticle immunoassay (CMIA) method, which has 98% sensitivity and 97% specificity.<sup>8</sup> There are no official guidelines on which signal to cutoff (S/CO) values determined by the CMIA method should trigger follow-up testing with

a confirmatory assay; as a result, the range values may vary among laboratories.

To perform a confirmatory assay on all reactive specimens in our study would have been too costly because nearly all of the specimens were from patients with only limited coverage provided by the Indonesian National Health Insurance. The results of previous studies<sup>7,9–11</sup> performed with different qualitative HBsAg assay methods have shown that the weakly reactive specimens (specimens with low cut-off index values) were the ones for which results should be verified using a confirmatory assay. Therefore, it is crucial to determine the reactive S/CO values that should trigger confirmatory HBsAg assay, so that the accuracy of the test results can be improved, therapy can be administered more quickly and more accurately, and the principles of quality and cost control can be applied. The objective of this study was to determine the S/CO values of HBsAg, determined using the CMIA method, that should trigger confirmatory testing, so that confirmatory testing can be carried out more selectively and efficiently.

## Materials and Methods

### Blood Specimens

A total of 19,645 specimens, from the emergency unit, inpatient ward, and outpatient clinic, were tested for HBsAg from October 2019 through June 2020 in our hospital central laboratory. All specimens were collected in plain tubes and were stored at room temperature before and during the HBsAg testing and confirmatory HBsAg testing. Serum specimens were isolated using centrifugation for 5 minutes at 2500g and immediately tested for HBsAg. All specimens for which the initial S/CO value was 0.90–100.00 were subjected to repeated HBsAg testing after high-speed centrifugation for 15 minutes at 16,000g. High-speed centrifugation was performed to reduce the possibility of lipemia, fibrin interference, or other particulate matter interference in the assay.<sup>12–14</sup> The specimens with S/CO values remained in the range of 0.90–100.00; those values triggered confirmatory HBsAg testing. For all specimens, confirmatory HBsAg testing was performed within less than 6 hours from when the specimens arrived in the laboratory.

### HBsAg and Confirmatory HBsAg Testing

The determination of serum HBsAg was performed using the HBsAg Qualitative II (REF 2G22) reagents on the ARCHITECT i2000 analyzer (Abbott Diagnostics). Every specimen was tested twice for HBsAg, once before and once after high-speed centrifugation. The specimens with S/CO remained in the range of 0.90–100.00 were then subjected to confirmatory testing using the HBsAg Qualitative II Confirmatory (REF 2G23) reagents on the ARCHITECT i1000 analyzer. Imprecision tests using positive and negative control materials were performed for the HBsAg assay (CV, 1.81% and 6.96%, respectively); positive control material was used for the confirmatory HBsAg assay (CV, 1.41%).

The ARCHITECT i2000 and i1000 analyzers used the CMIA method. In the Architect HBsAg Qualitative II assay, serum specimens, anti-HBs coated paramagnetic microparticles, and anti-HBs acridinium-labeled conjugate underwent reactions. HBsAg present in the specimen binds to anti-HBs coated microparticles and to anti-HBs acridinium-labeled conjugate. The resulting chemiluminescent reaction is measured and

compared to the cutoff signal. If the signal in the specimen is greater than or equal to the cutoff signal ( $S/CO \geq 1.00$ ), the specimen is considered to be reactive for HBsAg.<sup>13</sup>

The ARCHITECT HBsAg Qualitative II Confirmatory assay is based on the neutralization procedure that utilizes human anti-HBs. There are 2 different pretreatment reagents in the assay. Pretreatment reagent 1 contains human anti-HBs, whereas pretreatment reagent 2 does not. Each of the pretreatment reagents is incubated with the specimen material in different reaction vessels in the analyzer. The neutralized HBsAg in the specimen is blocked from binding to the anti-HBs coated microparticles. A specimen is considered to have tested positive if the signal for the nonneutralized specimen (incubated with pretreatment reagent 2) result is greater than or equal to the cutoff ( $S/CO \geq 0.70$ ) and the signal of the neutralized specimen (incubated with pretreatment reagent 1) is reduced by at least 50% compared with the nonneutralized specimen.<sup>15</sup> The interpretation of the confirmatory result of each specimen was automatically performed by the analyzer, and the result was shown on the analyzer screen.

### Statistical Analysis

We analyzed the data using SPSS, version 20 (IBM) and Excel, version 2016 (Microsoft). The specimens were grouped based on the S/CO values and confirmatory HBsAg results. The difference of S/CO values after high-speed centrifugation between the group with the reactive confirmatory HBsAg results and the group with the nonreactive confirmatory HBsAg results was analyzed using Mann-Whitney testing. ROC analysis was performed to determine the S/CO value after high-speed centrifugation.

### Results

There were 161 specimens with initial S/CO values of 0.90–100.00; these specimens were subjected to high-speed centrifugation and repeat HBsAg testing. Of the 132 specimens with S/CO values of 0.90–100.00 after high-speed centrifugation, 102 specimens were confirmed as being reactive, via confirmatory HBsAg assay. The discrepancy between the HBsAg and confirmatory HBsAg results was found in 22.7% of the specimens with S/CO values of 0.90–100.00 (30 of 132 specimens). There were 18,290 true-negative specimens, so the false-positive rate of the qualitative HBsAg assay in this study was 0.16%. The characteristics

**TABLE 1. Characteristics of Study Patients and Their Specimen Results**

Variable	Confirmed Reactive, No. <sup>a</sup>	Nonreactive, No. <sup>b</sup>	Total <sup>c</sup>
Age range (y), mean (SD)	49.97 (16.8)	44.9 (15.9)	48.9 (16.7)
0–18, No.	5	2	7
19–40, No.	19	5	24
41–60, No.	52	19	71
>60, No.	26	4	30
Sex, No. (%)			
Male	64 (62.7)	15 (50.0)	79 (59.8)
Female	38 (37.3)	15 (50.0)	53 (40.2)

<sup>a</sup>*n* = 102.

<sup>b</sup>*n* = 30.

<sup>c</sup>*n* = 132.

of subjects whose blood specimens included in this study are listed in **TABLE 1**.

We observed a greater percentage of confirmed reactive HBsAg results in the group with higher S/CO values. Specimens with S/CO values after high-speed centrifugation of 0.90–5.00 had 59.1% confirmed reactive results, whereas 100% were confirmed as reactive in the group with S/CO values of >10.00 (**TABLE 2**).

The median of the S/CO values after high-speed centrifugation in the confirmed reactive group was 8.25, whereas it was 1.68 in the nonreactive group ( $P < .001$ ). ROC analysis was performed for S/CO values after the high-speed centrifugation was completed. The range of S/CO values that triggered mandatory confirmatory HBsAg test was analyzed. The lower limit was the S/CO value with 100% sensitivity and the highest specificity, and the upper limit was the S/CO value with the specificity of 100% and the highest sensitivity (**FIGURE 1**). Based on the results of our ROC analysis, S/CO values of 0.98 (100% sensitivity, 3.3% specificity) to 9.32 (47.1% sensitivity, 100% specificity) should trigger confirmatory HBsAg assay. The AUC was 83.3%, with a  $P$  value of  $< .001$  (**FIGURE 2**).

The clinical profile of subject individuals with discrepant HBsAg results (reactive initial HBsAg results but nonreactive confirmatory HBsAg results) was based on the diagnosis stated in the medical records. The most common diagnoses found were hypertension, diabetes mellitus, chronic kidney disease, and community-acquired pneumonia. Most of the subjects had more than 1 of the previously stated diagnoses.

**TABLE 2. Confirmatory HBsAg Results Based on HBsAg S/CO Values**

S/CO Values After High-Speed Centrifugation	Confirmed Reactive, No.	Nonreactive, No.	Total Specimens, No.
0.90–5.00	39	27	66
5.01–10.00	17	3	20
10.01–100.00	46	0	46
Total specimens	102	30	132

HBsAg, hepatitis B surface antigen; S/CO, signal to cutoff.

## Discussion

Laboratory testing plays an important role in diagnosing and monitoring HBV infection, with HBsAg as the most frequent serological marker being tested.<sup>16</sup> Reactive HBsAg test results indicate HBV infection. However, the window period between the disappearance of HBsAg and the emergence of anti-HBs in patient serum sometimes makes diagnosing HBV infection more complicated.<sup>7</sup> Using high-sensitivity HBsAg assay could partially solve the problem but would also increase the risk of false-positive results. Most false-positive results originated from the weakly reactive specimens.<sup>17</sup>

The percentage of the HBsAg specimens that needed to be followed up with confirmatory HBsAg testing in this study was less than 1%; this value was quite similar to the value reported by Shao et al.<sup>7</sup> Most of the specimens included were from men with a mean age of 48.9 years. The results were in accordance with the positive HBsAg prevalence in Indonesia, which is highest in men and within the group aged 45–49 years.<sup>18</sup>

Most of the specimens (77%) included in this research had reactive confirmatory results, in accordance with the findings of previous studies conducted with a different HBsAg assay method. Our results showed that mostly weakly reactive HBsAg specimens would be confirmed to be reactive via the HBsAg confirmatory assay, with the median S/CO of the reactive confirmatory group being significantly higher than the nonreactive one. The findings of previous studies from Shao et al.<sup>7</sup> and Sholikhah et al.<sup>11</sup> using the electrochemiluminescence immunoassay (ECLIA) method also yielded reactive confirmatory HBsAg results in approximately 60% and 88% of weakly reactive HBsAg specimens, respectively. The results of this study were also in line with the research performed by Purnamawaty et al.,<sup>10</sup> for which the results included reactive confirmatory HBsAg results in 63.8% of the HBsAg specimens examined using the enzyme-linked fluorescent assay (ELFA) method.

The range of the S/CO values in HBsAg testing that should trigger confirmatory testing, as determined in this study, was based on the lowest and the highest S/CO cutoff values. The lowest cutoff value is the S/CO value with 100% sensitivity and the highest specificity, such that all the reactive HBsAg specimens that need to be confirmed will be included. The highest cutoff value is the S/CO value with 100% specificity and the highest sensitivity, such that all the test specimens not requiring a confirmatory HBsAg

**FIGURE 1. Range of signal to cutoff (S/CO) values that must be followed by confirmatory hepatitis B surface antigen assay: sensitivity/specificity of various S/CO cutoff values.**

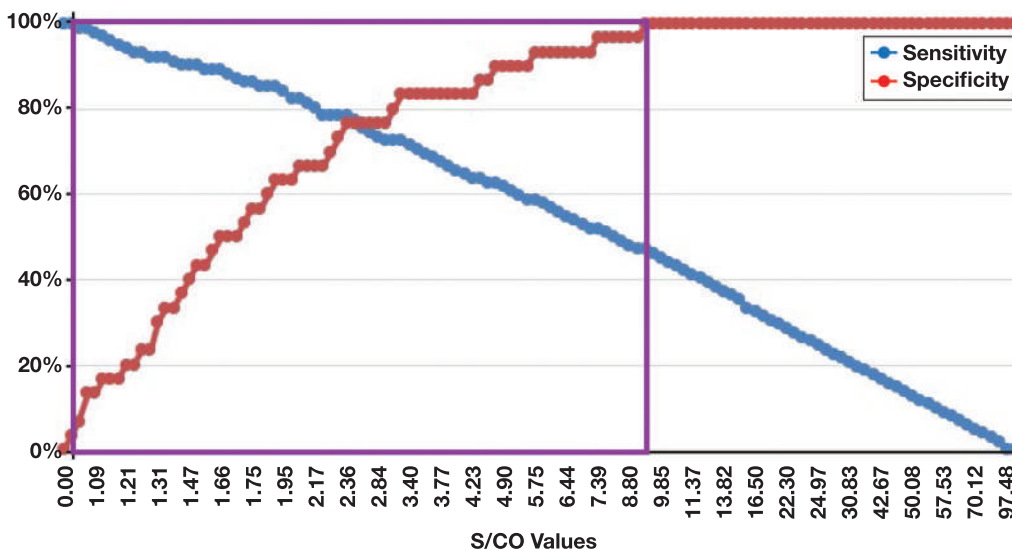
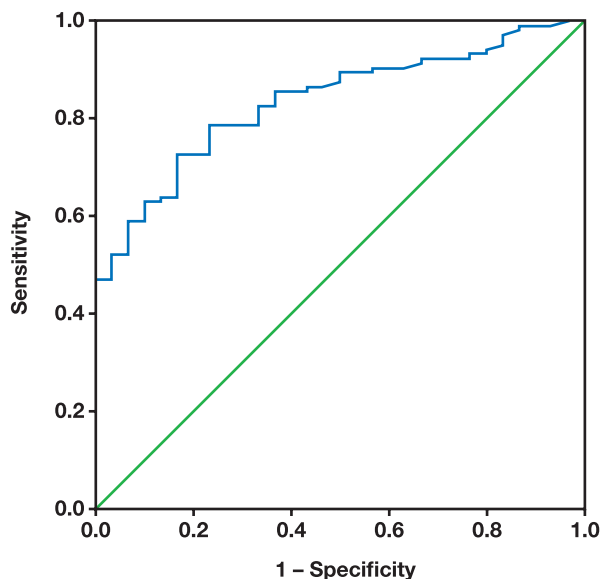


**FIGURE 2.** Receiver operating characteristic curve of signal to cutoff values after high-speed centrifugation (area under the curve, 83.3% [ $P < .001$ ]).



test will be excluded. Thus, the range of the HBsAg S/CO values that should trigger confirmatory HBsAg testing is 0.98–9.32.

In this study, all 30 specimens with nonreactive confirmatory testing results had S/CO of  $<10.00$ , and all specimens that had S/CO of  $>10.00$  were confirmed as reactive. The percentage of confirmed reactive specimens was greater in the group of specimens with a higher S/CO value. Most of the specimens with nonreactive confirmatory testing results had S/CO of  $<5.00$ . These results may become a basis in determining the HBsAg S/CO value that merits confirmatory HBsAg testing using the CMIA method.

Chang et al<sup>19</sup> mentioned that discrepant HBsAg results could be found in patients with chronic kidney disease receiving hemodialysis. Arleevskaya et al<sup>20</sup> reported that rheumatoid-factor formation could be triggered by bacterial infections such as *Klebsiella pneumoniae* or *Chlamydia pneumoniae* infection. Xu et al<sup>21</sup> found that rheumatoid-factor interference could increase or decrease the S/CO value in HBsAg assays using the ELISA method. However, the causes of discrepant HBsAg results in our study cannot be ascertained, due to limited information regarding the cause of pneumonia and the fact that no further testing was performed to examine the rheumatoid factor levels in the specimens.

## Conclusion

Based on the results of this study, the values of HBsAg S/CO determined via the CMIA method that need to be followed by confirmatory HBsAg tests were 0.98–9.32. Therefore, confirmatory HBsAg testing can be carried out more selectively and efficiently than in the past. Still, further studies are needed to determine the possible cause(s) of results discrepancies in HBsAg detection using the CMIA method.

## Personal and Professional Conflicts of Interest

The reagents used in this study were supplied by PT Abbott Products Indonesia.

## REFERENCES

- World Health Organization. Global hepatitis report, 2017. 2017. <https://www.who.int/hepatitis/publications/global-hepatitis-report2017/en/>. Accessed July 27, 2019.
- Thio CL, Hawkins C. Hepatitis B virus and hepatitis Delta virus. In: Bennett JE, Dolin R, Blaser MJ, eds. *Mandell, Douglas and Bennett's Principles and Practice of Infectious Diseases*. 8th ed. Philadelphia, PA: Elsevier Saunders; 2015:1815–1839.e7.
- Pusat Data dan Informasi Kemenkes RI. The situation of hepatitis B disease in Indonesia in 2017 [article in Indonesian]. 2017. <https://pusdatin.kemkes.go.id/article/view/18122600001/situasi-penyakit-hepatitis-b-di-indonesia-tahun-2017.html>. Accessed July 27, 2019.
- Veselsky SL, Walker TY, Fenlon N, Teo CG, Murphy TV. Discrepant hepatitis B surface antigen results in pregnant women screened to identify hepatitis B virus infection. *J Pediatr*. 2014;165(4):773–778.
- World Health Organization. Hepatitis B. <https://www.who.int/news-room/fact-sheets/detail/hepatitis-b>. Accessed July 27, 2019.
- World Health Organization. Guidelines on hepatitis B and C testing. 2017. doi: 10.1007/s00216-014-7926-1.
- Shao H, Li Y, Xu W, Zhou X. Increased need for testing to confirm initial weakly reactive results for hepatitis B virus surface antigen. *Lab Med*. 2012;43(4):15–17.
- İnan N, Demirel A, Ünsür EK, et al. Comparison of chemiluminescence microparticle immunoassay and electrochemiluminescence immunoassay for detection of HBsAg. *Viral Hepatitis J*. 2015;20(3):101–105.
- Chu F-Y, Su F-H, Cheng S-H, et al. Hepatitis B surface antigen confirmatory testing for diagnosis of hepatitis B virus infection in Taiwan. *J Med Virol*. 2011;83(9):1514–1521.
- Purnamawaty S, Handayani I, Nurulita A, Bahrun U. Determination of reactive HBsAg cut-off that need confirmatory test. *Indones J Clin Pathol Med Lab*. 2018;24(3):261–265.
- Sholikah A, Intansari US, Sukorini U. Determination of reactive HBsAg cutoff index (COI) based on confirmatory HBsAg assay in Dr. Sardjito General Hospital Yogyakarta [article in Indonesian]. 2018. <http://etd.repository.ugm.ac.id/penelitian/detail/155740>. Accessed July 27, 2019.
- Kasmierczak SC. Interferences of hemolysis, lipemia, and high bilirubin on laboratory tests. In: Dasgupta A, Sepulveda JL, eds. *Accurate Results in the Clinical Laboratory: A Guide to Error Detection and Correction*. 2nd ed. Philadelphia, PA: Elsevier; 2019:57–67.
- ARCHITECT System HBsAg Qualitative II [package insert]. Abbott Laboratories; 2013.
- Gaće M, Prskalo ZS, Dobrijević S, Mayer L. Most common interferences in immunoassays. *Libri Oncol*. 2015;43(1–3):23–27.
- ARCHITECT System HBsAg confirmatory assay [package insert]. Abbott Laboratories; 2014.
- Turgeon ML. Viral hepatitis. In: Turgeon ML, ed. *Immunology and Serology in Laboratory Medicine*. 6th ed. Philadelphia, PA: Elsevier; 2018:286–315.
- Dufour DR. Hepatitis B surface antigen (HBsAg) assays—are they good enough for their current uses? *Clin Chem*. 2006;52(8):1457–1459.
- Muljono DH. Epidemiology of hepatitis B and C in Republic of Indonesia. *Euroasian J Hepatogastroenterol*. 2017;7(1):55–59.
- Chang J-M, Huang C-F, Chen S-C, et al. Discrepancy between serological and virological analysis of viral hepatitis in hemodialysis patients. *Int J Med Sci*. 2014;11(5):436–441.
- Arleevskaya MI, Kravtsova OA, Lemerle J, Renaudineau Y, Tsibulkin AP. How rheumatoid arthritis can result from provocation of the immune system by microorganisms and viruses. *Front Microbiol*. 2016;7:1–14.
- Xu L, Wang X, Ma R, et al. False decrease of HBsAg S/CO values in serum with high-concentration rheumatoid factors. *Clin Biochem*. 2013;46(9):799–804.

# Elevated Lactate Dehydrogenase Concentrations in Plasma Compared to Serum

Crystal Bockoven, MD,<sup>1,2</sup> Robert C. Benirschke, PhD,<sup>1,2</sup> and Hong-Kee Lee, PhD<sup>1,2\*</sup>

<sup>1</sup>Department of Pathology and Laboratory Medicine, NorthShore University HealthSystem, Evanston, IL, USA; and <sup>2</sup>Department of Pathology, University of Chicago Pritzker School of Medicine, Chicago, IL, USA  
\*To whom correspondence should be addressed. [hlee@northshore.org](mailto:hlee@northshore.org)

**Keywords:** clinical chemistry, oncology, lactate dehydrogenase, plasma, serum, platelets

**Abbreviations:** LDH, lactate dehydrogenase; RBC, red blood cell; WBC, white blood cell; SST, serum separator tubes; PST, plasma separator tubes; CI, confidence interval.

*Laboratory Medicine* 2022;53:479–482; <https://doi.org/10.1093/labmed/lmac026>

## ABSTRACT

**Objective:** To evaluate the difference in lactate dehydrogenase (LDH) concentrations in plasma vs serum specimens in our patient population.

**Materials and Methods:** We measured LDH in 110 paired plasma and serum specimens over a 2-week period. Hemolytic indices were performed on each specimen. These paired specimens were drawn in a single setting and stored under the same conditions. For the last 14 paired specimens, cell counts were performed on the plasma/serum.

**Results:** Plasma LDH was on average 22% higher than serum LDH. There was no difference in the hemolytic indices between the plasma and the serum specimens. In the last 14 specimens, cell counts revealed increased platelets in the plasma specimens compared to the serum specimens.

**Conclusion:** We propose switching back to using serum for LDH testing because there was unpredictable elevation in plasma LDH concentrations. These elevations in LDH levels may be linked to the platelets present in plasma and that may lyse or become activated with storage at refrigerated temperature.

Lactate dehydrogenase (LDH) is an enzyme that plays an important role in cellular energy production and is present in many different tissues including the heart, liver, kidney, muscle, and blood. Elevated levels of LDH in serum can be used clinically to aid in disease monitoring, evaluating treatment, and predicting prognosis. Serum LDH may be elevated in multiple malignancies including lymphomas and leukemias. In some hematologic malignancies, it plays an important role as a prognostic marker. In addition, LDH may be monitored regularly in some malignancies because elevations in LDH levels could suggest disease progression or disease relapse. Serum LDH is useful in monitoring for disease progression because it is measured using a noninvasive test; elevation of serum LDH can also serve as a prompt for further and more expensive diagnostic evaluations. False elevations in LDH can lead to unnecessary investigations and anxiety in patients.

Serum LDH can be separated into multiple different isoenzymes, with each isoenzyme being a tetramer made up of 2 different subunits. Studies have shown that LDH is an intracellular enzyme that is released during cellular damage.<sup>1</sup> For this reason, LDH levels are susceptible to false elevations when any in vitro cell lysis occurs. Common examples include red blood cell (RBC), white blood cell (WBC), and platelet lysis.

When our hospital implemented total laboratory automation, the preferred specimen type was switched from serum to plasma. The switch was made to accommodate more chemistry tests in a single tube to reduce blood loss. Our oncologists who used LDH concentrations to monitor disease progression in their patients with hematologic malignancies noticed an increased number of results above the reference range. Upon further investigation, these patients had no other evidence of disease progression except elevated LDH results. This finding led the oncologists to alert the laboratory to look into the validity of our reference range. A few articles have described clinically significant increases in LDH in heparinized plasma specimens compared to serum specimens on the Roche analyzer.<sup>2-5</sup> However, the reason has not been clearly stated. Hence, the goal of our study was to evaluate whether there was a difference in LDH levels in heparinized plasma compared to serum and to postulate the possible reasons for differences. With the lack of literature explaining the differences in serum vs plasma LDH levels, we hope this information and awareness will be useful to other laboratories if they are experiencing similar challenges.

## Materials and Methods

### Specimen Selection

Paired plasma and serum specimens were used for the study. The 110 specimens were randomly selected, without knowing the patient diagnosis. The median age of the patients was 67 years, with an interquartile range between ages 54 and 76 years. Sex distribution included 70 women (64%) and 40 men (36%). The paired specimens were drawn in a single setting. Serum was collected in serum separator tubes (SST) and plasma was collected in plasma separator tubes (PST) containing lithium heparin. All collection tubes were from Becton Dickinson (Becton Dickinson, NJ).

The specimens were stored at refrigerated temperature for 1 day before analysis. Paired serum and plasma specimens were analyzed at the same time.

### LDH Analysis

One hundred ten paired serum and plasma specimens were collected over a 2-week period. The LDH analyses were performed using the Roche cobas c502 analyzer (Roche Diagnostics, IN). Hemolytic indices were performed on each specimen. In the Roche LDH assay, LDH catalyzes the conversion of L-lactate to pyruvate and reduces nicotinamide adenine dinucleotide in the process. The catalytic LDH activity is proportional to the initial rate of nicotinamide adenine dinucleotide plus hydrogen formation and is determined by photometrically measuring the increase in absorbance. For the last 14 paired specimens, cell counts were performed using a Sysmex XN-9000 analyzer (Sysmex America, IL) to evaluate whether there were cells present in the plasma or serum. Deming regression and Bland-Altman difference plots were used to analyze the data.

### LDH Analysis in Donor Platelets

We measured LDH in 10 donor platelet specimens that were unrelated to the 110 paired serum/plasma specimens and performed LDH analyses using the Roche cobas c502 analyzer. We measured LDH on day zero, when all 10 specimens were kept at room temperature. The platelet count was performed using the Sysmex XN-9000 analyzer. The 10 specimens were then kept in the freezer for 1 day, and LDH and platelet counts were performed after thawing the platelet specimens.

## Results

Linear regression (**FIGURE 1**) shows a correlation between plasma and serum LDH concentrations with a slope of 0.72 (95% confidence interval [CI], 0.51–0.93) and an intercept of 114.49 (95% CI, 73.44–155.53). The correlation was low with an  $R^2 = 0.3$ . This low correlation was likely because of the unpredictable release of LDH by platelets in the plasma specimens. Bland-Altman difference plots (**FIGURE 2**) show that plasma LDH was on average 61 U/L higher than serum LDH. This translated to a 22% higher LDH measurement in plasma compared to serum. **FIGURE 3** shows a shift in LDH concentrations between the paired plasma and serum specimens ( $P < .05$  using paired Wilcoxon test). The same shift was observed when subgroup analysis was performed, considering age and sex ( $P < .05$ ). There was no difference in the hemolytic indices between plasma and serum ( $P = .55$  using paired Wilcoxon test; **FIGURE 4**). For the last 14 paired specimens, RBCs were unchanged and WBCs showed no statistically significant difference ( $P = .18$ ). However, there was an increased number of platelets in plasma compared to serum ( $P < .05$ ; **TABLE 1**).

**FIGURE 1.** Comparison of plasma vs serum lactate dehydrogenase (LDH) results in paired specimens.  $y = 0.72x + 114.5$ ;  $R^2 = 0.3$ . Deming regression showing the correlation between plasma and serum LDH concentrations in the 110 paired plasma and serum specimens. The black line displays the regression equation, with 95% confidence intervals shaded in gray.

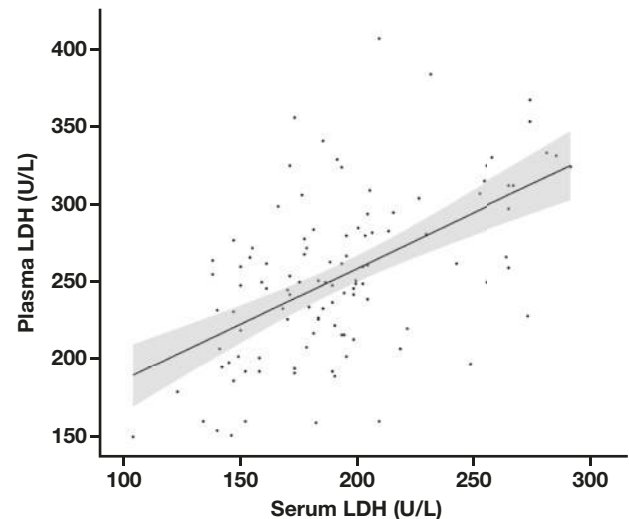
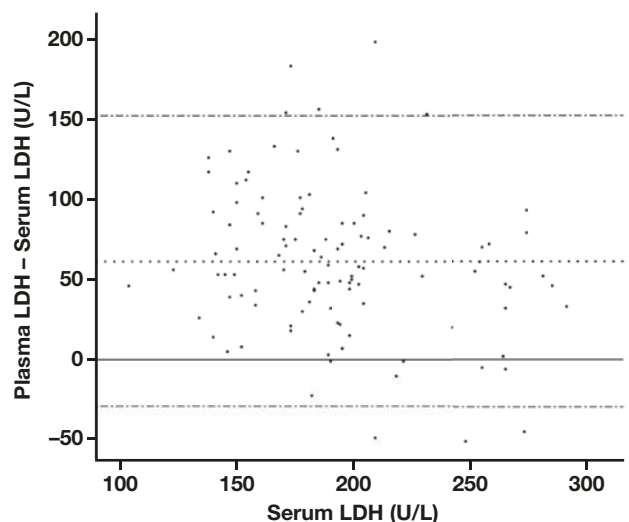


**FIGURE 2.** Bland-Altman difference plot of plasma and serum lactate dehydrogenase (LDH) concentrations in paired specimens ( $n = 110$ ) showing plasma minus serum concentrations of LDH. The dotted line represents the average difference, and the dotted-dashed line represents 2 standard deviations below and above the mean.



An experiment using 10 different donor platelet specimens was performed to investigate the amount of LDH in the platelets. Platelet counts and LDH analyses were performed on the platelet specimens on day zero. All 10 specimens were then frozen for 1 day and reanalyzed. Freezing the platelets caused degranulation to occur, leading to the release of intracellular LDH. **TABLE 2** shows that freezing the platelets did not cause significant changes ( $P = .13$ ) in the platelet counts but that LDH concentration increased 44% to 599% ( $P < .05$ ). This experiment indicated that platelets contain a high concentration of LDH. Excess

**FIGURE 3.** Distribution of plasma and serum lactate dehydrogenase (LDH) results in paired specimens (n = 110). The histogram shows serum (white) and plasma (dark gray) LDH concentrations in paired specimens. Light gray bars indicate overlap between the 2 groups at that LDH value. Statistical significance between the 2 groups is indicated by the bracket. \* $P < .05$  using paired Wilcoxon test.

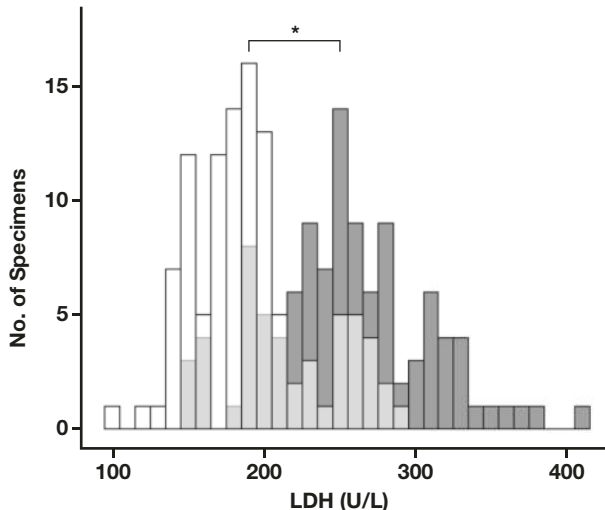
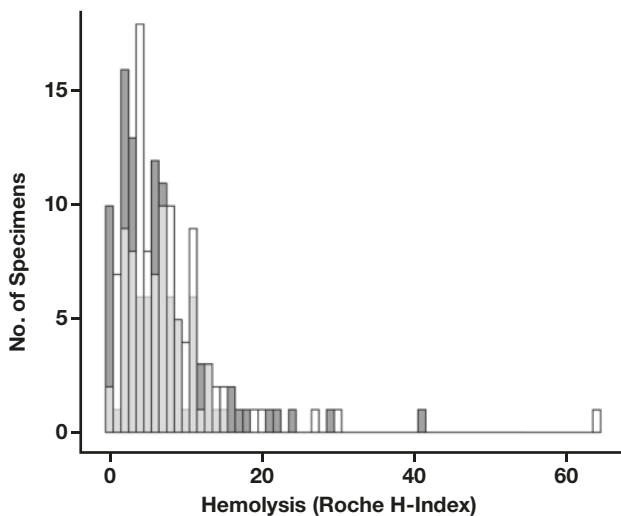


**FIGURE 4.** Distribution of H-index values in paired plasma and serum specimens. The histogram shows H-index values for the paired serum (white) and plasma (dark gray) specimens. Light gray bars indicate overlap between the 2 groups at that H-index value. The 2 groups were not statistically different.



platelets left in centrifuged plasma specimens can lead to an unpredictable elevation of LDH that is not reflective of the true physiological state of the patient. Centrifuged serum specimens contain a minimal amount of residual platelets, so LDH measurements using serum specimens are expected to be more accurate and reproducible.

To ensure that temperature did not significantly change the concentration of LDH in serum, a specimen stability experiment was performed. Fifteen random specimens that were unrelated to the 110 paired serum/plasma or 10 donor platelet specimens were

analyzed at room temperature (25°C), after refrigeration for 1 day (4°C–8°C), and after freezing for 1 day (–70°C). No statistically significant differences were observed between the 3 groups ( $P > .10$  for all comparisons).

## Discussion

Oncologists commonly use LDH to monitor disease progression in patients with hematologic malignancies. Switching specimen types from serum to plasma indicated an upward trend in the LDH levels. It is also important to note that serum and plasma LDH levels can be increased in a variety of nonmalignant conditions because they become elevated with cellular damage in many tissues. Because LDH is also present in the heart, skeletal muscle, and liver, myocardial infarction and liver diseases such as hepatocarcinoma, hepatitis, and cirrhosis can lead to elevation in serum LDH levels. Diseases affecting muscle, such as myositis, may also cause alterations in serum LDH levels. Patients with hematologic malignancies may also have other diseases that may alter serum LDH levels. Hence, nonspecific elevation of serum LDH levels is usually followed by further diagnostic investigation. Falsely elevated LDH can lead to unnecessary investigations. It is therefore important to ensure that the LDH level is accurately measured in the most appropriate specimen type.

Evaluating the paired plasma vs serum specimens using the same analyzer showed that LDH was consistently higher in the plasma specimens. Miles et al<sup>2</sup> found a 21% increase in LDH levels in plasma compared to serum, which is consistent with our data. One potential reason is that LDH is released from the breakdown or activation of cells in the specimens during storage or transportation. In our last 14 specimens, there were minimal amounts of RBCs and WBCs present; however, there was an increase in the number of platelets in plasma compared to serum (TABLE 1). Lysis or the activation of platelets could occur during storage or transportation of specimens before analysis. The effect is more evident in plasma because no clotting occurs before separating plasma from cells. The clotting process in serum tubes may entrap the platelets to prevent them from lysis or activation. Because platelets are small in size, they may leach up the gel barrier in PST upon standing, leading to an unpredictable release of LDH when they lyse, as shown by our platelet degranulation experiment.

Overall, serum is the preferred specimen type for LDH analysis<sup>7</sup> because of an unpredictable increase in plasma LDH concentrations. Although this phenomenon was not tested on an alternative platform, the authors believe that this phenomenon is not platform-specific because most methods use the same principle for analyzing LDH. Bausset et al<sup>8</sup> also showed that serum specimens that were centrifuged 4 hours after clotting still produced acceptable LDH results, which further support serum as the preferred specimen type for LDH analysis.

## Conclusion

The results from our studies showed that an unpredictable increase in plasma LDH concentration can occur upon storage because of the leaching of platelets across the gel barriers in PST. Minimal or no leaching of platelets across the gel barriers can occur in SST because platelets are entrapped in the clot. Therefore, blood collected in SST is the preferred specimen type for LDH analysis. Expanding the reference range of LDH to accommodate both plasma and serum specimen types

**TABLE 1. LDH and Cell Count Results from 14 PST and SST Specimens**

Specimen ID	PST				SST			
	LDH (U/L)	WBC ( $\times 10^3/\mu\text{L}$ )	RBC ( $\times 10^6/\mu\text{L}$ )	PLT ( $\times 10^3/\mu\text{L}$ )	LDH (U/L)	WBC ( $\times 10^3/\mu\text{L}$ )	RBC ( $\times 10^6/\mu\text{L}$ )	PLT ( $\times 10^3/\mu\text{L}$ )
1	201	0.69	<1	29	158	<0.10	<1	2
2	341	0.19	<1	52	185	<0.10	<1	3
3	266	<0.10	<1	15	154	<0.10	<1	<1
4	280	<0.10	<1	41	203	<0.10	<1	1
5	207	<0.10	<1	51	141	<0.10	<1	<1
6	261	<0.10	<1	13	204	<0.10	<1	2
7	226	<0.10	<1	25	183	<0.10	<1	<1
8	384	<0.10	<1	9	231	<0.10	<1	1
9	277	<0.10	<1	15	147	<0.10	<1	<1
10	186	<0.10	<1	17	147	<0.10	<1	1
11	285	<0.10	<1	8	200	<0.10	<1	<1
12	150	<0.10	<1	35	104	<0.10	<1	1
13	222	0.11	<1	27	190	<0.10	<1	3
14	325	<0.10	<1	66	171	<0.10	<1	1

LDH, lactate dehydrogenase; PLT, platelets; PST, plasma separator tubes; RBC, red blood cell; SST, serum separator tubes; WBC, white blood cell.

**TABLE 2. Platelet Counts and LDH Results Before and After Freezing Donor Platelets**

Donor Platelet	Day Zero		Post Frozen Day 1		% Change in PLT	% Change in LDH
	PLT Count ( $\times 10^3/\mu\text{L}$ )	LDH (U/L)	PLT Count ( $\times 10^3/\mu\text{L}$ )	LDH (U/L)		
1	1769	2400	1096	3459	-38	44
2	1056	486	1006	2297	-5	373
3	1159	412	1177	2384	-2	479
4	1105	514	880	1920	20	274
5	1177	525	1280	3455	-9	558
6	777	940	910	2825	-17	201
7	1351	771	1311	2035	-3	164
8	1514	340	1469	2375	-3	599
9	1047	448	722	1944	-31	334
10	833	430	697	1460	-16	240

LDH, lactate dehydrogenase; PLT, platelets.

would not be ideal because the leaching of platelets into plasma was inconsistent and unpredictable.

## REFERENCES

- Panteghini M, Bais R. Serum enzymes. In: Rifai N, Horvath AR, Wittwer CT, eds. *Tietz Textbook of Clinical Chemistry and Molecular Diagnostics*. 6th ed. St Louis, MO: Elsevier; 2018:404–434.
- Miles RR, Roberts RF, Putnam AR, Roberts WL. Comparison of serum and heparinized plasma samples for measurement of chemistry analytes. *Clin Chem*. 2004;50(9):1704–1706.
- Ladenson JH, Tsai LB, Michael JM, Kessler G, Joist JH. Serum versus heparinized plasma for eighteen common chemistry tests. *Am J Clin Pathol*. 1974;62(4):545–552.
- Bakker AJ, Mirchi B, Dijkstra JT, Reitsma F, Syperda H, Zijlstra A. IFCC method for lactate dehydrogenase measurement in heparin plasma is unreliable. *Clin Chem*. 2003;49(4):662–664.
- Liu Z, Wang W, He CS. Comparison of serum and plasma lactate dehydrogenase in postburn patients. *Burns*. 2000;26(1):46–48.
- Handin RI, Valeri CR. Improved viability of previously frozen platelets. *Blood*. 1972;40(4):509–513.
- Bais R, Philcox M. Approved recommendation on IFCC methods for the measurement of catalytic concentration of enzymes. Part 8. IFCC method for lactate dehydrogenase (l-lactate: NAD + oxidoreductase, EC 1.1.1.27). *Eur J Clin Chem Clin Biochem*. 1994;32(8):639–655.
- Bausset O, Juvet O, Staller-Gobelli C, Milano E, Bausset JP. Impact of serum-clot contact time on lactate dehydrogenase and inorganic phosphorus serum levels. *Pract Lab Med*. 2017;7:36–40.

# Erythrocyte Sedimentation Rate in Patients with Renal Insufficiency and Renal Replacement Therapy

Anna Buckenmayer, MD,<sup>1,\*</sup> Lotte Dahmen, MD,<sup>1</sup> Joachim Hoyer, MD,<sup>1</sup> Sahana Kamalanabhaiah, MD,<sup>1</sup> Christian S. Haas, MD<sup>1</sup>

<sup>1</sup>Department of Internal Medicine, Nephrology & Intensive Care Medicine, Phillips University, Marburg, Germany; \*To whom correspondence should be addressed. [buckenma@med.uni-marburg.de](mailto:buckenma@med.uni-marburg.de)

**Keywords:** erythrocyte sedimentation rate, chronic kidney disease, peritoneal dialysis, hemodialysis, inflammation, renal replacement therapy

**Abbreviations:** ESR, erythrocyte sedimentation rate; MM, multiple myeloma; PMR, polymyalgia rheumatica; GCA, giant-cell arteritis; CKD, chronic kidney disease; ESRD, end-stage renal disease; RRT, renal replacement therapy; HD, hemodialysis; PD, peritoneal dialysis; KT, kidney transplantation; AKI, acute kidney injury; CRP, C-reactive protein; MDRD, Modification of Diet in Renal Disease; eGFR, estimated glomerular filtration rate; NA, nonapplicable

*Laboratory Medicine* 2022;53:483–487; <https://doi.org/10.1093/labmed/lmac018>

## ABSTRACT

**Background:** Determination of the erythrocyte sedimentation rate (ESR) is a simple diagnostic tool for estimating systemic inflammation. It remains unclear whether ESR is influenced by renal disease or renal replacement therapy (RRT).

**Objective:** To report the incidence and extent of ESR elevations in patients with chronic kidney disease (CKD) and the possible impact of RRT.

**Methods:** We performed a single-center, retrospective study in inpatients with or without renal disease and in those with RRT, comparing ESR levels and other laboratory and clinical information.

**Results:** A total of 203 patients were included. On average, ESR was elevated (mean [SD], 51.7 [34.6] mm/h), with no statistically significant difference between the patient groups. Only those receiving PD showed significantly higher ESR (78.3 [33.1] mm/h;  $P < .001$ ).

**Conclusions:** ESR testing can be used without restriction in patients with CKD and in patients undergoing hemodialysis and who have received kidney transplantation; however, this measurement should be monitored carefully in patients with PD.

Determination of the erythrocyte sedimentation rate (ESR) involves a simple laboratory test for estimating systemic inflammation. Easy availability, simple implementation, and low cost make the ESR a potentially useful tool in clinical practice. Acute-phase proteins deplete the negative charge between erythrocytes, leading to a faster agglomeration of erythrocytes and increase in the ESR.<sup>1</sup>

Common diseases associated with ESR elevations are severe infectious diseases, tumors, vasculitis, and possibly severe anemia.<sup>2</sup> Low sensitivity and specificity, however, impair the validity of ESR testing for revealing an inflammatory response. By contrast, an extremely elevated ESR is a reliable parameter for ruling in multiple myeloma (MM) and is found in most cases of polymyalgia rheumatica (PMR) and giant-cell arteritis (GCA)<sup>3</sup>; in fact, these disorders can be easily ruled out by a normal ESR.<sup>1</sup> Classically, the ESR is assessed after 1 and 2 hours, respectively, although it is sufficient to determine only the 1-hour value.<sup>4</sup> In the literature, normal ESR values are 6–20 mm/hour in women and 3–15 mm/hour in men, whereas an ESR of >70–100 mm/hour is interpreted as being an extremely elevated ESR.<sup>1</sup>

Articles in 2 publications<sup>5,6</sup> suggest that renal disease may be another cause of ESR elevation. Chronic kidney disease (CKD) affects 10%–15% of the worldwide population<sup>7</sup>; the global prevalence of end-stage renal disease (ESRD) with need of RRT is estimated at 0.07%.<sup>8</sup> In Europe, hemodialysis (HD) is by far the most common RRT (82%), followed by peritoneal dialysis (PD; 13%) and kidney transplantation (KT; 5%).<sup>9</sup> Signs of low-grade inflammation are commonly observed in patients with CKD, as well as in patients undergoing dialysis.<sup>10</sup> These observations are believed to be the combined result of several factors, including increased production and decreased clearance of proinflammatory cytokines, as well as acidosis and oxidative stress caused by uremia.<sup>11</sup> Contact with bioincompatible dialysis membranes may play an additional role.<sup>12</sup>

So far, data for ESR in patients with CKD and those undergoing RRT are insufficient or inconsistent, and the diagnostic benefit of ESR testing remains unclear. Further, the effect of comorbidities has not been studied, to our knowledge. Bathon et al<sup>13</sup> found an increased ESR in 93% of patients with HD, concluding that determination of ESR is useless in this patient group. In contrast, Brouillard et al<sup>14</sup> found only a normal to mildly increased ESR. Values from both studies were comparable to those in the general population.<sup>13,14</sup> Personal observations in our clinical practice suggest a moderately increased ESR in patients with HD, independent from the underlying disease and comorbidities, but pointed to a significantly elevated ESR in patients with PD. So far, data on ESR in acute kidney injury (AKI) are sparse and mainly case-related.

The objectives of this retrospective pilot study were as follows. First, we sought to determine a possible correlation between ESR and the extent of renal insufficiency. Second, we aimed to see whether ESR differs between patients with and without CKD. Our third goal was to analyze whether RRT modes affect ESR, and our fourth was to evaluate a potential correlation between ESR and other laboratory parameters and comorbidities.

## Methods

We provide a cross-sectional, descriptive study of patients admitted to the Department of Nephrology at the University Hospital in Marburg, Germany. Inpatients between January 2019 and January 2021 were retrospectively screened for the ESR value available at the time of admission. All patients with available ESR measurement with and without kidney disease, including those undergoing any RRT, were included. Eligible patients were classified into 5 groups: patients without renal disease (group 1, no RD), patients with acute kidney disease and CKD at various stages (group 2, RD), patients with ESRD receiving hemodialysis (group 3, HD), patients with ESRD receiving peritoneal dialysis (group 4, PD), and patients with ESRD receiving KT (group 5, KT).

ESR was determined by the Westergren method in specimen material collected into a blood tube blood collection container (Sarstedt); the analysis took place after 60 minutes of sedimentation at room temperature.<sup>4</sup> Increased ESR was defined as  $\geq 25$  mm/hour, with values of  $\geq 80$  mm/hour considered to be extremely elevated.<sup>15</sup> ESR values were correlated with the following laboratory parameters, assessed during routine workup using automatic analyzers (AU5800, Beckman Coulter; and Sysmex XN, Sysmex): C-reactive protein (CRP), leucocytes, creatinine, estimated glomerular filtration rate (eGFR to define CKD; as determined by the Modification of Diet in Renal Disease [MDRD] formula<sup>16</sup>), urea, hemoglobin, and protein. Also, information regarding the underlying renal disease and comorbidities was obtained from the medical records and discharge letters provided by the nephrologists in charge of the patients.

Data were analyzed using SPSS software, version 27 (IBM) and Microsoft Excel, version 16 (2020; Microsoft). We analyzed the correlation between ESR and laboratory parameters and comorbidities, respectively, including calculation of a correlation coefficient, in a linear model. One-way ANOVA and Tukey post hoc analysis were used to compare different groups. We assessed normal distribution via the Shapiro-Wilk test; homogeneity of variances was asserted using the Levene test. Data are represented as mean (SD), unless otherwise stated. These study results may help in the care of future patients, in that the results will aid health care professional in more quickly identifying certain medical conditions in patients with renal diseases when ESR is used as a screening tool. The study was given a waiver by the Ethics Committee, Philipps University, Marburg, Germany.

## Results

Overall, 203 patients (mean [SD] age, 63.1 [18.6] years; median, 65.0 years; range, 18–95 years) were included in this study, with comparable numbers of male patients (104 [51.2%]) and female patients (99 [48.8%]; **TABLE 1**). In total, 82 individuals had CKD stage 1–5, of whom 36 presented with additional AKI and 9 patients showed AKI without preexisting CKD. Hypertensive and/or diabetic nephropathy

was the predominant cause for CKD and ESRD (41.8%), followed by glomerulonephritis (21.5%). The remaining individuals had a variety of underlying renal diseases. Among them, 76 patients had ESRD: 28 of those patients received HD, 19 were treated with PD, and 29 patients received KT as RRT; 45 patients had no kidney disease. Arterial hypertension was the most common comorbidity, with the highest prevalence in patients with RRT. Patients undergoing hemodialysis represented the oldest population (70.1 [13.7] years), and patients with PD were significantly younger (48.3 [11.8] years). Kidney transplant recipients received RRT for the longest amount of time (151.5 [203.5] months). The mean ESR of the total population was elevated (51.7 [34.6] mm/h; range, 0–150 mm/h), with ESR being normal in 54 patients ( $< 25$  mm/h); 54 patients had an extremely elevated ESR ( $> 80$  mm/h).

Assessment of the ESR in the 5 different subject groups showed comparable values in the no-RD group (48.2 [30.2] mm/h), the RD group (51.5 [35.3] mm/h), the HD group (45.8 [31.8] mm/h), and the KT group (46.4 [37.1] mm/h). However, ESR was significantly higher in patients with PD (78.3 [33.1] mm/h;  $P < .001$ ) with only 2 outliers in this population (**FIGURE 1**). Equal variances being assumed ( $P = .24$  based on mean), ESR was normally distributed for the no-RD and PD groups but not for the RD, HD, and KT groups ( $\alpha = 0.05$ ). The level of ESR differed statistically significant for the different populations ( $F[4.198] = 3.44$ ;  $P = .01$ ;  $\eta^2 = 0.065$ ).

Tukey post hoc analysis revealed a significant difference ( $P < .05$ ) between ESR levels of the PD group individually, compared with all other groups: PD vs no-RD (30.02; 95% CI, 4.55–55.39), PD vs RD (26.81; 3.11–50.51), PD vs HD (32.44; 4.77–60.11), and PD vs KT (31.85 [4.37–59.33]). In fact, there was a significant difference between PD group and all other groups taken together (78.3 [33.1] mm/h; vs all other patients, 49.0 [33.7] mm/h;  $P < .001$ ; **TABLE 2**). Most biochemical parameters (leucocytes, C-reactive protein, protein, hemoglobin) did not differ significantly between the groups. As we expected, urea levels were significantly higher in patients with RD or RRT, compared with patients not having RD (96.1 [73.3] mg/dL vs 48.3 [68.4] mg/dL;  $P < .001$ ; **TABLE 2**). We were intrigued to learn that there was no significant correlation between ESR and CRP in the entire study population, possibly due to the wide range of the ESR values (variance, 25–140 mm/h). We note that the ESR significantly correlated with CRP in all subgroups but not in patients with HD or PD receiving RRT (**TABLE 3**). As expected, the ESR was higher in patients with vasculitis, active tumors, GCA, and PMR or MM (data not shown); however, this was not true for the PD group.

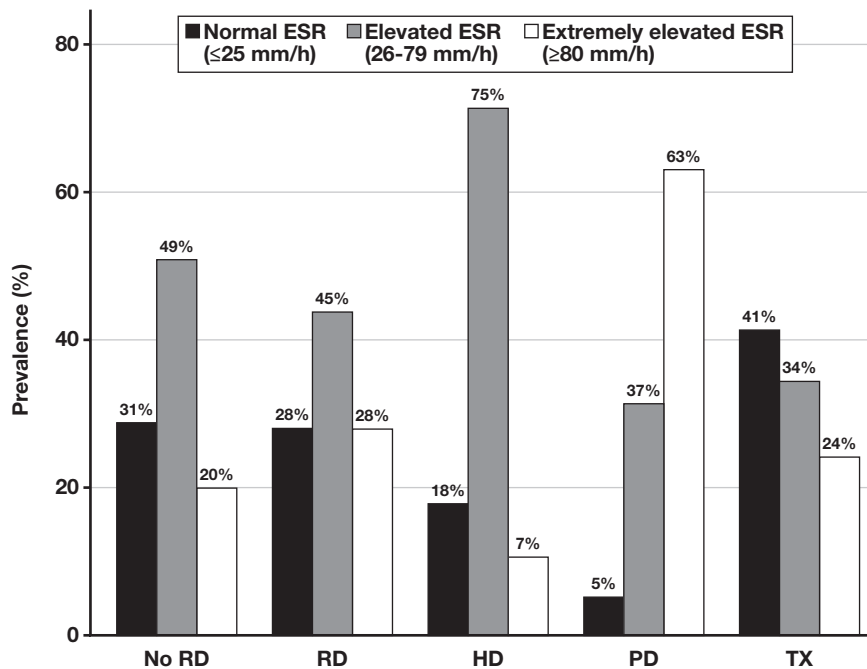
## Discussion

ESR testing is an unspecific yet easy, quick, and inexpensive diagnostic means of screening for systemic inflammation. Despite the lack of specificity offered by the assay, an elevated ESR may point to an underlying disorder and/or inflammatory problem, whereas an extremely elevated ESR is helpful in establishing the diagnosis of PMR and GCA, or MM, respectively. So far, there are conflicting data regarding whether CKD affects the ESR, thereby compromising the validity of the ESR test. Indeed, the findings reported in previous publications<sup>13,17</sup> suggest a general ESR increase in patients with CKD, possibly caused by decreased clearance of proinflammatory cytokines, oxidative stress, and metabolic acidosis but also by dialysis-related factors, such as extracorporeal membranes, impurities in the water used in dialysis, or foreign material

**TABLE 1. Baseline Characteristics of the Study Population**

Variable	Group					Total
	No RD	RD	HD	PD	TX	
No.	45	82	28	19	29	203
Male/Female, No.	20/25	39/43	20/8	12/7	13/16	104/99
Age (y), mean (SD)	60.7 (20.3)	67.5 (18.5)	70.1 (13.7)	48.3 (11.8)	57.3 (17.1)	63.1 (18.6)
Diabetes, No. (%)	8 (17.8%)	23 (28.0%)	14 (50.0%)	5 (26.3%)	10 (34.5%)	60 (29.6%)
Hypertension, No. (%)	30 (66.7%)	63 (76.8%)	28 (100%)	19 (100%)	24 (82.8%)	164 (80.8%)
Coronary heart disease, No. (%)	8 (17.8%)	26 (31.7%)	15 (53.6%)	4 (21.0%)	6 (20.7%)	59 (29.1%)
Vasculitis, No. (%)	3 (6.7%)	4 (4.9%)	2 (7.1%)	1 (5.2%)	3 (10.3%)	13 (6.4%)
GCA/PMR, No. (%)	4 (8.9%)	4 (4.9%)	0	0	0	8 (3.9%)
Active tumor, No. (%)	3 (6.7%)	9 (11.0%)	2 (7.1%)	0	3 (10.3%)	17 (8.4%)
Severe infection, No. (%)	15 (33.3%)	18 (21.9%)	7 (25.0%)	0	8 (27.6%)	48 (23.7%)
Time from start RRT (mo), mean (SD)	NA	NA	15.6 (16.9)	31.0 (32.8)	151.5 (203.5)	26.7 (92.6)

GCA, giant-cell arteritis; HD, hemodialysis; KT, kidney transplant; NA, not applicable; PD, peritoneal dialysis; PMR, polymyalgia rheumatica; RD, renal disease; RRT, renal replacement therapy.

**FIGURE 1. Prevalence of erythrocyte sedimentation rate (ESR) levels (normal, elevated, extremely elevated). HD, hemodialysis; KT, kidney transplantation; PD, peritoneal dialysis; RD, renal disease.****TABLE 2. Laboratory Parameters of the Study Participants (n = 203)**

Analyte	Group, Mean (SD)					Total
	No RD	RD	HD	PD	TX	
ESR (mm/h)	48.2 (30.2)	51.5 (35.3)	45.8 (31.8)	78.3 (33.1)	46.4 (37.1)	51.7 (34.6)
Leukocytes ( $\times 10^3/\mu\text{L}$ )	8.7 (3.8)	8.3 (4.0)	7.0 (2.2)	8.9 (2.9)	7.9 (3.3)	8.2 (3.6)
C-reactive protein (mg/L)	71.0 (84.6)	40.2 (56.4)	61.0 (76.5)	38.1 (36.4)	54.3 (92.0)	51.6 (71.3)
Creatinine (mg/dL)	0.7 (0.2)	2.7 (2.2)	6.1 (2.3)	10.9 (4.6)	2.6 (1.3)	3.7 (3.9)
Urea (mg/dL)	48.3 (68.4)	109.5 (82.9)	114.5 (59.9)	111.7 (32.1)	101.9 (52.1)	95.7 (73.3)
Protein (g/L)	64.0 (8.8)	62.6 (10.3)	61.7 (7.5)	66.1 (5.4)	66.7 (7.9)	63.7 (9.0)
Hemoglobin (g/dL)	11.4 (2.2)	11.4 (2.7)	9.9 (2.1)	10.0 (1.4)	10.6 (2.1)	11.2 (1.7)

ESR, erythrocyte sedimentation rate; HD, hemodialysis; PD, peritoneal dialysis; RD, renal disease; TX, kidney transplant.

**TABLE 3. Correlation of ESR with Laboratory Parameters**

Analyte	Pearson Correlation Coefficient <i>r</i>					
	No RD	RD	HD	PD	KT	Total
C-reactive protein	0.471 <sup>a</sup>	0.308 <sup>a</sup>	0.253	0.428	0.534 <sup>a</sup>	0.338 <sup>a</sup>
Leucocytes	0.156	0.140	−0.007	0.219	−0.014	0.141 <sup>b</sup>
Creatinine	−0.05	0.27	−0.040	0.212	0.345	0.221
Urea	0.024	0.216	−0.150	0.071	0.201	0.134 <sup>a</sup>
Protein	0.047	−0.151	0.093	−0.076	−0.096	−0.044
Hemoglobin	−0.258	−0.300 <sup>a</sup>	−0.392 <sup>b</sup>	−0.501 <sup>b</sup>	−0.567 <sup>a</sup>	−0.024
Time from start of RRT	NA	NA	0.007	−0.017	0.315	0.086

ESR, erythrocyte sedimentation rate; HD, hemodialysis; KT, kidney transplant; NA, not applicable; PD, peritoneal dialysis; RD, renal disease; RRT, renal replacement therapy.

<sup>a</sup>Significant correlation ( $P < .01$ , 2-tailed).

<sup>b</sup>Significant correlation ( $P < .05$ , 2-tailed).

such as could be generated during hemodialysis or could come from peritoneal dialysis catheters.

Chronic inflammation is considered to have an impact on cardiovascular mortality<sup>18</sup>; in fact, patients with CKD and ESRD are at significantly higher risk for cardiovascular events.<sup>11,19</sup> The findings reported in a publication by Al-Homrany<sup>20</sup> included an extremely elevated ESR in 1 of 3 patients with ESRD. Conversely, other study reports, including one by Brouillard et al,<sup>14</sup> did not reveal find any significant higher ESRs in patients with CKD. We were interested to learn that patients with AKI consistently have a likelihood for impaired outcome with respect to mortality and kidney function, independent from comorbidities.<sup>21</sup> It is conceivable that an associated inflammatory response may contribute to this result, and that it might be reflected by an elevated ESR.

In the present study, we investigated the ESR in 45 patients without and 158 patients with a renal disease, including those receiving RRT (TABLE 1). In contrast to our clinical impressions before the study, we could not find any evidence for significant higher ESR values in patients with renal disease, compared with those having normal kidney function (TABLE 2), suggesting that ESR testing may also be worthwhile as a screening tool in this population. In fact, the ESR was also significantly elevated in all patients with renal disease and a diagnosis of MM, GCA, or PMR, as extensively described elsewhere for the general population.<sup>22,23</sup>

We note that prevalence of an extremely elevated ESR is comparable in patients with and without renal insufficiency, including patients with ESRD having HD or receiving KT. However, ESR values in the PD group were ordinarily extremely elevated (TABLE 2). Previous data<sup>10</sup> suggest that chronic inflammation caused by a combination of systemic and intraperitoneal inflammation could lead to elevated levels of acute-phase proteins, thereby also raising the ESR.

Conceivably, intraperitoneal catheters, exposure to endotoxins, and high glucose concentrations via the dialysate and complement activation result in an inflammatory response, as previously suggested by elevated CRP levels in 12%–65% of patients with PD.<sup>24</sup> However, in the present study, we were unable to confirm significantly higher CRP levels in the PD group; instead, our findings showed a trend to levels below average (38.1 [36.4] mg/L vs 51.6 [71.3] mg/L;  $P$  value nonsignificant). These findings are supported by data presented by Haubitz et al,<sup>25</sup> which show chronically elevated CRP levels in patients with ESRD who have HD but not in patients who have only PD. However, comparing patients with HD and those with PD may be problematic due to different baseline characteristics—eg, patients with PD generally are significantly younger and have

fewer comorbidities than patients with HD. In fact, we would be interested in testing whether switching the RRT modality affects ESR levels.

KT recipients are considered to have fewer acute-phase proteins, possibly as a result of the immunosuppressive therapy.<sup>12</sup> Nevertheless, our study does not confirm a notable impact of this therapy on the ESR. We were interested to notice a significant negative correlation between the ESR and hemoglobin levels in all patients with kidney disease (correlation coefficient,  $-0.30$ ;  $P < .01$ ; TABLE 3); consistent with previous study findings, we did not see these results in patients without renal disease.<sup>26,27</sup> It is possible that renal anemia contributes to this observation because the ESR is affected by increased velocity of the upward plasma flow and faster fallout of red blood cells.<sup>28</sup> In our findings, neither etiology of the renal disease (data not shown) nor time receiving RRT correlated with the ESR (TABLE 3). Leukocytes and CRP showed a weak correlation only in the no-RD and RD groups ( $P < .001$ ; TABLE 3); we did not observe this result in patients receiving RRT (results nonsignificant). This finding is consistent with data from Panichi et al,<sup>29</sup> which show a stronger correlation in patients without CKD ( $r = 0.46$  in patients with creatinine clearance  $>20$  mL/min vs  $r = 0.32$  in those with creatinine clearance  $<20$  mL/min). Thus, it is conceivable that elevated ESR values in patients with HD or PD may not reflect an inflammatory state associated with bacterial or viral infection.<sup>30</sup>

The limitations of the present study are its retrospective study design, monocentric data acquisition, and the missing ESR values in a large number of individuals, thereby minimizing the eligibility for the study. Also, data were assessed only in hospitalized patients, possibly undermining the transferability of the study results on an outpatient population. Elevated CRP levels in most of the patients (70.2%) may suggest an acute problem, representing a potential source of bias in data interpretation. We believe that comparing data from a healthy control group, patients with defined stable CKD, or patients with ESRD who are receiving ambulatory RRT would be interesting. Further, a longitudinal study design with repeatedly measured ESR in the same patient population could clarify whether elevated ERS levels might be due to an acute situation or result from chronic inflammation.

## Conclusions

Our findings demonstrate that ESR does not differ among various stages of renal insufficiency; that it can be used as a screening tool without restriction in patients with renal insufficiency; that it is significantly

increased in patients with ESRD and PD, although it seems not to be affected by HD and in renal transplant recipients; and that it has only some correlation with the selected parameters. Further studies would be helpful in understanding these observations and defining the possible role of various RRT options in ESRD.

## Acknowledgments

This study received a waiver in April 2021 by the Ethics Committee, Philipps University, Marburg, Germany. The datasets used or analyzed during the current study are available from the corresponding author on reasonable request.

## REFERENCES

1. Tishkowsky K, Gupta V. Erythrocyte sedimentation rate (ESR). In: *StatPearls*. StatPearls Publishing; 2020.
2. Olshaker JS, Jerrard DA. The erythrocyte sedimentation rate. *J Emerg Medicine*. 1997;15(6):869–874.
3. Levy SL, Bull AD, Nestel AR. How common is inflammatory marker-negative disease in giant cell arteritis? *Eye (Lond)*. 2013;27(1):106–108.
4. Jou JM, Lewis SM, Briggs C, et al, for the International Council for Standardization in Haematology (ICSH). ICSH review of the measurement of the erythrocyte sedimentation rate. *Int J Lab Hematol*. 2011;33(2):125–132.
5. Levay PF, Retief JH. Causes of high erythrocyte sedimentation rates in an inpatient population. *S Afr Med J*. 2005;95(1):45–46.
6. Shusterman N, Kimmel PL, Kiechle FL, Williams S, Morrison G, Singer I. Factors influencing erythrocyte sedimentation in patients with chronic renal failure. *Arch Intern Med*. 1985;145(10):1796–1799.
7. Levin A, Tonelli M, Bonventre J, et al. Global kidney health 2017 and beyond: a roadmap for closing gaps in care, research, and policy. *Lancet*. 2017;390(10105):1888–1917.
8. Himmelfarb J, Vanholder R, Mehrotra R, Tonelli M. The current and future landscape of dialysis. *Nat Rev Nephrol*. 2020;16(10):573–585.
9. Kramer A, Pippias M, Noordzij M, et al. The European Renal Association – European Dialysis and Transplant Association (ERA-EDTA) Registry Annual Report 2015: a summary. *Clin Kidney J*. 2018;11(1):108–122.
10. Pecoits-Filho R, Stenvinkel P, Wang AY-M, Heimbürger O, Lindholm B. Chronic inflammation in peritoneal dialysis: the search for the holy grail? *Perit Dial Int*. 2004;24(4):327–339.
11. Akchurin OM, Kaskel F. Update on inflammation in chronic kidney disease. *Blood Purif*. 2015;39(1–3):84–92.
12. Argani H, Mozaffari S, Zedefatah Y, Rahbani M. Acute phase reactants in hemodialysis and renal transplantation. *Transplant Proc*. 2002;34(6):2420–2421.
13. Bathon J, Graves J, Jens P, Hamrick R, Mayes M. The erythrocyte sedimentation rate in end-stage renal failure. *Am J Kidney Dis*. 1987;10(1):34–40.
14. Brouillard M, Reade R, Boulanger E, et al. Erythrocyte sedimentation rate, an underestimated tool in chronic renal failure. *Nephrol Dial Transplant*. 1996;11(11):2244–2247.
15. Herburger D. *Comparison of the Electrochemical Behavior of Human Blood with the Blood Sedimentation Rate [book in German]*. Diplomarbeiten Agentur Diplom.de; 1992.
16. Inal BB, Oguz O, Emre T, et al. Evaluation of MDRD, Cockcroft-Gault, and CKD-EPI formulas in the estimated glomerular filtration rate. *Clin Lab*. 2014;60(10):1685–1694.
17. Warner DM, George CRP. Erythrocyte sedimentation rate and related factors in end-stage renal failure. *Nephron*. 1991;57(2):248–248.
18. Willerson JT. Inflammation as a cardiovascular risk factor. *Circulation* 2004;109(21\_suppl\_1):II-2–II-10.
19. Cobo G, Lindholm B, Stenvinkel P. Chronic inflammation in end-stage renal disease and dialysis. *Nephrol Dial Transplant*. 2018;33(suppl 3):35–40.
20. Al-Homrany M. The significance of extreme elevation of the erythrocyte sedimentation rate in hemodialysis patients. *Saudi J Kidney Dis Transpl*. 2002;13(2):141–145.
21. Coca SG, Yusuf B, Shlipak MG, Garg AX, Parikh CR. Long-term risk of mortality and other adverse outcomes after acute kidney injury: a systematic review and meta-analysis. *Am J Kidney Dis*. 2009;53(6):961–973.
22. Chan FLY, Lester S, Whittle SL, Hill CL. The utility of ESR, CRP and platelets in the diagnosis of GCA. *BMC Rheumatol*. 2019;3:14.
23. Koshariar C, Van den Bruel A, Oke JL, et al. Early detection of multiple myeloma in primary care using blood tests: a case-control study in primary care. *Br J Gen Pract*. 2018;68(674):e586–e593.
24. Wang AY-M. Consequences of chronic inflammation in peritoneal dialysis. *Semin Nephrol*. 2011;31(2):159–171.
25. Haubitz M, Brunkhorst R, Wrenger E, et al. Chronic induction of C-reactive protein by hemodialysis, but not by peritoneal dialysis therapy. *Perit Dial Int*. 1996;16(2):158–162.
26. Alende-Castro V, Alonso-Sampedro M, Vazquez-Temprano N, et al. Factors influencing erythrocyte sedimentation rate in adults: new evidence for an old test. *Medicine (Baltim)*. 2019;98(34):e16816.
27. Kanfer EJ, Nicol BA. Haemoglobin concentration and erythrocyte sedimentation rate in primary care patients. *J R Soc Med*. 1997;90(1):16–18.
28. Bridgen M. Clinical utility of the erythrocyte sedimentation rate. *Am Fam Physician*. 1999;60(5):1443–1450.
29. Panichi V, Migliori M, De Pietro S, et al. C reactive protein in patients with chronic renal diseases. *Ren Fail*. 2001;23(3–4):551–562.
30. Paydar-Darian N, Kimia AA, Monuteaux MC, et al. C-reactive protein or erythrocyte sedimentation rate results reliably exclude invasive bacterial infections. *Am J Emerg Med*. 2019;37(8):1510–1515.

# Usefulness of AFP, PIVKA-II, and Their Combination in Diagnosing Hepatocellular Carcinoma Based on Upconversion Luminescence Immunochemistry

Song-gao Zhang, MMed,<sup>1,2</sup> and Yi Huang, MD<sup>1,2,3,4</sup>

<sup>1</sup>Provincial Clinical College, Fujian Medical University, Fuzhou, China, <sup>2</sup>Department of Clinical Laboratory, Fujian Provincial Hospital, Fuzhou, China, <sup>3</sup>Central Laboratory, Fujian Provincial Hospital, Fujian, China, <sup>4</sup>Center for Experimental Research in Clinical Medicine, Fujian Provincial Hospital, Fuzhou, China; \*To whom correspondence should be addressed. [hyi8070@126.com](mailto:hyi8070@126.com)

**Keywords:** AFP, PIVKA-II, upconverting phosphor technology, lateral-flow assay, hepatocellular carcinoma, POCT

**Abbreviations:** HCC, hepatocellular carcinoma; LC, liver cirrhosis; AASLD, American Association for the Study of Liver Diseases; EASL, European Association for the Study of the Liver; AFP,  $\alpha$ -fetoprotein; PIVKA-II, prothrombin induced by vitamin K absence or antagonist-II; DCP, des- $\gamma$ -carboxy prothrombin; HCC, hepatocellular carcinoma; LC, liver cirrhosis; UCPs, upconverting phosphors; LF, lateral flow; UPT-LF, upconverting phosphor technology-based lateral flow; POCT, point-of-care test; ECLIA, electrochemiluminescence immunoassay; CLEIA, chemiluminescent enzyme immunoassay; BCLC, Barcelona Clinic Liver Cancer; LoD, limit of detection; YI, Youden index

*Laboratory Medicine* 2022;53:488–494; <https://doi.org/10.1093/labmed/lmac027>

## ABSTRACT

**Objectives:** To evaluate the prognostic values of serum PIVKA-II (prothrombin induced by vitamin K absence-II) and  $\alpha$ -fetoprotein (AFP) and the combination of these analytes for identifying hepatocellular carcinoma (HCC), and to analyze the correlation between biomarkers and clinicopathological features of HCC.

**Methods:** The levels of PIVKA-II and AFP in 331 case individuals were determined by upconverting phosphor technology-based immune lateral flow (UPT-LF) assay. We used the ROC curve to determine the diagnostic value; the relationships between the biomarkers and clinicopathological features of HCC also were analyzed.

**Results:** AFP and PIVKA-II have good diagnostic performance in the diagnosis of HCC; the best AUC was 0.76, 0.74. High levels of PIVKA-II were more advantageous than AFP in predicting tumor size, portal-vein embolism, and vascular invasion (all  $P < .05$ ).

**Conclusion:** Levels of PIVKA-II and AFP showed good diagnostic value for HCC, but the level of PIVKA-II was more closely related to the clinicopathological features of HCC.

Hepatocellular carcinoma (HCC) is a malignant tumor caused by canceration of liver cells, which is the third-highest cause of cancer-related deaths worldwide, with occult onset, rapid progression, early metastasis, and limited treatment options.<sup>1</sup> According to the annual projections, it is estimated that 1 million people will die due to liver cancer in 2030.<sup>1</sup> Liver cirrhosis (LC) is the most important risk factor for HCC in the developing world.<sup>2</sup> The liver diagnosis and treatment guidelines formulated by the American Association for the Study of Liver Diseases (AASLD) and the European Association for the Study of the Liver (EASL) recommend monitoring high-risk patients every 6 months.<sup>3,4</sup>

AFP ( $\alpha$ -fetoprotein) is the most widely used serum tumor biomarker for screening, disease evaluation, and prognosis of patients with HCC. However, most researchers<sup>5–7</sup> state that AFP testing yields high false-positive or false-negative rates, and that serum levels of AFP may increase significantly in patients with LC or chronic hepatitis. Also, serum levels of AFP do not reveal significant abnormalities in >30% of patients with HCC.

Prothrombin induced by vitamin K absence or antagonist-II (PIVKA-II), or des- $\gamma$ -carboxy prothrombin (DCP), was first reported to be overexpressed in the serum of patients with HCC by Libman et al in 1984.<sup>8</sup> PIVKA-II has high specificity for HCC not expressed in LC and chronic hepatitis and is an alternative tumor biomarker of AFP; there is poor correlation between PIVKA-II and AFP.<sup>9,10</sup> The expression level of PIVKA-II was highly correlated with portal vein invasion, tumor size, intrahepatic metastasis, tumor recurrence, and recurrence after treatment.<sup>11–15</sup> Further, compared with AFP, PIVKA-II has better prediction performance for patients at higher risk of developing HCC.<sup>16,17</sup> For instance, Caviglia et al<sup>18</sup> reported that when serum PIVKA-II is  $\geq 55$  mAU/mL, 56.9% (41/72) of patients with cirrhosis without HCC developed HCC during the 36 months of follow-up ( $P < .001$ ). However, several large case-control study reports have concluded that the sensitivity, specificity, and accuracy of serum PIVKA-II for HCC were 48%–62%, 81%–98%, and 59%–84%, respectively; serum AFP measurements for HCC were 40%–54%, 88%–97%, and 64%–76%, respectively.<sup>19,20</sup>

Given the deficiency of PIVKA-II and AFP in the diagnosis of HCC, combined detection is an effective detection method that can improve the sensitivity or specificity of disease diagnosis based on the existing biomarkers. The combined detection of PIVKA-II and AFP increased the sensitivity to 78.3%, which is significantly higher than that of PIVKA-II (51.9%) and AFP (57.5%); the diagnostic accuracy was also improved by 8.26%–13.42% and 1.12%–2.69%, respectively.<sup>21</sup> Also, the NPV of diagnosis for HCC can be greatly improved by use of the combined method.<sup>22</sup>

Upconverting phosphors (UCPs) is a lanthanide-containing entity (along with Yb<sup>3+</sup>, Er<sup>3+</sup>, and the submicrometer-sized particle) that has a special composition and structure and can emit visible light when excited by infrared light. It has a cleaner background and higher sensitivity and stability, owing to its special crystal structure.<sup>23</sup> Combining UCPs as fluorescent labels with the immune lateral flow (LF) assay (upconverting phosphor technology-based LF [UPT-LF] assay) provides a solid foundation for accurate quantitative detection of analytes with rapid and high sensitivity. Currently, the UPT-LF assays suitable for point-of-care test (POCT) have been developed for the sensitive detection of bacteria, nucleic acid, tumor markers, etc.<sup>24–26</sup> The sensitivity and specificity of the UPT-LF test card used by Huang et al<sup>27</sup> to detect serum PIVKA-II in 228 patients with HCC was 71.49% and 88.89%, respectively.

Until now, the detection methods used in case-control studies on the diagnostic performance of PIVKA-II and AFP are the electrochemiluminescence immunoassay (ECLIA) and chemiluminescent enzyme immunoassay (CLEIA).<sup>28,29</sup> However, retrospective studies on serum PIVKA-II and AFP levels measured via UPT-LF assay (evaluation of the value of single and combined testing in the diagnosis of HCC) rarely report relevant information, nationally or internationally. To address this gap in the literature, we retrospectively analyzed serum PIVKA-II and AFP levels quantitatively measured via UPT-LF assay, to provide a reliable theoretical basis for more rapid and accurate POCT measurement in clinical diagnosis, curative-effect monitoring, and prognostic evaluation of HCC.

## Materials and Methods

### Study Subjects

A total of 331 cases were included in this study, including 103 cases of LC and 228 cases of HCC. All serum specimens were collected in Fujian Provincial Hospital from June 2015 through December 2019, all the subject individuals gave informed written consent and were approved by the Fujian Provincial Hospital Ethics Review Committee and Ethics Ref: 2016 [K2016-10-28]. All the patients in the LC group were confirmed based on their clinical examination findings in combination with ultrasound, CT scan, and MRI results, or liver biopsy. All patients in the HCC group were confirmed by liver biopsy after ultrasound or liver surgery; liver metastases, cholangiocarcinoma, or mixed liver cancer served as excluding factors. Also, patients who had recently taken warfarin or received any chemotherapy (including sorafenib) at any point in their lives were excluded.

The clinical staging of HCC was based on the BCLC (Barcelona Clinic Liver Cancer) staging system. All serum specimens were preserved in accordance with the following requirements: 5 mL of peripheral venous blood was collected under conditions of early-morning fasting, left at room temperature for 2 hours, centrifuged at 1500g for 5 minutes to

separate the serum, dispensed in 2 tubes, and frozen at –80°C from 1.5 months to 2 years until use.

### Determination of PIVKA-II and AFP, and Grouping of Patients

Serum AFP measurements were determined using a diagnostic kit for AFP testing. The sensitivity was 5.0 ng/mL; the cutoff for HCC diagnosis was 7.0 ng/mL, and the linear range was 5.0–1000.0 ng/mL.

The limit of detection (LOD) of the UPT-LF assay for serum PIVKA-II was 2.66 ng/mL, the cut-off for HCC diagnosis was 25.3 ng/mL, and the linear range was 4.8–20,000.0 ng/mL. PIVKA-II and AFP were measured in the same serum specimens. If the AFP level was >1000.0 ng/mL or the PIVKA-II level >20,000.0 ng/mL, the original specimen was manually diluted based on the previous results, according to the kit instructions.

In this study, patients with HCC were divided into 4 groups based on the median levels of serum PIVKA-II and AFP (higher than the median level is called *high level* and lower than the median is called *low level*). The patients in the PIVKA-II low-level and AFP high-level groups were categorized into the GA group; the PIVKA-II high-level and AFP low-level groups into the GP group; the PIVKA-II high-level and AFP high-level groups into the GH group; and the PIVKA-II low-level and AFP low-level groups into the GL group. Also, to analyze the relationship between serum PIVKA-II, AFP levels, and tumor stage, tumor size, vascular invasion, and other tumor characteristics of patients with HCC, we compared data from the patients in the PIVKA-II high-level and low-level groups (H<sub>PIVKA-II</sub> group vs L<sub>PIVKA-II</sub> group) and data from the AFP high-level and low-level groups (H<sub>AFP</sub> group vs L<sub>AFP</sub> group).

### Statistical Analysis

All statistical analysis was performed on Microsoft Excel 2013 (Microsoft) or SPSS software, version 24.0 (IBM); MedCalc software, version 19.0, was used for statistical mapping. Mann-Whitney *U* testing was used for continuous variable comparison, and  $\chi^2$  testing or Fisher exact testing was used for categorical variable comparison. The serum levels of PIVKA-II and AFP were expressed as median (IQR). To determine the best cutoff value of PIVKA-II and AFP for the identification of HCC and LC, a ROC curve was constructed, the AUC was calculated and compared, and the best Youden index (YI) was used as the basis for determining the cutoff in diagnosing HCC. Variables included in the statistical analysis included age, sex, etiology, Child-Pugh classification of liver function, total bilirubin, AST, ALT, and albumin. The combination of PIVKA-II and AFP positivity was defined as occurring when at least 1 of the biomarkers tests positive. The Spearman  $\rho$  correlation factor was calculated to identify relationships between the PIVKA-II and AFP values.  $P < .05$  was considered statistically significant.

## Results

### Basic Characteristics of Patients and Biomarker Levels

Of the 331 patients studied, 228 had HCC and 103 had LC that excluded HCC. The basic patient characteristics are shown in **TABLE 1**. The HCC and LC groups contained significantly more men than women ( $P < .001$ ), with a median age of 56 years (IQR, 47–63 years) in the HCC group and 58 years (IQR, 41–66 years) in the LC group. The etiological statistics showed that HBV infection was the main cause of HCC (82.0%) and LC (80.6%); HCV infection was less than 15%, and other nonviral causes were <10%.

**TABLE 1. Baseline Characteristics of the Study Patients (n = 331)**

Variable	HCC Group (n = 228)	LC Group (n = 103)	P Value
Sex, male, No. (%)	199 (87.3%)	71 (68.9)	<.001
Age, median (IQR)	56 (47–63)	58 (41–66)	.25
Etiology, No. (%)			.02
HBV	187 (82.0%)	83 (80.6%)	
HCV	31 (13.6%)	13 (12.6%)	
Other	10 (4.4%)	7 (6.8%)	
Child-Pugh class, No. (%)			<.001
A	188 (82.4%)	76 (73.8%)	
B	24 (10.5%)	17 (16.5%)	
C	16 (7.0%)	10 (9.7%)	
Laboratory findings, median (IQR)			
AST, U/L	49.25 (29.01–74.56)	34.14 (26.03–51.24)	.02
ALT, U/L	52.23 (34.54–72.37)	33.27 (21.59–46.16)	.01
Albumin, g/L	38.06 (34.41–44.59)	42.83 (36.44–46.91)	.03
Total bilirubin, $\mu$ mol/L	24.22 (18.78–29.43)	23.19 (16.21–28.07)	.17
PIVKA-II, ng/mL	52.39 (20.52–322.77)	10.89 (6.09–19.05)	<.001
AFP, ng/mL	165.39 (18.91–627.40)	4.21 (2.54–5.69)	<.001

AFP,  $\alpha$ -fetoprotein; HCC, hepatocellular carcinoma; LC, liver cirrhosis; PIVKA-II, prothrombin induced by vitamin K absence or antagonist-II.

The results of liver-function assessment by Child-Pugh classification showed that most of the liver function in both groups took place during the compensatory period, among which the proportion of Child-Pugh A in the HCC group was 82.4%, and that in the LC group was 73.8%. The median levels of serum PIVKA-II and AFP in the HCC group were 52.39 ng/mL (IQR, 20.52–322.77 ng/mL) and 165.39 ng/mL (IQR, 18.91–627.40 ng/mL), respectively, which were significantly higher than those in the LC group (10.89 ng/mL [IQR, 6.09–19.05 ng/mL] and 4.21 ng/mL [IQR, 2.54–5.69 ng/mL], respectively), with statistical significance ( $P < .001$ ).

As shown in **TABLE 2**, among the 228 patients with HCC, 36.8% had tumor vascular invasion, 11.4% had distant metastasis, and 25.9% had portal vein embolism. Most of the patients (51.3%) had tumor nodule diameter between 3 and 5 cm, and almost half of those were multiple tumor nodules. The proportion of patients with HCC who had well-differentiated, moderately differentiated, and poorly differentiated tumor margins is 1:9:4. HCC mainly displays poor to moderate differentiation, accounting for 92.5% of the total. According to the BCLC staging system for HCC, the number of patients in BCLC categories 0 + A, B, C, and D was 73 (32.0%), 79 (34.6%), 64 (28.1%), and 12 (5.3%), respectively; most of patients had disease in the middle-late stage.

### Relationship Between the Levels of Serum PIVKA-II and AFP

The relationship between PIVKA-II and AFP was analyzed by Spearman correlation testing. **FIGURE 1** shows the correlations between the biomarkers, the Spearman coefficient ( $r$ ) between PIVKA-II and AFP was 0.469 ( $P < .001$ ).

### Diagnostic Performance of PIVKA-II and AFP in Differentiating HCC from LC

The serum PIVKA-II and AFP levels measured quantitatively via UPT-LF assay were analyzed by ROC curve, and the results showed that the AUC

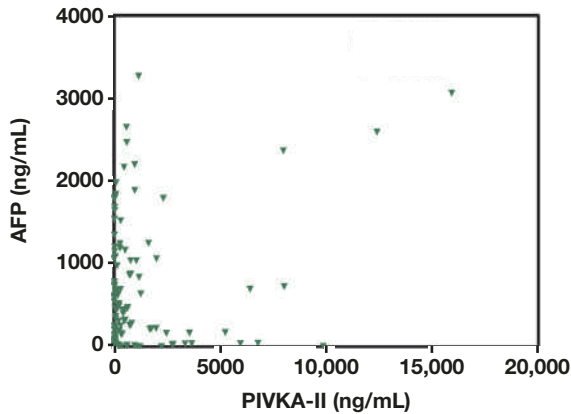
**TABLE 2. Clinical Features of HCC (n = 228)**

Variable	No. (%)
Vascular invasion	84 (36.8%)
Tumor metastasis	26 (11.4%)
Portal vein embolism	59 (25.9%)
Tumor size, diameter (cm)	
$\leq 3$	67 (29.3%)
$>3$ to $<5$	117 (51.3%)
$\geq 5$	44 (19.3%)
No. of tumor nodules	
1	102 (44.7%)
$\geq 2$	126 (55.3%)
Tumor grade	
Well-differentiated	17 (7.5%)
Moderately differentiated	145 (63.6%)
Poorly differentiated	66 (28.9%)
BCLC stage	
0 + A	73 (32.0%)
B	79 (34.6%)
C	64 (28.1%)
D	12 (5.3%)

BCLC, Barcelona Clinic Liver Cancer; HCC, hepatocellular carcinoma.

of PIVKA-II (cutoff = 25.3 ng/mL) was not different from those in AFP (cutoff = 7.0 ng/mL [ $Z = 0.73$ ;  $P = .47$ ]). The sensitivity of combined detection (PIVKA-II or AFP had positive results, or the combination was defined as having positive results) was enhanced to 73.68%. However, the diagnostic performance (AUC) did not improve (AFP vs combined:  $P = .70$ ;

**FIGURE 1.** The correlation between serum levels of prothrombin induced by vitamin K absence or antagonist-II (PIVKA-II) and  $\alpha$ -fetoprotein (AFP) ( $r = 0.469$ ;  $P < .001$ ).



PIVKA-II vs combined:  $P = .25$ ) on the basis of ensuring the specificity (82.52%), as shown in **TABLE 3** and **FIGURE 2**.

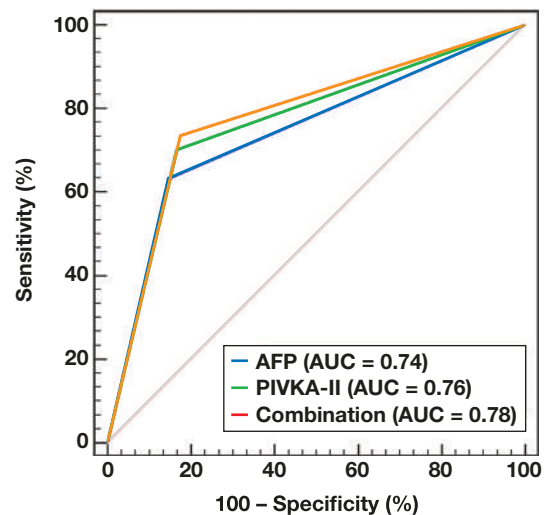
### Diagnostic Performance of AFP And PIVKA-II For Changing Cut-off Value

Currently, the cutoff values of serum PIVKA-II and AFP in most clinical laboratories are 40.0 mAU/mL and 20.0 ng/mL, respectively.<sup>28,30</sup> We also performed ROC analysis to obtain the diagnostic performance (AUC), which also showed no difference between serum PIVKA-II and AFP in discriminating HCC from LC ( $Z = 0.41$ ;  $P = .69$ ). Despite that the sensitivity (68.86%) of the combined detection increased significantly, the AUC (0.77) remained unchanged (AFP vs Combined:  $P = .22$ ; PIVKA-II vs Combined:  $P = .43$ ; see **TABLE 4** and **FIGURE 3**).

### Correlation Between Serum PIVKA-II And AFP Levels and Clinicopathological Features of HCC

The median levels of serum PIVKA-II and AFP were 52.39 ng/mL and 165.39 ng/mL, respectively. For the patients in the GA group, PIVKA-II was  $<52.39$  ng/mL and AFP  $>165.39$  ng/mL; for the GP group, PIVKA-II was  $>52.39$  ng/mL and AFP  $<165.39$  ng/mL. For the GH group, PIVKA-II was  $>52.39$  ng/mL and AFP  $>165.39$  ng/mL. For the GL group, PIVKA-II was  $<52.39$  ng/mL and AFP  $<165.39$  ng/mL. The  $\chi^2$  test results showed that tumor size, portal vein embolization, and vascular invasion in the GP and GH group were significantly different from those in the GA and GL group (all  $P < .05$ ), but there was no significant difference between the GH and GP group or between the GA and GL group (all  $P > .05$ ). There was a statistically significant difference in the number of tumors between the GP/GH and GA groups ( $P < .01$ ), but little difference between the GP and GH groups ( $P > .05$ ). The number of patients with BCLC stage B–D in the GP/GA/GH group was much higher

**FIGURE 2.** ROC curve comparing serum levels of prothrombin induced by vitamin K absence or antagonist-II (PIVKA-II),  $\alpha$ -fetoprotein (AFP), and a combination of PIVKA-II and AFP in patients with hepatocellular carcinoma (HCC) vs liver cirrhosis (LC).



than that in the GL group ( $P < .001$ ), but no significant differences were observed among the GP, GA, and GH groups ( $P > .05$ ). Also, no significant differences were observed in the proportion of Child-Pugh A/B/C among the 4 groups ( $P > .05$ ), as shown in **Supplementary Table 1**.

Further, the clinicopathological characteristics of patients with HCC were analyzed based on the median level of PIVKA-II and AFP, and the correlation between the  $H_{PIVKA-II}$  group and  $L_{PIVKA-II}$  group or the  $H_{AFP}$  group and the  $L_{AFP}$  group was compared with respect to the main clinical features of HCC. The results of statistical analysis indicated that the number of tumors in the  $H_{AFP}$  group was significantly higher than that in the  $L_{AFP}$  group ( $P < .01$ ). However, there were significant differences in tumor size, number of tumors, portal vein embolism, vascular invasion, and BCLC stage B–D between the  $H_{PIVKA-II}$  group and the  $L_{PIVKA-II}$  group (all  $P < .01$ ; **Supplementary Table 2**).

### Discussion

Currently, electrochemical luminescence or chemiluminescence assay based on fully automatic immunoanalyzers are predominantly used to detect the serum level of serum tumor markers in the laboratory. Although these analysis systems have high sensitivity and accuracy, a substantial amount of time and cost has been spent in the process of specimen analysis.

The UPT-LF assay is a kind of solid-phase immunoassay pattern in which the UCPs doped with rare earth  $Ln^{3+}$  with a unique upconverting

**TABLE 3.** Diagnostic Value of AFP and PIVKA-II in Differentiating HCC from LC

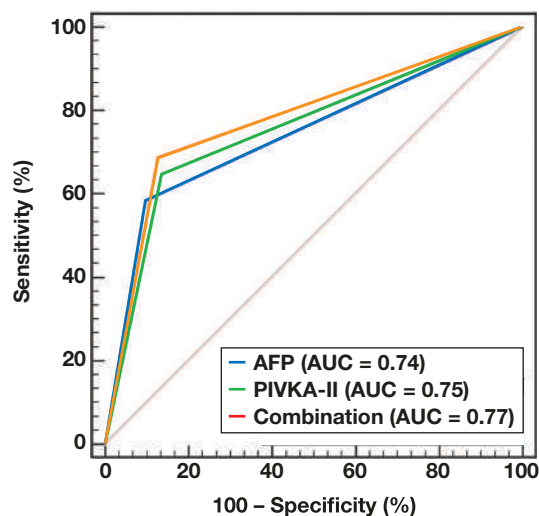
Variable	Sensitivity (%)	Specificity (%)	PPV (%)	NPV (%)	Accuracy (%)	AUC (95% CI)
PIVKA-II	70.18	83.50	90.39	55.84	74.32	0.76 (0.72–0.81)
AFP	63.16	85.44	90.56	51.16	70.09	0.74 (0.69–0.79)
PIVKA-II and AFP	73.68	82.52	90.32	58.62	76.43	0.78 (0.73–0.83)

AFP,  $\alpha$ -fetoprotein; AUC, area under the curve; HCC, hepatocellular carcinoma; NPV, negative predictive value; PIVKA-II, prothrombin induced by vitamin K absence or antagonist-II; PPV, positive predictive value.

**TABLE 4. Diagnostic Performance of Biomarkers after Changing the Cutoff Value**

Variable	Sensitivity (%)	Specificity (%)	PPV (%)	NPV (%)	Accuracy (%)	AUC (95% CI)
PIVKA-II	64.91	86.41	91.35	52.66	71.60	0.75 (0.71-0.80)
AFP	58.33	90.29	93.00	49.47	68.27	0.74 (0.69-0.79)
PIVKA-II and AFP	68.86	87.38	92.35	55.90	74.62	0.77 (0.73-0.82)

AFP,  $\alpha$ -fetoprotein; AUC, area under the curve; NPV, negative predictive value; PIVKA-II, prothrombin induced by vitamin K absence or antagonist-II; PPV, positive predictive value.

**FIGURE 3. ROC curve comparing serum levels of prothrombin induced by vitamin K absence or antagonist-II (PIVKA-II),  $\alpha$ -fetoprotein (AFP), and a combination of PIVKA-II and AFP in patients with hepatocellular carcinoma (HCC) vs liver cirrhosis (LC) after changing the cutoff value.**

phenomenon are used as reports; an immunochromatographic strip is used as the reaction carrier; and a fully portable UPT-3A-1800 biosensor (Beijing Hotgen Biotech) is used as the immunoassay analyzer, which requires no more than 15 minutes to obtain the analytical results. Thus, the UPT-LF assay has a high signal-to-noise ratio and is suitable for POCT.<sup>31</sup>

Also, the sensitivity of quantitative analysis of analytes can be improved 100-fold, compared with that of colloidal gold.<sup>32</sup> In this study, we used the test card based on the UPT-LF assay to detect serum PIVKA-II and AFP. The diagnostic kit for AFP has been used in other clinical laboratories, and the test results of serum PIVKA-II assay were consistent with those of the LumipulseG PIVKA-II detection kit (CLEIA assay; Fujirebio Diagnostics), the coefficient for the correlation ( $R^2$ ) was 0.901 ( $P < .01$ ).<sup>27</sup>

The basic characteristic of 228 patients with HCC and 103 patients with LC were analyzed, and the results showed that both HCC and LC were common in middle-aged and elderly people. HBV infection was one of the main causes, as reported in a previous study from the United States.<sup>33</sup> Further analysis of the clinicopathological features of patients with HCC showed that vascular invasion and portal vein embolization were common in the HCC group (36.8% and 25.9%, respectively). Also, mainly, the tumors were moderately and poorly differentiated, and the well-differentiated cases accounted for only 7.5% of the total. The median levels of serum PIVKA-II and AFP in the HCC group were significantly higher than those in the LC group.

Although AFP has been used in clinical auxiliary diagnosis of HCC for many years, it has not been recommended by the AASLD or the EASL

for its poor sensitivity, especially for the diagnosis of early HCC.<sup>34</sup> For example, the 20 ng/mL measurement used as the cutoff value and the sensitivity (41%–65%) were undesirable.<sup>35</sup> The sensitivity, specificity, AUC, PPV, and NPV of using 7.0 ng/mL as the cutoff value were 63.16%, 85.44%, 0.74 (95% CI, 0.69–0.79), 90.56%, and 51.16%; and that of 20 ng/mL were 58.33%, 90.29%, 0.74 (0.69–0.79), 93.00%, and 49.47%, in this study. No difference in AUC was observed between the 2 cutoff values, which was in line with the findings of Park et al.<sup>36</sup>

PIVKA-II is a kind of abnormal prothrombin that lacks one to several glutamic acid residues and normal coagulation function in protein molecular structure; its expression is mainly related to hypoxia and vitamin K.<sup>37</sup> The analysis results showed that performance of PIVKA-II at a cutoff value of 25.3 ng/mL was similar to that of Poté et al.<sup>38</sup> and was better than that of 40 ng/mL for HCC diagnosis, with sensitivity of 70.18% (vs 64.91%), specificity of 83.50% (vs 86.41%), and an AUC of 0.76 (95% CI, 0.72–0.81) (vs 0.75 [0.71–0.80]), a PPV of 90.39% (vs 91.35%), and a NPV of 55.84% (vs 52.66%).

Poor correlation was also observed between the level of serum PIVKA-II and AFP in our study<sup>9,10</sup>; the Spearman coefficient ( $r$ ) was 0.469. To enhance the performance of discrimination of HCC from LC, we further explored the performance of combined detection for HCC. Our analysis showed a significant increase in combined detection sensitivity (73.68%) at the UPT-LF assay–recommended cutoff value of 25.3 ng/mL for PIVKA-II and 7.0 ng/mL for AFP but a slight decrease in specificity (82.52%). Also, the AUC (0.78 [95% CI, 0.73–0.83]) was similar to the single detection (AFP vs combined:  $P = .70$ ; PIVKA-II vs combined:  $P = .25$ ).

In addition, the performance at the usual clinical cutoff value of 40.0 ng/mL for PIVKA-II and 20.0 ng/mL for AFP was marginally better than that at the recommended cutoff value, with sensitivity of 68.86%, specificity of 87.38%, and an AUC of 0.77 (95% CI, 0.73–0.82). These findings were not consistent with those of Lim et al.,<sup>28</sup> who reported that the diagnostic value of PIVKA-II combined with AFP was superior to that of AFP or PIVKA-II, with sensitivity of 52.9%, specificity of 97.1%, and an AUC of 0.85 (0.82–0.88).

HCC is characterized by a strong proliferative activity and unlimited replicative proficiency, insensitivity to growth-inhibiting signals, escape of apoptosis, sustained angiogenesis, tissue evasion, and metastasis. These features are closely related to tumor biological behavior, which are the main reasons for short survival and high mortality of patients.<sup>28</sup>

Our analysis revealed that patients with HCC who were categorized into the GP and GH groups tended to have larger tumor-nodule sizes, most of which were massive HCC. These patients also were more likely to develop portal vein embolization with vascular invasion, which indicates that PIVKA-II protein expression level may be positively correlated with the number of tumor cells and can also promote the occurrence of portal vein embolism and vascular

invasion of HCC.<sup>39</sup> However, no significant difference was observed in the aforementioned characteristics between the GA and GL groups (all  $P > .05$ ), or between GP and GH groups (all  $P > .05$ ), which might be an indication that serum PIVKA-II level was more closely related to biological behavior of HCC cells than serum AFP level.<sup>33</sup> The number of tumor nodules in the GP and GH groups was more than that in the GA group (both  $P < .01$ ), whereas that in the GA group was more than that in the GL group ( $P < .05$ ), which showed that the level of serum PIVKA-II and serum AFP was related to the number of tumor nodules but was more closely related to the level of serum PIVKA-II. These findings were consistent with those reported in previous studies.<sup>20,40</sup>

Further data analysis showed that the number of patients having BCLC stage B–D disease in the GH/GP/GA group was much higher than that in the GL group ( $P < .001$ ), and that in the GH group was higher than that in the GP/GA group, although no statistically significant differences were observed between them ( $P > .05$ ). Accordingly, we speculated that the levels of serum PIVKA-II and AFP were closely related to tumor progression, and if they rise simultaneously, it means that the HCC is more likely to progress to the middle-late stage. These findings were similar to those reported by Hatanaka et al.<sup>41</sup>

In conclusion, ours is the first review in the literature, to our knowledge, of serum PIVKA-II and AFP measured by the UPT-LF assay that provides a rapid and reliable POCT method for the quantitative detection of biomarkers and that demonstrates comparable discrimination performance for HCC vs LC. However, combined detection was unable to enhance the diagnostic performance of disease discrimination based on ensuring specificity. Further, we found that the levels of serum PIVKA-II and AFP were closely related to multiple clinicopathological features of HCC, but PIVKA-II seems to be most useful for the evaluation of clinical severity and the prognosis of HCC.

Despite these findings, our study was subject to some limitations. The number of specimens we studied is small, our study lacks comparison of levels of preoperative and postoperative serum biomarkers, and we have gathered no follow-up data to explore the correlation between biomarkers and survival rate of patients. In future research, we will supplement the deficiencies of this study, provide more data support for the determination of serum PIVKA-II and AFP via UPT-LF assay, and promote the POCT application of tumor biomarkers.

## Acknowledgments

This work was supported by the Startup Fund for scientific research, Fujian Medical University (2019QH1158), and the medical innovation program of Fujian province (2017-CX-4).

## REFERENCES

- Villanueva A. Hepatocellular carcinoma. *N Engl J Med*. 2019;380(15):1450–1462.
- Fattovich G, Stroffolini T, Zagni I, Donato F. Hepatocellular carcinoma in cirrhosis: incidence and risk factors. *Gastroenterology*. 2004;127(5-suppl-S1):S35–S50.
- El-Serag HB, Mason AC. Rising incidence of hepatocellular carcinoma in the United States. *N Engl J Med*. 2003;20(5):745–750.
- Hasegawa K, Kokudo N, Makuuchi M, et al. Comparison of resection and ablation for hepatocellular carcinoma: a cohort study based on a Japanese nationwide survey. *J Hepatol*. 2013;58(4):724–729.
- Di Bisceglie AM, Hoofnagle JH. Elevations in serum alpha-fetoprotein levels in patients with chronic hepatitis B. *Cancer*. 1989;64(10):2117–2120.
- Bae JS, Park SJ, Park KB, et al. Acute exacerbation of hepatitis in liver cirrhosis with very high levels of alpha-fetoprotein but no occurrence of hepatocellular carcinoma. *Korean J Intern Med*. 2005;20(1):80–85.
- Sherman M, Peltekian KM, Lee C. Screening for hepatocellular carcinoma in chronic carriers of hepatitis B virus: incidence and prevalence of hepatocellular carcinoma in a North American urban population. *Hepatology*. 1995;22(2):432–438.
- Liebman HA, Furie BC, Tong MJ, et al. Des- $\gamma$ -carboxy (abnormal) prothrombin as a serum marker of primary hepatocellular carcinoma. *N Engl J Med*. 1984;310(22):1427–1431.
- Motohara K, Kuroki Y, Kan H, Endo F, Matsuda I. Detection of vitamin K deficiency by use of an enzyme-linked immunosorbent assay for circulating abnormal prothrombin. *Pediatr Res*. 1985;19(4):354–357.
- Yoon YJ, Han K-H, Kim DY. Role of serum prothrombin induced by vitamin K absence or antagonist-II in the early detection of hepatocellular carcinoma in patients with chronic hepatitis B virus infection. *Scand J Gastroenterol*. 2009;44(7):861–866.
- Tang W, Miki K, Kokudo N, et al. Des- $\gamma$ -carboxyprothrombin expression in cancer and/or non-cancer liver tissues: association with survival of patients with resectable hepatocellular carcinoma. *Oncol Rep*. 2005;13(1):25–30.
- Koike Y, Shiratori Y, Sato S, et al. Des-gamma-carboxy prothrombin as a useful predisposing factor for the development of portal venous invasion in patients with hepatocellular carcinoma: a prospective analysis of 227 patients. *Cancer*. 2001;91(3):561–569.
- Nakamura S, Nouso K, Sakaguchi K, et al. Sensitivity and specificity of des-gamma-carboxy prothrombin for diagnosis of patients with hepatocellular carcinomas varies according to tumor size. *Am J Gastroenterol*. 2006;101(9):2038–2043.
- Kaibori M, Matsui Y, Yanagida H, et al. Positive status of  $\alpha$ -fetoprotein and des- $\gamma$ -carboxy prothrombin: important prognostic factor for recurrent hepatocellular carcinoma. *World J Surg*. 2004;28(7):702–707.
- Dohmen K, Shigematsu H, Irie K, Ishibashi H. Clinical characteristics among patients with hepatocellular carcinoma according to the serum levels of alpha-fetoprotein and des- $\gamma$ -carboxy prothrombin. *Hepatogastroenterology*. 2003;50(54):2072–2078.
- Loglio A, Iavarone M, Facchetti F, et al. The combination of PIVKA-II and AFP improves the detection accuracy for HCC in HBV Caucasian cirrhotics on long-term oral therapy. *Liver Int*. 2020;40(8):1987–1996.
- Ricco G, Cosma C, Bedogni GB, et al. Modeling the time-related fluctuations of AFP and PIVKA-II serum levels in patients with cirrhosis undergoing surveillance for hepatocellular carcinoma. *Cancer Biomark*. 2020;29(2):189–196.
- Caviglia GP, Ciruolo M, Abate ML, et al. Alpha-fetoprotein, protein induced by vitamin K absence or antagonist II and glypican-3 for the detection and prediction of hepatocellular carcinoma in patients with cirrhosis of viral etiology. *Cancers (Basel)*. 2020;12(11):3218.
- Kamel MM, Saad MF, Mahmoud AA, Edries AA, Abdel-Moneim AS. Evaluation of serum PIVKA-II and MIF as diagnostic markers for HCV/HBV induced hepatocellular carcinoma. *Microb Pathog*. 2014;77:31–35.
- Ji J, Wang H, Li Y, et al. Diagnostic evaluation of des-gamma-carboxy prothrombin versus  $\alpha$ -fetoprotein for hepatitis B virus-related hepatocellular carcinoma in China: a large-scale, multicentre study. *PLoS One*. 2016;11(4):e0153227e153227.
- Kim Y, Park Y-H, Hwang S, et al. Diagnostic role of blood tumor markers in predicting hepatocellular carcinoma in liver cirrhosis patients undergoing liver transplantation. *Ann Transplant*. 2016;21:660–667.
- Gentile I, Buonomo AR, Scotto R, et al. Diagnostic accuracy of PIVKA-II, alpha-fetoprotein and a combination of both in diagnosis of hepatocellular carcinoma in patients affected by chronic HCV infection. *In Vivo*. 2017;31(4):695–700.

23. Li L, Zhou L, Yu Y, et al. Development of up-converting phosphor technology-based lateral-flow assay for rapidly quantitative detection of hepatitis B surface antibody. *Diagn. Microbiol Infect Dis Sci.* 2009;63(2):165–172.
24. Zhao Y, Wang H, Zhang P, et al. Rapid multiplex detection of 10 foodborne pathogens with an up-converting phosphor technology-based 10-channel lateral flow assay. *Sci Rep.* 2016;6:21342. doi:10.1038/srep21342.
25. Zuiderwijk M, Tanke HJ, Sam Niedbala R, Corstjens PLAM. An amplification-free hybridization-based DNA assay to detect *Streptococcus pneumoniae* utilizing the up-converting phosphor technology. *Clin Biochem.* 2003;36(5):401–403.
26. Chen Z, Zheng W, Huang P, et al. Lanthanide-doped luminescent nano-bioprobes for the detection of tumor markers. *Nanoscale.* 2015;7(10):4274–4290.
27. Huang Y, Zhang S, Zheng Q, et al. Development of up-converting phosphor technology-based lateral flow assay for quantitative detection of serum PIVKA-II: inception of a near-patient PIVKA-II detection tool. *Clin Chim Acta.* 2019;488:202–208.
28. Lim TS, Kim DY, Han K-H, et al. Combined use of AFP, PIVKA-II, and AFP-L3 as tumor markers enhances diagnostic accuracy for hepatocellular carcinoma in cirrhotic patients. *Scand J Gastroentero.* 2016;51(3):1–10.
29. Oeda S, Iwane S, Takasaki M, et al. Optimal follow-up of patients with viral hepatitis improves the detection of early-stage hepatocellular carcinoma and the prognosis of survival. *Intern Med.* 2016;55(19):2749–2758.
30. Tsugawa D, Fukumoto T, Kido M, et al. The predictive power of serum  $\alpha$ -fetoprotein and des- $\gamma$ -carboxy prothrombin for survival varies by tumor size in hepatocellular carcinoma. *Kobe J Med Sci.* 2015;61(5):E124–E131.
31. Corstjens PLAM, De Dood CJ, Kornelis D, et al. Tools for diagnosis, monitoring and screening of *Schistosoma* infections utilizing lateral-flow based assays and upconverting phosphor labels. *Parasitology.* 2014;141(14):1841–1855.
32. Liu X, Zhao Y, Sun C, et al. Rapid detection of aBcr in foods with an up-converting phosphor technology-based lateral flow assay. *Sci Rep.* 2016;6:34926. doi:10.1038/srep34926.
33. Eslam M, Khattab MA, Harrison SA. Insulin resistance and hepatitis C: an evolving story. *Gut.* 2011;60(8):1139–1151.
34. Trevisani F, D’Intino PE, Morsellilabate AM, et al. Serum  $\alpha$ -fetoprotein for diagnosis of hepatocellular carcinoma in patients with chronic liver disease: influence of HBsAg and anti-HCV status. *J Hepatol.* 2001;34(4):570–575.
35. Gao J, Song P. Combination of triple biomarkers AFP, AFP-L3, and PIVAKII for early detection of hepatocellular carcinoma in China: expectation. *Drug Discov Ther.* 2017;11(3):168–169.
36. Park SJ, Jang JY, Jeong SW, et al. Usefulness of AFP, AFP-L3, and PIVKA-II, and their combinations in diagnosing hepatocellular carcinoma. *Medicine.* 2017;96(11):e5811.
37. Stenflo J, Fernlund P, Egan W, Roepstorff P. Vitamin K dependent modifications of glutamic acid residues in prothrombin. *P Natl Acad Sci USA.* 1974;71(7):2730–2733.
38. Poté N, Cauchy F, Albuquerque M, et al. Performance of PIVKA-II for early hepatocellular carcinoma diagnosis and prediction of microvascular invasion. *J Hepatol.* 2015;62(4):848–854.
39. Kim HS, Park JW, Jang JS, et al. Prognostic values of  $\alpha$ -fetoprotein and protein induced by vitamin K absence or antagonist-II in hepatitis B virus-related hepatocellular carcinoma: a prospective study. *J Clin Gastroenterol.* 2009;43(5):482–488.
40. Truong BX, Yano Y, Van VT, et al. Clinical utility of protein induced by vitamin K absence in patients with chronic hepatitis B virus infection. *Biomed Rep.* 2013;1(1):122–128.
41. Hatanaka T, Kakizaki S, Shimada Y, et al. Early decreases in  $\alpha$ -fetoprotein and des- $\gamma$ -carboxy prothrombin predict the antitumor effects of hepatic transarterial infusion chemotherapy with cisplatin (CDDP) powder in patients with advanced hepatocellular carcinoma. *Intern Med.* 2016;55(16):2163–2171.

# Anticardiolipin IgA as a Potential Risk Factor for Pregnancy Morbidity in Patients with Antiphospholipid Syndrome

Xiaodan Zhai MD,<sup>1</sup> Shuo Yang MD,<sup>1</sup> and Liyan Cui PhD,<sup>1\*</sup>

<sup>1</sup>Department of Laboratory Medicine, Peking University Third Hospital, Beijing, China \*To whom correspondence should be addressed. [cliyan@163.com](mailto:cliyan@163.com)

**Keywords:** anticardiolipin IgA, pregnancy, antiphospholipid antibodies, fetal loss, anti- $\beta$ 2 glycoprotein I, antiphospholipid syndrome

**Abbreviations:** APS, antiphospholipid syndrome; aPLs, antiphospholipid antibodies; LA, lupus anticoagulant; aCL, anticardiolipin; a $\beta$ 2GPI, anti- $\beta$ 2 glycoprotein I; SNAPS, seronegative APS; HGB, hemoglobin; PLT, platelet; Fib, fibrinogen; TCHO, total cholesterol

*Laboratory Medicine* 2022;53:495–499; <https://doi.org/10.1093/labmed/lmac028>

## ABSTRACT

**Background:** Antiphospholipid syndrome (APS) is an autoimmune disorder that is characterized by venous or arterial thrombosis and/or obstetric morbidity in the constant presence of persistent antiphospholipid antibodies (aPLs). In patients with APS, the relationship between production of immunoglobulin (Ig)A antiphospholipid antibodies and adverse events in pregnancy is still unclear. As a result of massive trials, the clinical efficiency of IgA-aPLs is used to evaluate pregnancy outcomes in patients with APS.

**Methods:** We enrolled 381 female patients with APS and 93 healthy pregnant women. Silica clotting time ratio, dilute Russell viper venom time (dRVVT) ratio, and 6 aPLs, including IgA/IgG/IgM isotypes a $\beta$ 2GPI and IgA/IgG/IgM isotypes anticardiolipin (aCL), were detected using commercial kits.

**Results:** We found no significant differences in laboratory parameters between patients with APS and the control group. The total prevalence of aCL IgA was 2.9%; the prevalence of a $\beta$ 2GPI IgA was 3.4%. Only 1.3% of the individuals who tested aCL-positive (5/381) had isolated aCL IgA. Similarly, isolated a $\beta$ 2GPI IgA was present in only 0.8% (3/381) of the a $\beta$ 2GPI-positive subjects. Meanwhile, aCL IgA showed the maximum area under the curve (AUC) of 0.666 (95% CI, 0.60–0.73;  $P < .001$ ), followed by dRVVT ratio (AUC = 0.649; 0.58–0.72;  $P < .001$ ).

**Conclusion:** Positive aCL IgA and a $\beta$ 2GPI IgA ratios were extremely low for each isolated isotype of aPLs. For patients with APS who experienced fetal loss, aCL IgA may be utilized as a risk factor for pregnancy loss among patients with APS. Establishing a standardized diagnosis of IgA aPLs is also important for these patients.

Antiphospholipid syndrome (APS) is an autoimmune disorder that is characterized by venous or arterial thrombosis and/or obstetric morbidity when in the constant presence of persistent antiphospholipid antibodies (aPLs).<sup>1</sup> A revised international consensus statement on laboratory classification criteria for APS includes lupus anticoagulant (LA), anticardiolipin (aCL), and anti- $\beta$ 2 glycoprotein I (a $\beta$ 2GPI) antibodies (the IgG or IgM isotypes).<sup>2</sup> The patients have typical clinical manifestations, which highly suggests APS, but the aPLs criteria remain constantly negative. These patients have been classified as having seronegative APS (SNAPS) by Hughes and Khamashta.<sup>3</sup>

Patients with SNAPS also have an increased risk of thrombotic occurrences and pregnancy morbidities. The findings of numerous studies, such as Murthy et al,<sup>4</sup> show that noncriteria aPLs, particularly a $\beta$ 2GPI IgA, in patients with SNAPS may indicate a significantly increased risk of thrombosis. Nevertheless, IgA isotype testing is not included in classification criteria for APS.

Now the International Consensus Task Force on aPLs suggests that IgA screening for aCL and a $\beta$ 2GPI should be undertaken when all other relevant test results are truly negative and APS is still suspected.<sup>5</sup> Because the clinical value of testing IgA aPLs remains unclear, the primary aim of our study was to measure IgA aCL and IgA a $\beta$ 2GPI antibodies in well-diagnosed female patients with APS who have experienced fetal loss, thereby providing more convincing evidence for detecting noncriteria aPLs.

## Materials and Methods

### Patients and Serum Specimen Testing

From January 2019 through December 2019, 381 female patients with APS and 93 healthy pregnant women were enrolled in this retrospective research study at the Third Hospital of Peking University, Beijing, China. All patients were residents of China. In this research, duplicate

patients were excluded, and only the first test results of patients who had multiple aPLs features observed during this period were considered. All patients satisfied the 2006 Sydney Classification Criteria.<sup>6</sup> The study was approved by the Ethics Committee of Peking University Third Hospital.

Silica clotting time (SCT) and dilute Russell viper venom time (dRVVT) were measured using the ACLTOP 700 instrument (Werfen), serum levels of aCL IgG/IgM/IgA and aβ2GPI IgG/IgM/IgA were tested using CIA (QUANTA Flash assays, Inova Diagnostics). The QUANTA Flash assays were performed on the BIO-FLASH instrument (Biokit). The cut-off value for positivity of SCT ratio was set at 1.16 because the positivity of the dRVVT ratio was set at 1.11 based on the recommendations of the manufacturer. The cutoff values for positivity of other aPLs were set at 20 CU based on the recommendations of the manufacturer.

### Statistical Analysis

The result of the normally distribution data is expressed as mean (SD). The frequency of categorical data is being used to convey the description data. We used the Student *t*-test for continuous variables conforming to normal distribution;  $\chi^2$  test was used for categorical variables; Mann-Whitney *U* testing was used for continuous variables that did not conform to normal distribution. The receiver operating characteristic (ROC) curve was used to compute the area under the curve (AUC). SPSS software, version 21.0 (IBM) was used to evaluate the quantitative data in our study; 2-tailed *P* values of .05 were considered to be statistically significant.

## Results

### Characteristics of Patients

We tested aCL and aβ2GPI antibodies of IgG, IgM, and IgA isotypes in serum specimens from 381 female patients with APS and 93 healthy pregnant women. The cohort demographic characteristics are depicted in **TABLE 1**. There was no statistically significant difference in laboratory parameters between patients with APS and healthy pregnant women

**TABLE 1. Demographic Data of 381 Female Patients with APS and 93 Healthy Pregnant Women<sup>a</sup>**

Variable	Patients with APS (n = 381)	93 Healthy Pregnant Women (n = 93)	Total No.
Age (y)			
≤30	58 (15.2)	27 (29.0)	85
31–60	323 (84.8)	66 (71.0)	389
Distribution of patients			
Rheumatology	358 (94.0)	0	358
Reproductive center	1 (0.3)	0	1
Gynecology	2 (0.5)	93 (100)	95
Hematology	18 (4.7)	0	18
Other	2 (0.5)	0	2
Obstetric complications			
Early pregnancy loss	376 (98.7)	—	—
Eclampsia/preeclampsia	1 (0.3)	—	—
Late fetal loss	4 (1.0)	—	—

APS, antiphospholipid syndrome.

<sup>a</sup>Data given as No. (%) except where specified.

(**TABLE 2**). Most of the patients had been treated at the Department of Rheumatology and Immunology. In total, 381 patients were diagnosed with APS according to the revised 2006 Sydney criteria for APS.

### Distribution of Antiphospholipid Antibodies

In general, the total percentage of positive aPLs in the pregnant patients with APS was significantly higher, compared with the healthy pregnant women. The most common aPL was the SCT ratio in patients with APS (19.4%), followed by the dRVVT ratio (14.4%). The overall prevalence of aCL was 17.8%, and the most common isotype was aCL IgG (11.8%). Overall, 13.6% were aβ2GPI, with aβ2GPI IgG being the most common isotype (10.5%). The overall prevalence of aCL IgA was 2.9%, and that of aβ2GPI IgA was 3.4% (**TABLE 3**).

At the same time, we observed that only 1.3% (5/381) of the patients with APS had isolated aCL IgA. Similarly, isolated aβ2GPI IgA only accounted for 0.8% (3/381) of patients with APS. We found that aPL-IgA positivity in patients with APS was usually accompanied by IgG or IgM aPLs. The cross-positivity for aCL and aβ2GPI demonstrated that IgA isotypes are also less frequently detected aPLs (**FIGURE 1**).

ROC analysis was conducted to evaluate the predictive value of aPLs in patients with fetal loss vs patients with healthy pregnancy (**FIGURES 2 and 3**). aCL IgA showed the largest AUC, of 0.666 (95% CI, 0.60–0.73; *P* < .001), followed by the dRVVT ratio (AUC, 0.649; 0.58–0.72; *P* < .001; **TABLE 4**). The AUC of aβ2GPI IgA was 0.601 (0.53–0.67; *P* = .003). The combination with antiphospholipid antibodies can improve diagnostic efficiency; however, aCL IgA combined with LA could not better enhance sensitivity (**FIGURE 3, TABLE 4**). Overall, aCL IgA could be regarded as a risk factor for patients with APS related to fetal loss.

### Discussion

The clinical epidemiology of APS has a high incidence and complex pathogenesis, which involves many aspects such as aPLs-induced cell activation, inhibition of anticoagulant and fibrinolytic systems, inflammatory response, complement activation, and oxidative stress. Moreover, the clinical manifestations are complex and varied, which can involve multiple organs and systems throughout the body. According to the 14th International Congress on Antiphospholipid Antibodies Task Force, low aPLs positivity may be associated with adverse outcomes in pregnancy, although the classification standard requires continuous high-titer aPLs positivity.<sup>7</sup> The analysis of published IgA aCL data shows that the general weakness of these data, deriving from the observational cross-sectional studies, is in their lack of prospective confirmation or that they provide control groups of insufficient size.

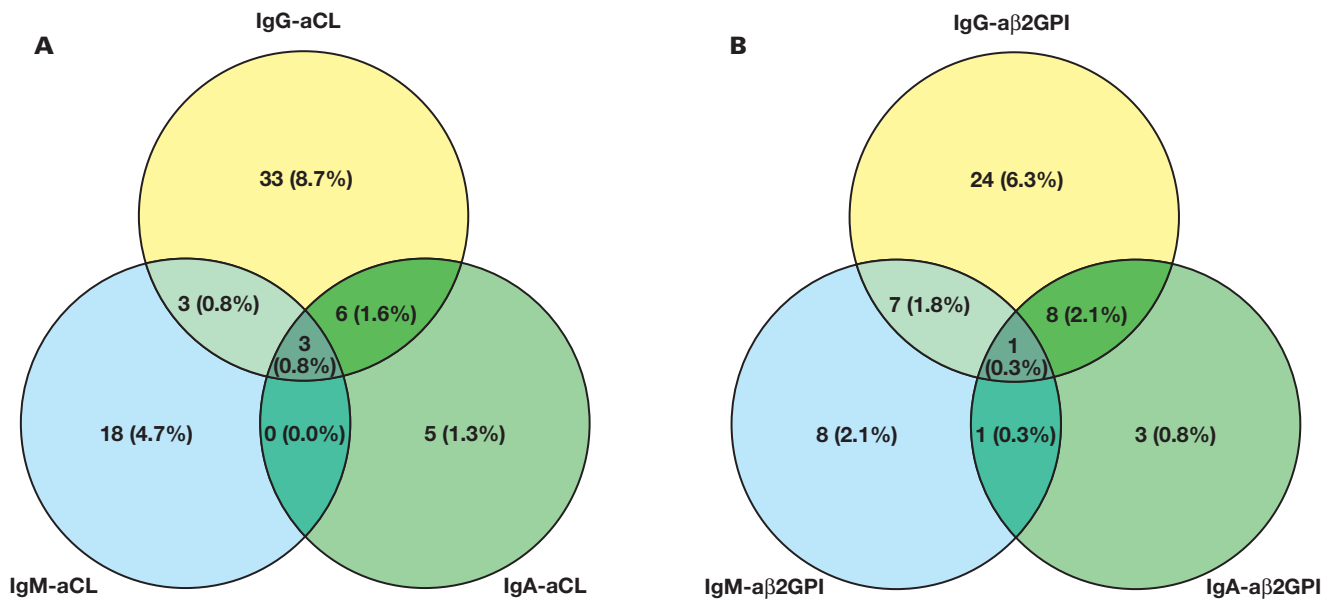
We analyzed the aPLs profile of 381 female subjects with APS from the Chinese general population. We found no significant differences in laboratory parameters between patients with APS and healthy pregnant women. The results indicated that aPLs involve many aspects such as aPLs-induced cell activation, inhibition of anticoagulant, fibrinolytic systems, and so forth. At the same time, we observed the relationship between variables such as SCT ratio, dRVVT ratio, aPLs, and pregnancy outcomes in patients with APS. We found that the total prevalence of aCL IgA in patients with APS was 2.9%, and the total prevalence of aβ2GPI IgA was 3.4% in the present study.

Two previous works of research<sup>8,9</sup> indicated that in terms of epidemiology, the prevalence of aCL IgA is between 1.6% and 10%, and the prevalence of aβ2GPI IgA is between 1.6% and 10%.<sup>10,11</sup> These findings

**TABLE 2. Laboratory Findings of 381 Female Patients with APS and 93 Healthy Pregnant Women**

Laboratory Parameter	Female Patients with APS (n = 381), X±S	Healthy Pregnant Women (n = 93), X±S	t	P Value
WBC (10 <sup>9</sup> /L)	7.09 ± 4.47	6.96 ± 2.59	0.86	.93
HGB (g/L)	130.42 ± 9.29	126.86 ± 10.30	1.20	.24
PLT (10 <sup>9</sup> /L)	201.23 ± 69.32	228.29 ± 63.28	1.22	.23
PT (s)	11.30 ± 0.83	11.13 ± 0.61	0.66	.51
APTT (s)	40.13 ± 19.05	32.27 ± 4.38	1.29	.21
Fib (g/L)	3.17 ± 0.61	3.37 ± 0.58	1.02	.32
TCHO (mmol/L)	4.71 ± 0.97	5.06 ± 0.72	1.10	.29
LDL-C (mmol/L)	2.77 ± 0.86	3.10 ± 0.76	1.08	.29
HDL-C (mmol/L)	1.47 ± 0.34	1.47 ± 0.34	0.049	.96

APS, antiphospholipid syndrome; Fib, fibrinogen; HDL-C, high-density lipoprotein cholesterol; HGB, hemoglobin; LDL-C, low-density lipoprotein cholesterol; PLT, platelet; TCHO, total cholesterol.

**FIGURE 1. Venn diagrams revealing multipositive antiphospholipid antibodies in the antiphospholipid syndrome group. aCL, anticardiolipin.**

are similar to those revealed by our research. The antibody cutoff value is based on the recommendations by the manufacturer in our study.

The cross-positivity for aCL and aβ2GPI demonstrated that aPL-IgA positivity in patients with APS was accompanied by IgG or IgM aPLs. However, these results differ from those of previous studies, such as Frodlund et al<sup>12</sup> and Ruiz-García et al,<sup>13</sup> whose study results demonstrated that the prevalence of isolated IgA aPLs were higher than in our study.

ROC curve analysis revealed that aCL IgA showed the largest AUC, of 0.666 (95% CI, 0.60–0.73;  $P < .001$ ), followed by the dRVVT ratio (AUC = 0.649; 0.58–0.72;  $P < .001$ ). In this study, the total prevalence of the dRVVT ratio was 14.4%. At the same time, Lockshin et al<sup>14</sup> showed that as many as 43% of pregnant women who tested positive for LA had adverse pregnancy outcomes and that aCL and aβ2GPI combined with LA could not better predict adverse pregnancy outcomes, compared with LA only. Therefore, LA is the main predictor of adverse pregnancy outcomes.

However, Seheult et al<sup>15</sup> showed that direct oral administration of anticoagulants and heparin would interfere with the detection of LA, leading to false-positive test results. Besides, dabigatran and apixaban expanded the time of aPTT and modified Russell venom dilution testing.<sup>16</sup>

In this study, aCL IgA showed high diagnostic efficacy for fetal loss in patients with APS. A recent analysis revealed a similar conclusion, namely, that aCL IgA was related to obstetric complications.<sup>17</sup> Certain previous study reports<sup>18–22</sup> also indicated that there was a relationship between aCL IgA and thrombosis. And one study<sup>23</sup> indicated that aβ2GPI IgM was the major type of aPL in patients with APS who had experienced fetal loss. Further, aβ2GPI IgA can be used as an independent predictor for APS-related events.<sup>18</sup> There was a correlation between decrease in antiphospholipid antibody titer and improvement in pregnancy outcomes.<sup>23</sup> These conclusions were controversial due to differences in the inclusion criteria of the study population, ethnic distribution, and the statistical methods used in the study.

**FIGURE 2.** Receiver operating characteristic analysis of the antiphospholipid isotype in patients with antiphospholipid syndrome who have experienced fetal loss. aCL, anticardiolipin; dRVVT, dilute Russell viper venom time; SCT, silica clotting time.

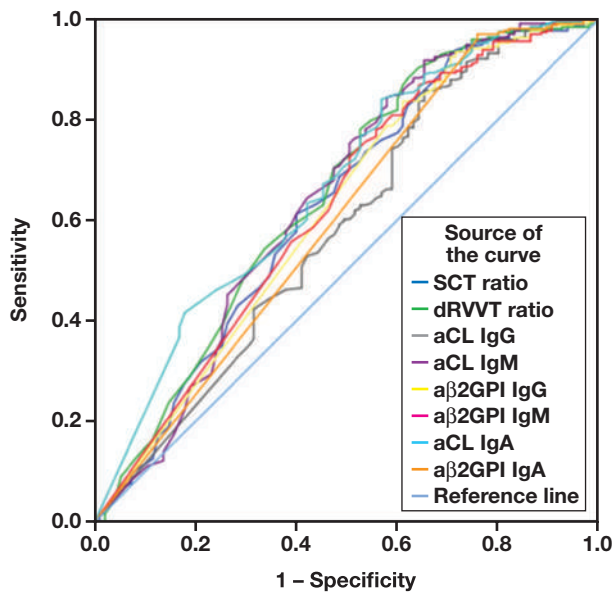


**FIGURE 3.** Receiver operating characteristic analysis of the combination antiphospholipid antibody isotype in patients with antiphospholipid syndrome. aCL, anticardiolipin; LA, lupus anticoagulant.

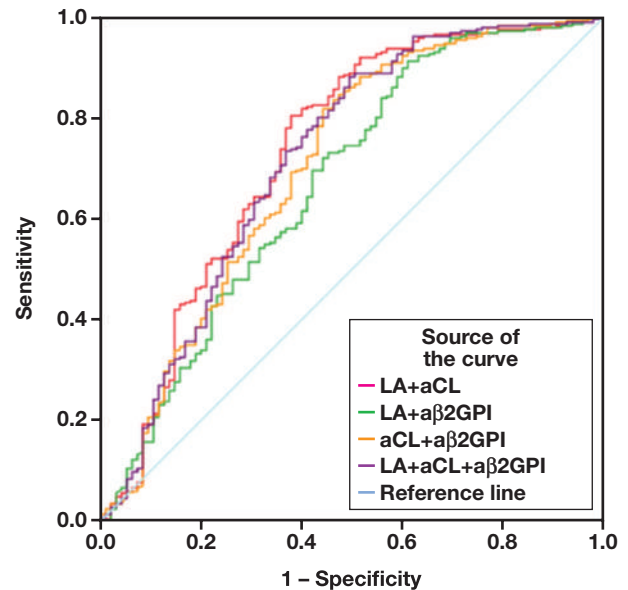


**TABLE 3.** Distribution of Antiphospholipid Antibodies in Patients with APS and Healthy Pregnant Women<sup>a</sup>

Variable	Patients with APS (n = 381)		Healthy Pregnant Women (n = 93)
	Total Positivity	Isolated Positivity	Total Positivity
SCT ratio	74 (19.4)	33 (8.7)	0
dRVVT ratio	55 (14.4)	11 (2.9)	1 (1.1)
aCL	68 (17.8)	—	—
aCL IgG	45 (11.8)	33 (8.7)	0
aCL IgM	24 (6.3)	18 (4.7)	0
aCL IgA	11 (2.9)	5 (1.3)	0
aβ2GPI	52 (13.6)	—	—
aβ2GPI IgG	40 (10.5)	24 (6.3)	0
aβ2GPI IgM	17 (4.5)	8 (2.1)	0
aβ2GPI IgA	13 (3.4)	3 (0.8)	0

aCL, anticardiolipin; APS, antiphospholipid syndrome; dRVVT, dilute Russell viper venom time; SCT, silica clotting time.

<sup>a</sup>Data given as No. (%).

**TABLE 4.** ROC Curve Analysis of the aPL Isotype in Patients with APS

Variable	AUC	P Value	95% CI	Sensitivity	Specificity	Youden Index
SCT ratio	0.629	<.001	.56–.70	93.0	29.5	0.225
dRVVT ratio	0.649	<.001	.58–.72	90.2	35.8	0.260
aCL IgG	0.584	.01	.51–.65	85.7	34.7	0.204
aCL IgM	0.642	<.001	.57–.71	84.3	42.1	0.264
aβ2GPI IgG	0.618	.001	.55–.69	83.6	38.9	0.225
aβ2GPI IgM	0.624	<.001	.56–.69	86.7	35.8	0.225
aCL IgA	0.666	<.001	.60–.73	83.9	43.2	0.271
aβ2GPI IgA	0.601	.003	.53–.67	96.9	24.2	0.211
LA+aCL	0.732	<.001	.67–.80	80.4	62.1	0.425
LA+aβ2GPI	0.671	<.001	.60–.74	91.3	38.9	0.302
aCL+aβ2GPI	0.704	<.001	.64–.77	81.8	55.8	0.376
LA+aCL+aβ2GPI	0.719	<.001	.65–.79	88.1	50.5	0.386

aCL, anticardiolipin; APS, antiphospholipid syndrome; dRVVT, dilute Russell viper venom time; LA, lupus anticoagulant; ROC, receiver operating characteristic; SCT, silica clotting time.

There are some limitations to our study. The study investigates the diagnostic efficacy of IgA isotypes for adverse pregnancy outcomes in patients with APS, but we cannot control anticoagulant therapy, such as low-molecular-weight heparin. Also, different detection systems or kits may change the sensitivity and diagnostic efficiency.<sup>24</sup> Finally, we could not distinguish between primary and secondary APS in patients with APS. The value of IgA aPLs is still difficult to calculate; this problem could be solved in future studies. This research is in continuous development because the clinical relevance of these antibodies is far from being completely clarified.

## Conclusion

In conclusion, positive aCL IgA and a $\beta$ 2GPI IgA were very low when it came to each isolated isotype of aPLs. For patients with APS who had experienced fetal loss, aCL IgA showed perfect diagnostic efficacy. Further, aCL IgA may be considered a predictor for fetal loss in patients with APS. Establishing a standardized diagnosis of IgA aPLs is also critical for these patients.

## Acknowledgments

This work was supported by the National Natural Science Foundation of China (grant No. 62071011).

## REFERENCES

- Liu T, Gu J, Wan L, et al. "Non-criteria" antiphospholipid antibodies add value to antiphospholipid syndrome diagnoses in a large Chinese cohort. *Arthritis Res Ther*. 2020;22(1):33.
- Cáliz Cáliz R, Díaz Del Campo Fontecha P, Galindo Izquierdo M, et al. Recommendations of the Spanish Rheumatology Society for Primary Antiphospholipid Syndrome. Part I: diagnosis, evaluation and treatment [in Spanish]. *Reumatol Clin*. 2020;16(2 Pt 1):71–86.
- Hughes GRV, Khamashta MA. 'Seronegative antiphospholipid syndrome': an update. *Lupus*. 2019;28(3):273–274.
- Murthy V, Willis R, Romay-Penabad Z, et al. Value of isolated IgA anti- $\beta$ 2-glycoprotein I positivity in the diagnosis of the antiphospholipid syndrome. *Arthritis Rheum*. 2013;65(12):3186–3193.
- Lakos G, Favaloro EJ, Harris EN, et al. International consensus guidelines on anticardiolipin and anti- $\beta$ 2-glycoprotein I testing: report from the 13<sup>th</sup> International Congress on Antiphospholipid Antibodies. *Arthritis Rheum*. 2012;64(1):1–10.
- Miyakis S, Lockshin MD, Atsumi T, et al. International consensus statement on an update of the classification criteria for definite antiphospholipid syndrome (APS). *J Thromb Haemost*. 2006;4(2):295–306.
- Bertolaccini ML, Amengual O, Andreoli L, et al. 14<sup>th</sup> International Congress on Antiphospholipid Antibodies Task Force. Report on antiphospholipid syndrome laboratory diagnostics and trends. *Autoimmun Rev*. 2014;13(9):917–930.
- Palomo I, Pereira J, Alarcón M, et al. Prevalence and isotype distribution of antiphospholipid antibodies in unselected Chilean patients with venous and arterial thrombosis. *Clin Rheumatol*. 2004;23(2):129–133.
- Kahles T, Humpich M, Steinmetz H, Sitzer M, Lindhoff-Last E. Phosphatidylserine IgG and beta-2-glycoprotein I IgA antibodies may be a risk factor for ischaemic stroke. *Rheumatology (Oxford)*. 2005;44(9):1161–1165.
- Hsieh K, Knöbl P, Rintelen C, et al. Is the determination of anti-beta2 glycoprotein I antibodies useful in patients with venous thromboembolism without the antiphospholipid syndrome? *Br J Haematol*. 2003;123(3):490–495.
- Veres K, Lakos G, Kerényi A, et al. Antiphospholipid antibodies in acute coronary syndrome. *Lupus*. 2004;13(6):423–427.
- Frodlund M, Vikerfors A, Grosso G, et al. Immunoglobulin A antiphospholipid antibodies in Swedish cases of systemic lupus erythematosus: associations with disease phenotypes, vascular events and damage accrual. *Clin Exp Immunol*. 2018;194(1):27–38.
- Ruiz-García R, Serrano M, Martínez-Flores JÁ, et al. Isolated IgA anti- $\beta$ 2 glycoprotein I antibodies in patients with clinical criteria for antiphospholipid syndrome. *J Immunol Res*. 2014;2014:704395.
- Lockshin MD, Kim M, Laskin CA, et al. Prediction of adverse pregnancy outcome by the presence of lupus anticoagulant, but not anticardiolipin antibody, in patients with antiphospholipid antibodies. *Arthritis Rheum*. 2012;64(7):2311–2318.
- Seheult JN, Meyer MP, Bontempo FA, Chibisov I. The effects of indirect- and direct-acting anticoagulants on lupus anticoagulant assays: a large, retrospective study at a coagulation reference laboratory. *Am J Clin Pathol*. 2017;147(6):632–640.
- Martinuzzo ME, Barrera LH, D'adamo MA, Otaso JC, Gimenez MI, Oyhamburu J. Frequent false-positive results of lupus anticoagulant tests in plasmas of patients receiving the new oral anticoagulants and enoxaparin. *Int J Lab Hematol*. 2014;36(2):144–150.
- Žigon P, Podovšovnik A, Ambrožič A, et al. Added value of non-criteria antiphospholipid antibodies for antiphospholipid syndrome: lessons learned from year-long routine measurements. *Clin Rheumatol*. 2019;38(2):371–378.
- Tortosa C, Cabrera-Marante O, Serrano M, et al. Incidence of thromboembolic events in asymptomatic carriers of IgA anti  $\beta$ 2 glycoprotein-I antibodies. *PLoS One*. 2017;12(7):e0178889.
- Murthy V, Willis R, Romay-Penabad Z, et al. Value of isolated IgA anti- $\beta$ 2-glycoprotein I positivity in the diagnosis of the antiphospholipid syndrome. *Arthritis Rheum*. 2013;65(12):3186–3193.
- Despierres L, Beziane A, Kaplanski G, et al. Contribution of anti- $\beta$ 2 glycoprotein I IgA antibodies to the diagnosis of anti-phospholipid syndrome: potential interest of target domains to discriminate thrombotic and non-thrombotic patients. *Rheumatology (Oxford)*. 2014;53(7):1215–1218.
- Mattia E, Ruffatti A, Tonello M, et al. IgA anticardiolipin and IgA anti- $\beta$ 2 glycoprotein I antibody positivity determined by fluorescence enzyme immunoassay in primary antiphospholipid syndrome. *Clin Chem Lab Med*. 2014;52(9):1329–1333.
- Serrano M, Martínez-Flores JA, Norman GL, Naranjo L, Morales JM, Serrano A. The IgA isotype of Anti- $\beta$ 2 glycoprotein I antibodies recognizes epitopes in domains 3, 4, and 5 that are located in a lateral zone of the molecule (L-shaped). *Front Immunol*. 2019;10:1031.
- Song Y, Wang H-Y, Qiao J, Liu P, Chi H-B. Antiphospholipid antibody titers and clinical outcomes in patients with recurrent miscarriage and antiphospholipid antibody syndrome: a prospective study. *Chin Med J (Engl)*. 2017;130(3):267–272.
- Martínez-Flores JA, Serrano M, Alfaro J, et al. Heterogeneity between diagnostic tests for IgA anti-beta2 glycoprotein I: explaining the controversy in studies of association with vascular pathology. *Anal Chem*. 2013;85(24):12093–12098.

# Topical Application of Methyl Nicotinate Solution Enhances Peripheral Blood Collection

YuLi Zhu, MA,<sup>1,\*</sup> Wei Xu, BA,<sup>1,\*</sup> LiangLiang OuYang, BA,<sup>1,\*</sup> Hong Wang, MA,<sup>1</sup> WeiWei Mao, BA,<sup>1</sup> HuiXiang Zhou, BA,<sup>1</sup> Chao Shen, PhD,<sup>1</sup> ZhiJian Hu, MA,<sup>1</sup> YunChang Tan, MA,<sup>2,\*</sup>

<sup>1</sup>Department of Laboratory, Affiliated Hospital of Jiujiang University, Jiujiang City, China. <sup>2</sup>Department of General Surgery, Affiliated Hospital of Jiujiang University, Jiujiang City, China.\*To whom correspondence should be addressed. [tanyunchang3@163.com](mailto:tanyunchang3@163.com) \*\*These authors contributed equally to this study.

**Keywords:** methyl nicotinate solution, nicotinic acid, peripheral blood, blood collection, routine blood tests, T lymphocyte subsets, topical application

*Laboratory Medicine* 2022;53:500–503; <https://doi.org/10.1093/labmed/lmac033>

## ABSTRACT

**Objective:** The purpose of this study was to investigate whether local application of methyl nicotinate solution can change the content and proportion of blood cells in peripheral blood samples and to determine whether this treatment is a safe and reliable method for improving peripheral blood collection.

**Methods:** Routine blood analysis and flow cytometry were used to analyze the contents and proportions of blood cells and T lymphocyte subsets in peripheral blood samples. Experimental blood specimens were collected from earlobes treated with different concentrations of methyl nicotinate solution, and the control group consisted of blood specimens collected from untreated earlobes.

**Results:** The blood flow in the earlobe was significantly increased after methyl nicotinate solution stimulation, especially when the methyl nicotinate solution concentration was greater than  $10^{-4}$  mol/L. There were no significant changes in the proportions of white blood cells, red blood cells, platelets, neutrophils, eosinophils, basophils, monocytes, or lymphocytes in the peripheral blood obtained from earlobes treated with methyl nicotinate solution. The proportion of T lymphocytes increased in the experimental group, but this difference was not significant.

**Conclusion:** Local application of methyl nicotinate solution is a feasible method for improving peripheral blood collection, especially for

patients with venous blood collection phobia or an inability to provide venous blood samples.

Peripheral blood collection has many advantages; for example, this approach causes minimal pain, is convenient, and allows the collection of low volume blood samples. Peripheral blood collection is often used for rapid tests that require small blood volumes, such as routine blood tests and blood glucose level tests (blood glucose strip method). Currently, the fingertip, earlobe, and heel are the most common areas used for peripheral blood collection. However, due to the rapid coagulation mechanism, poor blood circulation, and other factors, peripheral blood collection may be difficult in some patients. Small amounts of bleeding and poor bleeding often occur during collection, and it is often necessary to manually squeeze the site of blood collection, which can easily lead to blood sample contamination, such as infiltration of tissue fluid and clotting. Research by Han et al<sup>1</sup> shows that difficulties in conducting routine blood tests with peripheral blood specimens are primarily caused by insufficient blood volume (67.8%). Therefore, measures to improve peripheral blood collection are urgently needed.

Nicotinic acid, also known as vitamin B<sub>3</sub>, is one of 13 essential vitamins in the human body; nicotinic acid and nicotinamide, a derivative of nicotinic acid in the human body, are both soluble in water and alcohol, and their properties are relatively stable.<sup>2</sup> Nicotinic acid dilates peripheral blood vessels and is used in the clinic for the treatment of migraine, tinnitus, inner ear vertigo, etc.<sup>2</sup> Studies have shown that nicotinic acid derivatives can stimulate mast cells to release prostaglandin D<sub>2</sub>, which induces vasodilation, vascular permeability, and blood flow, and causes skin flushing.<sup>3</sup> In a study on the use of nicotinic acid-mediated skin flushing in the diagnosis of depression, a laser Doppler instrument was used to analyze the movement of blood cells in microvessels, and the results showed that skin treated with methyl nicotinate solution had significantly increased blood flow.<sup>4</sup> Another study showed that the topical application of nicotinic acid and nonivamide is a possible method for improving capillary blood collection for immunological assessments.<sup>5</sup> In this study, we locally applied methyl nicotinate solution to induce vasodilation to improve peripheral blood collection. However, it is not clear whether the local application of methyl nicotinate solution to induce vasodilation affects the contents and proportions

of blood cells, especially immune cells, in peripheral blood samples. In this study, blood samples were collected from the tips of the earlobes of women aged between 18 and 35 years; one earlobe of each woman was treated with methyl nicotinate solution, and the untreated contralateral earlobe was used as the control. Blood cells and T lymphocyte subsets were analyzed to determine whether the local application of methyl nicotinate solution is a safe and reliable method for inducing vascular dilation and improving peripheral blood collection.

## Methods and Materials

### Subjects

A total of 45 volunteers were recruited for the study. The enrollment criteria were as follows: (1) 18- to 35-year-old females; (2) no past or present diseases, such as abnormal liver and kidney function, heart disease, cerebrovascular disease, or mental disease; and (3) sufficient audiovisual and comprehension abilities. The exclusion criteria were as follows: (1) recent use of vitamin immunosuppressants and other related drugs or (2) pregnancy, breastfeeding, or planning for pregnancy. Each volunteer provided written informed consent, and the study was approved by the Ethics Committee of the Affiliated Hospital of Jiujiang University.

### Blood Flow in the Earlobe After Stimulation with Methyl Nicotinate Solution

According to the procedure described by Messamore et al,<sup>4</sup> the blood flow of the earlobe was measured after stimulation with methyl nicotinate solution. In this part of the study, 45 volunteers were recruited, and a total of 90 earlobes were randomly assigned to 6 groups: a  $10^{-5}$  mol/L methyl nicotinate group ( $n = 15$  earlobes), a  $10^{-4}$  mol/L methyl nicotinate group ( $n = 15$  earlobes), a  $10^{-3}$  mol/L methyl nicotinate group ( $n = 15$  earlobes), a  $10^{-2}$  mol/L methyl nicotinate group ( $n = 15$  earlobes), a  $10^{-1}$  mol/L methyl nicotinate group ( $n = 15$  earlobes), and a control group ( $n = 15$  earlobes). An electrode was attached to the earlobe, and a laser Doppler probe (Perimed, PeriFlux5000 system) was used to measure the baseline blood cell movement in the microvessels. Then, the electrode was removed, the bottom of a double-sided plastic hole was exposed, 0.5 cm diameter filter paper was placed in the hole, a pipette gun was used to remove 50  $\mu$ L of methyl nicotinate solution of different concentrations ( $10^{-5}$  mol/L,  $10^{-4}$  mol/L,  $10^{-3}$  mol/L,  $10^{-2}$  mol/L, and  $10^{-1}$  mol/L), and the solutions of different concentrations were dispensed on the filter paper. The skin of the earlobe was soaked in methyl nicotinate solution for 10 minutes, the filter paper was removed, and blood cell movement was recorded again with a laser Doppler instrument. The blood flow is reported as perfusion units (PUs), and blood flow (PU) = the number of moving blood cells in the measurement area  $\times$  the average movement rate of blood cells.

### Collection of Blood from the Earlobe

One week after the completion of the first part of the experiment, the 45 volunteers recruited for this study were again randomly assigned to three groups: a  $10^{-3}$  mol/L methyl nicotinate group ( $n = 15$ ), a  $10^{-2}$  mol/L methyl nicotinate group ( $n = 15$ ), and a  $10^{-1}$  mol/L methyl nicotinate group ( $n = 15$ ). One earlobe of each volunteer was treated with methyl nicotinate solution and assigned to the experimental group, whereas the opposite lobe remained untreated and was assigned to the control group. One earlobe of each volunteer was covered with methyl

nicotinate solution. After 10 minutes, the earlobe was disinfected with alcohol-soaked cotton balls and then punctured with a disposable blood collection needle to allow the blood to flow naturally. After the first drop was gently wiped with a disinfected cotton ball, blood (approximately 0.2–0.3 mL) was collected into a 0.5 mL EDTAK2 anticoagulant tube. The puncture site was pressed with a dry cotton ball, and the volunteers were asked to apply pressure to the puncture site for 2 to 3 minutes. The blood was then mixed well in a mini vibrator and immediately sent for testing. The same method was used to collect blood from the distal lobe of the contralateral ear, which was not treated with nicotinic acid, and this sample served as the control.

### Specimen Testing

The 6-color direct immunofluorescence method was used for T lymphocyte subset analysis. Fluorescently labeled antibodies (BD) were added to the whole blood samples, and these antibodies bound to their corresponding antigens on the membranes of the white blood cells. After incubation in a light-protection chamber and hemolysis, an FACSCanto II flow cytometer (BD) was used for analysis. The absolute numbers of T lymphocyte subsets in the samples were determined. Routine blood tests were performed using a CAL8000 (Mindray).

### Statistical Analysis

GraphPad Prism 7.0 software was used to analyze the data and generate the corresponding charts. ANOVA or a paired *t*-test was used to analyze the data. The *t*-test was two-sided in this study, and  $P < .05$  was considered statistically significant.

## Results

### Changes in Blood Flow to the Earlobe After Methyl Nicotinate Solution Stimulation

The results showed a significant increase in blood flow to the earlobe after methyl nicotinate solution stimulation, especially when the concentration of the methyl nicotinate solution was greater than  $10^{-4}$  mol/L. The blood flow in the earlobes treated with methyl nicotinate solution at concentrations of  $10^{-4}$  mol/L,  $10^{-3}$  mol/L,  $10^{-2}$  mol/L, and  $10^{-1}$  mol/L was significantly different from that in the control earlobes (FIGURE 1). No participants in the study reported adverse events or withdrew from the study because of adverse events.

### Comparison of Routine Blood Indexes between the Experimental Group and the Control Group

The results showed that the differences in the proportions of white blood cells, red blood cells, platelets, neutrophils, eosinophils, basophils, monocytes, and lymphocytes in the peripheral blood samples from the earlobes stimulated with methyl nicotinate solution compared with those in the samples from the control earlobes were not statistically significant (TABLE 1).

### Comparison of the Proportions of T Lymphocyte Subsets between the Experimental Group and the Control Group

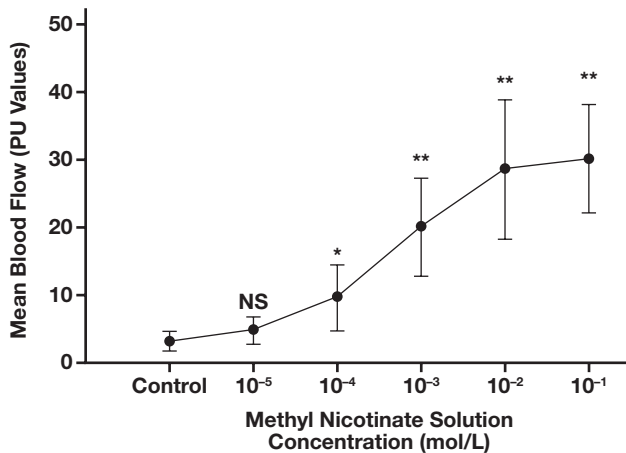
Further studies showed that the proportions of T lymphocyte subsets were increased in the experimental group, but the increase was not statistically significant (TABLE 2).

## Discussion

Under physiological conditions, after skin is stimulated by nicotinic acid, blood perfusion significantly increases, and skin erythema and edema can be observed. There are many different methods of evaluating the intensity of the skin-flushing reaction to nicotinic acid. For example, the intensity of the skin-flushing reaction to nicotinic acid can be semiquantitatively evaluated by visually assessing the degree of skin redness and swelling<sup>6,7</sup>; some studies have also analyzed changes in skin color depth or quantified the intensity of skin color after capturing

images with an optical spectrometer.<sup>8</sup> However, some studies showed that skin blood vessels can also significantly dilate when no changes in skin color can be observed by the naked eye. Therefore, the accuracy and reliability of the methods described above for detecting the intensity of changes in blood flow are limited.<sup>4</sup> In this study, following the method described by Messamore et al,<sup>4</sup> a laser Doppler instrument was used for the direct quantitative measurement of blood perfusion; this method can directly and accurately measure the changes in blood flow that are caused by different concentrations of nicotinic acid. In this study, similar to other studies, blood flow in the skin of earlobes significantly increased after nicotinic acid stimulation, especially when the methyl nicotinate solution concentration was greater than  $10^{-4}$  mol/L (FIGURE 1).

**FIGURE 1.** Changes in blood flow to the earlobe after methyl nicotinate solution stimulation. Data were analyzed by analysis of variance, and the values are expressed as the mean + SD, with  $n = 15$  for each group; \* $P < .005$ , \*\* $P < .001$ . NS, not significant; PU, perfusion unit.



The mechanism underlying the skin-flushing reaction to nicotinic acid is relatively clear. When nicotinic acid binds to specific G-protein-coupled receptors on dermal macrophages, adipocytes, and epidermal Langerhans cells, it can activate phospholipase  $A_2$  and hydrolyze membrane phospholipids, releasing arachidonic acid from the cell membrane. Prostaglandin  $D_2$  is produced from arachidonic acid by cyclooxygenase (COX-2), and prostaglandin  $D_2$  relaxes the smooth muscle of the skin capillary walls and dilates blood vessels, thereby causing a local skin-flushing reaction.<sup>9</sup> In an allergic state, prostaglandin  $D_2$  activates various immune cells, such as helper T cells, eosinophils, basophils, mast cells, and dendritic cells.<sup>10</sup> In addition, in combination with cysteine leukotriene E4 (LTE4), prostaglandin  $D_2$  alters helper T cell adhesion and migration as well as cytokine production.<sup>11</sup>

Our study showed that skin flushing in response to nicotinic acid did not significantly affect the contents and proportions of local blood cells, although the contents of T cell subsets in the experimental group increased nonsignificantly (TABLE 1 and TABLE 2). The results obtained in this

**TABLE 1.** Comparison of Routine Blood Indexes Between the Experimental Group and the Control Group<sup>a</sup>

	$10^{-3}$ mol/L Methyl Nicotinate			$10^{-2}$ mol/L Methyl Nicotinate			$10^{-1}$ mol/L Methyl Nicotinate		
	Treatment Group	Control Group	P	Treatment Group	Control Group	P	Treatment Group	Control Group	P
White blood cells ( $\times 10^9/L$ )	6.22 $\pm$ 1.37	6.13 $\pm$ 1.40	> .05	5.34 $\pm$ 1.59	5.58 $\pm$ 1.01	> .05	5.65 $\pm$ 0.97	5.72 $\pm$ 1.03	> .05
Red blood cells ( $\times 10^{12}/L$ )	4.67 $\pm$ 0.37	4.76 $\pm$ 0.42	> .05	4.65 $\pm$ 0.63	4.48 $\pm$ 0.35	> .05	4.58 $\pm$ 0.41	4.54 $\pm$ 0.33	> .05
Platelet ( $\times 10^9/L$ )	239 $\pm$ 60.9	234 $\pm$ 67.9	> .05	224 $\pm$ 44.4	223 $\pm$ 41.5	> .05	206 $\pm$ 39.7	209 $\pm$ 38.8	> .05
Neutrophils ( $\times 10^9/L$ )	3.88 $\pm$ 1.15	3.92 $\pm$ 1.13	> .05	3.27 $\pm$ 0.78	3.33 $\pm$ 0.75	> .05	3.45 $\pm$ 0.93	3.50 $\pm$ 0.89	> .05
Eosinophils ( $\times 10^9/L$ )	0.11 $\pm$ 0.08	0.13 $\pm$ 0.11	> .05	0.13 $\pm$ 0.12	0.13 $\pm$ 0.12	> .05	0.11 $\pm$ 0.09	0.10 $\pm$ 0.08	> .05
Basophil ( $\times 10^9/L$ )	0.02 $\pm$ 0.01	0.02 $\pm$ 0.01	> .05	0.02 $\pm$ 0.01	0.02 $\pm$ 0.01	> .05	0.02 $\pm$ 0.01	0.02 $\pm$ 0.01	> .05
Monocytes ( $\times 10^9/L$ )	0.40 $\pm$ 0.16	0.40 $\pm$ 0.15	> .05	0.37 $\pm$ 0.28	0.38 $\pm$ 0.26	> .05	0.31 $\pm$ 0.07	0.32 $\pm$ 0.06	> .05
Lymphocyte ( $\times 10^9/L$ )	1.64 $\pm$ 0.52	1.62 $\pm$ 0.52	> .05	1.77 $\pm$ 0.48	1.74 $\pm$ 0.49	> .05	1.65 $\pm$ 0.34	1.64 $\pm$ 0.33	> .05

<sup>a</sup>The treatment group was the group of earlobes stimulated with methyl nicotinate, and the control group was the group of the contralateral earlobe. A paired t-test was used to analyze the data, and the values are expressed as the mean  $\pm$  SD, with  $n = 15$  for each group.

**TABLE 2.** Comparison of T Lymphocyte Subsets Between Different Concentrations of Methyl Nicotinate Solution and the Control<sup>a</sup>

	$10^{-3}$ mol/L Methyl Nicotinate			$10^{-2}$ mol/L Methyl Nicotinate			$10^{-1}$ mol/L Methyl Nicotinate		
	Treatment Group	Control Group	P	Treatment Group	Control Group	P	Treatment Group	Control Group	P
CD3+	1733 $\pm$ 601	1693 $\pm$ 581	> .05	1687 $\pm$ 643	1585 $\pm$ 577	> .05	1676 $\pm$ 597	1643 $\pm$ 589	> .05
CD4+	922 $\pm$ 417	899 $\pm$ 418	> .05	937 $\pm$ 418	920 $\pm$ 424	> .05	967 $\pm$ 437	941 $\pm$ 420	> .05
CD8+	710 $\pm$ 275	675 $\pm$ 236	> .05	705 $\pm$ 287	663 $\pm$ 259	> .05	698 $\pm$ 253	688 $\pm$ 255	> .05

<sup>a</sup>The treatment group was the group of earlobes treated with methyl nicotinate, and the control group was the group of contralateral earlobes. Paired t-tests were used to analyze the data. Data are expressed as the mean  $\pm$  SD number of cells/ $\mu L$ , with  $n = 15$  for each group.

study are similar to those of Moro et al,<sup>5</sup> but this study quantitatively analyzed the changes in blood flow caused by treatment with methyl nicotinate solutions of different concentrations and whether methyl nicotinate solutions of different concentrations would change the composition and content of blood cells, especially immune cells. Adverse effects of nicotinic acid mainly include a burning sensation at the application site, local tingling, rash, blistering, paresthesia, cough, and dyspnea. However, none of the participants in the study reported adverse events or withdrew from the study due to adverse events. Therefore, local application of methyl nicotinate solution is a feasible method to improve the rate of peripheral blood collection success, especially for patients with venous blood collection phobia or who are unable to provide venous blood samples.

## Acknowledgments

This study was supported by the Science and Technology Research Project of Jiangxi Provincial Education Department (No. GJJ190939) and the Science and Technology Project of Jiangxi Provincial Health Commission (No. 20204283).

## REFERENCES

1. Han Z, He J, Xie X, et al. Investigation and analysis on the application of peripheral blood specimens for routine blood testing by laboratory physicians. *Ann Palliat Med*. 2021;10(9):9516–9522.
2. Djado S, Bajaj T. *NiacinBTI - StatPearls*. 2021. <https://pubmed.ncbi.nlm.nih.gov/31082080/>.
3. Papaliodis D, Boucher W, Kempuraj D, et al. Niacin-induced “flush” involves release of prostaglandin D2 from mast cells and serotonin from platelets: evidence from human cells in vitro and an animal model. *J Pharmacol Exp Ther*. 2008;327(3):665–672.
4. Messamore E, Hoffman WF, Janowsky A. The niacin skin flush abnormality in schizophrenia: a quantitative dose-response study. *Schizophr Res*. 2003;62(3):251–258.
5. Moro C, Bass J, Scott AM, et al. Enhancing capillary blood collection: The influence of nicotinic acid and nonivamide. LID - 10.1002/jcla.22142 [doi]. *J Clin Lab Anal*. 2017;31(6):e22142.
6. Bosveld-van HL, Knegeter R, Kluiters H, et al. Niacin skin flushing in schizophrenic and depressed patients and healthy controls. *Psychiatry Res*. 2006;143(2-3):303–306.
7. Smesny S, Rosburg T, Riemann S, et al. Impaired niacin sensitivity in acute first-episode but not in multi-episode schizophrenia. *Prostaglandins Leukot Essent Fatty Acids*. 2005;72(6):393–402.
8. Smesny S, Riemann S, Riehemann S, et al. Quantitative measurement of induced skin reddening using optical reflection spectroscopy—methodology and clinical application [in German]. *Biomed Tech (Berl)*. 2001;46(10):280–286.
9. Langbein K, Schmidt U, Schack S, et al. State marker properties of niacin skin sensitivity in ultra-high risk groups for psychosis—an optical reflection spectroscopy study. *Schizophr Res*. 2018;192:377–384.
10. Arima M, Fukuda T. Prostaglandin D(2) and T(H)2 inflammation in the pathogenesis of bronchial asthma. *Korean J Intern Med*. 2011;26(1):8–18.
11. Xue L, Fergusson J, Salimi M, et al. Prostaglandin D2 and leukotriene E4 synergize to stimulate diverse TH2 functions and TH2 cell/neutrophil crosstalk. *J Allergy Clin Immunol*. 2015;135(5):1358–1366.e1.

# Association of rs5742612 Polymorphism in the Promoter Region of *IGF1* Gene with Nonalcoholic Fatty Liver Disease: A Case-Control Study

Hossein Nobakht, MD,<sup>1</sup> Touraj Mahmoudi, MS,<sup>2</sup> Gholamreza Rezamand, MD,<sup>3,4</sup> Seidamir Pasha Tabaeian, MD,<sup>3,4</sup> Golnaz Jeddí, MS,<sup>5</sup> Asadollah Asadi, PhD,<sup>6</sup> Hamid Farahani, PhD,<sup>7,\*</sup> Reza Dabiri, MD,<sup>1</sup> Fariborz Mansour-Ghanaei, MD, AGAF,<sup>8</sup> Seyed Alireza Kaboli, MD,<sup>9</sup> Faramarz Derakhshan, MD,<sup>2</sup> and Mohammad Reza Zali, MD<sup>2</sup>

<sup>1</sup>Internal Medicine Department, Semnan University of Medical Sciences, Semnan, Iran, <sup>2</sup>Gastroenterology and Liver Diseases Research Center, Research Institute for Gastroenterology and Liver Diseases, Shahid Beheshti University of Medical Sciences, Tehran, Iran, <sup>3</sup>Department of Internal Medicine, School of Medicine, Iran University of Medical Sciences, Tehran, Iran, <sup>4</sup>Colorectal Research Center, Iran University of Medical Sciences, Tehran, Iran, <sup>5</sup>Department of Biology, Faculty of Basic Sciences, East Tehran Branch (Ghiamdasth), Islamic Azad University, Tehran, Iran, <sup>6</sup>Department of Biology, Faculty of Science, University of Mohaghegh Ardabili, Ardabil, Iran, <sup>7</sup>Department of Physiology and Pharmacology, School of Medicine, Qom University of Medical Sciences, Qom, Iran, <sup>8</sup>Division of Gastroenterology and Hepatology, Gastrointestinal and Liver Diseases Research Center (GLDRC), Guilan University of Medical Sciences, Rasht, Iran, <sup>9</sup>Department of Gastroenterology, School of Medicine, Hamadan University of Medical Sciences, Hamadan, Iran \*To whom correspondence should be addressed. farahani42@gmail.com

**Keywords:** *IGF1* gene, insulin, NAFLD, polymorphism, variant

**Abbreviations:** NAFLD, nonalcoholic fatty liver disease; IGF1, insulin-like growth factor 1; IR, insulin resistance; T2D, type 2 diabetes; SNV, single nucleotide variant; AST, aspartate aminotransferase; ALT, alanine aminotransferase; GGT, gamma glutamyl transferase; PCR, polymerase chain reaction; RFLP, restriction fragment length polymorphism; OR, odds ratio; 95% CI, 95% confidence interval; HOMA-IR, Homeostatic Model Assessment for Insulin Resistance.

*Laboratory Medicine* 2022;53:504–508; <https://doi.org/10.1093/labmed/lmac039>

## ABSTRACT

**Objective:** Nonalcoholic fatty liver disease (NAFLD) is an emerging global chronic liver disease encompassing a wide spectrum of disorders ranging from simple steatosis to nonalcoholic steatohepatitis, fibrosis, cirrhosis, and hepatocellular carcinoma. Considering the strong association between NAFLD and insulin resistance, and the vital role of insulin-like growth factor 1 (IGF1) in IR, we hypothesized that *IGF1* gene polymorphism might be associated with NAFLD.

**Methods:** A total of 302 subjects, including 149 patients with biopsy-proven NAFLD and 153 controls, were enrolled in this case-control

study. All the subjects were genotyped for the rs5742612 polymorphism of the *IGF1* gene using the polymerase chain reaction-restriction fragment length polymorphism method.

**Results:** The distribution of *IGF1* rs5742612 genotypes and alleles differed significantly between the cases with NAFLD and controls. The *IGF1* rs5742612 CC genotype compared with the TT genotype or the TT+TC genotype occurred more frequently in the cases than the controls and the differences remained significant after adjustment for confounding factors such as age and body mass index ( $P = .011$ , OR = 2.71, 95%CI = 1.16–5.85; and  $P = .032$ , OR = 2.29, 95% CI = 1.10–5.24, respectively).

**Conclusion:** For the first time, this study uncovered that the *IGF1* rs5742612 CC genotype compared with the TT genotype or the TT+TC genotype had a 2.71-fold or 2.29-fold increased risk for NAFLD, respectively.

Nonalcoholic fatty liver disease (NAFLD) is an emerging global chronic liver disease characterized by accumulation of triglycerides in hepatocytes without excessive alcohol consumption. NAFLD encompasses a broad spectrum of disorders ranging from simple steatosis to nonalcoholic steatohepatitis, fibrosis, cirrhosis, and hepatocellular carcinoma. Global prevalence of NAFLD among adults is estimated to range between 23% and 25%,<sup>1</sup> but its etiology has not yet been entirely elucidated. However, NAFLD is connected with abnormal glucose tolerance,<sup>2</sup> insulin resistance (IR),<sup>3,4</sup> type 2 diabetes (T2D),<sup>5</sup> and obesity.<sup>6</sup> In addition, a positive association between circulating insulin levels and NAFLD has been reported.<sup>7</sup> IR is the underlying cause of NAFLD independent of obesity and plays a major role in the pathogenesis of NAFLD. Insulin sensitivity is associated with the severity of histological progression of NAFLD.<sup>8</sup> Interestingly, patients with nonalcoholic steatohepatitis compared with those with simple fatty liver have more severe IR.<sup>9</sup> Finally, the rate of elevated liver enzymes levels is much higher in NAFLD patients with IR than those without IR.<sup>10</sup>

There is a biological interconnection between insulin and insulin-like growth factor (IGF) axes. IGF1 is largely produced by liver cells

and has a significant homology with insulin. There is a positive association between serum levels of IGF1 and insulin sensitivity.<sup>11</sup> Maybe more interestingly, patients with NAFLD have lower levels of circulating IGF1 and IGF1 mRNA than the controls.<sup>12–14</sup> Previous studies have also shown significant associations between *IGF1* gene polymorphisms and insulin secretion,<sup>15</sup> circulating insulin levels,<sup>16</sup> IR,<sup>15</sup> T2D,<sup>17</sup> and obesity.<sup>15</sup> Significant associations between polymorphisms in insulin pathway-related genes and NAFLD risk have also been found.<sup>18–20</sup> Accordingly, these observations led us to investigate the possible association of the rs5742612 polymorphism of the *IGF1* gene with NAFLD risk. The criteria for selecting this single nucleotide variant (SNV) was its commonly use in previous genetic studies and its position in the gene (promoter).

## Materials and Methods

### Study Population

This was a retrospective case-control study where 302 Iranian and genetically unrelated individuals (cases with biopsy-proven NAFLD [n = 149, age range, 32–86 years] and controls [n = 153, age range, 33–81 years]) were enrolled after informed consent. The present study had the approval of the Research Institute for Gastroenterology and Liver Diseases, Shahid Beheshti University of Medical Sciences Ethics Committee, following the principles of the Declaration of Helsinki. For the NAFLD group, participants were enrolled after a diagnosis of fatty liver defined by (1) ultrasonographic evidence of fatty liver; (2) high serum levels of liver enzymes including aspartate aminotransferase (AST), alanine aminotransferase (ALT), and gamma glutamyl transferase (GGT); (3) excluding patients with other causes of liver disease, such as that caused by alcohol abuse (alcohol consumption >70 g/wk. in women or >140 g/wk. in men), viral hepatitis, Wilson's disease, alpha-1 antitrypsin deficiency, or use of drugs likely to cause NAFLD; and (4) the confirmation of liver biopsy consistent with NAFLD by a seasoned pathologist who was blinded to clinical and laboratory data of the patients and analyzed the liver biopsy samples using Brunt's criteria. Grading of steatosis and necroinflammation was from 0 to 3 and staging of fibrosis was from 0 to 4.<sup>21</sup> For the control group, subjects who were free of elevated liver enzymes and viral hepatitis infection (examined by blood test), had no liver steatosis (examined by abdominal ultrasonography), and were not alcoholic or on regular medications were enrolled. Controls were recruited from medical students and the research staff of the Institute. All the participants were asked to complete self-administered questionnaires in which they listed their demographic, anthropometric, and clinical characteristics. The formula for calculation of body mass index (BMI) was weight in kilograms (kg) divided by height in meters squared (m<sup>2</sup>).<sup>22</sup>

### Genotyping

The genomic DNA was purified from 5 mL EDTA-anti-coagulated whole blood using phenol chloroform extraction and ethanol precipitation protocol and was stored at -20°C for further analysis.<sup>23</sup> The genotypes of *IGF1* rs5742612 were determined using the polymerase chain reaction-restriction fragment length polymorphism (PCR-RFLP) method. Genotyping was performed without the knowledge of case or control status of the participants by laboratory personnel. **TABLE 1** shows the details of the studied gene polymorphism and its PCR and

RFLP conditions.<sup>24</sup> PCR products were separated by 3% agarose gels after digestion with the restriction enzyme of BseI (Fermentas) in a water bath at 37°C overnight. They were then stained with ethidium bromide (0.5 µg/mL) and visualized with a UV transilluminator. The digestion pattern and the presence/absence of the BseI determined the genotypes of the *IGF1* rs5742612 variant for each subject. Around 20% of all the samples were genotyped twice to validate the genotyping results with a reproducibility of 100%.

### Statistical Analysis

SPSS statistics software for Windows, version 25.0 (SPSS) was used for statistical analyses. Continuous variables were expressed as mean (standard deviation) and compared using the *t*-test. Categorical clinical variables were presented as number (percent) and compared using the  $\chi^2$  test. To compare the allele frequencies between NAFLD and control groups, we also used the  $\chi^2$  test. Logistic regression analysis was performed to evaluate the association between the genotype frequencies and NAFLD risk and to adjust confounding factors. The measure of associations was assessed by the odds ratio (OR) and the corresponding 95% confidence interval (95% CI). Statistical significance level was considered  $P < .05$ .

### Results

Demographic, anthropometric, clinical, and biochemical characteristics of the study population are depicted in **TABLE 2**. Age and BMI of the NAFLD patients were significantly higher than the controls ( $P < .001$ ). The cases with NAFLD were also more likely to be male ( $P < .001$ ) and smoker ( $P = .008$ ) than the controls. Moreover, systolic blood pressure, diastolic blood pressure, and circulating levels of AST, ALT, and GGT were significantly different between the case and control groups, being higher in the case group ( $P < .001$ ).

The distribution of genotypes and alleles of the *IGF1* rs5742612 gene polymorphism in the cases with NAFLD and the controls is summarized in **TABLE 3**. Genotype and allele frequencies were significantly different between the two groups. The *IGF1* rs5742612 CC genotype compared with the TT genotype and the CC genotype compared with the TT+TC genotype occurred more frequently in the cases with NAFLD than the controls ( $P = .011$ , OR = 2.71, 95% CI = 1.16–5.85; and  $P = .032$ , OR = 2.29, 95% CI = 1.10–5.24, respectively). These differences remained significant even after adjustment for confounding factors including age, BMI, sex, smoking status, systolic blood pressure, and diastolic blood pressure.

### Discussion

In the current study, which has not been done before, the association of the *IGF1* rs5742612 polymorphism with NAFLD susceptibility was explored. We found that the *IGF1* rs5742612 CC genotype compared with the TT genotype or the TT+TC genotype increases the risk of NAFLD.

The investigation of the genetic aspect of diseases provides the opportunity to explore the relationships between complex phenotypes and genomic variation. NAFLD is a complex metabolic condition in which, like other complex diseases, the interactions between different genetic and environmental factors determine the presence and severity of the disease. Owing to the fairly small individual effects and complex

**TABLE 1. The Studied Variant in the *IGF1* Gene**

RFLP Products Size (bp)	Restriction Enzyme	PCR Product Size (bp)	Annealing Temperature	Primer Sequence (Forward and Reverse)	Gene (SNV) Location (Base Change)
C: 410	Bsll	410	67 °C	5'-GACAGTGACAGGCAGCCTAGTAGAAG-3'	<i>IGF1</i> (rs5742612)
T: 234 + 176				5'-CTGGGCATGAACACAAACG-3'	Promoter (T/C)

*IGF1*, insulin-like growth factor 1; PCR, polymerase chain reaction; RFLP, restriction fragment length polymorphism; SNV, single nucleotide variant.

**TABLE 2. General Characteristics of the Study Groups<sup>a</sup>**

Variables	Cases with Nonalcoholic Fatty Liver Disease (n = 149)	Controls (n = 153)	P Value
Age (years)	38.7 (9.2)	29.0 (7.3)	<.001
BMI (kg/m <sup>2</sup> )	29.3 (5.5)	23.7 (3.1)	<.001
Sex			
M	109 (73.1)	81 (52.9)	
F	40 (26.9)	72 (47.1)	<.001
Smoking history			
No	112 (75.1)	140 (91.5)	
Former	18 (12.1)	9 (5.9)	
Current	19 (12.8)	4 (2.6)	.008
SBP (mm Hg)	123.5 (15.1)	114.6 (13.3)	<.001
DBP (mm Hg)	74.9 (9.3)	69.4 (8.4)	<.001
AST (IU/L)	39.3 (17.5)	19.7 (7.1)	<.001
ALT (IU/L)	71.7 (41.1)	19.1 (10.6)	<.001
GGT (IU/L)	58.5 (31.9)	18.3 (8.2)	<.001
Steatosis			
Grade 0	—		
Grade 1	39 (26.2)		
Grade 2	80 (53.7)		
Grade 3	30 (20.1)		
Necroinflammation			
Grade 0	46 (30.9)		
Grade 1	57 (38.3)		
Grade 2	44 (29.5)		
Grade 3	2 (1.3)		
Fibrosis			
Stage 0	86 (57.7)		
Stage 1	56 (37.6)		
Stage 2	7 (4.7)		
Stage 3	—		
Stage 4	—		

ALT, alanine aminotransferase; BMI, body mass index; DBP, diastolic blood pressure; GGT, gamma glutamyl transferase; SBP, systolic blood pressure.

<sup>a</sup>Data are presented as mean (SD) or No. (%).

interactions of these genes, they will not be discovered easily. A common approach to identifying novel susceptibility genes for complex diseases like NAFLD is to study the SNVs in candidate genes; however, inconsistent findings are not rare in genetic association studies. The discrepancies may be explicated by variations in lifestyle or dietary factors, racial differences in genetic makeup, genotyped markers, statistical methods, or even differences in disease definition.<sup>25–27</sup> Nevertheless, considering

the fact that IR is of critical importance in NAFLD pathogenesis, it is reasonable to assume that insulin signaling pathway genes may play a role in the development and progression of NAFLD. Previous studies have demonstrated that the release of free fatty acids from adipose tissue and their influx into liver can be accelerated by IR.<sup>3,4,28</sup> The Homeostatic Model Assessment for Insulin Resistance (HOMA-IR) index has an independent predictive value for advanced liver fibrosis. To maintain glucose homeostasis in the patients with NAFLD, insulin secretion seems to increase to make up for low insulin sensitivity in these patients.<sup>29,30</sup> Previous reports have also shown that insulin and IGF axes are closely interrelated and IGF1 has diverse physiological functions. Notwithstanding the biological plausibility, there is no previous study that has explored the possible association between the *IGF1* rs5742612 polymorphism and the risk of NAFLD.

*IGF1*, as one of the most important members of IGF family, is encoded by *IGF1* gene. The gene consists of 5 exons and is situated on the long arm of chromosome 12. As a highly polymorphic gene with thousands of SNVs, *IGF1* has numerous biological functions, and any defects in it can result in IR, obesity, inflammation, and oxidative stress, which are implicated in the etiology of NAFLD. In this study, we demonstrated that there is a significant association between NAFLD and rs5742612 polymorphism located in the evolutionarily conserved region of *IGF1* promoter. Alterations in promoter sequence can influence protein expression.<sup>31</sup> The CC genotype of *IGF1* rs5742612 gene variant compared with the TT genotype or the TT+TC genotype was a risk factor for NAFLD. The promoter of *IGF1* gene is associated with IGF1 expression and the rs5742612 variant may change the level and functional activity of IGF1 protein. However, the molecular mechanism through which the rs5742612 polymorphism might affect the function of IGF1 needs to be elucidated. rs5742612 per se might not be functional biologically; instead it might be in linkage disequilibrium with another functional *IGF1* gene polymorphism. Alternatively, perhaps the rs5742612 C allele is less stable and translates less efficiently into IGF1 protein, in turn, reduces the biological response to IGF1, and lastly results in NAFLD. In agreement with the second hypothesis, the C allele was found to be positively associated with decreased insulin sensitivity, as well as increased insulin secretion, circulating insulin levels, BMI,<sup>15</sup> and risk of T2D.<sup>17</sup> Previous reports have also suggested significant associations between *IGF1* gene polymorphisms and insulin secretion,<sup>15</sup> serum insulin levels,<sup>16</sup> IR,<sup>15</sup> T2D,<sup>17</sup> obesity,<sup>15</sup> and circulating IGF1 levels.<sup>32</sup> Furthermore, IGF1 may prevent the development and progression of NAFLD by reducing IR and oxidative stress that are 2 major contributors in the pathogenesis of this disease.<sup>11–14,33,34</sup> Finally, IGF1 reduces the level of C-reactive protein as an inflammatory biomarker.<sup>35</sup> On the other hand, the secretion of IGF1 from hepatocytes can be suppressed by inflammatory cytokines including IL1 $\beta$ , IL6, and TNF $\alpha$ , which have a central role in the development of NAFLD.<sup>36</sup> Consequently, a growing body of evidence corroborates the hypothesis that IGF1 and its gene may play a role in the development and progression of NAFLD, and the finding of the present study, that

**TABLE 3. The Distribution of the *IGF1* Gene rs5742612 Polymorphism in the Cases with NAFLD and in the Controls<sup>a</sup>**

Gene (SNV)	Cases (n = 149)	Controls (n = 153)	Crude OR (95% CI) P Value	Adjusted <sup>b</sup> OR (95% CI) P Value
<i>IGF1</i> (rs5742612)				
Genotype-wise comparison				
TT	102 (68.5)	114 (74.5)	1.0 (reference)	1.0 (reference)
TC	32 (21.4)	32 (20.9)	1.05 (0.62–1.46) .907	1.17 (0.73–1.69) .786
CC	15 (10.1)	7 (4.6)	2.58 (1.14–5.34) .014	2.71 (1.16–5.85) .011
TC and CC	47 (31.5)	39 (25.5)	1.31 (0.75–2.45) .657	1.44 (0.85–2.12) .564
CC vs others	15 (10.1)	7 (4.6)	2.32 (1.17–5.38) .029	2.29 (1.10–5.24) .032
Allele-wise comparison				
T	236 (79.2)	260 (84.9)	1.0 (reference)	—
C	62 (20.8)	46 (15.1)	1.31 (0.62–1.74) .063	—

CI, confidence interval; *IGF1*, insulin-like growth factor 1; NAFLD, nonalcoholic fatty liver disease; OR, odds ratio; SNV, single-nucleotide variant.

<sup>a</sup>Data presented as No. (%).

<sup>b</sup>Adjusted for age, body mass index, sex, smoking status, systolic blood pressure, and diastolic blood pressure in genotype-wise comparisons.

the rs5742612 polymorphism of *IGF1* gene is associated with NAFLD, is in line with the evidence.

The present study had the following limitations: (1) Owing to the modest sample size, it was not sensible to perform sub-analyses. (2) The serum level of *IGF1* and insulin resistance (HOMA-IR) index were not measured due to budget limitations. (3) Because only one polymorphism in the *IGF1* gene was genotyped, the coverage of the gene for this genetic association study was not complete. (4) Unfortunately, there were no patients with advanced fibrosis (stage 3 or 4), those who are at the greatest risks of liver failure; hence we could not investigate the association between *IGF1* gene and these patients. (5) There was a significant difference between the cases and controls with regard to age due to not using age-matched controls. Notwithstanding the aforementioned limitations, the design of this study was good, and liver biopsy, which is generally considered as the gold standard method to confirm NAFLD diagnosis, was used. Moreover, it also had novel and interesting findings that were consistent with prior reports.

In conclusion, our findings revealed that genetic variants related to the insulin signaling pathway may have a role in NAFLD susceptibility. For the first time, we uncovered that the *IGF1* rs5742612 CC genotype compared with the TT genotype or the TT+TC genotype had at least a 2-fold increase in NAFLD risk. Interestingly, from a theoretical viewpoint, this observation is relevant, although it needs to be corroborated by future studies with more participants.

## Acknowledgments

The authors thank all patients and healthy blood donors for providing blood samples. This study was funded by Iran National Science Foundation (INSF) (grant No. 90005942); and Gastroenterology and Liver Diseases Research Center, Shahid Beheshti University of Medical Sciences (grant No. 1425).

## REFERENCES

1. Lazarus JV, Mark HE, Anstee QM, et al. Advancing the global public health agenda for NAFLD: a consensus statement. *Nat Rev Gastroenterol Hepatol*. 2022;19:60–78. doi:10.1038/s41575-021-00523-4.

2. Haukeland JW, Konopski Z, Linnestad P, et al. Abnormal glucose tolerance is a predictor of steatohepatitis and fibrosis in patients with non-alcoholic fatty liver disease. *Scand J Gastroenterol*. 2005;40:1469–1477. doi:10.1080/00365520500264953.
3. Eguchi Y, Eguchi T, Mizuta T, et al. Visceral fat accumulation and insulin resistance are important factors in nonalcoholic fatty liver disease. *J Gastroenterol*. 2006;41:462–469.
4. Brunt EM, Kleiner DE, Wilson LA, et al. Portal chronic inflammation in nonalcoholic fatty liver disease (NAFLD): a histologic marker of advanced NAFLD-clinicopathologic correlations from the Nonalcoholic Steatohepatitis Clinical Research Network. *Hepatology*. 2009;49:809–820.
5. Bellentani S, Scaglioni F, Marino M, et al. Epidemiology of non-alcoholic fatty liver disease. *Dig Dis*. 2010;28:155–161.
6. Dietrich P, Hellerbrand C. Non-alcoholic fatty liver disease, obesity and the metabolic syndrome. *Best Pract Res Clin Gastroenterol*. 2014;28:637–653.
7. Siddiqui MS, Fuchs M, Idowu MO, et al. Severity of nonalcoholic fatty liver disease and progression to cirrhosis associate with atherogenic lipoprotein profile. *Clin Gastroenterol Hepatol*. 2015;13:1000–1008.
8. Ohmi S, Ono M, Takata H, et al. Analysis of factors influencing glucose tolerance in Japanese patients with non-alcoholic fatty liver disease. *Diabetol Metab Syndr*. 2017;9:65.
9. Gholam PM, Flancbaum L, Machan JT, et al. Nonalcoholic fatty liver disease in severely obese subjects. *Am J Gastroenterol*. 2007;102:399–408.
10. Li M, Zhang S, Wu Y, et al. Prevalence of insulin resistance in subjects with nonalcoholic fatty liver disease and its predictors in a Chinese population. *Dig Dis Sci*. 2015;60:2170–2176.
11. Succurro E, Andreozzi F, Marini MA, et al. Low plasma insulin-like growth factor-1 levels are associated with reduced insulin sensitivity and increased insulin secretion in nondiabetic subjects. *Nutr Metab Cardiovasc Dis*. 2009;19:713–719.
12. Sumida Y, Yonei Y, Tanaka S, et al. Lower levels of insulin-like growth factor-1 standard deviation score are associated with histological severity of non-alcoholic fatty liver disease. *Hepatol Res*. 2015;45:771–781.
13. Chishima S, Kogiso T, Matsushita N, et al. The relationship between the growth hormone/insulin-like growth factor system and the histological features of nonalcoholic fatty liver disease. *Intern Med*. 2017;56:473–480.
14. Yao Y, Miao X, Zhu D, et al. Insulin-like growth factor-1 and non-alcoholic fatty liver disease: a systemic review and meta-analysis. *Endocrine*. 2019;65:227–237.
15. Wang R, Xu D, Liu R, et al. Microsatellite and single nucleotide polymorphisms in the insulin-like growth factor 1 promoter with insulin sensitivity and insulin secretion. *Med Sci Monit*. 2017;23:3722–3736.

16. Willems SM, Cornes BK, Brody JA, et al. Association of the IGF1 gene with fasting insulin levels. *Eur J Hum Genet.* 2016;24:1337–1343.
17. Zhang J, Chen X, Zhang L, et al. IGF1 gene polymorphisms associated with diabetic retinopathy risk in Chinese Han population. *Oncotarget.* 2017;8:88034–88042.
18. Dabiri R, Mahmoudi T, Sabzikarian M, et al. A 3'-untranslated region variant (rs2289046) of insulin receptor substrate 2 gene is associated with susceptibility to nonalcoholic fatty liver disease. *Acta Gastroenterol Belg.* 2020;83:271–276.
19. Nobakht H, Mahmoudi T, Sabzikarian M, et al. Insulin and insulin receptor gene polymorphisms and susceptibility to nonalcoholic fatty liver disease. *Arq Gastroenterol.* 2020;57:203–208.
20. Sabzikarian M, Mahmoudi T, Tabaeian SP, et al. The common variant of rs6214 in insulin like growth factor 1 (IGF1) gene: a potential protective factor for non-alcoholic fatty liver disease. *Arch Physiol Biochem.* 2020;1–6. doi: [10.1080/13813455.2020.1791187](https://doi.org/10.1080/13813455.2020.1791187).
21. Brunt EM, Janney CG, Di Bisceglie AM, et al. Nonalcoholic steatohepatitis: a proposal for grading and staging the histological lesions. *Am J Gastroenterol.* 1999;94:2467–2474.
22. Mahmoudi T, Karimi K, Karimi N, et al. Association of adiponectin receptor 1 gene - 106 C > T variant with susceptibility to colorectal cancer. *Meta Gene* 2016;9:210–214.
23. Mahmoudi T, Majidzadeh-A K, Karimi K, et al. Gly972Arg variant of insulin receptor substrate 1 gene and colorectal cancer risk in overweight/obese subjects. *Int J Biol Markers.* 2016;31:e68–e72.
24. Mahmoudi T, Majidzadeh-A K, Karimi K, et al. An exon variant in insulin receptor gene is associated with susceptibility to colorectal cancer in women. *Tumour Biol.* 2015;36:3709–3715.
25. Mahmoudi T, Arkani M, Karimi K, et al. The -4817 G>A (rs2238136) variant of the vitamin D receptor gene: a probable risk factor for colorectal cancer. *Mol Biol Rep.* 2012;39:5277–5282.
26. Nikzamir A, Esteghamati A, Hammedian AA, et al. The role of vascular endothelial growth factor +405 G/C polymorphism and albuminuria in patients with type 2 diabetes mellitus. *Mol Biol Rep.* 2012;39:881–886.
27. Mahmoudi T, Farahani H, Nobakht H, et al. Genetic variations in leptin and leptin receptor and susceptibility to colorectal cancer and obesity. *Iran J Cancer Prev* 2016;9:e7013.
28. Salamone F, Bugianesi E. Nonalcoholic fatty liver disease: the hepatic trigger of the metabolic syndrome. *J Hepatol.* 2010;53:1146–1147.
29. Atay K, Canbakan B, Koroglu E, et al. Apoptosis and disease severity is associated with insulin resistance in non-alcoholic fatty liver disease. *Acta Gastroenterol Belg.* 2017;80:271–277.
30. Fujii H, Imajo K, Yoneda M, et al. HOMA-IR: an independent predictor of advanced liver fibrosis in nondiabetic non-alcoholic fatty liver disease. *J Gastroenterol Hepatol.* 2019;34:1390–1395.
31. Mahmoudi T, Karimi K, Arkani M, et al. Resistin -420C>G promoter variant and colorectal cancer risk. *Int J Biol Markers.* 2014;29:e233–e238.
32. Yang CW, Li TC, Li CI, et al. Insulin like growth factor-1 and its binding protein-3 polymorphisms predict circulating IGF-1 level and appendicular skeletal muscle mass in Chinese elderly. *J Am Med Dir Assoc.* 2014;16:365–3670.
33. Federici M, Porzio O, Lauro D, et al. Increased abundance of insulin/insulin-like growth factor-I hybrid receptors in skeletal muscle of obese subjects is correlated with in vivo insulin sensitivity. *J Clin Endocrinol Metab.* 1998;83:2911–2915.
34. Nishizawa H, Takahashi M, Fukuoka H, et al. GH-independent IGF-I action is essential to prevent the development of nonalcoholic steatohepatitis in a GH-deficient rat model. *Biochem Biophys Res Commun.* 2012;423:295–300.
35. Hribal ML, Procopio T, Petta S, et al. Insulin-like growth factor-I, inflammatory proteins, and fibrosis in subjects with nonalcoholic fatty liver disease. *J Clin Endocrinol Metab.* 2013;98:E304–E308.
36. Ichikawa T, Nakao K, Hamasaki K, et al. Role of growth hormone, insulin-like growth factor 1 and insulin-like growth factor-binding protein 3 in development of non-alcoholic fatty liver disease. *Hepatol Int.* 2007;1:287–294.

# The Viability of Hematopoietic Progenitor Cell Grafts after Cryopreservation Does Not Predict Delayed Engraftment in Allogeneic Hematopoietic Stem Cell Transplantation

Emmanuel Fadeyi,<sup>1,\*</sup> Yafet T. Mamo,<sup>1</sup> Amit K. Saha,<sup>2</sup> Emily Wilson,<sup>1</sup> Gregory Pomper<sup>1</sup>

<sup>1</sup>Wake Forest University School of Medicine – Pathology, Winston-Salem, North Carolina, USA, <sup>2</sup>Wake Forest University School of Medicine – Anesthesiology, Winston-Salem, North Carolina, USA \*To whom correspondence should be addressed. [efadeyi@wakehealth.edu](mailto:efadeyi@wakehealth.edu)

**Keywords:** cellular therapy, hematopoietic stem cell, transplantation, peripheral blood stem cell, viability, engraftment

**Abbreviations:** PBSC, peripheral blood stem cell; TNC, total nucleated cell; HSCT, hematopoietic stem cell transplantation; 7AAD, 7-aminoactinomycin D; ANC, absolute neutrophil count; PLT, platelet; WBC, white blood cell; TTE, time to engraftment; AML, acute myeloid leukemia; HPC, hematopoietic progenitor cell.

*Laboratory Medicine* 2022;53:509–513; <https://doi.org/10.1093/labmed/lmac042>

## ABSTRACT

**Objective:** Due to the COVID-19 pandemic, more peripheral blood stem cell (PBSC) allogeneic grafts are being frozen and infused thawed. Our objective was to study the influence of graft viability on engraftment outcome in patients treated with PBSCs.

**Methods:** Using trypan blue stain, we compared total nucleated cell (TNC) viability of both fresh and thawed grafts in allogeneic PBSCs.

**Results:** The viability of thawed PBSC grafts median was 74%, and fresh was 99.0%. The median number of CD34 + cells/kg infused thawed was  $6.3 \times 10^6$ /kg and median time to neutrophil and platelet engraftment was 17.5 and 20 days. Median number of CD34 + cells/kg infused fresh was  $5.1 \times 10^6$ /kg and median time to neutrophil and platelet engraftment was 18 and 19 days. There were no statistically significant differences in the time to engraftment between the 2 groups.

**Conclusion:** A low TNC viability of thawed PBSC grafts does not have an effect on time to neutrophil and platelet engraftment when more than  $2.85 \times 10^6$  CD34 + cells/kg are infused.

Allogeneic hematopoietic stem cell transplantation (HSCT) is a successful treatment strategy for patients with hematologic malignancies, bone marrow failure syndromes, and some inherited disorders.<sup>1–4</sup> Assessing graft adequacy prior to myeloablative chemotherapy typically involves determining the viability of stem cells and the yield of stem cells by enumeration of stem/progenitor cells expressing the cell surface antigen CD34 at the time of leukapheresis.<sup>5</sup> The number and recovery of viable CD34+ cells and their ability to form colony-forming units are readily used for estimating graft quality at infusion if given either fresh or postthaw when the graft is cryopreserved. Most allogeneic hematopoietic progenitor cell (HPC) grafts are given as fresh infusions and are less commonly cryopreserved. However, due to the COVID-19 pandemic, more allogeneic HPC grafts are currently being cryopreserved to proactively prevent COVID-19 transmission from an asymptomatic donor who may test positive for COVID-19 postdonation. According to the US Food and Drug Administration, there have been no reported or suspected cases of transfusion-transmitted COVID-19 infection. Additionally, no cases of coronavirus transfusion transmission have been reported for the other highly pathogenic coronaviruses that have emerged in the past two decades: SARS-CoV (severe acute respiratory syndrome coronavirus) and MERS-CoV (Middle East respiratory syndrome).<sup>6</sup>

Reduced CD34+ cell viability due to cryopreservation has unknown effects on subsequent hematopoietic engraftment in allogeneic HSCT. The viability of the total nucleated cells (TNCs) in the graft can either be measured by microscope-based assays such as trypan blue staining or via flow cytometry based on staining using 7-aminoactinomycin D (7AAD) or propidium iodide. These methods do not detect cells in early apoptosis and may lead to overestimation of graft cell viability.<sup>7</sup> Graft quality assessed by 7AAD has been demonstrated to affect clinical outcome and may be inferior, leading to transplant-related mortality.<sup>7</sup>

We studied the influence of graft viability using trypan blue stain on engraftment outcome in 93 patients treated with allogeneic HSCT, comparing frozen-thawed to fresh infusions. A TNC viability of greater than 70% using trypan blue from the HPC graft was used as an indicator of successful engraftment.

## Materials and Methods

### Patients

There were 93 patients who underwent allogeneic HSCT at Wake Forest Baptist Medical Center between 2014 and 2020. A total of 56 patients

received grafts from unrelated donors. A total of 93 patients' PBSCs were analyzed. Of these, 49 patients received fresh infusion and 44 received frozen-thawed infusion.

Following informed consent, patients underwent allogeneic HSCT for various hematologic malignancies as shown in (TABLE 1). To mobilize CD34+ cells, donors received 1 dose of recombinant human granulocyte colony-stimulating factor, 10 µg/kg/d for 5 days. Leukapheresis was undertaken using either a COBE Spectra Apheresis System or a COBE Spectra Optia Apheresis System (Terumo) with up to 12–24 L of blood being processed for each collection. Target viable CD34+ PBSC yield was  $3.0 \times 10^6$  CD34+ cells/kg of recipient body weight. Disease-specific myeloablative chemotherapy was administered to each patient based on the clinical transplant protocol.

### PBSC Processing, Cryopreservation, Thawing, and Reinfusion

All fresh PBSC grafts were either processed immediately after collection or stored overnight at 4°C and processed the following morning. In the laboratory, all study PBSC apheresis collections underwent centrifugation at 600g for 20 minutes and plasma volume reduction. Centrifuged PBSC grafts were diluted 1:2 with cryoprotectant (dimethyl sulfoxide DMSO, Mylan Institutional), donor plasma, and Plasma-Lyte A Injection pH 7.4 (Baxter), transferred to Cryocyte freezing bags (Origen), and subjected to controlled-rate freezing in a liquid nitrogen freezing tank (CryoMed, Thermo Electro). PBSC grafts were stored in a vapor phase liquid nitrogen at -160°C in a monitored and alarmed purpose-specific tank. The PBSC grafts were all stored between 7 and 14 days but most were given between 7 and 10 days. PBSC grafts were thawed immedi-

ately prior to reinfusion in a 37°C water bath and infused through an IV syringe pushed slowly into the central venous access device.

### CD34+ Cell Enumeration and Viability Assay

Absolute CD34+ cell numbers and viability of PBSC grafts was determined using ISHAGE single platform methodology with a multi-color flow cytometer (FacsCalibur cell analyzer or Facs CANTO II, BD Biosciences). The viability of the progenitor cells was enumerated using microscope-based trypan blue staining. CD34+ cell enumeration was performed on each PBSC graft at the time of collection and postconcentration before cryopreservation. The CD34+ cells/kg dose listed for this study is the postconcentration value prior to cryopreservation; the dose is not adjusted for percent viability using trypan blue. The total dose of CD34+ cells/kg was recorded prior to both fresh and thawed infusion and immediately before the infusion.

### Engraftment Monitoring

Following PBSC infusion, daily blood counts were monitored and recorded. Neutrophil engraftment was defined as the first of three consecutive days postinfusion where peripheral blood neutrophil count (ANC) was at least  $0.5 \times 10^9/L$ . Platelet (PLT) engraftment was defined as the first of 3 consecutive days where platelet count was at least  $20 \times 10^9/L$  without PLT transfusion support in the preceding 7 days. Successful engraftment for both ANC and PLT was set at less than 21 days based on published studies.<sup>8–10</sup> Chimerism obtained up to day +100 was recorded for each transplant.

### Statistical Analysis

Statistical analysis was performed using IBM SPSS Statistics for Windows software version 26.0 (IBM). Results were analyzed using descriptive statistics to compare fresh and frozen-thawed infusion using viability percentage and engraftment. Comparison between groups was done using  $\chi^2$  tests for proportions and Student *t*-test for continuous variables, and results are presented as mean ± standard deviation. For variable failing in normality test nonparametric Mann-Whitney test was employed to assess group differences, and the results are presented as median ± range. Because stem cell data did not pass the Shapiro-Wilk normality test, nonparametric evaluation was performed. Spearman correlation tests were used to determine relationships between viability and other variables. To assess the association of event of engraftment less than 21 days for both fresh and frozen-thawed infusion, multiple linear regression was performed with all other independent variables as fixed effects. Collinearity was assessed using variance inflation factor and condition index, with values <10 indicating acceptability. Additionally, sensitivity analyses were performed to investigate effect of fresh and frozen-thawed infusion on range of ANC and PLT engraftment using Cox-regression analysis with Kaplan-Meier. A 2-tailed *P* value <.05 was considered statistically significant.

Wake Forest University Health Sciences' Institutional Review Board approved this data collection protocol.

### Results

There were no statistically significant differences in patient age, sex, weight, CD34+/kg dose, and TNC count infused between the 2 groups. (TABLE 1). There was a statistically significant difference in viability

TABLE 1. Patient Characteristics

	Fresh (n = 49)	Thawed (n = 44)	P Value
Age (y), mean (SD)	54.2 (15.7)	57.2 (12.5)	.343
Patient weight (kg), mean (SD)	84.5 (18.2)	89.8 (24.4)	.196
CD34+/kg infused, median (range)	$5.1 \times 10^6$ ( $2.16 \times 10^6$ – $12.5 \times 10^6$ )	$6.3 \times 10^6$ ( $2.85 \times 10^6$ – $11.8 \times 10^6$ )	.034
Total nucleated cell count infused, median (range)	$5.97 \times 10^{10}$ ( $1.50 \times 10^{10}$ – $14.44 \times 10^{10}$ )	$6.08 \times 10^{10}$ ( $4.05 \times 10^{10}$ – $14 \times 10^{10}$ )	.128
% Viability (trypan blue), median (range)	99 (85–100)	74 (33–89)	<.001
Sex (male, female) (No.)	26, 23	24, 20	.961
Type transplant (No.)			.623
Related	18	19	
Unrelated	31	25	
Disease (No.)			.619
AML/ALL	32	30	
Aplastic anemia	2	0	
Lymphoma (HL and NHL)	1	5	
MDS	10	7	
Myelofibrosis	4	2	

ALL, acute lymphoblastic leukemia; AML, acute myeloid leukemia; HL, Hodgkin lymphoma; MDS, myelodysplastic syndrome; NHL, non-Hodgkin lymphoma.

**TABLE 2. Multiple Logistic Regression for the Event (ANC  $0.5 \times 10^9/L$  and PLT  $20 \times 10^9/L$  Engraftment Less than 21 Days)**

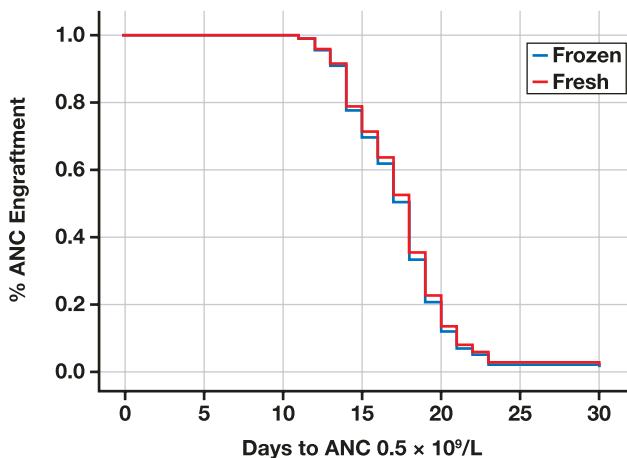
	Odds Ratio	95% CI for Odds Ratio		P Value
		Lower	Upper	
Fresh (Yes)	0.364	0.072	1.838	.221
Sex (male)	0.536	0.201	1.429	.212
Age	0.981	0.949	1.015	.281
Type transplant (related)	1.216	0.750	1.971	.428
Patient weight	0.982	0.961	1.004	.103
% Viability (trypan blue)	0.968	0.922	1.016	.189
Lymphoma (HL and NHL) with respect to AML/ALL	1.421	0.350	5.759	.623
MDS with respect to AML/ALL	1.847	0.340	10.033	.477

ALL, acute lymphoblastic leukemia; AML, acute myeloid leukemia; ANC, absolute neutrophil count; CI, confidence interval; HL, Hodgkin lymphoma; MDS, myelodysplastic syndrome; NHL, non-Hodgkin lymphoma; PLT, platelet.

**TABLE 3. Engraftment Outcome Analysis**

	Fresh (n = 49)	Thawed (n = 44)	P Value
Days to PLT $20 \times 10^9/L$ , median (range)	19 (9–79)	20 (12–39)	.503
Days to ANC $0.5 \times 10^9/L$ , median (range)	18 (11–23)	17.5 (11–30)	.608
Chimerism %, median (range)	99 (94–100)	99 (92–100)	.920
Event of ANC $0.5 \times 10^9/L$ and PLT $20 \times 10^9/L$ engraftment less than 21 days(n)	30	23	.682

ANC, absolute neutrophil count; PLT, platelet.

**FIGURE 1. Days to absolute neutrophil count (ANC)  $0.5 \times 10^9/L$ .**

percent between the 2 groups with a median of 74% for frozen-thawed and 99% for fresh infusion ( $P < .001$ ) (TABLE 1). Multivariate regression analysis was performed on all the covariates for engraftment less than 21 days. The odds ratio for ANC  $0.5 \times 10^9/L$  and PLT  $20 \times 10^9/L$  engraftment less than 21 days based on multiple logistic regression showed no statistically significant effects on fresh and frozen-thawed infusions, gender, age, transplant type, patient's weight, viability percent, and disease type (TABLE 2). Univariate analysis showed no significant differences in the outcomes of days to ANC and PLT engraftment, chimerism, and event of ANC and PLT engraftment less than 21 days between the 2 groups of fresh and frozen-thawed. (TABLE 3). There were 2 patients who received frozen-thawed grafts that failed engraft-

ment. The Cox-regression analysis using the Kaplan-Meier method for engraftment analysis between percent engraftment and days to ANC  $0.5 \times 10^9/L$  and PLT  $20 \times 10^9/L$  showed no statistically significant difference in engraftment between the 2 groups of fresh and frozen-thawed infusions (FIGURES 1 and 2).

## Discussion

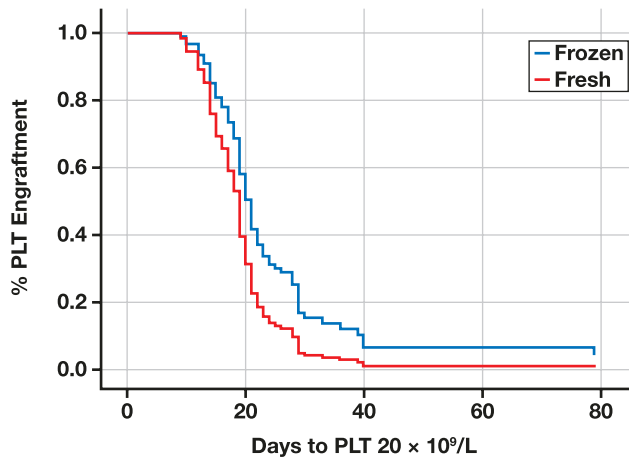
HSCT is currently an important treatment in the management of various hematologic malignancies. During HSCT, native hematopoietic cells of recipients are replaced by donor HPC, which then populate the recipient marrow and become the source of hematopoiesis. Various types of HSCT, based on donor-recipient human leukocyte antigen (HLA) compatibility, the origin of donor stem cells, and the type of conditioning regimen, can all affect the time for immune reconstitution. There is usually a predictable loss of CD34+ cells during processing and cryopreservation.

We found in our study that a higher percentage of viable TNC in the fresh grafts does not correlate with earlier engraftment of both ANC and PLT if the viability is above 70%. In Watz et al,<sup>7</sup> the authors found that grafts with higher white blood cell (WBC) concentrations ( $>300 \times 10^9/L$ ) had significantly lower viability of WBCs in frozen-thawed samples than grafts with WBC concentration of less than  $300 \times 10^9/L$ . Therefore, no clear correlation could be found when comparing the viability of WBCs using 7AAD on freshly arrived PBSC grafts compared to frozen-thawed vials.<sup>7</sup>

According to the Foundation for Accreditation of Cellular Therapy standard D8.1.3.1,<sup>11</sup> "for all cellular therapy products, a total nucleated cell count and viability measurement shall be performed"; however, there is no guidance on the method used to perform viability. We used trypan blue staining method in our laboratory as a quality indicator of viability for our frozen-thawed products to maintain the potency and the integrity of the cellular product. Others have used flow cytometric methods to determine viability of cryopreserved cellular therapy products that showed nearly identical cell viability to that of fresh cellular product graft 48 hours after collection.<sup>12</sup> In autologous transplantation, measurement of postthaw viable CD34+ cell count has been shown to be a valuable predictor of hematopoietic stem cell engraftment according to Lee et al.<sup>13</sup> Based on trypan blue viability results, there is no statistical difference in viable TNC between the two groups. This may explain why freeze-thaw has no effect on engraftment.

Based on our findings, measurement of postthaw viable TNC count using trypan blue when comparing fresh and frozen-thawed

**FIGURE 2.** Days to platelet (PLT)  $20 \times 10^9/L$ .



allogeneic transplantation has no effect on time to hematopoietic engraftment. Similar to our findings, Abrahamsen et al<sup>14</sup> found that using flow cytometry, the viable transplanted CD34+ cell dose measured postthaw does not predict engraftment. Likewise, in our study we found that there is no statistically significant difference in time to engraftment (TTE) between fresh and frozen-thawed allogeneic HSCT.

Several factors other than CD34+ cell dose determine engraftment potential in HSCT. These factors include the nature of the disease being treated, prior therapies, and the type of conditioning regimen, including whether the HPC is bone marrow derived or PBSCs.<sup>15,16</sup> In addition to whether the HPC is bone marrow vs PBSC, the cryopreservation storage time appears to have little or no effect on engraftment potential, and this has been confirmed by a number of observers.<sup>15,17</sup> In looking at the effect of donor graft cryopreservation on allogeneic HPC transplants outcomes, cryopreservation is safe during the COVID-19 pandemic and may be associated with slower engraftment, which may affect transplantation outcomes in some patients.<sup>18,19</sup>

Minimizing viable CD34+ cell loss during processing, cryopreservation and thawing is in part a function of quality assurance in the stem cell-processing laboratory. In our laboratory, we can expect, on average, a reduction of approximately 30% in viable TNC using trypan blue staining. Therefore, a TNC viability of 70% following processing and cryopreservation was set as a quality indicator of viability and potency of the frozen-thawed grafts.

It has been shown in autologous transplants by Allan et al<sup>20</sup> that cryopreservation and processing of autologous stem cell collections significantly reduces the number of viable CD34+ cells available for reinfusion. The number of viable CD34+ cells reinfused is associated with time to hematopoietic engraftment in autologous transplantation. This has not been our experience with frozen-thawed allogeneic transplantation based on the presented data. The median dose of CD34+ cells was actually higher for the frozen-thawed grafts than for the fresh grafts and yet there was no difference in TTE, although the median viable CD34+ cells are similar between the 2 groups. Above a minimal threshold, the dose of CD34+ cells infused is not associated with time to either ANC or PLT engraftment. According to Allan et al,<sup>20</sup> measuring CD34+ cell viability may be useful in quality assessments of stem cell processing and may identify patients at risk of delayed engraftment. This may not necessarily translate to allogeneic HSCTs. There were 2 patients who received

**TABLE 4.** Patients with Failed Engraftment

	Patient 1	Patient 2
Type	Frozen	Frozen
Age (y)	62	67
Patient weight (kg)	66	80
CD34+/kg infused	$2.85 \times 10^6$	$5.02 \times 10^6$
Total nucleated cell count infused	$4.95 \times 10^{10}$	$6.75 \times 10^{10}$
% Viability (trypan blue)	83	86
Sex	Female	Male
Type Transplant (No.)	Related	Unrelated
Disease (No.)	AML	Myelofibrosis

frozen-thawed grafts with graft failures, one with myelofibrosis and the other with acute myeloid leukemia (AML). Both patients had identical TNC viabilities and similar patient characteristics (see TABLE 4). According to Gupta et al,<sup>21</sup> the success of allogeneic transplant in patients with myelofibrosis is associated with significant risk of regimen-related toxicities, graft failure, and graft-versus-host disease. Leukemia relapse continues to be the main cause of graft failures in patients with acute leukemia following allogeneic HSCT.<sup>22,23</sup>

The Kaplan-Meier curves demonstrate no difference in days to both ANC and PLT engraftment between the groups of frozen-thawed and fresh infusions. Watz et al<sup>7</sup> found in their study of quality of stem cell grafts using 7AAD for viability that the time to engraftment as measured by PLT count and ANC was similar for patients receiving low and better quality grafts; therefore, no clear correlation could be found when comparing the viability of WBCs using 7AAD on fresh and frozen-thawed PBSCs. This is similar to the results of our study when using trypan blue viability.

There are some limitations of our study. First, this study was performed at a single stem cell-processing laboratory and may not be generalizable to other processing laboratories with alternative way of determining viability such as using 7AAD. However, 7AAD is comparable to trypan blue staining in determining stem cell viability. Second, we did not take into consideration the different diseases of the patient and the different types of conditioning regimen that might be required for each disease and how this might affect engraftment or transplant outcomes. We only reviewed the viability of the PBSC grafts prior to infusion and assessed for engraftment. Third, we did not account for the HLA-mismatched donor-recipient pairs nor did we consider differences between related and unrelated donor-recipient pairs, which might affect graft outcomes. Fourth, there is a difference in median cell dose between the 2 groups, with the patients that received the frozen-thawed product having a slightly higher median dose than those receiving the fresh product. Jeyaraman et al<sup>24</sup> conducted a retrospective analysis that showed autologous stem cell transplant can be safely performed with a noncryopreserved CD34+ cell dose of  $<2 \times 10^6/kg$  range ( $1.22$  to  $1.97 \times 10^6/kg$ ). Sureda et al<sup>25</sup> showed that a higher CD34+ cell dose/kg will lead to an early engraftment. However, given the lower viability in the frozen-thawed grafts, there seems to be no significant difference in the total viable CD34+ cells/kg infused between the 2 groups.

In conclusion, we investigated the difference in low TNC viability between the frozen-thawed infusion of allogeneic PBSC grafts compared to the fresh infusion of allogeneic PBSC grafts and assessed for delayed engraftment. The data shows that low TNC viability of the

frozen-thawed grafts was not associated with delayed TTE. Engraftment following PBSC infusion does not depend on the viability assessment using trypan blue stain for both frozen-thawed and fresh infusions.

## REFERENCES

1. Remberger M, Ackefors M, Berglund S, et al. Improved survival after allogeneic hematopoietic stem cell transplantation in recent years: a single-center study. *Biol Blood Marrow Transplant*. 2011;17(11):1688–1697. doi:10.1016/j.bbmt.2011.05.001.
2. Ringden O, Remberger M, Svahn BM, et al. Allogeneic hematopoietic stem cell transplantation for inherited disorders: experience in a single center. *Transplantation* 2006;81(5):718–725. doi:10.1097/01.tp.0000181457.43146.36.
3. Thomas ED, Buckner CD, Banaji M, et al. One hundred patients with acute leukemia treated by chemotherapy, total body irradiation, and allogeneic marrow transplantation. *Blood* 1977;49(4):511–533.
4. Ringdén O, Karlsson H, Olsson R et al. The allogeneic graft-versus-cancer effect. *Br J Haematol* 2009;147(5):614–633.
5. Bender JG, To LB, Williams S, et al. Defining a therapeutic dose of peripheral blood stem cells. *J Hematother Winter* 1992;1(4):329–341.
6. <https://www.fda.gov/vaccines-blood-biologics/safety-availability-biologics/updated-information-blood-establishments-regarding-novel-coronavirus-covid-19-outbreak>
7. Watz E, Remberger M, Ringden O, et al. Quality of the hematopoietic stem cell graft affects the clinical outcome of allogeneic stem cell transplantation. *Transfusion*. 2015;55(10):2339–2350. doi:10.1111/trf.13143.
8. Yahng SA, Lee JW, Kim Y, et al. New proposed guidelines for early identification of successful myeloid and erythroid engraftment in hematopoietic stem cell transplantation. *J Clin Lab Anal*. 2014;28(6):469–477. doi:10.1002/jcla.21712.
9. Martinelli G, Trabetti E, Farabegoli P, et al. Early detection of bone marrow engraftment by amplification of hypervariable DNA regions. *Haematologica* 1997;82(2):156–160.
10. Bitan M, Or R, Shapira MY, et al. Successful engraftment following allogeneic stem cell transplantation in very high-risk patients with busulfan as a single agent. *Haematologica*. 2005;90(8):1089–1095.
11. *FACT-JACIE International Standards for Hematopoietic Cellular Therapy Product Collection, Processing, and Administration*. 7th ed. European Society for Blood and Marrow Transplantation; 2018:122.
12. Kim KM, Huh JY, Hong SS, et al. Assessment of cell viability, early apoptosis, and hematopoietic potential in umbilical cord blood units after storage. *Transfusion*. 2015;55(8):2017–2022. doi:10.1111/trf.13120.
13. Lee S, Kim S, Kim H, et al. Post-thaw viable CD34 (+) cell count is a valuable predictor of haematopoietic stem cell engraftment in autologous peripheral blood stem cell transplantation. *Vox Sang*. 2008;94(2):146–152. doi:10.1111/j.1423-0410.2007.01009.x.
14. Abrahamsen JF, Wentzel-Larsen T, Bruserud O. Autologous transplantation: the viable transplanted CD34+ cell dose measured post-thaw does not predict engraftment kinetics better than the total CD34+ cell dose measured pre-freeze in patients that receive more than 2x10(6) CD34+ cells/kg. *Cytotherapy*. 2004;6(4):356–362. doi:10.1080/14653240410004925.
15. D’Rozario J, Parisotto R, Stapleton J, et al. Pre infusion, post thaw CD34+ peripheral blood stem cell enumeration as a predictor of haematopoietic engraftment in autologous haematopoietic cell transplantation. *Transfus Apher Sci*. 2014;50(3):443–450. doi:10.1016/j.transci.2014.02.021.
16. Majado MJ, Salgado-Cecilia G, Blanquer M, et al Cryopreservation impact on blood progenitor cells: influence of diagnoses, mobilization treatments, and cell concentration. *Transfusion* 2011;51(4):799–807. doi:10.1111/j.1537-2995.2010.02885.x.
17. Liseth K, Ersvær E, Abrahamsen JF, et al. Long-term cryopreservation of autologous stem cell grafts: a clinical and experimental study of hematopoietic and immunocompetent cells. *Transfusion* 2009;49(8):1709–1719. doi:10.1111/j.1537-2995.2009.02180.x.
18. Hsu JW, Farhadfar N, Murthy H, et al. The effect of donor graft cryopreservation on allogeneic hematopoietic cell transplantation outcomes: a center for international blood and marrow transplant research analysis. Implications during the COVID-19 pandemic. *Transplant Cell Ther* 2021 Jun;27(6):507–516. doi:10.1016/j.jtct.2021.03.015.
19. Hamadani M, Zhang MJ, Tang XY et al. Graft cryopreservation does not impact overall survival after allogeneic hematopoietic cell transplantation using post-transplantation cyclophosphamide for graft-versus-host disease prophylaxis. *Biol Blood Marrow Transplant*. 2020;26(7):1312–1317.
20. Allan DS, Keeney M, Howson-Jan K, et al. Number of viable CD34 (+) cells reinfused predicts engraftment in autologous hematopoietic stem cell transplantation. *Bone Marrow Transplant*. 2002 Jun;29(12):967–972. doi:10.1038/sj.bmt.1703575.
21. Gupta V, Hari P, Hoffman R. Allogeneic hematopoietic cell transplantation for myelofibrosis in the era of JAK inhibitors. *Blood* 2012;120(7):1367–1379. doi:10.1182/blood-2012-05-399048.
22. Piemontese S, Boumendil A, Labopin M, et al; Acute Leukemia Working Party of the European Society for Blood and Marrow Transplantation (EBMT). Leukemia relapse following unmanipulated haploidentical transplantation: a risk factor analysis on behalf of the ALWP of the EBMT. *J Hematol Oncol* 2019;12(1):68. doi:10.1186/s13045-019-0751-4.
23. Xuan L, Liu Q. Maintenance therapy in acute myeloid leukemia after allogeneic hematopoietic stem cell transplantation. *J Hematol Oncol* 2021;14(1):4. doi:10.1186/s13045-020-01017-7.
24. Jeyaraman P, Borah P, Dayal N, et al. Adequate engraftment with lower hematopoietic stem cell dose. *Clin Lymphoma Myeloma Leuk*. 2020 Apr;20(4):260–263. doi:10.1016/j.clml.2019.12.018.
25. Sureda A, Chabannon C, Masszi T, et al. Analysis of data collected in the European Society for Blood and Marrow Transplantation (EBMT) Registry on a cohort of lymphoma patients receiving plerixafor. *Bone Marrow Transplant*. 2020;55(3):613–622. doi:10.1038/s41409-019-0693-z.

# Reduced Immune Response and Neutralizing Antibody Activity to the SARS-CoV-2 Vaccination in Patients with a History of Solid Organ Transplant

Deborah French, PhD,<sup>1,2,\*</sup> Chui Mei Ong, BS,<sup>3</sup> Paul Patel, PhD,<sup>4</sup> Marisa Zuk, BS,<sup>4</sup> and Alan H. B. Wu, PhD<sup>1,3</sup>

<sup>1</sup>Department of Laboratory Medicine, University of California San Francisco, San Francisco, CA, USA, <sup>2</sup>UCSF Health Clinical Laboratories, San Francisco, CA, USA, <sup>3</sup>Clinical Laboratories, Zuckerberg San Francisco General Hospital, San Francisco, CA, USA <sup>4</sup>ET Healthcare, Palo Alto, CA USA. \*To whom correspondence should be addressed. [deborah.french@ucsf.edu](mailto:deborah.french@ucsf.edu)

**Keywords:** SARS-CoV-2, COVID-19, vaccination, immune response, solid organ transplant, antibodies

**Abbreviations:** RBD, receptor binding domain; RFUs, relative fluorescence units; RLUs, relative light units; ACE2, angiotensin-converting enzyme 2 protein.

*Laboratory Medicine* 2022;53:514–522; <https://doi.org/10.1093/labmed/lmac038>

## ABSTRACT

**Objective:** Three SARS-CoV-2 vaccinations and boosters are available. We determined whether solid organ transplant patients mounted an immune response to the vaccinations and whether the antibodies had neutralizing activity compared to healthcare worker controls and monoclonal gammopathy patients.

**Methods:** Remnant plasma was obtained from vaccinated solid organ transplant, allogeneic stem cell transplant, monoclonal gammopathy patients, and healthcare worker controls. Samples positive on a SARS-CoV-2 IgG assay (detects spike protein and nucleocapsid) were run on a SARS-CoV-2 in vitro neutralizing antibody assay and a nucleocapsid-specific SARS-CoV-2 IgG assay.

**Results:** Only 25% of solid organ transplant patients produced antibodies to SARS-CoV-2 vaccination. Of these, 90% had neutralizing activity against wild type virus, but reduced activity to the variants compared to monoclonal gammopathy patients and healthcare worker controls, particularly the delta variant, for which only 50% had neutralizing antibody activity.

**Conclusion:** Solid organ transplant patients should consider protecting themselves against future SARS-CoV-2 infection.

As of March 3, 2022, the SARS-CoV-2 virus has infected over 441 million people worldwide resulting in >5.9 million deaths.<sup>1</sup> Along with masking and social distancing measures, development, approval, and implementation of vaccines is key to stopping the further spread of highly infectious viral infections. To date, the Pfizer-BioNTech (BNT162b2) and Moderna (mRNA-1273) vaccinations were given full US Food and Drug Administration approval on August 23, 2021, and January 31, 2022, respectively. They are both 2-dose vaccines based on mRNA technology. The Johnson and Johnson Janssen vaccine (JNJ-78436735) was given emergency use authorization on February 27, 2021, and is based on a modified adenovirus vector.

Patients who undergo a solid organ or stem cell transplant at any stage of life are required to take medications that suppress the immune system to prevent rejection of the transplanted organ or cells. However, this leaves the patients vulnerable to infection. From a study in the United Kingdom, having a solid organ transplant was associated with greater than 3 times increased risk of death from COVID-19 after adjustment for age.<sup>2</sup> Due to this degree of immunosuppression, organ transplant patients were prioritized to have earlier access to the vaccines should they wish to receive them.

As can be appreciated, immunocompromised individuals may have a lower immune response to vaccinations. In a study of 242 kidney transplant patients, 28 days after the first dose of the Moderna vaccine, only 10.8% of these patients had a positive IgG serology test.<sup>3</sup> This was further confirmed in another study of 436 transplant patients that were a median of 20 days postvaccination with either the Pfizer or Moderna vaccine where only 17% of patients had a detectable antibody response.<sup>4</sup> These authors also found that an antibody response to the vaccines was less likely in transplant patients receiving antimetabolite maintenance immunosuppression therapy (mycophenolate) than in transplant patients receiving other types of therapy.<sup>4</sup> It should be noted, however, that 20 or 28 days may not be a sufficient time period in which to mount an adequate immune response. In a follow-up study, the authors investigated the antibody response in 658 solid organ transplant patients after both doses of the vaccine.<sup>5</sup> They found that 15% of these patients had an antibody response after dose 1 and dose 2 of the vaccine, 46% of these patients had no antibody response after either dose, and 39% had no antibody response after dose 1 but developed an antibody response after dose 2 of the vaccine. The previous finding that patients receiving antimetabolite therapy were less likely to have an immune response to the vaccine was

mirrored in this study, where 57% of patients taking antimetabolites had no antibody response after doses 1 and 2, 35% had no antibody response after dose 1 but developed one after dose 2, and 8% of patients had an antibody response after dose 1 and dose 2.<sup>5</sup>

In a liver transplant-specific study of 161 patients, it was found that antibodies were detectable in 34% of patients after dose 1 (median of 21 days postdose) and 81% after dose 2 at a median of 30 days after the dose and that 39% of patients receiving 2 vaccine doses on antimetabolite therapy vs 5% not on antimetabolite therapy were nonresponders.<sup>6</sup> A later study investigated B-cell and T-cell responses in 16 solid organ transplant patients vs 23 immunocompetent controls and found that only 37% of solid organ transplant patients vs 100% of immunocompetent controls developed anti-SARS-CoV-2 IgG antibodies to the spike protein.<sup>7</sup> Further, only 56% of transplant patients had a detectable T-cell response.<sup>7</sup>

In a previous study of 93 multiple myeloma patients, it was found that 56% had a positive SARS-CoV-2 IgG spike protein antibody response after the first dose of either the Pfizer or Oxford-AstraZeneca (AZD1222; viral vector vaccine) vaccines.<sup>8</sup> In another study,<sup>9</sup> it was found that patients with a history of monoclonal gammopathy had a similar antibody response to the Pfizer, Moderna, and Janssen SARS-CoV-2 vaccines as healthcare worker controls. Therefore, the objective of this study was to investigate the SARS-CoV-2 IgG antibody response in patients who had a history of solid organ or stem cell transplant. Further, this study aimed to determine whether the antibodies that were produced by the transplant patients and patients with a history of monoclonal gammopathy had neutralizing activity towards the different strains of the virus *in vitro* compared to healthcare worker controls.

## Materials and Methods

### Patient Samples

Institutional review board approval from the University of California San Francisco was obtained for this study. Medical records were reviewed for patients who had laboratory orders placed for tacrolimus, everolimus, sirolimus, and cyclosporine in April and May 2021. If these patients had received either both doses of a SARS-CoV-2 Pfizer or Moderna vaccination or the single dose of the Janssen vaccination and had a medical history of either solid organ or allogeneic stem cell transplant, they were included in this study. Remnant plasma samples sent to the laboratory for routine clinical testing for these patients were retrieved and stored frozen at  $-20^{\circ}\text{C}$  ( $n = 40$ ).

Remnant serum samples from patients with a history of monoclonal gammopathy ( $n = 12$ ) that had a SARS-CoV-2 vaccination and had a positive SARS-CoV-2 IgG response from the assay described below that detects antibodies against both the spike protein and nucleocapsid were obtained and used as a disease control group. Additional information regarding these patients has been described.<sup>9</sup> Written consent was not required, as remnant samples sent to the laboratory for routine patient care were used for this study.

Healthcare worker controls ( $n = 20$ ) from Zuckerberg San Francisco General Hospital were recruited and blood samples were drawn (gold top tubes). Written consent was obtained from all subjects. The date(s) of vaccination and type of vaccine received was self-reported.

### SARS-CoV-2 IgG Antibody Assay

The Pylon 3D automated immunoassay system was used to quantitatively measure IgG antibodies as previously described<sup>10</sup> on the residual plasma samples retained from the transplant patients. Briefly, this assay is a sandwich-based assay. Fifteen microliters of plasma was mixed with 105  $\mu\text{L}$  diluent in the sample well. The probe, coated with Protein G targeting IgG, was immersed in the sample well for 360 seconds, followed by a wash sequence. The probe was then transferred to a well containing biotinylated SARS-CoV-2 spike receptor binding domain (RBD) (Arg319-Phe541) for a 180 second incubation. The biotinylated RBD binds SARS-CoV-2 specific IgG. Following a wash sequence, the probe was then incubated with a Cy5-streptavidin (Cy5-SA) polysaccharide conjugate reagent for 30 seconds followed by a wash sequence. Fluorescence signal from the bound Cy5-SA on the probe tip was then measured. This assay detects both the nucleocapsid and spike protein of SARS-CoV-2 and therefore cannot differentiate between antibodies produced as a result of COVID-19 infection or those produced due to vaccination. The quantitative assay produces a result of relative fluorescence units (RFUs), and a cutoff of 50 RFUs was considered as positive.<sup>10</sup> RFUs are determined for patient samples based on comparison with a calibration curve ranging from 1  $\mu\text{g}/\text{mL}$  to 300  $\mu\text{g}/\text{mL}$  of SARS-CoV-2 human IgG standard spiked into negative human serum. The assay is linear to 300  $\mu\text{g}/\text{mL}$  corresponding to 6976 RFUs. Therefore, the higher the number of RFUs, the greater the antibody response.

### SARS-CoV-2 IgG Nucleocapsid Antibody Assay

The samples from transplant patients that were positive on the SARS-CoV-2 IgG antibody assay described above were run on a chemiluminescent microparticle immunoassay designed to detect only antibodies against the nucleocapsid protein of the virus on the Architect i2000 instrument (Abbott Laboratories). This assay uses SARS-CoV-2 antigen coated paramagnetic microparticles that are incubated with the patient sample, allowing the IgG antibodies in the sample to bind to the antigen. There is a washing step: anti-human IgG acridinium-labeled conjugate is added, creating a reaction mixture, which is incubated, and the addition of a pre-trigger and trigger solution cause a chemiluminescent reaction, which is measured in relative light units (RLUs). There is a direct relationship between the amount of IgG antibodies in the patient sample and the RLUs detected. The result is reported as an index based on dividing the sample result by the calibrator result to determine whether a patient sample is positive or negative for the antibodies. The cut-off index for positivity is  $\geq 1.4$  S/C (sample result divided by calibrator result).

### SARS-CoV-2 In Vitro Neutralizing Antibody Assay

The Pylon neutralizing antibody assay is a competitive binding assay. Twenty-six microliters of plasma was mixed with 104  $\mu\text{L}$  of assay buffer containing biotinylated recombinant angiotensin-converting enzyme 2 protein (ACE2) in the sample well. The probe, coated with SARS-CoV-2 spike RBD (Arg319-Phe541), was immersed in the sample well and incubated for 720 seconds. The biotinylated ACE2 competes with any neutralizing antibody present in the sample to bind the immobilized RBD on the probe. Following a wash sequence, the probe was then incubated with streptavidin conjugated to cyanine 5 (Cy5-SA) for 30 seconds, followed by a wash sequence. Fluorescence signal from the bound Cy5-SA on the probe tip was measured.

The amount of fluorescence signal measured is inversely proportional to the amount of neutralizing antibody present in the sample. The result output is a ratio index value ( $B/B_0$ ), where  $B$  is the fluorescence signal measurement for the sample and  $B_0$  is a preestablished value determined by testing negative pre-COVID-19 sera and is the fluorescent measurement for maximum binding. The cutoff index value used in this study was 0.73 using 30 pre-COVID-19 control serum samples. Any index value above 0.73 was negative (-) for neutralizing antibody and any below 0.73 was positive (+); the lower the signal, the more neutralizing antibody activity in the patient sample. Neutralizing antibody activity against the following variants of SARS-CoV2 was investigated: D614G (original variant), B.1.1.7 (alpha variant), B.1.351 (beta variant), B.1.1.28 (gamma variant) and B.1.617 (delta variant). The between-batch imprecision of this assay was  $\leq 10\%$  for all variants. All patient samples that had a positive IgG antibody assay result were used in the neutralizing antibody assay.

### Data Analysis

Data analysis was performed in Excel (Microsoft). For each of the variants, a  $2 \times 2 \chi^2$  test was performed comparing the positive neutralizing antibody assay results between the combined group of patients with a history of monoclonal gammopathy and healthcare worker controls vs the solid organ transplant patients (that were positive in the SARS-CoV-2 IgG antibody assay) using MedCalc v.19.6.4. A  $P$  value of  $< .05$  was deemed significant.

## Results

### Study Population

The demographic information for the 40 transplant patients included in this study can be seen in **TABLE 1**. Out of 40 patients, 13 were female and 27 were male with a mean and median age of 67 and 69 years, respectively (range, 28–87 years). Fifteen of the patients had previously had a kidney transplant, 8 had a liver transplant, 9 had a lung transplant (3 of which were bilateral), 5 had a heart transplant, 2 had allogeneic stem cell transplants, and 1 patient had a heart and lung transplant. Mean and median time since transplant was 6.8 and 5.8 years, respectively (range, 0.5–22.8 years). Twenty-five patients received the Pfizer vaccine, 13 patients received the Moderna vaccine, and 2 patients received the Janssen vaccine. The mean and median time since the first or only dose of the vaccine were 71 and 73 days, respectively (range, 14–100 days).

Demographic information for the 12 patients with a history of monoclonal gammopathy run on the SARS-CoV-2 neutralizing antibody assay and included in this study can be seen in **TABLE 2** and from the healthcare worker controls in **TABLE 3**.

### SARS-CoV-2 IgG Antibodies in Solid Organ and Stem Cell Transplant Patients

Of the 40 transplant patients included in this study, only 10 had a positive SARS-CoV-2 IgG antibody test (25%) (**TABLE 4**). Of the 10 patients that were positive, 2 had a heart transplant, 1 had a heart and lung transplant, 3 had a kidney transplant, 3 had a liver transplant, and 1 had a lung transplant. Of the 3 patients that had a SARS-CoV-2 IgG result of  $>500$  RFUs, all of them had liver transplants. The liver transplant patient with the highest SARS-CoV-2 IgG result

was only receiving tacrolimus as immunosuppressive therapy and it had been 22.8 years since the transplant. The other 2 liver transplant patients with RFUs of  $>500$  were taking mycophenolate and tacrolimus, and sirolimus and tacrolimus, respectively, and it had been 2.2 and 8.1 years since their respective transplants. Neither of the two patients who had undergone allogeneic stem cell transplant had a positive SARS-CoV-2 IgG antibody test.

The SARS-CoV-2 IgG RFUs showed a positive trend with increasing time since second dose of the vaccination in the 40 transplant patients (**FIGURE 1**). Increasing age had a slightly positive trend with RFUs in the 40 transplant patients and 20 healthcare worker controls, but a slightly negative trend with RFUs in the 12 patients with a history of monoclonal gammopathy (**FIGURE 2**). Further, the SARS-CoV-2 IgG RFUs also showed a slight positive trend with days since second dose of the Moderna vaccine and the Pfizer vaccine in the transplant patients (**FIGURE 3**).

### SARS-CoV-2 IgG Nucleocapsid Antibody Assay

Of the 10 patients that had a positive antibody result on the assay described above, 9 had sufficient sample remaining to be tested on a SARS-CoV-2 IgG assay that only detected antibodies to the nucleocapsid protein. All 9 samples were negative on this assay, indicating that the antibody response seen in the previously described assay was directed at the spike protein. This result could indicate that the antibodies were from the vaccine and not from prior infection, or that the sample was taken from these patients after sufficient time had passed from SARS-CoV-2 infection that the nucleocapsid antibody titer had decreased. For the 1 patient that did not have sufficient sample remaining to perform this assay, chart review did not indicate a prior COVID-19 infection.

### In Vitro Neutralizing Antibody Assay

The samples from solid organ transplant patients ( $n = 10$ ), patients with a history of monoclonal gammopathy ( $n = 12$ ) and from 20 healthcare worker controls that had detectable SARS-CoV2 IgG antibodies were run on the in vitro surrogate neutralizing antibody assay. A cutoff of 0.73 was used to determine whether the sample was positive for neutralizing antibodies, with the lower the number, the more neutralizing activity that was observed. The healthcare worker control samples all had neutralizing antibody activity for the original variant of the virus and for the other variants, but they were less effective for these other variants (**TABLE 5**). The patient samples from patients with a history of monoclonal gammopathy all had neutralizing antibody activity for the original variant of the virus, the alpha variant (B.1.1.7) and the delta variant (B.1.617). With one exception, 11 out of 12 patients (92%) with monoclonal gammopathy had neutralizing antibody activity to all of the variants (**TABLE 6**). The one exception (8%) had no neutralizing antibody activity against either the beta or gamma variants (B.1.351 and B.1.1.28, respectively) (**TABLE 6**). Nine out of 10 solid organ transplant patient samples had neutralizing antibody activity for the original variant of the virus (90%). Two out of 10 patient samples had no neutralizing antibody activity for the alpha variant (B.1.1.7; 20%), 3 out of 10 patient samples had no neutralizing antibody activity for the beta variant (B.1.351; 30%), 3 out of 10 patients had no neutralizing antibody activity for the gamma variant (B.1.1.28; 30%), and 5 out of 10 patients had no neutralizing antibody activity for the delta variant (B.1.617; 50%) (**TABLE 7**).

**TABLE 1. Demographic Information for the 40 Solid Organ or Allogenic Stem Cell Transplant Patients Included in the Study**

Patient	Age, y/Sex	Days Since Dose 1, 2	Vaccine	Transplant Type	Years Since Transplant	Current Immunosuppressant Medications
1	67/M	67, 40	P	Heart	2.1	Everolimus, tacrolimus
2	69/F	79, 58	P	Heart	8.0	Mycophenolate, tacrolimus
3	69/M	71, 42	P	Heart	4.4	Everolimus, mycophenolate, tacrolimus
4	50/F	48, 20	M	Heart	12.7	Mycophenolate, tacrolimus
5	61/M	67, 41	M	Heart	2.8	Mycophenolate, tacrolimus
6	28/F	50, 29	P	Heart and lung	4.8	Mycophenolate, prednisone, tacrolimus
7	78/F	56, 28	M	Kidney	9.0	Azothioprine, prednisone, tacrolimus
8	68/M	68, 47	P	Kidney	2.9	Mycophenolate, prednisone, tacrolimus
9	71/M	64, 25	P	Kidney	4.3	Mycophenolate, prednisone, tacrolimus
10	45/F	76, 23	P	Kidney	0.7	Mycophenolate, prednisone, tacrolimus
11	71/M	77, 55	P	Kidney	6.0	Mycophenolate, prednisone, tacrolimus
12	87/M	93, 72	P	Kidney	7.1	Mycophenolate, tacrolimus
13	57/M	14, NA	J	Kidney	3.6	Mycophenolate, prednisone, tacrolimus
14	68/M	76, 48	M	Kidney	7.7	Mycophenolate, prednisone, tacrolimus
15	67/M	74, 53	P	Kidney	18.0	Mycophenolate, prednisone, tacrolimus
16	72/F	72, 47	P	Kidney	0.8	Mycophenolate, prednisone, tacrolimus
17	70/F	73, 45	P	Kidney	3.6	Mycophenolate, prednisone, tacrolimus
18	78/F	93, 65	M	Kidney	8.4	Prednisone, tacrolimus
19	74/M	100, 72	M	Kidney	0.9	Mycophenolate, prednisone, tacrolimus
20	68/M	85, 63	P	Kidney	4.2	Mycophenolate, tacrolimus
21	63/M	61, 40	P	Kidney	11.6	Mycophenolate, prednisone, tacrolimus
22	81/M	93, 65	M	Liver	22.8	Tacrolimus
23	69/F	66, 38	M	Liver	8.1	Sirolimus, tacrolimus
24	73/M	97, 65	M	Liver	7.4	Mycophenolate, prednisone, tacrolimus
25	66/M	73, 52	P	Liver	3.1	Mycophenolate, tacrolimus
26	66/F	71, 30	P	Liver	8.4	Mycophenolate, tacrolimus
27	67/M	73, 44	M	Liver	2.2	Mycophenolate, tacrolimus
28	60/M	44, NA	J	Liver	4.9	Mycophenolate, tacrolimus
29	74/F	62, 35	P	Liver	19.4	Prednisone, tacrolimus
30	71/M	67, 25	P	Lung	5.7	Mycophenolate, prednisone, tacrolimus
31	73/F	82, 61	P	Lung	12.6	Everolimus, mycophenolate, prednisone, tacrolimus
32	56/F	37, 16	P	Lung	13.8	Mycophenolate, prednisone, tacrolimus
33	58/M	71, 47	P	Lung	8.7	Prednisone, sirolimus, tacrolimus
34	55/M	44, 23	P	Lung	8.1	Mycophenolate, prednisone, tacrolimus
35	75/M	93, 65	M	Lung	6.1	Mycophenolate, prednisone, tacrolimus
36	74/M	69, 30	P	Lung, bilateral	6.1	Everolimus, prednisone, tacrolimus
37	73/M	89, 60	M	Lung, bilateral	3.5	Mycophenolate, prednisone, tacrolimus
38	69/M	78, 50	P	Lung, bilateral	3.7	Everolimus, mycophenolate, prednisone, tacrolimus
39	72/M	82, 60	P	Stem cell, allogeneic	2.8	Prednisone, tacrolimus
40	69/M	85, 56	M	Stem cell, allogeneic	0.5	Tacrolimus

J, Janssen vaccine; M, Moderna vaccine; NA, not applicable; P, Pfizer vaccine.

A  $2 \times 2$   $\chi^2$  test was performed comparing the percentage of positive neutralizing antibody responses in the combined healthcare worker controls and patients with a history of monoclonal gammopathy group vs the solid organ transplant patients (TABLE 8). The solid organ trans-

plant patients had similar neutralizing antibody activity to the original SARS-CoV-2 strain ( $P = .0736$ ), but a significantly lower neutralizing antibody activity to the alpha ( $P = .0104$ ), beta ( $P = .0125$ ), and gamma ( $P = .0125$ ), and particularly the delta variant ( $P < .0001$ ) of SARS-CoV-2.

**TABLE 2. Demographic Information for Patients with a History of Monoclonal Gammopathy Run on the SARS-CoV-2 Neutralizing Antibody Assay**

Patient	Age, y/Sex	Days Since Dose 1, 2	Vaccine	Diagnosis
1	66/M	70, 37	P	MGUS
2	76/M	47, 20	M	MM not in remission
3	66/M	60, 32	M	SMM
4	49/F	66, 38	M	MM in remission with hypogammaglobulinemia
5	73/M	69, 41	M	MGUS
6	58/M	52, 21	M	MM in remission with hypogammaglobulinemia
7	38/M	19, NA	J	MGUS
8	66/F	60, 42	M	MGUS
9	60/F	71, 42	M	MGUS
10	66/M	73, 53	P	Free light chain amyloidosis
11	79/M	44, 16	M	MGUS
12	67/M	33, 5	M	MM not in remission

J, Janssen vaccine; M, Moderna vaccine; MGUS, monoclonal gammopathy of unknown significance; MM, multiple myeloma; NA, not applicable; P, Pfizer vaccine; SMM, smoldering multiple myeloma.

**TABLE 3. Demographic Information for Healthcare Worker Controls Run on the SARS-CoV-2 Neutralizing Antibody Assay**

Control	Age, y/Sex	Days Since Dose 1, 2	Vaccine
1	29/F	80, 52	M
2	28/M	57, 29	M
3	36/M	62, 41	P
4	54/F	91, 69	P
5	66/M	51, 30	P
6	41/F	79, 48	M
7	35/F	92, 62	M
8	59/F	52, 24	M
9	36/M	109, 88	P
10	32/F	102, 72	M
11	52/F	108, 87	P
12	39/F	116, 94	P
13	66/F	110, 89	P
14	28/M	89, 67	P
15	47/F	103, 82	P
16	32/F	112, 91	P
17	46/M	114, 93	P
18	46/F	127, 96	P
19	41/M	112, 93	P
20	39/M	115, 94	P

M, Moderna vaccine; P, Pfizer vaccine.

**TABLE 4. SARS-CoV-2 IgG Antibody Detection by Transplant Type**

Transplant Type	Total No.	No. (%) Positive for COVID IgG
Heart	5	2 (40)
Heart and lung	1	1 (100)
Kidney	15	3 (20)
Liver	8	3 (38)
Lung	9	1 (11)
Allogeneic stem cell	2	0 (0)

## Discussion

This study aimed to determine the SARS-CoV-2 IgG antibody response in patients who had a history of solid organ or allogeneic stem cell transplant and had received the SARS-CoV-2 vaccination. Only 25% of these patients had a positive SARS-CoV-2 IgG antibody response based on a positive cutoff of 50 RFUs. This is in line with reports in kidney transplant patients and other solid organ transplant patients.<sup>3-7</sup>

Transplant patients need to be maintained on immunosuppressant therapies to prevent rejection of the transplanted organ, but a balance must be maintained between preventing rejection and the side effects

of these medications. Liver transplant patients tend to be maintained on lower levels of immunosuppressants than other solid organ transplant recipients<sup>6</sup> and it is also possible to withdraw immunosuppressant

treatment completely in selected patients.<sup>11</sup> This may be a plausible explanation for the increased SARS-CoV-2 IgG antibody response that was observed in liver transplant patients in this study compared to other solid organ transplants. Further, in this study, the majority of patients were receiving mycophenolate. Immunosuppression regimens including mycophenolate have previously been reported to be associated with a reduction in antibody production to the SARS-CoV-2 vaccine in solid organ transplant patients after both the first and second doses of the vaccine.<sup>4,5</sup>

Because the vaccines were designed around the original SARS-CoV-2 spike protein that was detected, the expectation would be that these antibodies would have neutralizing activity towards the original variant, which is what was found in this study of control healthcare workers and patients with a history of monoclonal gammopathy, and to a lesser extent, in solid organ transplant patients. These antibodies produced from the vaccines also seem to have neutralizing activity for the variants in the spike protein in healthcare worker controls and patients with a history of monoclonal gammopathy, and to a significantly lesser degree, in the solid organ transplant patients, for the alpha, beta, and gamma variants but especially for the delta variant (B.1.617), in which only 50% of solid organ transplant patients that

**FIGURE 1.** Linear regression correlation between relative fluorescence units obtained on the SARS-CoV-2 IgG antibody assay and days since vaccination and dose 2 for solid organ and allogenic stem cell transplant patients.  $y = 4.9724x - 41.476$ ;  $R^2 = 0.017$ .

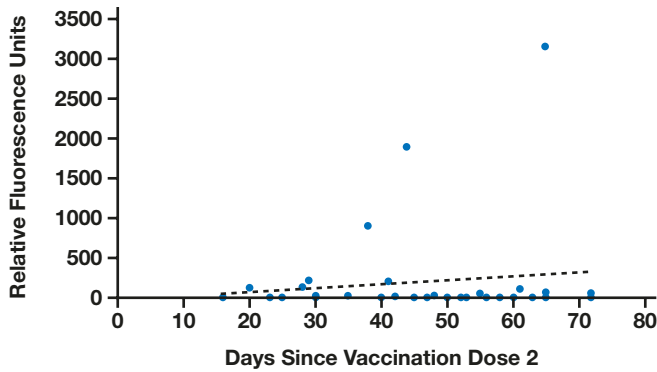


**FIGURE 2.** Linear regression correlation between relative fluorescence units obtained on the SARS-CoV-2 IgG antibody assay and age of the patient when the sample was collected for solid organ and allogenic stem cell transplant patients ( $y = 9.2119x - 441.28$ ;  $R^2 = 0.0264$ ) (A), patients with a history of monoclonal gammopathy ( $y = 15.391x - 3848.2$ ;  $R^2 = 0.0073$ ) (B), and healthcare worker controls ( $y = 7.3828x - 780.74$ ;  $R^2 = 0.0091$ ) (C).

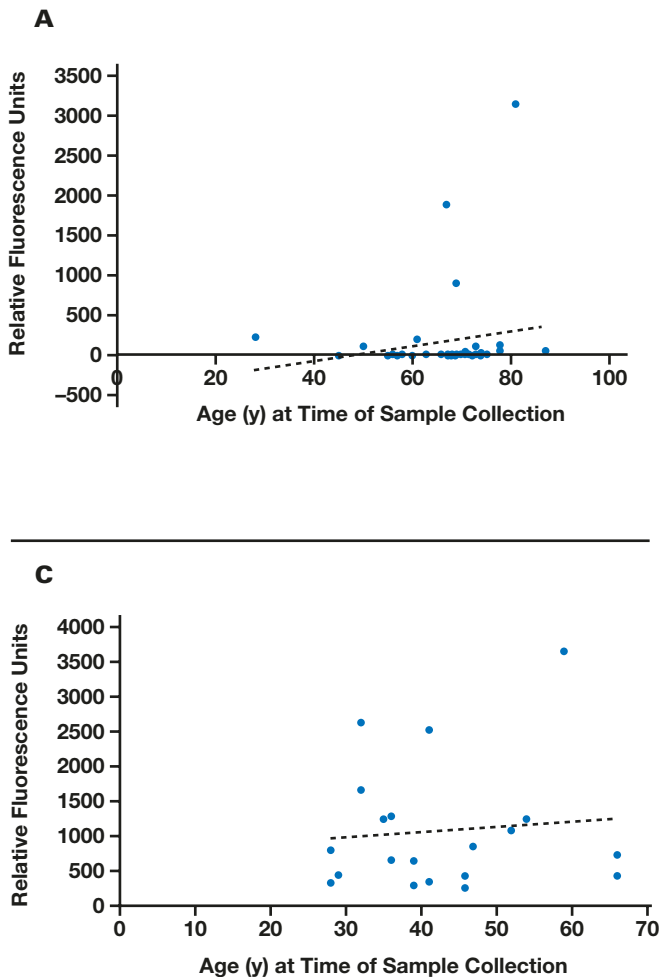


**FIGURE 3.** Linear regression correlation between relative fluorescence units obtained on the SARS-CoV-2 IgG antibody assay and days since vaccination dose 2 for the Moderna vaccine ( $y = 3.0557x - 344.29$ ;  $R^2 = 0.0026$ ) (A) and Pfizer vaccine ( $y = 0.0531x - 19.211$ ;  $R^2 = 0.0003$ ) (B) for solid organ and allogeneic stem cell transplant patients.

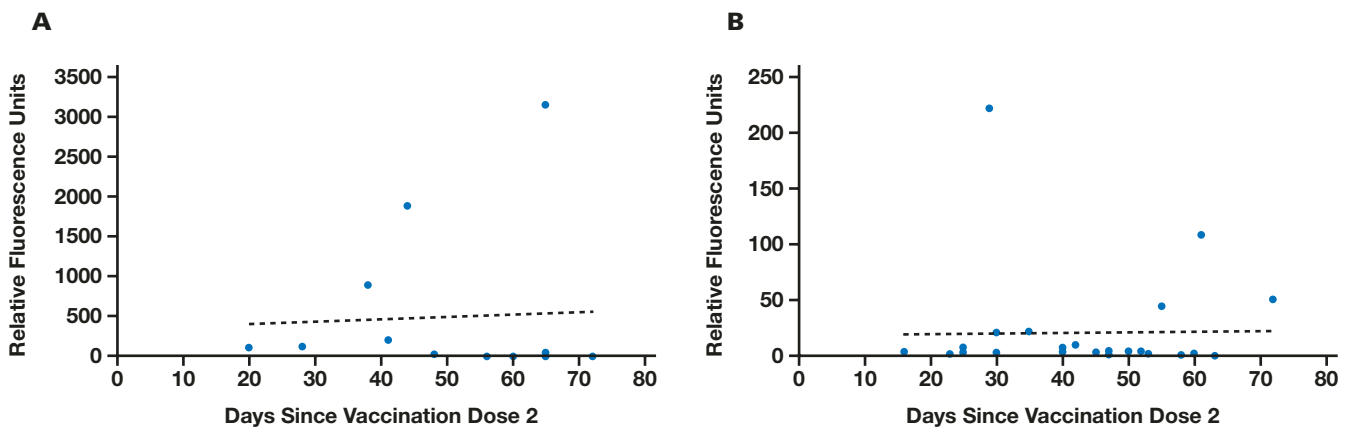


**TABLE 5.** In Vitro Neutralizing Antibody Activity in Healthcare Worker Controls

Control	Original Variant D614G		Alpha Variant B.1.1.7		Beta Variant B.1.351		Gamma Variant B.1.1.28		Delta Variant B.1.617	
	Index (B/B0)	Result (+, -)	Index (B/B0)	Result (+, -)	Index (B/B0)	Result (+, -)	Index (B/B0)	Result (+, -)	Index (B/B0)	Result (+, -)
1	0.01	(+)	0.09	(+)	0.08	(+)	0.06	(+)	0.07	(+)
2	0.02	(+)	0.11	(+)	0.09	(+)	0.09	(+)	0.07	(+)
3	0.08	(+)	0.34	(+)	0.25	(+)	0.24	(+)	0.25	(+)
4	0.07	(+)	0.29	(+)	0.27	(+)	0.24	(+)	0.19	(+)
5	0.17	(+)	0.52	(+)	0.46	(+)	0.43	(+)	0.39	(+)
6	0.01	(+)	0.08	(+)	0.07	(+)	0.07	(+)	0.04	(+)
7	0.03	(+)	0.18	(+)	0.16	(+)	0.19	(+)	0.12	(+)
8	0.01	(+)	0.04	(+)	0.04	(+)	0.04	(+)	0.02	(+)
9	0.17	(+)	0.59	(+)	0.57	(+)	0.51	(+)	0.47	(+)
10	0.01	(+)	0.06	(+)	0.05	(+)	0.06	(+)	0.04	(+)
11	0.14	(+)	0.38	(+)	0.38	(+)	0.37	(+)	0.30	(+)
12	0.41	(+)	0.67	(+)	0.55	(+)	0.55	(+)	0.52	(+)
13	0.32	(+)	0.71	(+)	0.66	(+)	0.65	(+)	0.57	(+)
14	0.13	(+)	0.35	(+)	0.54	(+)	0.42	(+)	0.31	(+)
15	0.06	(+)	0.26	(+)	0.24	(+)	0.25	(+)	0.14	(+)
16	0.03	(+)	0.13	(+)	0.13	(+)	0.12	(+)	0.08	(+)
17	0.10	(+)	0.34	(+)	0.29	(+)	0.29	(+)	0.24	(+)
18	0.33	(+)	0.70	(+)	0.66	(+)	0.67	(+)	0.54	(+)
19	0.20	(+)	0.52	(+)	0.47	(+)	0.46	(+)	0.43	(+)
20	0.19	(+)	0.57	(+)	0.50	(+)	0.48	(+)	0.42	(+)

had a positive antibody response had neutralizing activity towards it. To our knowledge, this is the first study to document this finding, which is particularly relevant as the delta variant was the most fatal SARS-CoV-2 variant in a number of countries around the world. This information should be disseminated to solid organ transplant patients so that they are aware that they may have an attenuated response to the SARS-CoV-2 vaccines and they should continue to employ risk-reduction strategies such as social distancing and wearing masks to protect themselves, as well as obtaining a booster vaccine dose that is available for each type of vaccine and has been shown to illicit an an-

tibody response in solid organ transplant patients who previously had no detectable antibody titers.<sup>12</sup>

There are several limitations to this study, including the very small number of patients included. There is no baseline antibody concentration data from these patients, and there are no data on the SARS-CoV-2 infection history. Further, 1 patient that had a positive antibody response to the SARS-CoV-2 spike protein assay had insufficient sample remaining to be run on the SARS-CoV-2 assay for nucleocapsid-directed antibodies. Although the SARS-CoV-2 IgG RFUs showed a positive trend with increasing time since the second dose of the vaccination as well as

**TABLE 6. In Vitro Neutralizing Antibody Activity in Patients with a History of Monoclonal Gammopathy**

Patient	Original Variant D614G		Alpha Variant B.1.1.7		Beta Variant B.1.351		Gamma Variant B.1.1.28		Delta Variant B.1.617	
	Index (B/B0)	Result (+, -)	Index (B/B0)	Result (+, -)	Index (B/B0)	Result (+, -)	Index (B/B0)	Result (+, -)	Index (B/B0)	Result (+, -)
1	0.07	(+)	0.08	(+)	0.44	(+)	0.45	(+)	0.37	(+)
2	0.15	(+)	0.16	(+)	0.83	(-)	0.90	(-)	0.44	(+)
3	0.03	(+)	0.03	(+)	0.39	(+)	0.37	(+)	0.17	(+)
4	0.06	(+)	0.06	(+)	0.30	(+)	0.34	(+)	0.31	(+)
5	0.01	(+)	0.02	(+)	0.29	(+)	0.27	(+)	0.14	(+)
6	0.03	(+)	0.03	(+)	0.36	(+)	0.34	(+)	0.21	(+)
7	0.01	(+)	0.01	(+)	0.10	(+)	0.09	(+)	0.03	(+)
8	0.00	(+)	0.03	(+)	0.05	(+)	0.04	(+)	0.01	(+)
9	0.01	(+)	0.05	(+)	0.06	(+)	0.06	(+)	0.02	(+)
10	0.01	(+)	0.07	(+)	0.18	(+)	0.15	(+)	0.06	(+)
11	0.00	(+)	0.04	(+)	0.08	(+)	0.08	(+)	0.02	(+)
12	0.01	(+)	0.02	(+)	0.22	(+)	0.21	(+)	0.10	(+)

**TABLE 7. In Vitro Neutralizing Antibody Activity in Solid Organ Transplant Patients**

Patient	Original Variant D614G		Alpha Variant B.1.1.7		Beta Variant B.1.351		Gamma Variant B.1.1.28		Delta Variant B.1.617	
	Index (B/B0)	Result (+, -)	Index (B/B0)	Result (+, -)	Index (B/B0)	Result (+, -)	Index (B/B0)	Result (+, -)	Index (B/B0)	Result (+, -)
4	0.57	(+)	0.66	(+)	0.74	(-)	0.80	(-)	0.84	(-)
5	0.29	(+)	0.54	(+)	0.66	(+)	0.70	(+)	0.68	(+)
6	0.38	(+)	0.64	(+)	0.65	(+)	0.31	(+)	0.62	(+)
7	0.43	(+)	0.67	(+)	0.72	(+)	0.68	(+)	0.87	(-)
12	0.40	(+)	0.68	(+)	0.72	(+)	0.80	(-)	0.99	(-)
18	0.99	(-)	0.82	(-)	1.26	(-)	0.43	(+)	0.89	(-)
22	0.02	(+)	0.05	(+)	0.11	(+)	0.13	(+)	0.06	(+)
23	0.64	(+)	0.12	(+)	0.50	(+)	0.40	(+)	0.18	(+)
27	0.02	(+)	0.07	(+)	0.14	(+)	0.11	(+)	0.05	(+)
31	0.65	(+)	0.81	(-)	0.78	(-)	0.77	(-)	0.96	(-)

**TABLE 8.  $2 \times 2 \chi^2$  Test Comparing the Number of Samples with a Positive Neutralizing Antibody Response to the Different SARS-CoV-2 Variants Between the Healthcare Worker Controls and Monoclonal Gammopathy Patient Group vs the Solid Organ Transplant Group<sup>a</sup>**

SARS-CoV-2 Strain	Health Care Worker Controls and Monoclonal Gammopathy Patients (n = 32)	Solid Organ Transplant Patients (n = 10)	P Value
Original variant D614G	32 (100)	9 (90)	.0736
Alpha variant B.1.1.7	32 (100)	8 (80)	.0104
Beta variant B.1.351	31 (96.9)	7 (70)	.0125
Gamma variant B.1.1.28	31 (96.9)	7 (70)	.0125
Delta variant B.1.617	32 (100)	5 (50)	<.0001

<sup>a</sup>Data are given as No. (%).

with increasing age in the solid organ transplant patients, the number of samples is low and so it is unclear whether these trends would be reproducible in larger data sets.

## Conclusions

The majority of solid organ and stem cell transplant patients included in this study did not mount a sufficient immune response against the

SARS-CoV-2 vaccinations to produce a positive IgG antibody titer. Further, in those that did have detectable antibodies, they were found to have lower neutralizing activity to all known variants of the SARS-CoV-2 virus compared to both healthcare worker controls and patients with a history of monoclonal gammopathy, most particularly the delta variant (B.1.617). Therefore, it seems prudent that these solid organ and stem cell transplant patients should obtain a third vaccination dose and a booster dose and continue to follow precautions to limit their exposure

to SARS-CoV-2 until herd immunity is achieved, as their response to the vaccinations seems to be attenuated.

## Acknowledgments

This work was supported by the University of California San Francisco Department of Laboratory Medicine.

## Disclosure

P.P. and M.Z. are employees of ET Healthcare and performed the neutralizing antibody test for which data are included in this article.

## REFERENCES

1. Johns Hopkins University. Coronavirus Resource Center. <https://coronavirus.jhu.edu/>. Accessed March 3, 2022.
2. Williamson EJ, Walker AJ, Bhaskaran K, et al. Factors associated with COVID-19-related death using OpenSAFELY. *Nature*. 2020;584(7821):430–436.
3. Bentomane I, Gautier-Vargas G, Cognard N, et al. Weak anti-SARS-CoV-2 antibody response after the first injection of an mRNA COVID-19 vaccine in kidney transplant recipients. *Kidney Int*. 2021;99(6):1487–1489.
4. Boyarsky BJ, Werbel WA, Avery RK, et al. Immunogenicity of a single dose of SARS-CoV-2 messenger RNA vaccine in solid organ transplant recipients. *JAMA*. 2021;325(17):1784–1786.
5. Boyarsky BJ, Werbel WA, Avery RK, et al. Antibody response to 2-dose SARS-CoV-2 mRNA vaccine series in solid organ transplant recipients. *JAMA*. 2021;325(21):2204–2206.
6. Strauss AT, Hallett AM, Boyarsky BJ, et al. Antibody response to severe acute respiratory syndrome-coronavirus-2 messenger RNA vaccines in liver transplant recipients. *Liver Transpl*. 2021;27(12):1852–1856.
7. Miele M, Busà R, Russeli G, et al. Impaired anti-SARS-CoV2 humoral and cellular immune response induced by Pfizer–BioNTech BNT162b2 mRNA vaccine in solid organ transplanted patients. *Am J Transplant*. 2021;21(8):2919–2921.
8. Bird S, Panopoulou A, Shea RL, et al. Response to first vaccination against SARS-CoV-2 in patients with multiple myeloma. *Lancet Hematol*. 2021;8(6):e389–e392.
9. Wu AHB, Wang CC, Ong CM, et al. Adequate antibody response to COVID-19 vaccine in patients with monoclonal gammopathies and light chain amyloidosis. *Lab Med*. 2022. doi: [10.1093/labmed/lmac113](https://doi.org/10.1093/labmed/lmac113).
10. Lynch KL, Whiteman JD, Lacanienta NP, et al. Magnitude and kinetics of anti-severe acute respiratory syndrome coronavirus 2 antibody responses and their relationship to disease severity. *Clin Infect Dis*. 2021;72(2):301–308.
11. Moini M, Schilsky ML, Tichy EM. Review on immunosuppression in liver transplantation. *World J Hepatol*. 2015;7(10):1355–1368.
12. Werbel WA, Boyarsky BJ, Ou MT, et al. Safety and immunogenicity of a third dose of SARS-CoV-2 vaccine in solid organ transplant recipients: a case series. *Ann Intern Med*. 2021;174(9):1330–1332.

# Highly Sensitive Serum miRNA Panel for the Diagnosis of Hepatocellular Carcinoma in Egyptian Patients with HCV-Related HCC

Ayman Yosry,<sup>1</sup> Naglaa Zayed,<sup>1</sup> Reham M. Dawood,<sup>2</sup> Marwa K. Ibrahim,<sup>2</sup> Marwa Elsharkawy,<sup>3</sup> Sherif M. Ekladius,<sup>3</sup> Ahmed Khairy,<sup>1</sup> Aisha Elsharkawy,<sup>1</sup> Marwa Khairy,<sup>1</sup> Shereen Abdel Alem,<sup>1</sup> Noha G. Bader El Din,<sup>2</sup> Mostafa K. El Awady,<sup>2</sup> Zeinab Abdellatif<sup>1,\*</sup>

<sup>1</sup>Endemic Medicine and Hepatology Department, Faculty of Medicine, Cairo University, Cairo, Egypt, <sup>2</sup>Microbial Biotechnology Department, Genetic Engineering Division, National Research Centre, Dokki, Giza, Egypt, <sup>3</sup>Clinical and Chemical Pathology Department, Faculty of Medicine, Cairo University, Cairo, Egypt \*To whom correspondence should be addressed. [zynabelkhateb@gmail.com](mailto:zynabelkhateb@gmail.com); [zeinab.soliman@medicine.cu.edu.eg](mailto:zeinab.soliman@medicine.cu.edu.eg)

**Keywords:** miRNA, hepatocellular carcinoma, hepatitis C virus, HCV, liver cirrhosis, advanced liver fibrosis

**Abbreviations:** miRNA, micro RNA; HCC, hepatocellular carcinoma; HCV, hepatitis C virus; OR, odds ratio; CI, confidence interval; mRNA, messenger RNA; ALT, alanine aminotransferase; AST, aspartate aminotransferase; AFP, alpha-fetoprotein; RT-PCR, reverse transcription–polymerase chain reaction; ROC, receiver operating characteristic; AUC, area under the curve; EMT, epithelial-mesenchymal transition.

*Laboratory Medicine* 2022;53:523–529; <https://doi.org/10.1093/labmed/lmac045>

## ABSTRACT

**Objective:** This study aimed at exploring the potential role of a panel of serum micro-RNA (miRNA) markers in liver fibrosis and hepatocellular carcinoma (HCC) diagnosis in patients with chronic hepatitis C virus (HCV) infection.

**Methods:** The study included 157 chronic HCV patients and 62 HCC patients who presented to the Cairo University Center for Hepatic Fibrosis, Endemic Medicine Department, from 2015 to 2017. Relevant clinical and laboratory data were collected and sera were subjected to miRNA expression profiling. Eleven miRNA markers were studied and receiver operating characteristic curves were constructed to investigate the best cutoff values of the miRNAs that showed altered expression in HCC compared to HCV-associated advanced fibrosis.

**Results:** miRNA expression profiling revealed 5 miRNAs (miR-124, miR-141, miR-205, miR-208a, miR-499a) were significantly

upregulated and 2 miRNAs were significantly downregulated (miR-103a, miR-15a) in HCC compared to advanced fibrosis patients. No significant difference was observed in miRNA expression between advanced fibrosis and early hepatic fibrosis apart from a significant downregulation of miR-155-5p in advanced fibrosis.

**Conclusion:** Serum miRNAs could serve as potential diagnostic tools for the diagnosis of HCC.

Hepatocellular carcinoma (HCC) is a primary hepatic malignancy and represents the fourth leading cause of cancer deaths worldwide.<sup>1</sup> In Egypt, it represents the fourth most common cancer.<sup>2</sup> Previous epidemiological studies have revealed a rise in the incidence of HCC in Egypt,<sup>3,4</sup> which could be attributed to the higher survival of cirrhotic patients,<sup>5</sup> improvement of screening programs and HCC diagnosis, and the increase in HCV incidence.<sup>6</sup>

Early diagnosis of HCC gives the opportunity for curative treatment (odds ratio [OR], 2.24; 95% confidence interval [CI], 1.99–2.52) and prolonged survival (OR, 1.90; 95% CI, 1.67–2.17).<sup>7</sup> Nonetheless, current diagnostic and surveillance methods for HCC have many limitations. For example, radiologic tools have low sensitivity for detecting small hepatic lesions<sup>8</sup>; moreover, the sensitivity and specificity of serologic tests (eg, alpha-fetoprotein [AFP], des-gamma-carboxy prothrombin) are insufficient for early diagnosis.<sup>9–11</sup>

MicroRNAs (miRNAs) are a class of short noncoding RNAs that inhibit gene expression by degrading messenger RNA (mRNA) or suppressing mRNA translation through complementary binding to their specific target mRNAs in the 3′-untranslated region.<sup>12,13</sup> Recent studies have proposed that miRNAs are involved in different basic biological processes, including cell proliferation, apoptosis, and differentiation.<sup>14,15</sup>

Current evidence suggests that miRNAs play an important role in HCC progression and have the potential for diagnostic and therapeutic HCC strategies.<sup>16,17</sup>

In this study, reverse transcription–polymerase chain reaction (RT-PCR) analysis was done, targeting 11 miRNAs that had previously

manifested differential expression in our laboratory in HCV-associated advanced fibrosis and HCC compared to patients with HCV infection and no liver fibrosis.

## Materials and Methods

### Patient Population

This observational cross-sectional study included 157 patients with chronic HCV infection and 62 patients with HCC who were recruited from Cairo University Center for Hepatic Fibrosis, Endemic Medicine Department, between 2015 and 2017. The enrolled chronic hepatitis C patients aged 18 to 75 years with a detectable HCV RNA for more than 6 months and were divided into 80 patients with nonadvanced fibrosis (F0–F2) and 77 patients with advanced fibrosis (F3–F4) according to transient elastography measurement.

Detailed history taking, clinical assessment, and routine laboratory tests in the form of complete blood count, liver biochemical profiles including alanine aminotransferase (ALT), aspartate aminotransferase (AST), bilirubin, albumin, renal function tests, and AFP were performed.

Transient elastography examination was done for the enrolled patients with the use of a FibroScan (EchoSens FibroScan). Transient elastography was the reference method for hepatic fibrosis staging and we used the proposed cutoffs of < 7.1 kPa for nonsignificant fibrosis (F < 2), ≥ 7.1 kPa for significant fibrosis (F ≥ 2), ≥ 9.5 kPa for advanced fibrosis (F ≥ 3), and ≥ 12.5 kPa for liver cirrhosis (F4).<sup>18</sup>

Patients with HCC had been recently diagnosed according to the American Association for the Study of Liver Disease updated practice guidelines for the management of HCC.<sup>19</sup> All of them had HCV-related HCC and had not commenced any kind of treatment at the time of the study.

For miRNA marker selection, we did an extensive literature review to find the miRNAs that showed promising ability for diagnosing chronic hepatitis, liver fibrosis, and hepatocellular carcinoma. We aimed to validate these markers in Egyptian patients with chronic hepatitis C. The current work was preceded by a preliminary small scale study on a small number of Egyptian patients to test the potential validity of these markers in our situation. **TABLE 1** summarizes some of these important studies.<sup>20–29</sup>

### miRNA Extraction and Quantification

Extraction was carried out using the miRNeasy Mini Kit (Qiagen). The miRNeasy Mini Kit was used to extract miRNA and total RNA following the manufacturer's protocols. The miRNA concentration and purity were evaluated using NanoDrop (UV-VIS-Spectrophotometer Q 5000) before proceeding to the real-time PCR assays. Extracted RNA was stored at –80°C until use.

### SYBR Green-Based RT-PCR Analysis

According to the manufacturer's instructions, the cDNA buffered with miScript HiSpec Buffer was prepared from 60 ng purified miRNA using the miScript II RT Kit (SABiosciences). The cDNA was then diluted 1:5 in nuclease-free water. The quantitative RT-PCR was conducted using miScript miRNA PCR master mix (SABiosciences). Briefly, the cDNA template was mixed with 2x QuantiTect SYBR Green PCR Master Mix, 10x miScript Universal Primer, and RNase-

**TABLE 1. Summary of Previous Studies on the Selected miRNAs**

miRNA	Function
miR-200c and miR-141 <sup>20</sup>	Simultaneous silencing of miR-200c and miR-141 was likely to be responsible for the development of HCC-BDTT via ZEB1-directed EMT activation and Sec23a-mediated secretome.
miR-200a and miRNA -200 family <sup>21</sup>	Several studies revealed an association between miR-200 family and a variety of human diseases, especially cancer. Some research provided insight into possible mechanisms of carcinogenesis. Could have role in HCC diagnosis and prognosis.
miR-200a <sup>22</sup>	It was predicted that miR-200a bind to iron-bound transferrin receptor (TfR1) targets TfR1 and DMT1 expression, thereby inhibiting cell cycle progression and growth.
miR-15a-5p <sup>23</sup>	Overexpression of miR-15a-5p inhibited viability, proliferation, migration, and invasion of HepG2 cells. This study revealed Exo-miR-15a-5p from cancer cells inhibited PD1 expression in CD8+ T cells, which suppressed the development of HCC.
miR-155-5p <sup>24</sup>	miRNA-155-5p has been reported to play an oncogenic role in different human malignancies. Moreover, it was reported that there is an association of miR-155-5p with aggressive HCC both in vitro and in vivo.
miR-574-3p <sup>25</sup>	miR-574-3p has been reported as a tumor suppressor and potential therapeutic target in various types of cancer.
miR-103a <sup>26,27</sup>	Found to be one of the most highly expressed microRNAs in HCC tissues, upregulated in HCC tissue compared with the controls. Its high expression was associated with poor prognosis, and its overexpression promoted HCC cell growth and mobility. It was reported that miR-103a plays both an oncogenic and tumor suppressive role in various types of cancers. For example, miR-103 promotes proliferation and metastasis by targeting KLF4 in gastric cancer.
miR-208-3p <sup>28</sup>	In vivo test results revealed that miR-208-3p down-regulation inhibited HCC tumorigenesis in Hep3B cells. These findings suggested that miR-208-3p up-regulation is associated with HCC cell progression and may provide a new target for liver cancer treatment.
miR-205 <sup>29</sup>	In the context of EMT modulation, both miR-200 family and miR-205 are markedly downregulated in cancer. miR-200 and miR-205 have captured most of the attention as therapeutic targets.

EMT, epithelial-mesenchymal transition; HCC, hepatocellular carcinoma.

free water and then transferred to a custom-made microRNA PCR panel that included primers for 11 target miRNAs. These miRNAs were selected based on previous findings from this laboratory, which revealed dysregulation of their expression in early vs late fibrotic patients. The hsa-miRs were miR-141-3p, miR-155-5p, miR-200a-3p, miR-200c-3p, miR-205-5p, miR-208a-3p, miR-499a-5p, miR-103a-3p, miR-574-3p, and miR-15a-5p (SABiosciences). The SNORD6 miRNA was selected as a reference gene for normalization. The PCR custom plate was then tightly sealed by using heat sealing film.

Amplification reactions were done under the following conditions: initial incubation for 15 min at 95°C (preactivation HotStarTaq), accompanied by 40 cycles at 94°C for 15 s, 55°C for 30 s, and 70°C

**TABLE 2. Baseline Characteristics of the Study Population**

	Early Fibrosis (F0–F2) (n = 80)	Advanced Liver Fibrosis (F3–F4) (n = 77)	Hepatocellular Carcinoma (n = 62)	P Value <sup>a</sup>	P Value <sup>b</sup>
Age (y), median (IQR)	49 (43–57)	55 (50–61)	60 (57–65)	.0005	<.0001
Sex, No. (%)					
M	48 (60%)	42 (54.5%)	42 (67.8%)	.5	
F	32 (40%)	35 (45.5%)	15 (24.2%)	.02	
Diabetes mellitus, No. (%)	18 (22.5%)	32 (41.6%)	12 (19.4%)	.01	.01
Hypertension, No. (%)	16 (20%)	27 (35.1%)	6 (9.7%)	.03	.001
BMI (kg/m <sup>2</sup> ), mean (SD)	28.17 (3.95)	30.07 (5.68)	26.55 (3.97)	.3	.04
Hemoglobin (g/dL), mean (SD)	13.92 (1.71)	13.46 (1.79)	11.65 (1.71)	.1	<.0001
White blood cell count (×10 <sup>3</sup> /μL), median (IQR)	6.4 (4.97–8.05)	5.9 (4.3–8.2)	4.7 (3.8–6.6)	.2	.02
Platelet count (×10 <sup>3</sup> /μL), median (IQR)	241.5 (168.5–251)	156 (120–200)	121 (90–170)	<.0001	.008
ALT (IU/L), median (IQR)	39 (26–59)	50 (34–73)	40 (29–64)	.04	.2
AST (IU/L), median (IQR)	36 (23–48)	55 (37–75)	62 (45–84)	<.0001	.07
Total bilirubin (mg/dL), median (IQR)	0.6 (0.4–0.8)	0.79 (0.6–1)	1.4 (0.96–2.14)	.0001	<.0001
Albumin (g/dL), mean (SD)	4.17 (0.60)	3.89 (0.59)	3.15 (0.66)	.004	<.0001
CAP (dB/m), mean (SD)	229.10 (49.17)	239.52 (53.65)	209.28 (71.61)	.5	.1

ALT, alanine aminotransferase; AST, aspartate aminotransferase; BMI, body mass index; CAP, controlled attenuation parameter; IQR, interquartile range.

<sup>a</sup>P value between early fibrosis and advanced fibrosis.

<sup>b</sup>P value between advanced fibrosis and hepatocellular carcinoma.

**TABLE 3. The Studied miRNA Markers in Early vs Advanced Stage of Liver Fibrosis vs HCC<sup>a</sup>**

Marker	Early Stage Fibrosis (F0–F2) (n = 80)	Advanced Fibrosis (F3–F4) (n = 77)	Hepatocellular Carcinoma (n = 62)	P Value <sup>b</sup>	P Value <sup>c</sup>
miR-124-3p	0.83 (0.47–1.72)	0.93 (0.31–2.20)	2.81 (1.35–4.25)	.9	<.0001
miR-141-3p	1.90 (0.65–3.87)	1.96 (0.97–3.56)	7.11 (2.66–18.81)	.9	<.000
miR-155-5p	1.08 (0.62–2.23)	0.63 (0.29–1.94)	0.86 (0.25–1.14)	.02	.9
miR-200a-3p	0.85 (0.41–2.34)	1.47 (0.60–3.58)	2.39 (1.15–4.34)	.2	.2
miR-200c-3p	0.98 (0.36–2.52)	0.84 (0.27–1.96)	1.02 (0.23–2.27)	.2	.8
miR-205-5p	0.99 (0.49–2.08)	0.82 (0.38–1.40)	2.10 (0.76–5.16)	.2	<.0001
miR-208a	1.46 (0.40–15.13)	1.23 (0.57–4.85)	4.02 (1.16–12.72)	.6	.009
miR-499	1.56 (0.95–3.46)	1.74 (0.77–3.40)	5.68 (1.40–20.27)	.8	.003
miR-103a	0.77 (0.42–2.13)	0.71 (0.33–1.59)	0.18 (0.08–0.45)	.3	<.0001
miR-574	1.77 (0.99–2.95)	2.41 (0.81–5.38)	2.09 (0.41–7.87)	.2	.9
miR-15	0.76 (0.33–2.81)	0.78 (0.19–2.44)	0.22 (0.05–0.64)	.5	.0004

<sup>a</sup>Data are expressed as median (interquartile range).

<sup>b</sup>P value between early fibrosis and advanced fibrosis.

<sup>c</sup>P value between advanced fibrosis and hepatocellular carcinoma (HCC).

for 30 s. Amplification was carried out using the real-time Rotor-Gene PCR (Qiagen). Relative expression of each gene was estimated using the 2– $\Delta\Delta$ CT method, and gene expression variations were compared to the mean of the healthy population and expressed as fold-change. Each experiment was repeated 3 times and the mean was taken for illustration.

The study protocol complied with the ethical guidelines of the 1964 Declaration of Helsinki (2008 revision) and was approved by the ethics committee of the Faculty of Medicine, Cairo University. Written informed consent was obtained prior to sample collection.

### Statistical Analysis

Descriptive statistics were done; numeric variables were presented as mean (SD). The Shapiro-Wilk normality test was used to assess the dis-

tribution of numeric variables. The unpaired Student *t*-test was used to compare normally distributed variables, and the Mann-Whitney *U* test was used to compare those with abnormal distribution. The  $\chi^2$  test was used for categorical variables. The Spearman correlation coefficient was used to establish the correlation between miRNA markers. Receiver operating characteristic (ROC) analysis was performed and curves were constructed to assess the accuracy of miRNA markers in diagnosing HCC. STATA 15.1 software was used for the analysis. *P* values < .05 were deemed significant.

### Machine Learning Models

To predict HCC accurately, we ran multiple machine learning classification models using Python auto ML. The area under the curve (AUC)

of each model was computed by using 5-fold cross-validation, and the model with the highest AUC was chosen. To further help with the model interpretation, we generated feature importance plots as well as partial dependence plots to show the feature behavior. H2O AutoML library was used for this analysis.<sup>30</sup>

## Results

### Characteristics of the Study Population

Baseline characteristics of the study population are summarized in **TABLE 2**. The chronic HCV infection group included 80 patients with early fibrosis (F0–F2) and 77 patients with advanced hepatic fibrosis ( $\geq$ F3). In the HCC group, the median focal lesion size was 3.35 cm (2.5–5.4), 52.7% of lesions were single focal lesions, 51.8% were Barcelona Clinic Liver Cancer stage B, and 48.2% were stage A.

### Study miRNA Markers in the Diagnosis of Hepatic Fibrosis

This study revealed that there is no significant difference in miRNA expression in patients with chronic hepatitis C with any degree of hepatic fibrosis compared to those with no fibrosis (F0). Comparing the expression of miRNA markers in cases of advanced liver fibrosis (F3–F4) to those with early fibrosis (F0–F2), we noticed that miR-155-5p was significantly downregulated in advanced fibrosis (**TABLE 3**).

### miRNA Markers in HCC Diagnosis

Five miRNA markers were significantly upregulated in the sera of HCC patients compared to chronic HCV patients with advanced fibrosis;

**FIGURE 1.** Receiver operating characteristic (ROC) curves for diagnosis of the 5 upregulated microRNAs in hepatocellular carcinoma.

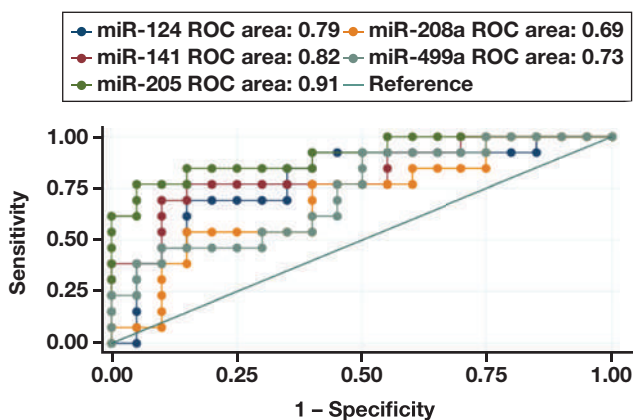


**TABLE 4.** Sensitivities, Specificities, and Best Cut-off Values of the 5 Upregulated miRNA Markers

Marker	Cut-off	AUROC (95% CI)	Sensitivity	Specificity	LR+	LR–	Accuracy
miR-124	1.22	0.79 (0.68–0.87)	80.70	68.18	2.54	0.28	75.25
miR-144	2.13	0.82 (0.68–0.91)	83.33	58.62	2.01	0.28	71.19
miR-205	1.58	0.90 (0.81–0.99)	85	85.19	5.74	0.18	85.11
miR-208a	2.75	0.69 (0.53–0.86)	70.59	62.5	1.88	0.47	65.85
miR-499a	1.39	0.73 (0.61–0.91)	82.35	54.17	1.80	0.33	65.85

AUROC, area under the receiver operating characteristic curve; LR, likelihood ratio.

namely, miR-124-3p, hsa-miR-141-3p, hsa-miR-205-5p, hsa-miR-208a-3p, hsa-miR-499a-5p. On the other hand, miR103a and miR15 showed significant downregulation in the HCC group compared to the advanced fibrosis group (**TABLE 3**).

### ROC Curves for the Discriminatory Power of miRNA Markers for Diagnosis of HCC

#### ROC Curves for miR-124-3p, miR-141-3p, miR-205-5p, miR-208a, miR-499 in Diagnosing HCC

ROC curves were constructed to determine the best cutoff values of miRNAs for the diagnosis of HCC. They revealed that miR-205 had the highest area under ROC: 0.9 (0.81–0.99) followed by miR-144 with 0.82 (0.68–0.91) and miR-124 with 0.79 (0.68–0.87) (**FIGURE 1** and **TABLE 4**). At a cutoff value of 1.58, miR-205 has a sensitivity of 85% and a specificity of 85.19 in the diagnosis of HCC.

#### ROC Curves for miR-103a, miR-15 for the Exclusion of HCC

On the other hand, miR-103a and miR-15 showed significant down expression in HCC compared to advanced liver fibrosis, with areas under ROC curves of 0.73 and 0.71, respectively (**FIGURE 2** and **TABLE 5**).

### Logistic Regression Analysis to Control for the Possible Confounding Effects of Age and Gender

Logistic regression analysis was performed to assess the predictability of these miRNA markers for the diagnosis of HCC, controlling for age and gender, as they showed a significant difference between advanced liver fibrosis and the HCC group. Analysis revealed that miR-124-3p, miR-141-3p, miR-205-5p, and miR-499 were significant predictors of HCC independent of age and gender. However, miR-208a added to the two downregulated miRs, miR-103a and miR-15, did not show significant predictability of HCC independent of age or gender (**TABLE 6**).

### Identification of the Best Diagnostic Biomarkers Using a Machine Learning Approach

In this study, we proposed a prediction model based on the machine learning algorithm to detect the association between relevant laboratory values, different miRNAs, and HCC. Notably, hemoglobin, total bilirubin, miR-155-5p, and miR-205-5p have significant diagnostic value for HCC (**FIGURE 3**). The area under the ROC curve for this model was 0.93 (**FIGURE 4**).

## Discussion

Early diagnosis of HCC is challenging. Currently, ultrasonographic examination is recommended by all guidelines with or without serum AFP test for early HCC detection. Cross-sectional imaging modalities are further recommended for liver nodules  $\geq 1$  cm. However, the sensitivity and specificity of these methods for HCC diagnosis remain unsatisfactory, particularly during early disease stages.<sup>31</sup>

miRNAs are considered as promising early diagnostic biomarkers of HCC despite the currently limited research programs and lack of practical translation. Together with other biomarkers, panels of deregulated miRNAs in the serum/plasma and/or exosomes are likely to play an important role in HCC diagnostics in the future.<sup>32</sup>

miRNAs are crucial gene regulators that are involved in the process of tumorigenesis. It had been proved that miRNAs can remain stable and be detected in various biological fluids, for example, human serum/plasma.<sup>33,34</sup>

This study revealed significant upregulation of 5 miRNA markers—miR-124-3p, miR-141-3p, miR-205-5p, miR-208a-3p, and miR-499a-5p—in the sera of HCC patients compared to liver cirrhosis.

In agreement with our results, a previous study revealed that miR-208a upregulation is associated with HCC progression.<sup>35</sup> In contrast to our findings, previous studies revealed significant downregulation of miR-124 in HCC tissues compared to nontumorous liver tissue.<sup>36</sup> Additionally, it has been reported that miR-124 could regulate HCC invasion and metastasis by regulating Rho-associated coiled-coil containing protein kinase 2 and enhancer of zeste homolog 2 (EZH2).<sup>37</sup>

Also, a previous study showed that miR-141 overexpression significantly reduces HCC proliferation, migration, and invasion through inhibiting epithelial-mesenchymal transition (EMT). More specifically, they found that miR-141-3p targets GP73 to reverse EMT, subsequently inhibiting HCC progression and metastasis.<sup>38</sup>

**FIGURE 2.** Receiver operating characteristic (ROC) curves for miR-103a and miR-15 in excluding hepatocellular carcinoma.

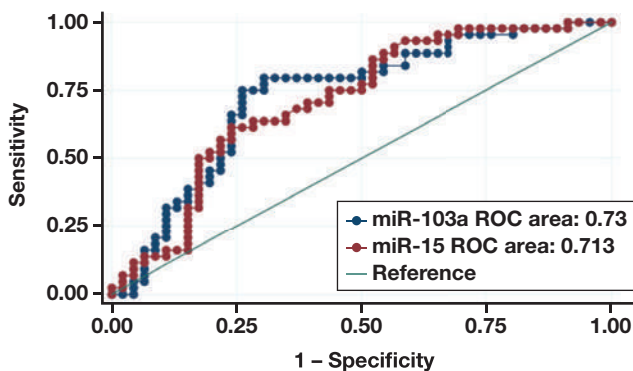


**TABLE 5.** Sensitivities, Specificities and Best Cut-off Values of miR-103a and miR-15 in Excluding HCC

Marker	Cut-off	AUROC (95% CI)	Sensitivity	Specificity	LR+	LR-	Accuracy
miR-103a	0.32	0.73 (0.66–0.85)	79.55	71.93	2.83	0.28	75.25
miR-15	0.27	0.71 (0.60–0.82)	70.45	60.87	1.80	0.48	65.65

AUROC, area under the receiver operating characteristic curve; LR, likelihood ratio.

As for miR-205, previous studies revealed that it is an important tumor suppressor, and its expression is reduced in the tissue of various malignancies compared to the adjacent tissue.<sup>39–42</sup> A previous study showed that miR-205 serum level is significantly reduced in HCC compared to liver cirrhosis and healthy control.<sup>43</sup>

Regarding miR-499, its association with HCV-associated HCC has not been reported in the literature to our knowledge. Nevertheless, previous studies revealed a link between has-miR-499 polymorphism and HBV-associated HCC development in Chinese patients.<sup>44</sup>

The reason behind the existence of miRNAs in plasma remains to be explained. Plasma miRNAs are generally considered to be a mixture of miRNAs released from cells of different tissues in the body, and estimating how many of them are released from the cancer cells is difficult. Some researchers suggest that cancer cells might pump these miRNAs into the circulation to eliminate their negative control on

**TABLE 6.** Logistic Regression Analysis for Predictors of Hepatocellular Carcinoma Compared to HCV-Associated Advanced Liver Fibrosis

	OR (95% CI)	P Value
<b>Model 1</b>		
miR-124-3p	1.81 (1.29–2.54)	.001
Age	1.12 (1.05–1.20)	.001
Sex	0.37 (0.13–1.09)	.07
<b>Model 2</b>		
miR-141-3p	1.15 (1.03–1.28)	.01
Age	1.09 (0.99–1.19)	.05
Sex	0.82 (0.23–2.94)	.8
<b>Model 3</b>		
miR-205-5p	1.12 (1.02–1.23)	.02
Age	1.11 (1.05–1.18)	<.0001
Sex	0.34 (0.15–0.79)	.01
<b>Model 4</b>		
miR-208a	1.06 (0.96–1.16)	.2
miR-499	1.20 (1.01–1.43)	.04
Age	1.07 (0.97–1.17)	.2
Sex	0.83 (0.15–4.73)	.8
<b>Model 5</b>		
miR-103a	1.002 (0.94–1.07)	.9
Age	1.11 (1.05–1.18)	<.0001
Sex	0.39 (0.18–0.87)	.02
<b>Model 6</b>		
miR-15	0.95 (0.85–1.05)	.3
Age	1.11 (1.04–1.17)	.001
Sex	0.47 (0.21–1.08)	.08

CI, confidence interval; OR, odds ratio.

**FIGURE 3.** Hepatocellular carcinoma prediction model based on a machine learning algorithm. Alb, albumin; AST, aspartate transferase; Bili, bilirubin; Hb, hemoglobin.

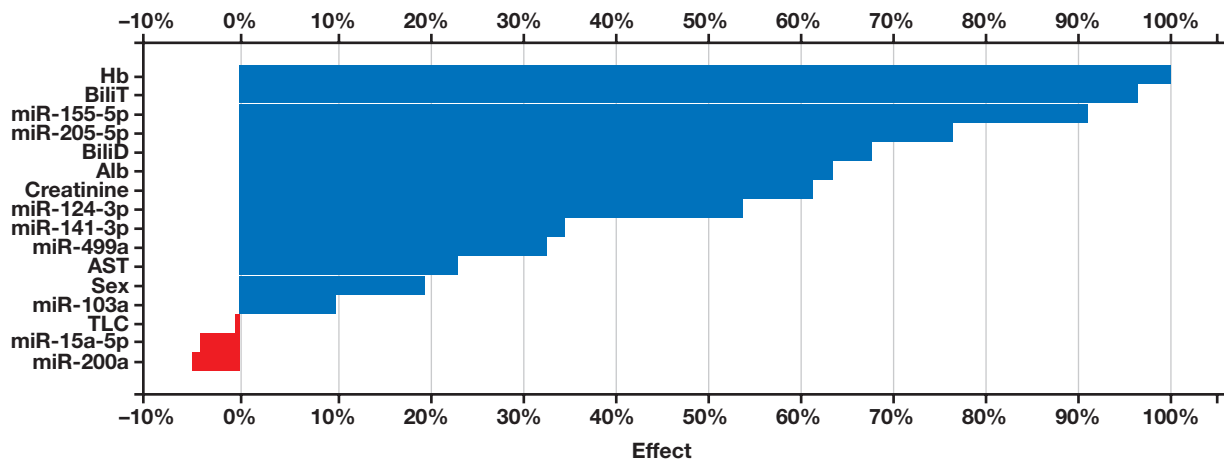
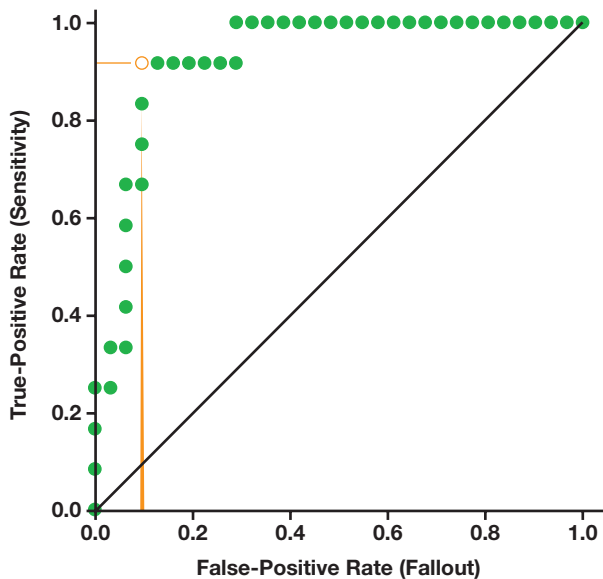


**FIGURE 4.** Receiver operating characteristic curve for the proposed model. Kolmogorov-Smirnov test = 0.8199; area under the curve = 0.9274.



tumor growth. This can explain our finding of serum upregulation of some of the miRNAs (miR-124, miR-141) that had been revealed to be downregulated in HCC tissues in other studies.<sup>45</sup>

Our results showed significant downregulation of miR-103a and miR-15. To the best of our knowledge, no previous studies evaluated the serum expression of these markers in HCC. Additionally, when we performed multivariable regression controlling for age and gender, neither marker showed statistical significance. This finding suggests that their expression could be attributed to differences in age between the advanced liver fibrosis group compared to the HCC group; however, further studies are needed.

A prediction model based on machine learning revealed that miR-155-5p and miR-205-5p have the highest relative importance in predicting HCC. miR-155-5p has been reported to play an oncogenic

role in various human malignancies; moreover, a previous study showed that it was highly overexpressed in HCC tissues and that miR-155-5p upregulation was significantly associated with the TNM stage.<sup>24</sup>

In conclusion, serum miRNA profiling revealed that HCV-associated HCC was associated with a significant change in a number of serum miRNAs in an Egyptian population. miR-124, miR-141, miR-205, miR-208a, and miR-499a were significantly higher in HCC cases compared to liver cirrhosis, whereas miR-103a and miR-15 were significantly lower in HCC sera. Serum miRNA profiling could serve as a clinically applicable tool for HCC diagnosis. However, studies with a larger sample size and other causes of HCC are needed to confirm these results.

### Funding

This work was supported by the scientific technology and development Fund (STDF fund: project ID 5274), Egypt.

### REFERENCES

- Villanueva A. Hepatocellular carcinoma. *N Engl J Med*. 2019;380(15):1450–1462. doi:10.1056/NEJMr1713263.
- Akinyemiju T, Abera S, Ahmed M, et al. The burden of primary liver cancer and underlying etiologies from 1990 to 2015 at the global, regional, and national level. *JAMA Oncol* 2017;3(12):1683–1691. doi:10.1001/jamaoncol.2017.3055.
- El-Zayadi A-R, Badran HM, Barakat EMFB, et al. Hepatocellular carcinoma in Egypt: a single center study over a decade. *World J Gastroenterol*. 2005;11(33):5193–5198.
- Abd-El salam S, Elwan N, Soliman H, et al. Epidemiology of liver cancer in Nile delta over a decade: a single-center study. *South Asian J Cancer*. 2018;7(1):24–26. doi:10.4103/sajc.sajc\_82\_17.
- Ziada DH, El Sadany S, Soliman H, et al. Prevalence of hepatocellular carcinoma in chronic hepatitis C patients in Mid Delta, Egypt: a single center study. *J Egypt Natl Canc Inst*. 2016;28(4):257–262. doi:10.1016/j.jnci.2016.06.001.
- El Serag HB. Epidemiology of hepatocellular carcinoma. *Clin Liver Dis*. 2001;5(1):87–107, vi.
- Singal AG, Pillai A, Tiro J. Early detection, curative treatment, and survival rates for hepatocellular carcinoma surveillance in patients

- with cirrhosis: a meta-analysis. *PLoS Med.* 2014;11(4):e1001624. doi:10.1371/journal.pmed.1001624.
8. Simmons O, Fetzter DT, Yokoo T, Marrero JA, Yopp A, Kono Y, et al. Predictors of adequate ultrasound quality for hepatocellular carcinoma surveillance in patients with cirrhosis. *Aliment Pharmacol Ther* 2017;45:169–177.
  9. Oka H, Tamori A, Kuroki T, Kobayashi K, Yamamoto S. Prospective study of alpha-fetoprotein in cirrhotic patients monitored for development of hepatocellular carcinoma. *Hepatology.* 1994;19(1):61–66.
  10. Marrero JA, Su GL, Wei W, et al. Des-gamma carboxyprothrombin can differentiate hepatocellular carcinoma from nonmalignant chronic liver disease in American patients. *Hepatology.* 2003;37(5):1114–1121. doi:10.1053/jhep.2003.50195.
  11. Seo SI, Kim HS, Kim WJ, et al. Diagnostic value of PIVKA-II and alpha-fetoprotein in hepatitis B virus-associated hepatocellular carcinoma. *World J Gastroenterol.* 2015;21(13):3928–3935. doi:10.3748/wjg.v21.i13.3928.
  12. Huang DH, Wang GY, Zhang JW, Li Y, Zeng XC, Jiang N. MiR-501-5p regulates CYLD expression and promotes cell proliferation in human hepatocellular carcinoma. *Jpn J Clin Oncol.* 2015;45(8):738–744. doi:10.1093/jjco/hyv063.
  13. Lu Y, Yue X, Cui Y, Zhang J, Wang K. MicroRNA-124 suppresses growth of human hepatocellular carcinoma by targeting STAT3. *Biochem Biophys Res Commun.* 2013;441(4):873–879. doi:10.1016/j.bbrc.2013.10.157.
  14. Otsuka M, Kishikawa T, Yoshikawa T, et al. MicroRNAs and liver disease. *J Hum Genet.* 2017;62(1):75–80. doi:10.1038/jhg.2016.53.
  15. Huang Y, Shen XJ, Zou Q, Wang SP, Tang SM, Zhang GZ. Biological functions of microRNAs: a review. *J Physiol Biochem.* 2011;67(1):129–139. doi:10.1007/s13105-010-0050-6.
  16. Bader El Din NG, Ibrahim MK, El-Shenawy R, et al. MicroRNAs expression profiling in Egyptian colorectal cancer patients. *IUBMB Life.* 2020;72(2):275–284. doi:10.1002/iub.2164.
  17. Huang S, He X. The role of microRNAs in liver cancer progression. *Br J Cancer.* 2011;104(2):235–240. doi:10.1038/sj.bjc.6606010.
  18. Tsochatzis EA, Gurusamy KS, Ntaoula S, Cholongitas E, Davidson BR, Burroughs AK. Elastography for the diagnosis of severity of fibrosis in chronic liver disease: a meta-analysis of diagnostic accuracy. *J Hepatol.* 2011;54(4):650–659. doi:10.1016/j.jhep.2010.07.033.
  19. Bruix J, Sherman M; American Association for the Study of Liver Diseases. Management of hepatocellular carcinoma: an update. *Hepatology.* 2011;53(3):1020–1022. doi:10.1002/hep.24199.
  20. Yeh TS, Wang F, Chen TC, et al. Expression profile of microRNA-200 family in hepatocellular carcinoma with bile duct tumor thrombus. *Ann Surg.* 2014;259(2):346–354.
  21. Mao Y, Chen W, Wu H, Liu C, Zhang J, Chen S. Mechanisms and functions of MiR-200 family in hepatocellular carcinoma. *Oncotargets Ther.* 2021;13:13479–13490.
  22. Greene CM, Varley RB, Lawless MW. MicroRNAs and liver cancer associated with iron overload: therapeutic targets unraveled. *World J Gastroenterol.* 2013;19(32):5212–5226.
  23. Zhang HY, Liang HX, Wu SH, Jiang HQ, Wang Q, Yu ZJ. Overexpressed tumor suppressor exosomal miR-15a-5p in cancer cells inhibits PD1 expression in CD8+ T cells and suppresses the hepatocellular carcinoma progression. *Front Oncol.* 2021. doi:10.3389/fonc.2021.622263.
  24. Fu X, Wen H, Jing L, et al. MicroRNA-155-5p promotes hepatocellular carcinoma progression by suppressing PTEN through the PI3K/Akt pathway. *Cancer Sci.* 2017;108(4):620–631. doi:10.1111/cas.13177.
  25. Zha Z, Jia F, Hu P, Mai E, Lei T. MicroRNA-574-3p inhibits the malignant behavior of liver cancer cells by targeting ADAM28. *Oncol Lett.* 2020;20(3):3015–3023.
  26. Liu Y, Zhang Y, Xiao B, et al. MiR-103a promotes tumour growth and influences glucose metabolism in hepatocellular carcinoma. *Cell Death Dis.* 2021;12(6):618.
  27. Zheng J, Liu Y, Qiao Y, Zhang L, Lu S. miR-103 promotes proliferation and metastasis by targeting KLF4 in gastric cancer. *Int J Mol Sci.* 2017;18:1–13.
  28. Yu P, Wu D, You Y, et al. miR-208-3p promotes hepatocellular carcinoma cell proliferation and invasion through regulating ARID2 expression. *Exp Cell Res.* 2015;336(2):232–241.
  29. Gregory PA, Bert AG, Paterson EL, et al. The miR-200 family and miR-205 regulate epithelial to mesenchymal transition by targeting ZEB1 and SIP1. *Nat Cell Biol.* 2008;10(5):593–601.
  30. LeDell E, Poirier S. H2O AutoML: Scalable automatic machine learning. 7th ICML Workshop on Automated Machine Learning (AutoML), July 2020. URL [https://www.automl.org/wp-content/uploads/2020/07/AutoML\\_2020\\_paper\\_61.pdf](https://www.automl.org/wp-content/uploads/2020/07/AutoML_2020_paper_61.pdf).
  31. Masuzaki R, Karp SJ, Omata M. New serum markers of hepatocellular carcinoma. *Semin Oncol.* 2012;39(4):434–439.
  32. Wang W, Wei C. Advances in the early diagnosis of hepatocellular carcinoma. *Genes Dis.* 2020;7(3):308–319.
  33. Mitchell PS, Parkin RK, Kroh EM, et al. Circulating microRNAs as stable blood-based markers for cancer detection. *Proc Natl Acad Sci USA.* 2008;105(30):10513–10518.
  34. Li Y, Jiang Z, Xu L, Yao H, Guo J, Ding X. Stability analysis of liver cancer-related microRNAs. *Acta Biochim Biophys Sin (Shanghai).* 2011;43(1):69–78. doi:10.1093/abbs/gmq114.
  35. Yu P, Wu D, You Y, et al. miR-208-3p promotes hepatocellular carcinoma cell proliferation and invasion through regulating ARID2 expression. *Exp Cell Res.* 2015;336(2):232–241. doi:10.1016/j.yexcr.2015.07.008.
  36. He RQ, Yang X, Liang L, Chen G, Ma J. MicroRNA-124-3p expression and its prospective functional pathways in hepatocellular carcinoma: a quantitative polymerase chain reaction, gene expression omnibus and bioinformatics study. *Oncol Lett.* 2018;15(4):5517–5532. doi:10.3892/ol.2018.8045.
  37. Zheng F, Liao YJ, Cai MY, et al. The putative tumour suppressor microRNA-124 modulates hepatocellular carcinoma cell aggressiveness by repressing ROCK2 and EZH2. *Gut* 2012;61(2):278–289. doi:10.1136/gut.2011.239145.
  38. Hou X, Yang L, Jiang X, et al. Role of microRNA-141-3p in the progression and metastasis of hepatocellular carcinoma cell. *Int J Biol Macromol.* 2019;128:331–339. doi:10.1016/j.ijbiomac.2019.01.144.
  39. Qin AY, Zhang XW, Liu L, et al. MiR-205 in cancer: an angel or a devil? *Eur J Cell Biol.* 2013;92(2):54–60. doi:10.1016/j.ejcb.2012.11.002.
  40. Yang G, Zhang P, Lv A, Liu Y, Wang G. MiR-205 functions as a tumor suppressor via targeting TGF-alpha in osteosarcoma. *Exp Mol Pathol.* 2016;100(1):160–166. doi:10.1016/j.yexmp.2015.12.010.
  41. Majid S, Dar AA, Saini S, et al. MicroRNA-205-directed transcriptional activation of tumor suppressor genes in prostate cancer. *Cancer.* 2010;116(24):5637–5649.
  42. Chen Z, Tang ZY, He Y, Liu LF, Li DJ, Chen X. miRNA-205 is a candidate tumor suppressor that targets ZEB2 in renal cell carcinoma. *Oncol Res Treat.* 2014;37(11):658–664.
  43. Zhu S, Liu W, Fu B, et al. Association of serum miR-205 with liver cirrhosis and cancer and its diagnostic significance. *Int J Clin Exp Med.* 2018;11(11):12375–12380.
  44. Xiang Y, Fan S, Cao J, Huang S, Zhang LP. Association of the microRNA-499 variants with susceptibility to hepatocellular carcinoma in a Chinese population. *Mol Biol Rep.* 2012;39(6):7019–7023. doi:10.1007/s11033-012-1532-0.
  45. Bai X, Liu Z, Shao X, et al. The heterogeneity of plasma miRNA profiles in hepatocellular carcinoma patients and the exploration of diagnostic circulating miRNAs for hepatocellular carcinoma. *PLoS One.* 2019;14(2):e0211581. doi:10.1371/journal.pone.0211581

# Seasonal Variation of Ferritin among Swedish Blood Donors

Johan Saldeen, MD, PhD,<sup>1</sup> Lena Carlsson, PhD,<sup>1</sup> Anders Larsson, MD, PhD<sup>1,\*</sup>

<sup>1</sup>Department of Medical Sciences, Uppsala University, Uppsala University Hospital, Uppsala, Sweden \*To whom correspondence should be addressed. [anders.larsson@akademiska.se](mailto:anders.larsson@akademiska.se)

**Keywords:** blood donors, ferritin, seasonal variation, anemia, iron deficiency, laboratory testing  
*Laboratory Medicine* 2022;53:530–532; <https://doi.org/10.1093/labmed/lmac053>

## ABSTRACT

**Objective:** Several biomarkers have been reported to exhibit a seasonal variation, which might also be associated with the seasonality observed for certain disorders, such as cardiovascular disease. Ferritin is a marker of iron stores but may be influenced by other factors including inflammation. The aim of this study was to determine whether there is a seasonal variation for plasma ferritin.

**Methods:** The study included all ferritin tests performed on blood donors between November 2009 and November 2016 in the county of Uppsala, Sweden.

**Results:** Median ferritin values were found to be highest in August to October (autumn) and lowest in April to May and December. The differences between the highest and lowest median values were 6 µg/L for males and 5 µg/L for females. This corresponds to approximately 12% difference for males and 15% difference for females.

**Conclusion:** A modest but statistically significant seasonal periodicity for ferritin was shown for blood donors.

As estimated by the World Health Organization, more than 110 million blood donations are made globally every year.<sup>1</sup> The blood components collected from these donors constitute an essential part of modern medicine. Due to the blood loss, however, blood donation is associated with a loss of iron, and maintaining an adequate iron homeostasis in the donor group is an important task.<sup>2,3</sup> In Danish high-frequency blood donors, iron deficiency defined as a ferritin

value <15 µg/L was found in 39% of premenopausal women, 22% of postmenopausal women, and 9% of men.<sup>4</sup> The majority of blood banks measure hemoglobin to screen for iron deficiency. However, the reduction in hemoglobin occurs rather late and a high proportion of blood donors may be iron-deficient despite acceptable hemoglobin values.<sup>5,6</sup> Moreover, even without anemia, iron deficiency is associated with a number of clinical adverse effects.<sup>2</sup> It is important to have additional methods to detect iron deficiencies before the reduction in hemoglobin values.

Ferritin is considered a good marker of iron stores in blood donors, and many blood banks use ferritin to monitor their blood donors.<sup>2,7</sup> In the absence of some concurrent diseases, ferritin is a sensitive marker of iron deficiency, which starts to decline long before changes in hemoglobin, erythrocyte size, or serum iron concentration may be observed.<sup>8</sup> Whereas a ferritin value <15 µg/L indicates iron deficiency, a value >100 µg/L generally indicates sufficient iron stores. Levels between 15 µg/L and 100 µg/L should be interpreted cautiously with respect to iron deficiency, as ferritin is an acute phase reactant and infections or inflammation may increase ferritin concentrations. Elevated levels, not always correlated with iron stores, may also be found in other disorders, some of which include certain leukemias and lymphomas, chronic alcohol consumption, obesity, nonalcoholic fatty liver disease, and the metabolic syndrome.<sup>8</sup>

In contrast to serum iron and transferrin saturation, ferritin has a nonsignificant diurnal rhythm.<sup>9</sup> A day-to-day variation of 5.9% or 14% (as observed in recent and older studies, respectively) may reflect fluctuations in ferritin synthesis or leakage from intracellular stores occurring in starvation, exercise, or inflammation.<sup>8</sup> Maes et al<sup>10</sup> reported a biannual variation for ferritin with a 29.3% difference in mean ferritin values between peak and trough months. The lowest ferritin values were observed during May and November. Another study using 2 riverine populations from the Brazilian Amazon showed higher mean ferritin values during the dry season.<sup>11</sup> With respect to a possible seasonal variation of ferritin, however, there are, to our knowledge, no large, published studies on blood donors.

Seasonal variations have been described for several factors that could potentially influence ferritin levels. Studies have shown seasonal variations in eating habits<sup>12,13</sup> and physical activity,<sup>14</sup> both in children and adults. Although differing between countries, the celebration of holidays often involves an increased intake of favorite foods.<sup>15</sup> There are also variations in infections and inflammation over the year.<sup>16,17</sup> Moreover, such factors have been associated with cardiovascular

disease, for which a seasonal variation has also been described.<sup>17,18</sup> In view of these notions, the aim of the present study was to investigate whether there is a seasonal variation for ferritin in blood donors.

## Materials and Methods

### Samples

The study was based on the routine plasma ferritin requests for blood donors in the county of Uppsala, Sweden. Test results together with age and sex were retrieved from the laboratory information system from November 2009 to November 2016. The study period was selected to cover several years to minimize the potential effects of a reagent batch having a different calibration. Also, we wanted to avoid potential effects of the COVID-19 pandemic and effects of instrument changes that could influence the assay results. In total, 99,994 ferritin results were included in the study. All donors were tested during this period. Only age (in years) and sex of the blood donor, date of sampling, and ferritin results were extracted for the statistical analysis. The study was performed in compliance with the Declaration of Helsinki and approved by the local ethical board at Uppsala University.

### Plasma Ferritin Assay

Blood was collected in Li-heparin tubes and plasma ferritin was analyzed the same day as the sampling at the Department of Clinical Chemistry, Uppsala University Hospital using an Architect c8200 instrument (Abbott Laboratories) with reagents (7K59-30) from the same manufacturer. The instrument had a total coefficient of variation of 4.3% at 28 µg/L and 3.0% at 164 µg/L.

### Statistical Analysis

Statistical analysis was performed using Statistica (StatSoft). Shapiro-Wilk test showed that the ferritin values were not normal distributed. Mann-Whitney *U* test was used to test for sex differences for the whole year. Kruskal-Wallis median test was used for nonparametric testing of ferritin values for individual months in relation to the whole year. Spearman rank correlations were used for testing correlations between ferritin and age.

## Results

### Ferritin Values in the Blood Donor Population

A total of 99,994 ferritin results were included in the study. Of these results, 46,426 were from male and 53,568 were from female blood donors. The median ages of females and males were 41 years (interquartile range, 26–52) and 45 years (30–56), respectively. The median ferritin value was 34 µg/L (22–50) for the female blood donors and 51 µg/L (35–83) for the male blood donors. Ferritin values less than 15 µg/L were found in 480 (1.0%) males and 5103 (9.5%) females, and 8476 (18.3%) male donors and 2288 (4.3%) female donors had ferritin values over 100 µg/L. There were weak but significant Spearman rank correlations between ferritin and age for the whole population ( $R = 0.12$ ;  $P < .0001$ ), for females ( $R = 0.23$ ;  $P < .0001$ ), and for males ( $R = -0.10$ ;  $P < .0001$ ).

### Seasonal Variation

There were significant seasonal variations for both male (Kruskal-Wallis  $P < .0001$ ) and female (Kruskal-Wallis  $P < .0001$ ) blood donors. The

**FIGURE 1.** Median (middle line) and interquartile ranges (top and bottom lines) for ferritin values for males and females in µg/L for individual months between November 2009 and November 2016 in the county of Uppsala, Sweden ( $P < .0001$ ).

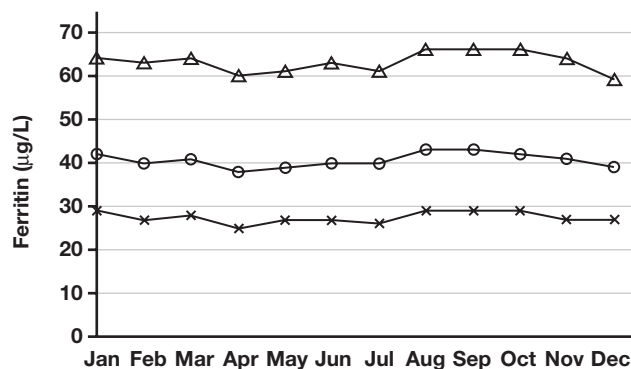
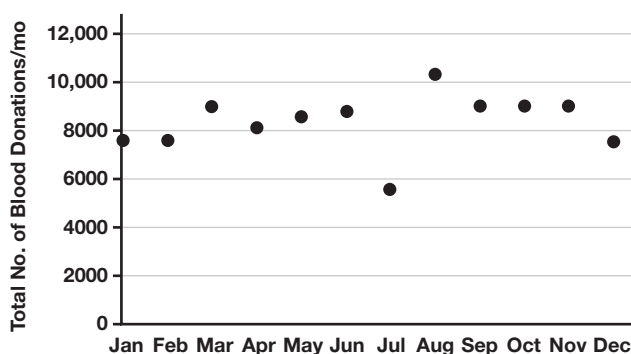


**FIGURE 2.** Number of blood donations divided per month of the year.



patterns were similar for males and females with the highest median values in August to October (autumn) and the lowest values in April to May (spring) and December (FIGURE 1). The differences between the highest and lowest median values were 6 µg/L for male and 5 µg/L for female blood donors. This corresponds to approximately 12% difference for males and 15% difference for females. The number of blood donations was lowest in July, but relatively stable over the rest of the year (FIGURE 2).

## Discussion

Ferritin is essential for iron homeostasis and is mainly used as a marker of total iron stores in humans. Iron staining of bone marrow biopsies is the gold standard for iron deficiency, but a low serum ferritin is also highly specific for iron depletion.<sup>19</sup> Ferritin is therefore a widely used biomarker for evaluation of iron status both in blood donors and in patients with suspected anemia. In the present study, approximately 1% of the male blood donors and 9.5% of the female blood donors had ferritin values <15 µg/L, indicating iron deficiency. This is lower than the prevalence of iron deficiency previously reported for Danish high-frequency blood donors.<sup>4</sup> In line with that study, however, there is a clear difference between the percentage of males and females with iron deficiency in our material. Whereas a negative correlation was found between ferritin and age in men, a significant positive correlation was observed in females. Both these correlations were weak with low

Spearman rank values. The finding is also in agreement with a lower percentage of iron deficiency reported in postmenopausal Danish women.<sup>4</sup> Presumably, the positive correlation between ferritin and age in females, at least for the most part, reflects the menopause effect on iron loss.

In contrast to iron and iron saturation, ferritin does not show any significant diurnal variation.<sup>9</sup> A seasonal variation can, however, be observed among blood donors in the present study, with the lowest median levels in April to May and December and the highest in August to October. We chose to study the seasonal variation of ferritin in blood donors rather than patients. Patient values may be influenced by a reduced availability of health care in connection with Christmas and summer holidays, implying a selection of more severely ill patients during those time periods. A lower number of donations during vacations means a longer recovery period to build up the iron stores. An effect could thus be higher ferritin values for the donor's first blood donation after the vacation. In the present study, the number of blood donations was lowest in July but relatively stable over the rest of the year (**FIGURE 2**). In Sweden, July is the main holiday month, and the hospitals reduce the number of beds. This means that blood donors may be away on vacation, reducing the number of donations, at the same time as the hospital demand is decreased. Both these changes will lead to a reduced number of blood donations. We did not observe a clear pattern between vacations and ferritin values.

The current observation of a seasonal variation for ferritin agrees with previous findings in a study on 26 healthy subjects<sup>10</sup> and is in line with the lower red blood cell counts, mean corpuscular volume, and hemoglobin values during winter to spring reported in a US population.<sup>20</sup> Maes et al<sup>10</sup> reported the lowest ferritin values in May and November, whereas our trough values occurred in April to May and December. We found a monthly peak to trough variation of 12% for males and 15% for females, which is clearly lower than the 29.3% reported by Maes et al<sup>10</sup> A seasonal variation with higher incidence during winter has also been described for both inflammation and cardiovascular disease.<sup>17,18</sup> A study on high-sensitivity C-reactive protein in healthy adults showed the highest levels in November and the lowest in May.<sup>16</sup> Cardiovascular disease, including coronary artery disease, is closely associated with inflammation, which is known to increase ferritin values.<sup>8</sup> Indeed, epidemiological studies have shown an association between increased ferritin levels and increased risk of coronary artery disease.<sup>21</sup> An increase of ferritin may also be found in lifestyle-associated conditions such as chronic alcohol consumption, nonalcoholic fatty liver disease, obesity, and the metabolic syndrome,<sup>8</sup> of which at least the latter has been shown to exhibit a seasonal variation with higher prevalence in winter.<sup>22</sup> A marked seasonal rhythm with increased intake of food during the fall<sup>12</sup> and less physical activity in winter than in summer<sup>14</sup> has also been described.

## Conclusion

Ferritin shows a clear seasonal variation in this cohort of blood donors, with the lowest median levels in April to May and December. Further studies are warranted to evaluate whether these changes also influence the number of deferrals for iron deficiency.

## Funding

The Uppsala University Hospital Research Fund, Sweden, supported this study.

## REFERENCES

1. World Health Organization. Global status report on blood safety and availability. 2016. <https://apps.who.int/iris/bitstream/handle/10665/254987/9789241565431-eng.pdf>. Accessed March 14, 2022.
2. Kiss JE, Vassallo RR. How do we manage iron deficiency after blood donation? *Br J Hematol*. 2018;181(5):590–603.
3. Mast AE. Low hemoglobin deferral in blood donors. *Transfus Med Rev*. 2014;28(1):18–22. doi:10.1016/j.tmr.2013.11.001.
4. Rigas AS, Sørensen CJ, Pedersen OB, et al Predictors of iron levels in 14,737 Danish blood donors: results from the Danish Blood Donor Study. *Transfusion*. 2014;54(3 Pt 2):789–796. doi:10.1111/trf.12518.
5. Baart AM, van Noord PAH, Vergouwe Y, et al. High prevalence of subclinical iron deficiency in whole blood donors not deferred for low hemoglobin. *Transfusion*. 2013;53(8):1670–1677. doi:10.1111/j.1537-2995.2012.03956.x.
6. Skikne B, Lynch S, Borek D, Cook J. Iron and blood donation. *Clin Haematol*. 1984;13(1):271–287.
7. O'Meara A, Infanti L, Stebler C, et al. The value of routine ferritin measurement in blood donors. *Transfusion*. 2011;51(10):2183–2188. doi:10.1111/j.1537-2995.2011.03148.x.
8. Nader R, Horvath AR, Wittwer CT. *Tietz Textbook of Clinical Chemistry and Molecular Diagnostics*. 6th ed. St Louis, MO: Elsevier; 2018.
9. Ridefelt P, Larsson A, Rehman J, Axelsson J. Influences of sleep and the circadian rhythm on iron-status indices. *Clin Biochem*. 2010;43(16–17):1323–1328. doi:10.1016/j.clinbiochem.2010.08.023.
10. Maes M, Bosmans E, Scharpé S, et al. Components of biological variation in serum soluble transferrin receptor: relationships to serum iron, transferrin and ferritin concentrations, and immune and haematological variables. *Scand J Clin Lab Invest*. 1997;57(1):31–41.
11. Rodrigues PCO, Ignotti E, Hacon SS. Association between weather seasonality and blood parameters in riverine populations of the Brazilian Amazon. *J Ped*. 2017;93(5):482–489.
12. de Castro JM. Seasonal rhythms of human nutrient intake and meal pattern. *Physiol Behav*. 1991;50(1):243–248. doi:10.1016/0031-9384(91)90527-u.
13. Kanikowska D, Sato M, Witowski J. Contribution of daily and seasonal biorhythms to obesity in humans. *Int J Biometeorol*. 2015;59(4):377–384. doi:10.1007/s00484-014-0871-z.
14. Kornide ML, Gillman MW, Rossner B, et al. US adolescents at risk for not meeting physical activity recommendations by season. *Pediatr Res*. 2018;84(1):50–56.
15. Helander EE, Wansink B, Chieh A. Weight gain over the holidays in three countries. *N Engl J Med*. 2016;375(12):1200–1202.
16. Chiriboga DE, Ma Y, Li W, et al. Seasonal and sex variation of high-sensitivity C-reactive protein in healthy adults: a longitudinal study. *Clin Chem*. 2009;55(2):313–321.
17. Wyse CA, Celis Morales CA, Ward J, et al. Population-level seasonality in cardiovascular mortality, blood pressure, BMI and inflammatory cells in UK biobank. *Ann Med*. 2018;50(5):410–419.
18. Marti-Soler H, Gubelmann C, Aeschbacher S, et al. Seasonality of cardiovascular risk factors: an analysis including over 230 000 participants in 15 countries. *Heart* 2014;100(19):1517–1523.
19. Knovich MA, Storey JA, Coffman LG, et al. Ferritin for the clinician. *Blood Rev*. 2009;23(3):95–104.
20. Liu B, Taioli E. Seasonal variations of complete blood count and inflammatory biomarkers in the US population—analysis of NHANES data. *PLoS One*. 2015;10(11):e0142382.
21. Salonen JT, Nyssönen K, Korpela H, et al. High stored iron levels are associated with excess risk of myocardial infarction in eastern Finnish men. *Circulation*. 1992;86(3):803–811.
22. Kamezaki F, Sonoda S, Nakata S, et al. Association of seasonal variation in the prevalence of metabolic syndrome with insulin resistance. *Hypertens Res*. 2013;36(5):398–402.

# EUS-FNA Diagnosis of a Metastatic Adult Granulosa Cell Tumor in the Stomach

Ilias P. Nikas, MD,<sup>1,\*</sup> Athanasia Sepsa, MD, PhD,<sup>2</sup> Evangelia Kleidaradaki, MD, MSc,<sup>3</sup> Charitini Salla, MD, PhD<sup>4</sup>

<sup>1</sup>School of Medicine, European University Cyprus, Nicosia, Cyprus, <sup>2</sup>Department of Pathology, Metropolitan Hospital, Athens, Greece, <sup>3</sup>Cytopathology Private Practice, Thessaloniki, Greece, <sup>4</sup>Department of Cytopathology, Hygeia and Mitera Hospital, Athens, Greece

\*To whom correspondence should be addressed. [i.nikas@euc.ac.cy](mailto:i.nikas@euc.ac.cy)

**Keywords:** cytopathology, ovarian cancer, immunohistochemistry, metastasis, cytology, neoplasm

**Abbreviations:** AGCT, adult granulosa cell tumors; EUS-FNA, endoscopic ultrasound-guided fine-needle aspiration; NET, neuroendocrine tumors; GIST, gastrointestinal stromal tumors.

*Laboratory Medicine* 2022;53:533–536; <https://doi.org/10.1093/labmed/lmac024>

## ABSTRACT

Granulosa cell tumors are uncommon ovarian neoplasms, predominantly of the adult type (AGCT). In this report, we present a rare case of a patient with metastatic AGCT to the stomach diagnosed with endoscopic ultrasound-guided fine-needle aspiration (EUS-FNA). A 61-year-old woman without a history of AGCT underwent both a vaginal and an abdominal ultrasound that showed a solid and cystic ovarian mass along with a solid mass in the gastric antral wall. Subsequently, an EUS-FNA was performed to assess the gastric lesion. Cytologic findings showed high cellularity, and the groups of neoplastic cells invaded the muscle layer of the stomach. Notably, these cells formed Call-Exner bodies, whereas some nuclei exhibited nuclear grooves. Immunohistochemistry was performed, revealing positivity for  $\alpha$ -inhibin, calretinin, and CD56 in the neoplastic cells, whereas chromogranin, synaptophysin, CD117, and DOG1 were negative. The combination of clinical presentation, radiology, cytomorphology, and immunohistochemistry could facilitate the diagnosis of metastatic AGCT and the management of such patients.

Granulosa cell tumors are uncommon ovarian neoplasms, comprising approximately 2% to 5% of all ovarian cancers. They belong to the family of sex cord stromal tumors and are predominantly adult granulosa cell

tumors (AGCT; 95%), rather than the juvenile type (5%). Studies have shown that AGCT present clinically with symptoms and signs caused by the presence of an adnexal mass, including abdominal pain or swelling.<sup>1–3</sup> Because AGCT are hormonally active, they secrete high levels of estrogen, often resulting in abnormal vaginal bleeding, and they pose a higher risk of patients developing endometrial hyperplasia and cancer.<sup>3,4</sup> They are considered low-grade and indolent ovarian malignancies that grow slowly, and staging is their most important prognostic factor. Most patients are diagnosed at stage I, exhibiting a favorable prognosis.<sup>1–3</sup> Of interest, 5- and 10-year survival rates of patients with AGCT have been reported to be 98% and 84%, respectively. Therefore, these patients exhibit a much better prognosis than patients with other more common ovarian cancers, such as serous ovarian carcinomas.<sup>5</sup> However, patients with AGCT require a long-term follow-up because this neoplasm may behave unpredictably and exhibit aggressive behavior in the long term. Notably, AGCT can recur or metastasize even many years after their initial detection; this may happen in patients initially diagnosed at stage I as well. Metastases of AGCT are mostly confined to the area of the pelvis and abdominal cavity (eg, peritoneum or omentum), yet more distant sites have also been reported, such as the liver, lung, and bones.<sup>1,2,6</sup>

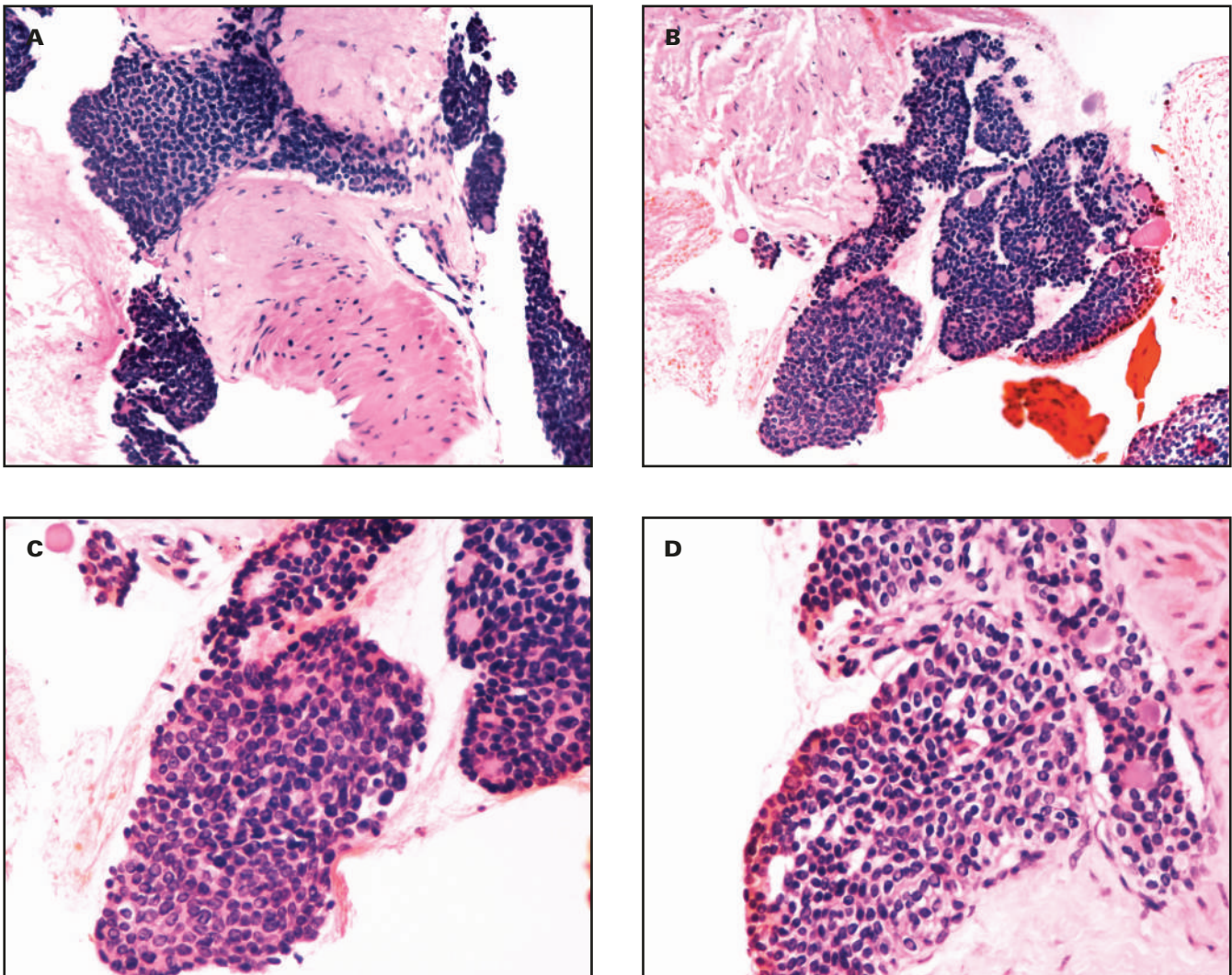
Fine-needle aspiration (FNA) is a modality that has been successfully utilized in the diagnosis of metastatic AGCT.<sup>2,7–11</sup> In this report, we present a case of a patient with metastatic AGCT to the stomach diagnosed with endoscopic ultrasound-guided (EUS) FNA. This is the first cytomorphologic description in the literature of a metastasis to this site diagnosed with this procedure.

## Case Description

A 61-year-old woman without a history of AGCT underwent both a vaginal and an abdominal ultrasound, which showed a solid and cystic ovarian mass and a solid mass in the gastric antral wall, respectively. Subsequently, an EUS-FNA was performed to assess the gastric lesion.

The material received was solely used to prepare a cell block. Subsequent H&E-stained slides showed high cellularity. The neoplastic cells were mostly arranged in syncytial groups invading the muscle layer of the stomach and also exhibited a tendency to form rosette-like structures (**FIGURE 1**). Neoplastic nuclei showed a monotonous appearance with ovoid shape and minimal atypia, and some of them exhibited nuclear grooves. Cytoplasm was of moderate amount, and the cell borders were ill-defined. No necrosis was found. The combination of clinical history (presence of a solid and cystic ovarian mass)

**FIGURE 1.** The H&E cell block cytomorphology of a metastatic adult granulosa cell tumor in the stomach wall. The neoplastic cells were mostly arranged in syncytial groups invading the muscle layer of the stomach and also exhibited a tendency to form Call-Exner bodies. A few of the neoplastic cells exhibited nuclear grooves (A and B,  $\times 200$ ; C and D,  $\times 400$ ).



and cytomorphology raised the possibility of an AGCT metastasis to the stomach. In this situation, the rosette-like structures would represent Call-Exner bodies. In the latter, the neoplastic granulosa cells are arranged around small lumens containing eosinophilic material, as we saw in our patient (FIGURE 1).

Immunohistochemistry was performed on the cell-block material. The neoplastic cells were positive for  $\alpha$ -inhibin, calretinin, and CD56 (FIGURE 2). In contrast, they were negative for chromogranin, synaptophysin, CD117, and DOG1.

Therefore, by combining the radiologic, cytomorphologic, and immunohistochemical findings, we developed a diagnosis of a metastatic AGCT to the stomach.

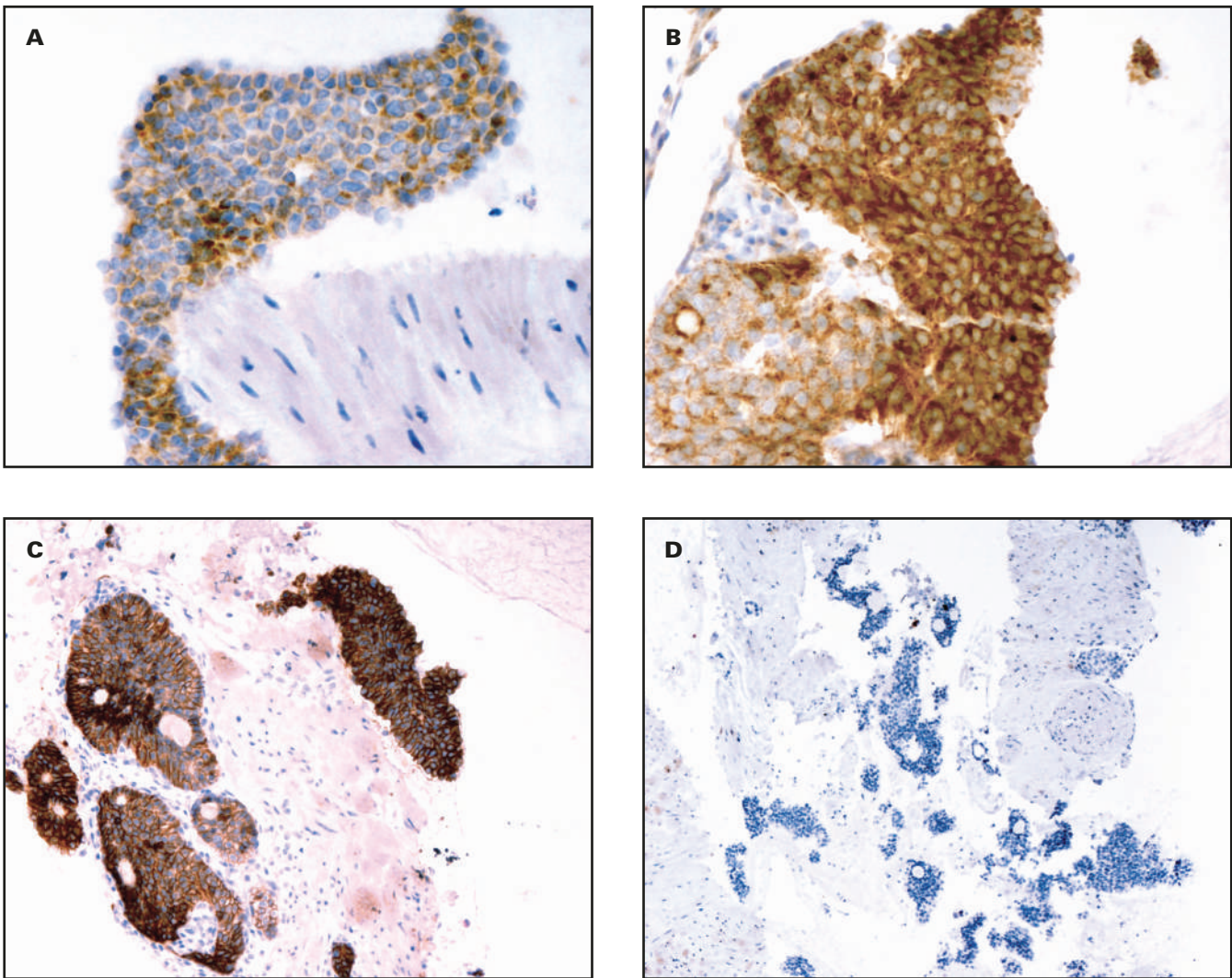
## Discussion

Research has shown that AGCT are low-grade ovarian malignancies derived from the granulosa cells of the ovarian follicles. Although most exhibit an indolent behavior, long-term follow-up is required

because a few can recur or metastasize even many years after the initial diagnosis.<sup>1,2,6</sup> Clinical history may be unavailable to the pathologist; thus, a diagnosis of metastatic AGCT can be difficult to make, especially when the specimen cellularity is inadequate for ancillary studies.<sup>2,8</sup> A few case series and reports describing cytologic diagnoses of metastatic AGCT have been published, where the latter has been found in sites such as the liver, lungs, bone, omentum, bowel, bladder, spleen, kidney, pleural and ascitic fluids, and lymph nodes.<sup>2,7-11</sup> A recent case series has effectively summarized the published literature on metastatic AGCT diagnosed with cytology.<sup>2</sup>

A diagnosis of metastatic AGCT can be suspected when the cytomorphology is classic, including the presence of Call-Exner bodies and nuclei with grooves.<sup>2</sup> Immunohistochemistry can confirm this suspicion because AGCT cells will most likely be positive for  $\alpha$ -inhibin, calretinin, and CD56.<sup>12</sup> Notably, the detection of the *FOXL2* mutation (missense point mutation; 402C→G), by either immunohistochemistry or sequencing, is an accurate diagnostic biomarker and pathognomonic

**FIGURE 2.** A selection of immunohistochemical stains performed on the cell block material of a metastatic adult granulosa cell tumor in the stomach wall (A,  $\alpha$ -inhibin  $\times 400$ ; B, calretinin  $\times 400$ ; C, CD56  $\times 200$ ; D, chromogranin  $\times 100$ ).



for AGCT. Furthermore, *FOXL2* immunohistochemistry is more sensitive than  $\alpha$ -inhibin and calretinin, besides being highly specific to highlight the presence of AGCT.<sup>1,13,14</sup>

For our patient, we formed our differential diagnosis list based on the location of the mass inside the stomach wall and the low-grade cytomorphology of the neoplasm. Low-grade lesions growing in the submucosa/muscularis can include gastric neuroendocrine tumors (NET), gastrointestinal stromal tumors (GIST), leiomyomas, and schwannomas. Studies have shown that NET are composed of cells with “salt and pepper” nuclei, albeit without grooves, that are positive for chromogranin and synaptophysin with immunohistochemistry.<sup>15</sup> Whereas GIST are positive for DOG1 and CD117, leiomyomas and schwannomas exhibit spindle-shaped morphology and immunopositivity for desmin and S100, respectively.<sup>16</sup>

## Conclusion

In conclusion, AGCT are malignant ovarian neoplasms with indolent behavior, yet they have an unpredictable malignant potential that prompts their long-term follow-up. The combination of clinical presentation,

radiology, cytomorphology, and immunohistochemistry can facilitate the diagnosis of metastatic AGCT and the management of such patients.

## REFERENCES

1. Färkkilä A, Haltia U-M, Tapper J, McConechy MK, Huntsman DG, Heikinheimo M. Pathogenesis and treatment of adult-type granulosa cell tumor of the ovary. *Ann Med*. 2017;49(5):435–447.
2. Harbhajanka A, Bitterman P, Reddy VB, Park J-W, Gattuso P. Cytomorphology and clinicopathologic correlation of the recurrent and metastatic adult granulosa cell tumor of the ovary: a retrospective review. *Diagn Cytopathol*. 2016;44(12):1058–1063.
3. Pectasides D, Pectasides E, Psyrris A. Granulosa cell tumor of the ovary. *Cancer Treat Rev*. 2008;34(1):1–12.
4. Bacalbasa N, Stoica C, Popa I, Mirea G, Balescu I. Endometrial carcinoma associated with ovarian granulosa cell tumors—a case report. *Anticancer Res*. 2015;35(10):5547–5550.
5. McConechy MK, Färkkilä A, Horlings HM, et al. Molecularly defined adult granulosa cell tumor of the ovary: the clinical phenotype. *J Natl Cancer Inst*. 2016;108(11):djw134.

6. Ahuja A, Iyer VK, Mathur S, Vijay MK. Fine needle aspiration cytology diagnosis of metastatic adult granulosa cell tumour showing Call-Exner bodies. *Cytopathology*. 2013;24(5):346–347.
7. Omori M, Kondo T, Yuminamochi T, et al. Cytologic features of ovarian granulosa cell tumors in pleural and ascitic fluids. *Diagn Cytopathol*. 2015;43(7):581–584.
8. Ylagan LR, Middleton WD, Dehner LP. Fine-needle aspiration cytology of recurrent granulosa cell tumor: case report with differential diagnosis and immunocytochemistry. *Diagn Cytopathol*. 2002;27(1):38–41.
9. Thirumala SD, Putti TC, Medalie NS, Wasserman PG. Skeletal metastases from a granulosa-cell tumor of the ovary: report of a case diagnosed by fine-needle aspiration cytology. *Diagn Cytopathol*. 1998;19(5):375–377.
10. Liu K, Layfield LJ, Coogan AC. Cytologic features of pulmonary metastasis from a granulosa cell tumor diagnosed by fine-needle aspiration: a case report. *Diagn Cytopathol*. 1997;16(4):341–344.
11. Shimizu K, Yamada T, Ueda Y, Yamaguchi T, Masawa N, Hasegawa T. Cytologic features of ovarian granulosa cell tumor metastatic to the lung. A case report. *Acta Cytol*. 1999;43(6):1137–1141.
12. Deavers MT, Malpica A, Liu J, Broaddus R, Silva EG. Ovarian sex cord-stromal tumors: an immunohistochemical study including a comparison of calretinin and inhibin. *Mod Pathol*. 2003;16(6):584–590.
13. Shah SP, Köbel M, Senz J, et al. Mutation of FOXL2 in granulosa-cell tumors of the ovary. *N Engl J Med*. 2009;360(26):2719–2729.
14. Al-Agha OM, Huwait HF, Chow C, et al. FOXL2 is a sensitive and specific marker for sex cord-stromal tumors of the ovary. *Am J Surg Pathol*. 2011;35(4):484–494.
15. Hirabayashi K, Zamboni G, Nishi T, Tanaka A, Kajiwara H, Nakamura N. Histopathology of gastrointestinal neuroendocrine neoplasms. *Front Oncol*. 2013;3:2.
16. Hirota S. Differential diagnosis of gastrointestinal stromal tumor by histopathology and immunohistochemistry. *Transl Gastroenterol Hepatol*. 2018;3:27.

# Macroprolactinoma-Induced Syndrome of Inappropriate Antidiuresis and Its Reversal with Dopamine Agonist Therapy

Amnon Schlegel, MD, PhD\*

Division of Endocrinology, Metabolism and Diabetes, Department of Internal Medicine, Spencer Fox Eccles School of Medicine, University of Utah, Salt Lake City; \*To whom correspondence should be addressed. amnons@u2m2.utah.edu

**Keywords:** SIAD, SIADH, hyponatremia, prolactinoma, cabergoline

**Abbreviations:** AVP, arginine vasopressin; SIAD, syndrome of inappropriate antidiuresis; ED, emergency department; TSH, thyroid-stimulating hormone; ACTH, adrenocorticotropic hormone; FSH, follicle-stimulating hormone; LH, luteinizing hormone

*Laboratory Medicine* 2022;53:537–539; <https://doi.org/10.1093/labmed/lmac025>

## ABSTRACT

Hyponatremia is an uncommon manifestation of pituitary adenomas. Herein, I report a case of syndrome of inappropriate antidiuresis (SIAD) caused by a macroprolactinoma that rapidly resolved with dopamine agonist therapy. A 29-year-old White woman presented with euvolemic, hypotonic hyponatremia, normal thyroid and glucocorticoid axes, and inappropriately concentrated urine. She was found to have a 1.2-cm sellar mass. Investigation of additional pituitary axes revealed an elevated prolactin level of 193.7 ng/mL. The SIAD experienced by the patient corrected rapidly with initiation of cabergoline. The patient could not tolerate dopamine agonist therapy, and after 1 year, she underwent transsphenoidal resection of the mass after the prolactin began to increase. Pathological examination confirmed the diagnosis of macroprolactinoma. There was no recurrence of the tumor, and the patient continued to have normonatremia and normoprolactinemia 7 years after her operation. To my knowledge, this is the first report in the literature of pathology-confirmed macroprolactinoma marked by SIAD that showed rapid normalization of water metabolism with dopamine agonist therapy.

Euvolemic, hypotonic hyponatremia with concentrated urine, along with normal adrenal and thyroid function and absence of renal disease and nonosmotic stimuli (various drugs, malignant neoplasms, infections, pulmonary diseases, and rare hereditary causes) of arginine vasopres-

sin (AVP) secretion meets the operational definition of syndrome of inappropriate antidiuresis (SIAD).<sup>1,2</sup> Because this disorder has a long differential diagnosis, careful history gathering and frugal laboratory and imaging evaluation are required for optimal therapy.

Herein, I report the case of a woman who presented with symptomatic hyponatremia caused by a macroprolactinoma. Macroadenomas rarely present with SIAD. To my knowledge, this is the first report in the literature of a pathological-examination--confirmed SIAD due to macroprolactinoma that rapidly responded to dopamine agonist therapy.

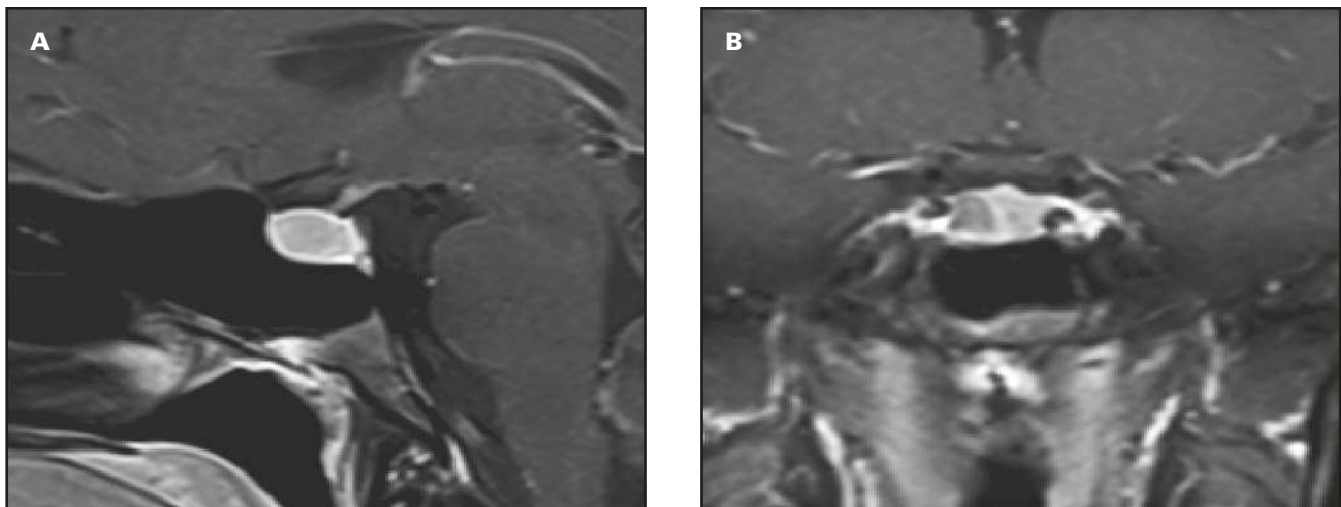
## Case Report

A 29-year-old White woman presented to an emergency department (ED) reporting dizziness, nausea, vomiting, and diarrhea. She had no fever and had normal heart rate, blood pressure, and peripheral oxygen saturation. Her serum sodium was 117 mmol/L (normal, 135–145 mmol/L); potassium, 4.2 mmol/L (normal, 3.6–5.0 mmol/L); chloride, 82 mmol/L (normal, 98–107 mmol/L); bicarbonate, 22 mmol/L (normal, 22–31 mmol/L); blood urea nitrogen, 6 mg/dL (normal, 8–18 mg/dL); creatinine, 0.72 mg/dL (normal, 0.70–1.20 mg/dL); glucose, 91 mg/dL (normal, 60–199 mg/dL); calcium, 8.5 mg/dL (normal, 8.5–10.5 mg/dL); magnesium, 0.70 mmol/L (normal, 0.69–1.07 mmol/L); and serum osmolality, 252 mOsm/kg (normal, 275–295 mOsm/kg). Here level of thyroid-stimulating hormone (TSH) was 4.12 mIU/L (normal, 0.27–4.20 mIU/L) and free thyroxine was 1.02 ng/dL (normal, 0.90–1.60 ng/dL). Her cortisol level was 22.3 µg/dL at 05:59 AM (normal, 6.2–19.4 µg/dL). She received fluid resuscitation, antiemetic therapy, and sodium chloride 1 g thrice daily orally. At 2 years and 6 months before presentation, her serum sodium level had been 138 mmol/L (normal range in a different laboratory, 137–145 mmol/L), and her TSH level was 2.680 mIU/L (normal, 0.47–4.68 mIU/L). Serial sodium values and other pertinent parameters are presented in **TABLE 1**.

Two weeks after starting sodium chloride tablets, her serum sodium measurement was 139 mmol/L. Her serum cortisol increased from 14.5 µg/dL to 29.2 µg/dL 60 minutes after injection of 250 µg of adrenocorticotropic hormone [ACTH] (1–24). ACTH drawn with the basal cortisol (at 08:28) was 16 pg/mL (normal, 6–58 pg/mL). Sodium chloride tablets were discontinued.

**TABLE 1. Select Laboratory Values and Treatments**

Timeline	Laboratory Value					Comment
	Serum Sodium (mmol/L)	Serum Osmolality (mOsm/kg)	Urine Sodium (mmol/L)	Urine Osmolality (mOsm/kg)	Prolactin	
30 mo before presentation	—	—	—	—	—	—
At time of presentation	117 (low)	252 (low)	—	—	—	Start NaCl tablets
2 wk after presentation	139	—	—	—	—	Stop NaCl tablets
5 wk after presentation	123 (low)	271 (low)	245 (inappropriately elevated)	639 (inappropriately concentrated)	193.7 (high)	Start cabergoline 0.25 mg twice/wk
12 h after first dose of cabergoline	133 (low)	—	—	—	—	—
36 h after first dose of cabergoline	135 (low)	283	111 (inappropriately elevated)	465	—	—
5 wk after presentation	138	—	—	—	12.5	—
7 wk after presentation	138	—	—	—	12.5	—
1 y after starting cabergoline	—	—	—	—	23.4	After stopping cabergoline temporarily
2 y after operation	138	—	—	—	9.1	—
7 y after operation	138	—	—	—	7.3	—

**FIGURE 1. Magnetic resonance image (MRI) of the brain of the patient, a 29-year-old White woman. Parasagittal (A) and coronal (B) T1 MRI showing the appropriately hyperintense neurohypophysis displaced inferoposteriorly by a 9 mm (craniocaudally) × 6 mm (transversely) × 12 mm (anteroposteriorly) macroprolactinoma.**

Three weeks later the patient presented to a second ED with the same symptoms that had prompted the first admission. Clinically, she had euolemia. Her serum sodium value was 123 mmol/L (normal, 137–145 mmol/L); serum osmolality was 271 mOsm/kg (normal, 280–303 mOsm/kg). Her spot urine osmolality had inappropriately risen to 639 mOsm/kg (normal range, 50–800 mOsm/kg when serum sodium is normal). Spot urine electrolyte values were as follows: sodium, 245 mmol/L; potassium, 33.7 mmol/L; chloride, 274 mmol/L; and creatinine, 65 mg/dL (all reported without normal ranges; however, a urine sodium value >20 mmol/L along with euolemic, hypotonic hyponatremia is consistent with SIAD, hypothyroidism, or glucocorticoid deficiency). SIAD was diagnosed based on the presence of euolemic, hypotonic hyponatremia, with inappropriately concentrated urine and normal thyroid and glucocorticoid axes. A 1-L daily fluid restriction was implemented.

Because the patient reported sustaining head trauma relating to her occupation, a brain magnetic resonance image (MRI) with and without gadolinium enhancement was obtained. The study revealed an anterior pituitary mass, with the greatest dimension being 11 mm; a dynamic pituitary protocol MRI indicated that the largest dimension of the mass was 12 mm (FIGURE 1). Normal posterior pituitary enhancement was observed in the sagittal T1-weighted images, although the mass posteriorly displaced the neurohypophysis. Visual field testing revealed no deficits. The patient reported having no galactorrhea, vision changes, or headaches, but stated that she had had irregular menses since menarche.

Additional interrogation of the adenohypophyseal function revealed hyperprolactinemia, without concurrent evidence of excess somatotrophic function; and normal gonadotrophic function. Specifically, the serum prolactin level was 193.7 ng/mL (normal, 2.8–26.0 ng/mL);

insulin-like growth factor 1 was 182 ng/mL (normal, 87–368 ng/mL); follicle-stimulating hormone (FSH), 3.2 IU/L (normal ranges: at the follicular phase of the menstrual cycle, 3.5–12.5 IU/L; midcycle, 4.7–215 IU/L; luteal phase, 1.7–7.7 IU/L; postmenopause, 25.8–134.8 IU/L); luteinizing hormone (LH), 1.8 IU/L (follicular phase, 2.4–12.6 IU/L; midcycle, 14.0–95.6 IU/L; luteal phase, 1.0–11.4 IU/L; postmenopause, 7.7–58.5 IU/L); and estradiol, 62 pg/mL (follicular phase: 27–122 pg/mL; midcycle, 95–433 pg/mL; luteal phase, 49–291 pg/mL; postmenopause, <41 pg/mL).

The patient received 0.25 mg of cabergoline. Her serum sodium measurement rose from 121 mmol/L to 133 mmol/L in the 12 hours after the dose and remained >135 mmol/L thereafter (normal, 137–145 mmol/L). Thirty-six hours after the first dose of cabergoline, the serum sodium value rose to 135 mmol/L, and the serum osmolality normalized to 283 mOsm/kg (normal, 280–303 mOsm/kg). Urine sodium improved to (appropriately diluted to) 111 mmol/L, as did the urine osmolality, to 465 mOsm/kg. Fluid restriction was liberalized, and she was discharged from the hospital with instructions to take cabergoline 0.25 mg twice weekly. After the third dose of cabergoline, her sodium value was 138 mmol/L (normal, 136–144 mmol/L), and her prolactin value was 12.5 ng/mL (normal, 2.6–26.0 ng/mL), and both values were unchanged 2 weeks later (TABLE 1).

Although the patient continued to have normonatremia while taking cabergoline, she could not tolerate the nausea, constipation, heavy menses, and anxiety caused by dopamine agonist therapy. After 1 year of cabergoline treatment with durable normonatremia and decrease in the tumor to 5.5 mm in its greatest dimension, the patient temporarily stopped taking cabergoline. As a result, her prolactin level rose to 23.4 ng/mL (normal, 2.6–26.0 ng/mL), and she elected to undergo transsphenoidal resection of the pituitary mass. The pathological specimen stained diffusely positive for prolactin. Postoperatively, she continued to have normonatremia and normoprolactinemia while not taking cabergoline. An MRI performed 6 months after her operation showed no tumor regrowth.

Two years after the operation, the serum sodium value was 138 mmol/L (normal, 136–144 mmol/L), and the prolactin value was 9.1 ng/mL (normal, 4.8–23.3 ng/mL). The TSH was elevated, at 8.350 IU/L (normal, 0.450–4.500 IU/L). The patient began thyroid replacement therapy for primary hypothyroidism. Seven years after her operation, the patient had a serum sodium level of 138 mmol/L (normal, 137–146 mmol/L); her prolactin level was 7.3 ng/mL (normal, 5.2–26.5 ng/mL), and TSH of 1.35 IU/L (normal, 0.45–4.67 IU/L).

## Discussion

Acquired SIAD due to pituitary-limited tumors is exceedingly rare. The largest case series (of which I am aware) of people with hyponatremia having sellar masses (n = 282)<sup>3</sup> revealed that sellar arachnoid cysts are the most likely to present with hyponatremia. However, adenohypophyseal tumors are rarely associated with hyponatremia. Other researchers<sup>4</sup> have theorized that the mechanism of inappropriate antidiuresis in prolactinoma is due to a lowering of the osmotic threshold for arginine vasopressin secretion, as reflected by a case individual with reset osmostat (ie, during hypertonic saline infusion, AVP secretion was triggered at a lower osmolality than normal). A concurrently reported case of SIAD due to macroprolactinoma, curiously, had unmeasurable AVP, as measured by then-available assays during hyponatremia. The patient had

a normal response to hypertonic challenge, with increased production of a peptide that coeluted with an AVP standard in a high-pressure liquid chromatography assay at a normal threshold concentration. The patient received bromocriptine for 13 months until he had achieved normonatremia and normal dilution of urine in response to hypotonic saline challenge.<sup>5</sup>

In contrast, my patient had rapid and sustained reversal of hyponatremia after initiation of the more potent dopamine agonist cabergoline. Further, she subsequently had immunohistochemical confirmation of a prolactin-secreting tumor at surgical resection. Her prolactin level was just below the 200 ng/mL cutoff recommended by the Endocrine Society for making the unequivocal diagnosis of prolactinoma.<sup>6</sup> The fact that the tumor shrank and the prolactin decreased with cabergoline indicates that this cutoff is, perhaps, too stringent.

In another, previously reported macroprolactinoma marked by SIAD,<sup>7</sup> transsphenoidal resection restored normal water metabolism, as with my patient; however, that other patient did not attempt a trial of dopamine agonist therapy. The rapid response to dopamine agonist therapy experienced by my patient suggests that disruption of dopaminergic input, per se, can rapidly restore normal AVPergic neuronal function. In the case of my patient and these other published cases, the patients had chronic hyponatremia and did not require urgent administration of hypertonic saline to reverse neurocognitive decline. Hypertonic saline and vasopressinergic antagonists are life-saving in acute, symptomatic hyponatremia but carry risks of overly rapid correction and attendant brain edema and herniation. Formulas to calculate water excess and rate of correction have become standards of care.<sup>8,9</sup>

To my knowledge, in the medical literature, my patient is the first person with prolactinoma-induced SIAD to achieve rapid restoration of normal water metabolism with dopamine agonist treatment. This resolution of SIAD preceded a decrease in tumor size, suggesting that dopamine or prolactin, but not a mass effect on AVPergic neurons, is what drove the inappropriate antidiuresis. Although rare, macroprolactinoma should be considered as a cause of SIAD.

## REFERENCES

1. Bartter FC, Schwartz WB. The syndrome of inappropriate secretion of antidiuretic hormone. *Am J Med.* 1967;42(5):790–806.
2. Loh JA, Verbalis JG. Disorders of water and salt metabolism associated with pituitary disease. *Endocrinol Metab Clin North Am.* 2008;37(1):213–234, x.
3. Bordo G, Kelly K, McLaughlin N, et al. Sellar masses that present with severe hyponatremia. *AACE Clin Case Rep.* 2014;20(11):1178–1186.
4. Ish-Shalom S, Ben-Haim S, Barzilai D, Hochberg Z. Low-set osmotic threshold for vasopressin release in a patient with prolactinoma. *Horm Res.* 1986;23(2):78–82.
5. Kern PA, Robbins RJ, Bichet D, Berl T, Verbalis JG. Syndrome of inappropriate antidiuresis in the absence of arginine vasopressin. *J Clin Endocrinol Metab.* 1986;62(1):148–152.
6. Melmed S, Casanueva FF, Hoffman AR, et al. Diagnosis and treatment of hyperprolactinemia: an Endocrine Society clinical practice guideline. *J Clin Endocrinol Metab.* 2011;96(2):273–288.
7. Saito T, Watanabe Y, Yuzawa M, et al. SIADH is only an atypical clinical feature in a patient with prolactinoma. *Intern Med.* 2007;46(10):653–656.
8. Adrogue HJ, Madias NE. Hyponatremia. *N Engl J Med.* 2000;342(21):1581–1589.
9. Spasovski G, Vanholder R, Allolio B, et al. Clinical practice guideline on diagnosis and treatment of hyponatremia. *Eur J Endocrinol.* 2014;170(3):G1–G47.

# Transient Pseudothrombocytopenia Detected 8 Months After COVID-19 Vaccination

Takakazu Higuchi, MD,<sup>1,\*</sup> Takao Hoshi, MT,<sup>2</sup> Astuko Nakajima, BS,<sup>2</sup> and Kosuke Haruki, MD<sup>2</sup>

<sup>1</sup>Blood Transfusion Department, Dokkyo Medical University Saitama Medical Center, Koshigaya, Japan, <sup>2</sup>Clinical Laboratory, Dokkyo Medical University Saitama Medical Center, Koshigaya, Japan; \*To whom correspondence should be addressed. [thiguchi@dokkyomed.ac.jp](mailto:thiguchi@dokkyomed.ac.jp)

*Laboratory Medicine* 2022;53:540–541; <https://doi.org/10.1093/labmed/lmac031>

## ABSTRACT

Pseudothrombocytopenia is an *in vitro* phenomenon of platelet aggregation due to conformational changes and exposure of cryptic antigens on the platelet surface caused by anticoagulants, leading to the aggregation of platelets and falsely lower automated platelet counts. Although it has no clinical relevance, it can lead to unnecessary fear, diagnostic errors, or unnecessary tests and interventions when unrecognized.

Pseudothrombocytopenia was detected in a 25-year-old woman 8 months after the second dose of mRNA COVID-19 vaccine, BNT162b2. The pseudothrombocytopenia was transient and the duration was shorter than 3 months. As pseudothrombocytopenia is not detected unless blood is drawn for other objectives, it is difficult to determine its true occurrence among recipients of vaccines. This case shows that pseudothrombocytopenia may develop transiently even months after COVID-19 vaccination and should be considered when thrombocytopenia is found in recipients of the vaccine to avoid unnecessary fear, diagnostic errors, or unnecessary tests and interventions.

## Case Report

The case is a 25-year-old woman taking rosuvastatin for familial hypercholesterolemia and having regular blood tests every 2 months. She received two doses of mRNA COVID-19 vaccine, BNT162b2, with a 3-week interval in March 2021. The platelet counts of the EDTA-2K-anticoagulated blood samples examined in May, July, and September did not show the aggregation of platelets and the platelet counts were  $348 \times 10^9/L$ ,  $281 \times 10^9/L$ , and  $302 \times 10^9/L$ , respectively (TABLE 1). The EDTA-2K anticoagulated blood drawn on the occasion of an annual health check in November, 8 months after the second vaccine dose, showed platelet aggregation, and blood was drawn again in an EDTA-2K anticoagulated tube and an FC Mix tube that contained sodium fluoride,

EDTA-2Na, and sodium citrate for anticoagulation. The platelet count in the EDTA-2K anticoagulant tube was  $63 \times 10^9/L$  and that in the other tube was  $90 \times 10^9/L$ . On microscopic peripheral blood examination, platelet aggregation was observed (FIGURE 1). The platelet count in the EDTA-2K anticoagulated tube was manually determined by counting the platelets in the sample diluted 100-fold in 1% ammonium oxalate solution with fluorescence microscopy and was  $179 \times 10^9/L$ . She did not have any signs or symptoms of bleeding and was diagnosed with pseudothrombocytopenia. The platelet count in the EDTA-2K anticoagulated sample drawn 3 weeks later had returned to her normal value of  $306 \times 10^9/L$ .

## Discussion

Hematological changes are frequently complicated with COVID-19 and thrombocytopenia is detected in 5% to 41.7% of patients.<sup>1,2</sup> Platelet count is lower in more severe diseases, and complex mechanisms are considered to contribute to the development of thrombocytopenia.<sup>1</sup> In addition to true thrombocytopenia, cases of pseudothrombocytopenia related to COVID-19 have been reported.<sup>3–7</sup> Pseudothrombocytopenia is an *in vitro* phenomenon of platelet aggregation due to the conformational changes and exposure of cryptic antigens on the platelet surface caused by anticoagulants, usually EDTA, leading to the aggregation of the platelets through the immune reaction between the exposed cryptic antigens and autoantibodies and falsely lower automated platelet counts.<sup>8</sup> Although pseudothrombocytopenia is observed in 0.03% to 0.27% of the general population, it is associated with some specific conditions such as autoimmune diseases, infections, pregnancy, and medications. Although it has no clinical relevance, it can lead to unnecessary fear, diagnostic errors or unnecessary tests and interventions, including platelet transfusion, when unrecognized.

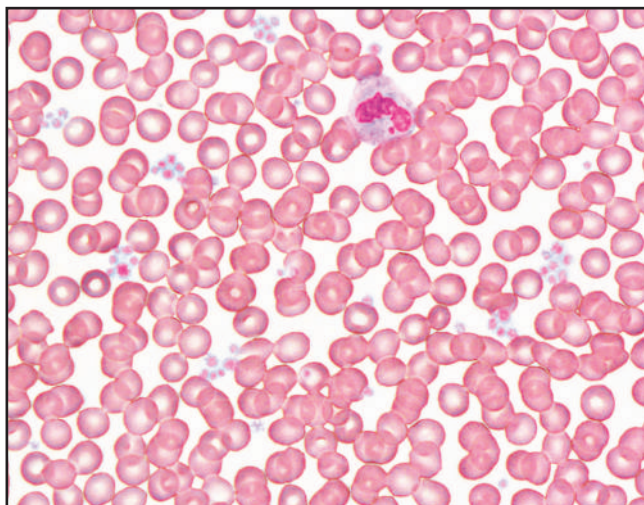
The efficacy of COVID-19 mRNA vaccines has been confirmed with acceptable safety profiles, and millions of people have been vaccinated worldwide. It is reported that they may cause a transient exacerbation of thrombocytopenia in patients with chronic immune thrombocytopenia;<sup>9</sup> however, they do not appear to be associated with newly developed immune thrombocytopenia, and the overall incidence of thrombocytopenia does not appear to increase after the vaccination.<sup>10</sup>

We reported a case of pseudothrombocytopenia associated with BNT162b2 COVID-19 mRNA vaccine observed 8 months after the second dose. A case of transient pseudothrombocytopenia in a recipient of Ad26.COVS.2 adenovirus vector vaccine has been reported.<sup>11</sup>

**TABLE 1. Blood Cell Counts of EDTA-2K Anticoagulated Samples**

Variables	May	July	Sept	Nov	Dec
White blood cells ( $\times 10^9/L$ )	7.1	4.7	5.0	5.0	5.1
Hemoglobin (g/dL)	11.7	11.1	11.5	12.0	11.7
Platelets ( $\times 10^9/L$ )	348	281	302	63	306

**FIGURE 1. Peripheral blood smear of the EDTA-2K anticoagulated sample. Relatively small and loose platelet aggregates were observed in November 2021 (May-Grünwald-Giemsa,  $\times 400$ ).**



The patient was taking methotrexate for psoriatic arthritis, and pseudothrombocytopenia was diagnosed 5 days after the vaccine. However, the incidence of pseudothrombocytopenia after COVID-19 vaccination is unknown and it appears difficult to be determined because, as pseudothrombocytopenia is not associated with bleeding tendency, it is not detected unless blood is drawn for objectives other than the evaluation of bleeding tendency. Thus, many cases of pseudothrombocytopenia could have been overlooked.

In a large nationwide study of BNT162b2 vaccine in Israel, the incidence of thrombocytopenia was 56 in 884,828 recipients and not different from that of controls during 21 days of follow-up.<sup>12,13</sup> However, the incidence of thrombocytopenia after this period is not known and that of pseudothrombocytopenia is all the more difficult to elucidate. In addition, as our patient developed transient pseudothrombocytopenia 8 months after vaccination, many cases of transient and/or late-onset pseudothrombocytopenia after the COVID-19 vaccination may have been unrecognized, and more cases of pseudothrombocytopenia could have been found with more frequent and prolonged follow-ups. Although anti-COVID-19 antibody levels were not measured in the present case, an observation that pseudothrombocytopenia persisted with positive IgG/IgM anti-COVID-19 antibodies 9 months after COVID-19 infection suggests that persistent high-titer anti-COVID-19 antibodies

induced by vaccination might be associated with the late-onset pseudothrombocytopenia in the present case.<sup>6</sup> However, this assumption needs to be verified in the similar cases. Pseudothrombocytopenia sometimes shows alternative periods without in vitro aggregation, and the duration of pseudothrombocytopenia in the present case was shorter than 3 months.<sup>8</sup> Thus, COVID-19 vaccination may lead to persisting, recurrent, or late-onset pseudothrombocytopenia.

Although it appears difficult to determine its true occurrence, the present case shows that pseudothrombocytopenia may develop transiently even months after COVID-19 vaccination and should be considered and properly evaluated when thrombocytopenia is found incidentally in recipients of the COVID-19 vaccine to avoid unnecessary fear and interventions.

## REFERENCES

1. Zhang Y, Zeng X, Jiao Y, et al. Mechanisms involved in the development of thrombocytopenia in patients with COVID-19. *Thromb Res.* 2020;193:110–115.
2. Lippi G, Plebani M, Henry BM. Thrombocytopenia is associated with severe coronavirus disease 2019 (COVID-19) infections: a meta-analysis. *Clin Chim Acta.* 2020;506:145–148.
3. Kuhlman P, Nasim J, Goodman M. Pan-pseudothrombocytopenia in COVID-19: a harbinger for lethal arterial thrombosis? *Fed Pract.* 2020;37:354–358.
4. Van Dijk R, Lauw MN, Swinkels M, Russcher H, Jansen AJG. COVID-19-associated pseudothrombocytopenia. *EJHaem.* 2021;2:475–477.
5. Li H, Wang B, Ning L, Luo Y, Xiang S. Transient appearance of EDTA dependent pseudothrombocytopenia in a patient with 2019 novel coronavirus pneumonia. *Platelets.* 2020;31:825–826.
6. Berezcki D, Nagy B, Kerényi A, et al. EDTA-induced pseudothrombocytopenia up to 9 months after initial COVID-19 infection associated with persistent anti-SARS-CoV-2 IgM/IgG seropositivity. *Lab Med.* 2021; Aug 20 [online ahead of print].
7. Can F, Gökçe D, Güney T, Akıncı S, Dilek İ. Massive platelet clumping on peripheral blood smear and pseudothrombocytopenia in a patient with COVID-19. *Balkan Med J.* 2021;38:194.
8. Lardinois B, Favresse J, Chatelain B, Lippi G, Mullier F. Pseudothrombocytopenia: a review on causes, occurrence and clinical implications. *J Clin Med.* 2021;10:594.
9. Kuter DJ. Exacerbation of immune thrombocytopenia following COVID-19 vaccination. *Br J Haematol.* 2021;195:365–370.
10. Welsh KJ, Baumbatt J, Chege W, Goud R, Nair N. Thrombocytopenia including immune thrombocytopenia after receipt of mRNA COVID-19 vaccines reported to the Vaccine Adverse Event Reporting System (VAERS). *Vaccine.* 2021;39:3329–3332.
11. Kemper M, Berssenbrügge C, Lenz G, Mesters RM. Vaccine-induced pseudothrombocytopenia after Ad26.COV2.S vaccination. *Ann Hematol.* 2021; Aug 10:1–2 [online ahead of print].
12. Barda N, Dagan N, Ben-Shlomo Y, Kepten E, Waxman J, Ohana R et al. Safety of the BNT162b2 mRNA Covid-19 vaccine in a nationwide setting. *N Engl J Med.* 2021;385:1078–1090.
13. Dagan N, Barda N, Balicer RD. Adverse effects after BNT162b2 vaccine and SARS-CoV-2 infection, according to age and sex. *N Engl J Med.* 2021;385:2299.

# Correction to: Quality Assessment and Clinical Utility of Plasma Obtained Via Apheresis vs That Obtained from Whole Blood

*Laboratory Medicine* 2022;53:542; <https://doi.org/10.1093/labmed/lmac091>

---

This is a correction to: Eiman Hussein, MD, PhD, Azza Aboul Enein, MD, Quality Assessment and Clinical Utility of Plasma Obtained Via

Apheresis vs That Obtained from Whole Blood, *Laboratory Medicine*, 2022, lmac029, <https://doi.org/10.1093/labmed/lmac029>.

In the originally published manuscript, there was an error in the opening section. The “Association for the Advancement of Book and Biotherapies (AABB)” should read “Association for the Advancement of Blood and Biotherapies (AABB).” This error has been corrected online.

# A Balanced Robertsonian Translocation in a Patient with a Janus Kinase 2–Positive Polycythemia Vera

Bernhard Strasser, MD,<sup>1,\*</sup> Christian Paar, PhD,<sup>1</sup> David Kiesl, MD,<sup>2</sup> Josef Tomasits, MD<sup>1</sup>

<sup>1</sup>Institute of Laboratory Medicine, Kepler-University-Hospital Linz, Linz, Austria; <sup>2</sup>Department of Hematology, Kepler-University-Hospital Linz, Linz, Austria\*To whom correspondence should be addressed. [bernhard.strasser@kepleruniklinikum.at](mailto:bernhard.strasser@kepleruniklinikum.at)

**Keywords:** Robertsonian translocation, JAK2, polycythemia vera, ddPCR, karyotype, myeloproliferative disorder

**Abbreviations:** BCR/ABL, breakpoint cluster region protein-Abelson murine leukemia viral oncogene homolog 1; JAK2, Janus kinase 2; ddPCR, digital droplet polymerase chain reaction.

*Laboratory Medicine* 2022;53:e101–e104; <https://doi.org/10.1093/labmed/lmab111>

## ABSTRACT

A male patient with a persistent, combined erythrocytosis, leukocytosis, and thrombocytosis without representative evidence of reactive increase emerged as having a myeloproliferative disorder. Molecular-biological assessment yielded Janus kinase 2–positive results, and the patient was diagnosed with polycythemia vera. In addition to these findings, further karyotyping accounted for a Robertsonian translocation. Because this rearrangement was a balanced variant, we concluded that this cytogenetic result might not significantly alter the diagnosis of polycythemia vera.

## Clinical History

We report a male patient aged 58 years referred to our hospital because of anamnestic reported erythrocytosis, leukocytosis, and thrombocytosis for more than half a year. Upon admission and subsequent blood analysis, the patient had leukocytes 10.6 G/L (3.9–8.8), thrombocytes 618 G/L (150–400), and polyglobulia with erythrocytes 6.4 T/L (4.2–5.5), hemoglobin 15.7 g/dL (14–17) and hematocrit 49.4% (36.2%–46.3%). In addition, a low count of erythropoietin was assessed. Because the patient's cardiorespiratory status could not sufficiently explain the polyglobulia as a reactive increase, the suspicion of a myeloproliferative disorder, primarily polycythemia vera, was expressed.

Consequently, a molecular-genetic laboratory program was carried out, including relevant biomarkers associated with myeloproliferative disorders. The analysis offered negative results for the breakpoint cluster

region protein-Abelson murine leukemia viral oncogene homolog 1 (BCR/ABL) translocation in both fluorescence in situ hybridization and quantitative polymerase chain reaction. Further investigations including calreticulin exon 9, Janus kinase 2 (JAK2) exon 12, and myeloproliferative leukemia of codons W515L/K/A and S505N also showed negative results. The patient was decisively positive for JAK2-V617F with a mutation allele frequency of 22.1% according to digital droplet polymerase chain reaction (ddPCR) of peripheral blood, as shown in **IMAGE 1**. Therefore, the patient met the major inclusion criteria for the diagnosis of a myeloproliferative disorder. Accordingly, a bone marrow biopsy was performed for further disease classification.

Subsequent cytomorphological investigations of the patient's bone marrow offered a coherent picture that substantiated the previous findings. In the hypercellular bone marrow, the erythrocytosis appeared strikingly proliferative, and staining with Berlin-blue dye revealed the typical iron deficiency of the reticuloendothelial system. A complementary immunohistochemical analysis further confirmed the diagnosis of polycythemia vera: The granulopoiesis (CD15, myeloperoxidase), the megakaryocytopoiesis (CD61, CD42b), and above all the erythrocytosis (CD71, glycophorin C) were quantitatively increased and the hemosiderin granules were not detectable. Reticulin staining showed a normal reticulin fiber network; therefore, in combination with an absence of leukoerythroblastosis in the peripheral blood smear, a prefibrotic stage of polycythemia vera or a post-polycythemia vera myelofibrosis was excluded.

Eventually, karyotyping analysis was performed on unstimulated (24 hours and 48 hours) bone marrow cultures. Surprisingly, an unexpected balanced Robertsonian translocation t(13;21)(q10;q10) was detected, as shown in **IMAGE 2**. The translocation was conclusively assumed to be a constitutional rather than an acquired translocation because all analyzed metaphases (20) were affected.

## Discussion

Although balanced Robertsonian translocations represent the most common human genetic chromosomal translocation,<sup>1</sup> with a rate of 1 in 1000 in newborns, little evidence is given in association with hematologic disorders as a possible contributor to pathogenesis. Generally, in balanced Robertsonian translocations, the phenotypical development is not affected, but predispositions to abortion, infertility, and hematologic disorders have been observed.<sup>2,3</sup> Prior publications with a hematologic context have predominantly described balanced Robertsonian translocations in patients with acute myeloid leukemia. In those

**IMAGE 1.** JAK2-V617F ddPCR analysis: Channel 1 = Mutated JAK2-V617F, Channel 2 = Wildtype JAK2 V617F. A01 – B01 positive control; C01 – negative control; D01 – no template control; C02 – D02 patient. A mutation allele frequency of 22.1% was assessed. JAK2, Janus kinase 2; ddPCR, digital droplet polymerase chain reaction.

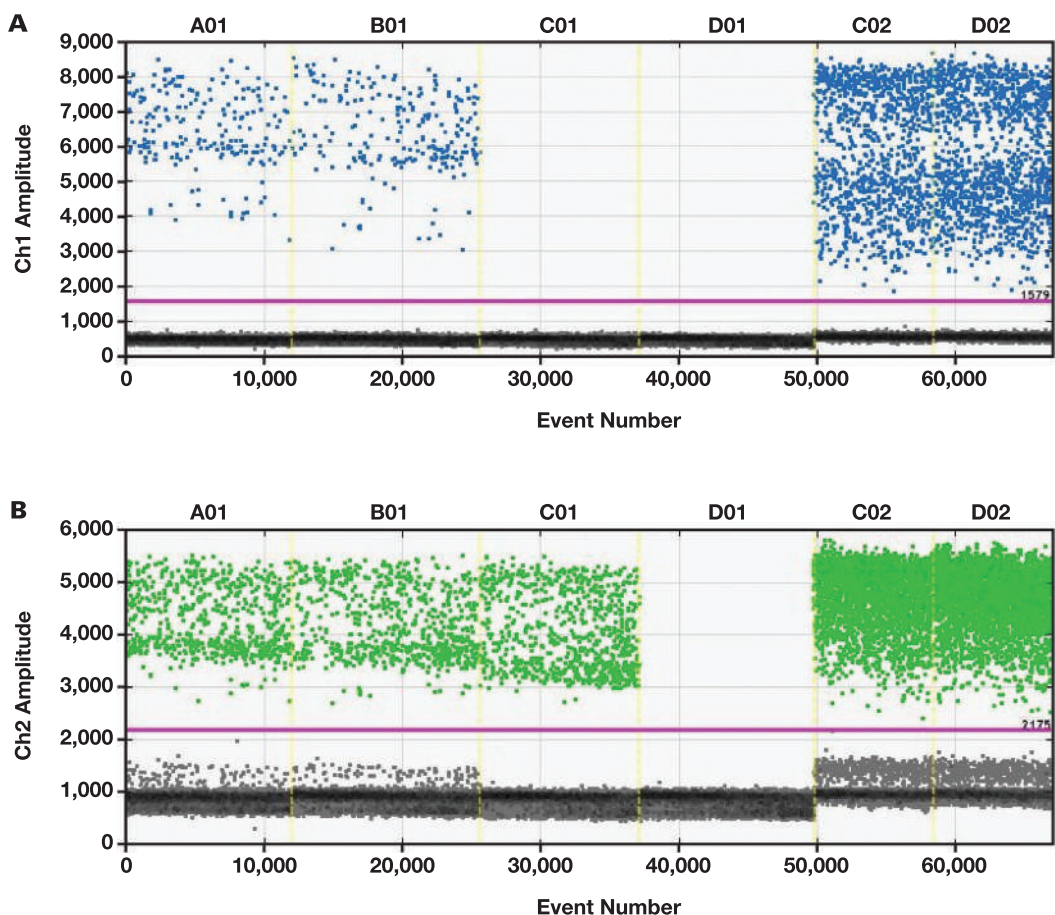
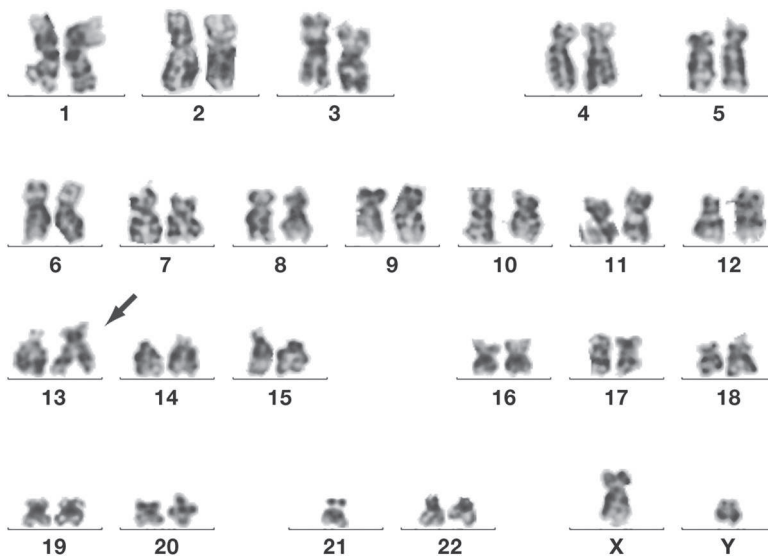


**IMAGE 2.** Karyogram of a male patient with a Robertsonian translocation in all metaphases and a loss of chromosome Y in 25% of metaphases. Karyotype: 44,X,Y,rob(13;21)(q10;q10)[3]/45,XY,rob(13;21)(q10;q10)[9].



patients, however, it is important to note that such aberrations have mostly been based on acquired genesis.<sup>4-7</sup>

In those reports, either a cytogenetic remission was commonly disclosed after introducing specific therapeutic regimes or the Robertsonian translocation occurred in the course of diagnostic disease monitoring as a secondary phenomenon in addition to already existing molecular-biological abnormalities, therefore proving the acquired nature of the translocation. The mechanism of Robertsonian translocations as a potential contributor to leukemogenesis is still not clear. Previous case reports provided the explanation that in acquired Robertsonian translocation partial trisomy or tetrasomy might increase gene dosage and therefore increase the risk of clonal evolution. Those assumptions were supported by a retrospective trial conducted by Welborn et al,<sup>1</sup> who investigated the impact of acquired Robertsonian translocations and isochromosomes on hematologic disorders. Of interest in that study, all of the detected acquired Robertsonian rearrangements resulted in a trisomic karyotype. In addition, a vast majority of those trisomies, on the basis of acquired Robertsonian translocation, were found to be the sole molecular biological abnormality. Those observations further indicated the potential of acquired Robertsonian translocation as a self-contained risk factor for hematologic disease development. Nevertheless, it is important to mention that those acquired variants are less prevalent than constitutional ones because Robertsonian translocations occur more frequently in meiosis than in mitosis.<sup>1,2,5,6</sup>

In our patient, we diagnosed a balanced Robertsonian translocation of congenital etiology in which the entire long arms of acrocentric chromosomes 13 and 21 fused—after breakage of the centromere—whereas the short arms were lost. The loss of the short arms is consistent with a normal phenotype because short arms of acrocentric chromosomes predominantly contain repeated satellite DNA sequences in tandem and repetitive ribosomal RNA. It is noteworthy that carriers of balanced Robertsonian translocations are at increased risk of producing unbalanced gametes and, consequently, of children with a similar condition. However, our patient did not have children nor wish to have children in the future, so further investigations regarding the patient's fertility or a human genetic analysis of family members was not required.<sup>8</sup>

When searching for myeloproliferative disorders in the literature, we could only identify 3 older studies that reported a Robertsonian translocation t(13;14) in patients with chronic myeloid leukemia.<sup>9-11</sup> No case report of balanced Robertsonian translocation in a patient with a polycythemia vera has been published before now.

### Laboratory Role in Diagnosis

In the case study we present, it is important to question the impact of laboratory analysis, specifically of the molecular-biological results, on the patient's outcome. In our patient, JAK2 positivity indisputably proved the diagnosis of a myeloproliferative disorder with BCR/ABL negativity according to World Health Organization diagnostic criteria.<sup>12</sup> Subsequent investigations, such as the subnormal erythropoietin level, persistent polyglobulia, and microscopic picture, enabled further classification as a polycythemia vera.<sup>12</sup>

Cytomorphological investigation of bone marrow represents one of the most important initial steps in the laboratory analysis of hematologic patients. Bone marrow biopsy was included in the major diagnostic criteria of polycythemia vera in the 2016 revised "WHO Classification of

Tumours of Haematopoietic and Lymphoid Tissues."<sup>12</sup> Our patient fulfilled these major diagnostic criteria because the bone marrow presented hypercellularity and panmyelosis (trilineage myeloproliferation) with a dominating proliferative erythrocytosis caused by the JAK2-V617F driver mutation. However, it is worth mentioning that microscopic differentiation of polycythemia vera and essential thrombocythemia is often challenging. In that context, the trilineage proliferation with pleomorphic megakaryocytes indicates a diagnosis of polycythemia vera. In contrast, in patients with essential thrombocythemia the megakaryocytic lineage is commonly affected and appears predominantly proliferative with enlarged megakaryocytes with hyperlobulated nuclei.<sup>12</sup>

In addition, the quantification of the allelic burden by ddPCR enabled a comprehensive follow-up in our patient comprising therapy guidance and a molecular-biological monitoring of minimal residual disease.<sup>13,14</sup> A few studies have referred to a higher mutation allelic frequency in polycythemia vera than in other myeloproliferative disorders. Lee et al<sup>15</sup> described a 40.7% ± 31.2% allelic burden in untreated patients, whereas Yow et al<sup>16</sup> reported a median JAK2-mutation allelic frequency of 48.8% in patients with polycythemia vera. Our patient had an initial mutation allele frequency of 22.1% in the peripheral blood and could be seen as having a comparatively low allelic burden.

We must also highlight that a loss of chromosome Y was detected in the karyotype analysis in 25% of our patient's analyzed metaphases. Even though the loss of chromosome Y represents the most frequently observed cytogenetic abnormality of the bone marrow analysis of male patients, it is necessary to differentiate whether this finding represents a disease-associated or an age-related phenomenon. The vast majority of publications in that context postulate a cutoff of 75% that must be overcome to discuss a disease-associated clone. Compared to our patient, who had a loss of chromosome Y in 25% of his analyzed metaphases, this result could be neglected as a natural occurrence of older age in a male patient. Above all, there is compelling evidence that the loss of chromosome Y represents an intermediate-to-favorable prognostic aberration in patients with hematologic disorders.<sup>17,18</sup>

Finally, we scrutinized the clinical significance of the Robertsonian translocation. The detection of the Robertsonian translocation was more or less a coincidence. Nevertheless, it underlines the necessity for karyotype analysis, even if myeloproliferative disorders usually do not present recurrent cytogenetic aberrations.<sup>19</sup> Considering the Robertsonian translocation, the balanced variant without a gain of gene material is much more favorable. In contrast, patients with an unbalanced translocation may suffer from multiple malformations to the point of Down syndrome or Patau syndrome.<sup>20-23</sup> Essentially, as reported in one of the most comprehensive studies in that scientific field, conducted by Schoemaker et al,<sup>2</sup> balanced Robertsonian rearrangements emerged as risk factors for childhood leukemia and non-Hodgkin lymphoma. Furthermore the Robertsonian translocation rob(13;14) resulted in a higher risk of breast cancer. Even though this prospective study found that even balanced variants of Robertsonian translocations are a relevant risk factor for specific hematologic and solid tumors, no prognostic conclusion or adverse patient outcomes could be confirmed. In particular, the overall mortality of patients harboring balanced Robertsonian translocations was lower (although not significantly lower) than that of the general population.<sup>2</sup>

Based on these findings, we report the case of a patient with a confirmed diagnosis of polycythemia vera. Because the patient also showed

a Robertsonian translocation, it was necessary to appraise that specific condition. Indeed, patients with balanced Robertsonian translocations commonly present a normal phenotype. Currently, no convincing data are available regarding balanced Robertsonian translocations that support an adverse outcome additional to the base diagnosis of polycythemia vera.

## Patient Follow-Up

Long-term medication with acetylsalicylic acid was prescribed as prophylaxis for thromboembolism, and a phlebotomy was performed to lower the hematocrit to 43% (<45%). A cytoreductive therapy has not yet been established because of the patient's age, clinical status, and, notably, the assessment of a favorable molecular-biological profile with an initial low allelic burden of JAK2 and nonadverse cytogenetic findings.

Furthermore, regular blood count monitoring was arranged with an external physician, and additional comprehensive assessments of hematologic parameters and monitoring of the patient's status have been scheduled at our institution for a period of 3 months (as of this writing).

## REFERENCES

1. Welborn J. Acquired Robertsonian translocations are not rare events in acute leukemia and lymphoma. *Cancer Genet Cytogenet.* 2004;151(1):14–35.
2. Schoemaker MJ, Jones ME, Higgins CD, Wright AF, Swerdlow AJ; United Kingdom Clinical Cytogenetics Group. Mortality and cancer incidence in carriers of balanced Robertsonian translocations: a national cohort study. *Am J Epidemiol.* 2019;188(3):500–508.
3. Warburton D. De novo balanced chromosome rearrangements and extra marker chromosomes identified at prenatal diagnosis: clinical significance and distribution of breakpoints. *Am J Hum Genet.* 1991;49(5):995–1013.
4. Ino T, Okamoto M, Tsuzuki M, Kamino I, Hirano M. An acquired Robertsonian 13;15 translocation in acute myelogenous leukemia (M5b). *Int J Hematol.* 1994;59(2):131–135.
5. Shimokawa T, Sakai M, Kojima Y, Takeyama H. Acute myelogenous leukemia (M5a) that demonstrated chromosomal abnormality of Robertsonian 13;21 translocation at onset. *Intern Med.* 2004;43(6):508–511.
6. Ma SK, Chow EY, Wan TS, Chan LC. Robertsonian translocation as an acquired karyotypic abnormality in leukaemia. *Br J Haematol.* 1997;98(1):213–215.
7. Chinnappan D, Philip A, Wu X, Pan A, Wyandt HE. Acquired Robertsonian translocations in two leukemia patients. *Cancer Genet Cytogenet.* 2001;131(2):104–108.
8. Chang YW, Chen LC, Chen CY, et al. Robertsonian translocations: an overview of a 30-year experience in a single tertiary medical center in Taiwan. *J Chin Med Assoc.* 2013;76(6):335–339.
9. Kohno S, Sandberg AA. Ph1-positive CML in a 13;14 translocation carrier. *Med Pediatr Oncol.* 1978;5(1):61–64.
10. Bown N, Yule SM, Evans J, Kernahan J, Reid MM. Chronic myelomonocytic leukemia with t(13;14) in a child. *Cancer Genet Cytogenet.* 1992;60(2):190–192.
11. Goh KO, Bauman AW, Townes PL. Myeloproliferative disorder in a t(13q14q) carrier. *Cancer.* 1980;45(2):327–329.
12. Barbui T, Thiele J, Gisslinger H, et al. The 2016 WHO classification and diagnostic criteria for myeloproliferative neoplasms: document summary and in-depth discussion. *Blood Cancer J.* 2018;8(2):15.
13. Haslam K, Langabeer SE. Monitoring minimal residual disease in the myeloproliferative neoplasms: current applications and emerging approaches. *Biomed Res Int.* 2016;2016:7241591.
14. Vannucchi AM, Verstovsek S, Guglielmelli P, et al. Ruxolitinib reduces JAK2 p.V617F allelic burden in patients with polycythemia vera enrolled in the RESPONSE study. *Ann Hematol.* 2017;96(7):1113–1120.
15. Lee E, Lee KJ, Park H, et al. Clinical implications of quantitative JAK2 V617F analysis using droplet digital PCR in myeloproliferative neoplasms. *Ann Lab Med.* 2018;38(2):147–154.
16. Yow KS, Liu X, Chai CN, et al. Relationship of JAK2 (V617F) allelic burden with clinico-haematological manifestations of Philadelphia-negative myeloproliferative neoplasms. *Asian Pac J Cancer Prev.* 2020;21(9):2805–2810.
17. Wiktor AE, Van Dyke DL, Hodnefield JM, Eckel-Passow J, Hanson CA. The significance of isolated Y chromosome loss in bone marrow metaphase cells from males over age 50 years. *Leuk Res.* 2011;35(10):1297–1300.
18. Wong AK, Fang B, Zhang L, Guo X, Lee S, Schreck R. Loss of the Y chromosome: an age-related or clonal phenomenon in acute myelogenous leukemia/myelodysplastic syndrome? *Arch Pathol Lab Med.* 2008;132(8):1329–1332.
19. Andrieux JL, Demory JL. Karyotype and molecular cytogenetic studies in polycythemia vera. *Curr Hematol Rep.* 2005;4(3):224–229.
20. Al-Alaiyan S, Al-Omran H, Kattan H, Sakati N, Nyhan WL. Down syndrome and recurrent abortions resulting from Robertsonian translocation 21q21q. *Ann Saudi Med.* 1995;15(4):391–392.
21. Wilch ES, Morton CC. Historical and clinical perspectives on chromosomal translocations. *Adv Exp Med Biol.* 2018;1044:1–14.
22. Hook EB. Unbalanced Robertsonian translocations associated with Down's syndrome or Patau's syndrome: chromosome subtype, proportion inherited, mutation rates, and sex ratio. *Hum Genet.* 1981;59(3):235–239.
23. Zhao WW, Wu M, Chen F, et al. Robertsonian translocations: an overview of 872 Robertsonian translocations identified in a diagnostic laboratory in China. *PLoS One.* 2015;10(5):e0122647.

# Resolving Pseudohyponatremia: Validation of Plasma Sodium on Radiometer ABL800 Blood Gas Analyzers for Immediate Reflex Testing

Michael A. Vera, BA, Angela Sutphin, BSc, MT(ASCP), Lisa Hansen, BSc, Joe M. El-Khoury, PhD\*

Department of Laboratory Medicine, Yale School of Medicine, New Haven, Connecticut; \*To whom correspondence should be addressed. [joe.el-khoury@yale.edu](mailto:joe.el-khoury@yale.edu)

**Keywords:** blood gas analyzer, electrolyte exclusion effect, method validation, plasma, pseudohyponatremia, pseudohyponatremia, sodium determination, volume displacement effect, whole blood

**Abbreviations:** ISEs, ion-selective electrodes; POC, point-of-care.

*Laboratory Medicine* 2022;53:e105–e108; <https://doi.org/10.1093/labmed/lmab114>

## ABSTRACT

**Objective:** To perform validation of plasma sodium on blood gas analyzers to reflexively correct erroneous measurements by ion-selective electrodes (ISEs).

**Methods:** We compared remnant specimens of whole blood and plasma collected by lithium heparin vacutainer with normal protein concentrations and no lipemia. Whole-blood specimens were tested for sodium concentration on the ABL800 Flex blood gas analyzer, followed by centrifugation for plasma separation, and repeat sodium determination on an aliquot of the plasma only. Also, plasma specimens were analyzed by indirect ISE on the Cobas 8000 series and by direct ISE on the ABL800 Flex for instrument comparison.

**Results:** Plasma aliquots yielded comparable results to the parent whole-blood specimen, with an average change of  $-1.33$  mmol/L ( $R^2 = 0.9727$ ). Comparison of indirect ISE to direct ISE similarly yielded comparable results, with an average change of  $+0.8$  mmol/L ( $R^2 = 0.9016$ ).

**Conclusion:** Plasma is a valid specimen matrix for use on blood gas analyzers for sodium determination, eliminating the need for re-collection of whole-blood specimens from patients with pseudohyponatremia.

In clinical laboratory testing, measurement of electrolytes (sodium, potassium, and chloride) is commonly performed by potentiometric methodologies relying on ion-selective electrodes (ISEs).<sup>1</sup> These are among the most commonly performed tests worldwide, and consequently, laboratories typically use high-throughput chemistry analyzers.

Testing is performed by analysis of plasma or serum using an indirect ISE method, requiring significant specimen dilution—1:20 to 1:34.<sup>2</sup> A consequence of the dilutional step necessitates back-calculation to produce an electrolyte concentration in the original specimen, relying on a critical assumption that the matrix of serum/plasma is predominantly aqueous. In healthy individuals, serum and plasma is approximately 93% aqueous material, in which the electrolytes are dissolved, and 7% solids (ie, lipids, proteins). Deviations in this ratio, caused by dyslipidemias and liver or kidney disorders in which hypo- or hyperproteinemia is present, can produce over- or underestimated concentrations of electrolytes by indirect ISE.<sup>1</sup> Collectively, this phenomenon is known as the *electrolyte exclusion effect* or *volume displacement effect*.<sup>3</sup>

Of all electrolytes, sodium is often the most affected, due to its relatively high plasma concentration and narrow physiological range. Potassium and chloride are also analytically affected by the phenomenon. However, due to lower plasma concentrations and larger physiological ranges, the absolute change in concentration is usually not clinically significant.<sup>3</sup> Findings from previous studies<sup>4,5</sup> have demonstrated a spurious increase in sodium concentration in cases of an absence of proteins (total protein  $<3$  g/dL) and spurious decreases in sodium concentration in the presence of excess proteins (total protein  $>9$  g/dL) or lipids (L-Index  $>700$ ), known as *pseudohyper-* and *pseudohyponatremia*, respectively. In such cases, these erroneous measurements may go undetected, or results may be canceled, and the patient redrawn from treatment with no true resolution.

A proposed solution is the usage of blood gas analyzers or point-of-care (POC) devices, which employ direct ISE methods on undiluted whole blood.<sup>6,7</sup> Without a required dilutional step, direct analyzers are not affected by the volume-displacement effect and can more accurately determine sodium concentration in such cases. However, these instruments are only validated for use on whole-blood specimens, not plasma or serum, requiring patients be redrawn when confirmatory analysis by direct ISE is needed.

Because these devices are typically accessible for laboratories, and to facilitate usage of direct ISE for cases of pseudohyper- and

pseudohyponatremia, our study aim was to validate the analysis of plasma using blood gas analyzers for sodium measurement. Doing so would consequently enable laboratories to establish rules for the detection of plasma specimens potentially affected by the volume-displacement effect and to reflex those specimens to direct ISE for more accurate sodium determination.<sup>5</sup> This step would minimally impact normal laboratory or clinical practice while eliminating these cases of erroneous sodium measurement.

## Methods

### Sodium Measurement and Specimen Collection

Direct sodium measurement was performed on the ABL800 Flex instrument (Radiometer). Indirect sodium measurement was performed on the ISE module of the Cobas 8000 series analyzer (F. Hoffman-La Roche, Ltd.). Specimens used in this study were leftover specimens, collected in lithium heparin vacutainer tubes, previously analyzed in the Yale New Haven Hospital Chemistry Laboratory. Specimens were stored between 2°C–8°C and used within 1 week of initial collection but reanalyzed on Roche and Radiometer instruments within 1 hour for the comparison study.

### Statistical Analysis

An allowable error of sodium measurement  $\pm 4$  mmol/L was used for all method comparison studies.<sup>4</sup> Statistical analysis was performed using EP Evaluator and JMP Pro 15. Results were analyzed by linear regression and mean analysis.

### Direct Sodium Whole Blood and Plasma Comparison

Whole-blood specimens ( $n = 45$ ) were analyzed directly for sodium concentration, immediately followed by centrifugation (2254g; 7 minutes). Separated plasma was aliquoted to a new tube, followed by a repeat direct sodium measurement.

### Direct and Indirect Plasma Method Comparison

Plasma specimens ( $n = 95$ ) selected for study were lightly vortexed before analysis by indirect and direct methods. To avoid confounding variables, only specimens with no apparent interferences were utilized in this study. Exclusion criteria consisted of specimen with H-Index  $> 30$ , L-Index  $> 15$ , and I-Index  $> 5$ . Also, to further avoid the volume-displacement effect, only specimens with a total protein within the reference interval of 6.6–8.7 g/dL were utilized, as protein concentrations outside of the normal range are known to cause a difference.<sup>4</sup> Specimens were analyzed indirectly first, immediately followed by direct measurement within 1 hour.

### Precision, Linearity, and Carryover

Radiometer precision was determined using quality control material at 3 levels (125, 140, and 159 mmol/L). Interassay precision was determined by 3 replicate runs at each level a day over 7 days ( $n = 60$ ). Intra-assay precision was determined by 20 measurements at each level within 1 run ( $n = 60$ ). Linearity determination utilized additional quality-control material at 3 different levels (83, 147, and 173 mmol/L), with 4 replicate runs at each level.

The potential for carryover was analyzed by using Radiometer calibrator material at 2 levels (115 and 167 mmol/L). Measurement of the

115 mmol/L material was performed after 2 sample measurements of the high- or low-concentration material. High and low material were alternated throughout the study, with 5 replicate runs at each level ( $n = 21$ ). Mean measurement of the 115 mmol/L material after low (low-low mean) and high (high-low mean) runs were used to assess carryover.

## Results

### Direct Sodium Whole Blood and Plasma Comparison

A total of 45 whole-blood specimens were compared with plasma over a sodium concentration range of 119 to 141 mmol/L, with a mean of 131 mmol/L. The difference between matrices was within the allowable error ( $\pm 4$  mmol/L) for all specimens (FIGURE 1), with an average bias of  $-1.33$  mmol/L.

### Direct and Indirect Plasma Method Comparison

A total of 95 plasma specimens were compared between both direct and indirect methods. The range in sodium concentrations by indirect measurement was from 126 to 147 mmol/L, with a mean of 138 mmol/L. The difference between instruments was within the allowable error ( $\pm 4$  mmol/L) for all specimens (FIGURE 2) with an average bias of  $+ 0.8$  mmol/L.

### Precision, Linearity, and Carryover

Intra-assay CV was determined to be 0.4% for low and middle concentrations (125 and 140 mmol/L) and 0.5% for the high concentration (159 mmol/L). Interassay CV was determined to be 0.3% for the low and high concentrations, and 0% for the middle concentration. The assay demonstrated strong linearity, with a CV of 0% and  $R^2 = 1$ .

Mean low concentration after a low-concentration specimen (low-low) was 114.8 mmol/L, and mean low concentration after a high-concentration specimen (high-low) was 114.6 mmol/L. These measurements represented minimal carryover of  $-0.2$  mmol/L.

## Discussion

In comparing whole blood to plasma on the Radiometer ABL800 Flex, there were minimal variations in sodium concentration, with an average bias of  $-1.33$  mmol/L ( $R^2 = 0.9727$ ). Also, there were minimal variations when comparing plasma sodium by indirect ISE on the Roche Cobas 8000 series analyzer to the direct ISE of the blood gas analyzer, with an average bias of  $+ 0.8$  mmol/L ( $R^2 = 0.9016$ ). In both cases, all tested specimens were within a total allowable error of  $\pm 4$  mmol/L. The findings of this study demonstrate plasma as a valid specimen type for the measurement of sodium on the blood gas analyzer, with comparable results to indirect ISE.

A limitation of indirect ISE is the volume-displacement effect, caused by a required dilution step during analysis.<sup>2</sup> This phenomenon occurs specifically in patients with hypoproteinemia (TP  $< 3.0$  g/dL), hyperproteinemia (TP  $> 9$  g/dL), or hyperlipidemia (L-Index  $> 700$ ) because it causes a shift in the percent volume of nonsoluble solids in plasma or serum.<sup>4,5</sup> The effect can result in spurious sodium measurements, known as pseudohyper- or pseudohyponatremia.

Generally, these erroneous measurements may be undetected or canceled, or the patient may have a specimen redrawn without resolution. Blood gas analyzers validated for measurement of electrolytes in

**FIGURE 1.** Comparison of whole blood and plasma sodium measurement on the ABL800 Flex (Radiometer). Red lines in both figures represent a total allowable error of  $\pm 4$  mmol/L. A, Linear regression of whole blood and plasma sodium determinations. The dashed line represents linear regression ( $y = 0.9584x + 6.7766$ ,  $R^2 = 0.9727$ ). The shaded area represents the 95% confidence range for the regression. B, Bias in plasma sodium concentration, compared with whole-blood determination.

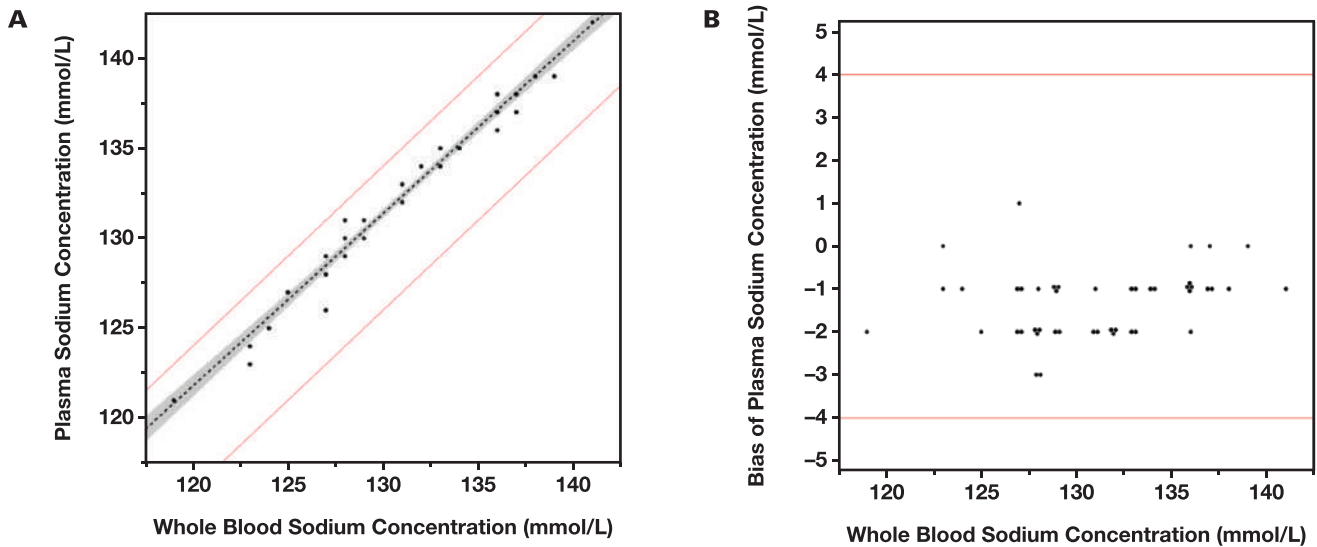
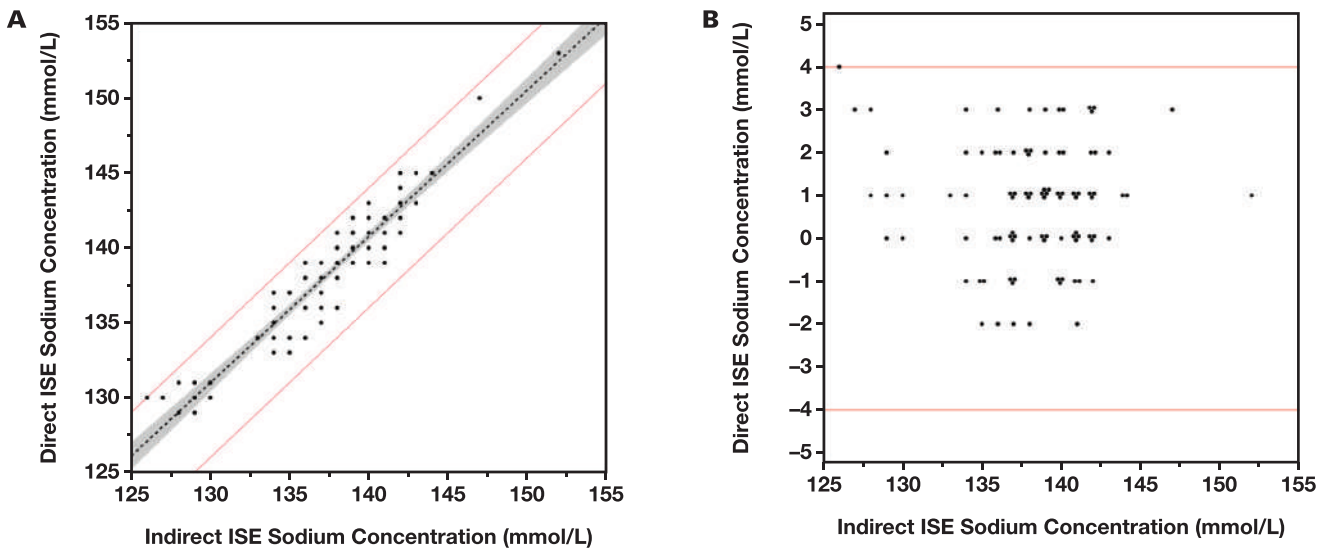


**FIGURE 2.** Comparison of indirect and direct sodium measurement on the Cobas ISE (F. Hoffman-La Roche, Ltd.) and ABL Flex 800 (Radiometer) instruments, respectively. The red line in both figures represents the total allowable error of  $\pm 4$  mmol/L. A, Linear regression of indirect and direct ion-selective electrodes (ISE) sodium determinations. The dashed line represents linear regression ( $y = 0.9767x + 4.0274$ ,  $R^2 = 0.9016$ ). The shaded area represents the 95% confidence range for the regression. B, Bias in direct ISE sodium concentration, compared to indirect ISE determination.



whole blood avoid this dilution step in measurement, and instead measure the ion electrical potential directly in the plasma water of the matrix. Sodium concentration, in this case, is independent of the volume of nonaqueous components because this is only a required consideration in the dilutional analysis of indirect ISE.<sup>8</sup> Thus, blood gas analyzers present an alternative solution, being consequently free from the volume-displacement effect. Most electrolyte testing occurs in plasma or serum; hence, these study findings demonstrate that these specimens may be

tested on the aforementioned devices. The findings provide an accessible solution to the problem of pseudohyper- and pseudohyponatremia.

This process is far more manual than indirect ISE testing, and thus not recommended for high-throughput routine practice. However, laboratories can create rules for the identification of specimens potentially affected by the volume-displacement effect and reflex the testing to POC blood gas analyzers, if available in the core laboratory, for accurate sodium measurement.

## Conclusion

Plasma specimens are a valid matrix for usage on blood gas analyzers for the purpose of sodium determinations. Blood gas analyzers and similar POC devices utilize direct ISE methodology that is free from erroneous electrolyte determinations by the volume-displacement effect. Conversely, common high-throughput chemistry analyzers utilize indirect ISE with a required dilutional step that can lead to erroneous electrolyte determinations. Laboratories should similarly validate plasma on blood gas analyzers and POC devices. Also, they should update rules for the detection of pseudohyper- and pseudohyponatremia so these specimens can be easily reflexed for more accurate sodium determinations, without the need for re-collection of whole blood.

## REFERENCES

1. Weisberg LS. Pseudohyponatremia: a reappraisal. *Am J Med.* 1989;86(3):315–318.
2. Goyal B, Datta SK, Mir AA, Ikkurthi S, Prasad R, Pal A. Increasing glucose concentrations interfere with estimation of electrolytes by indirect ion selective electrode method. *Indian J Clin Biochem.* 2016;31(2):224–230.
3. Chopra P, Datta SK. Discrepancies in electrolyte measurements by direct and indirect ion selective electrodes due to interferences by proteins and lipids. *J Lab Physicians.* 2020;12(2):84–91.
4. Katrangi W, Baumann NA, Nett RC, Karon BS, Block DR. Prevalence of clinically significant differences in sodium measurements due to abnormal protein concentrations using an indirect ion-selective electrode method. *J Appl Lab Med.* 2019;4(3):427–432.
5. Koch CD, Vera MA, Messina J, Price N, Durant TJS, El-Khoury JM. Preventing pseudohyponatremia: Intralipid®-based lipemia cutoffs for sodium are inappropriate. *Clin Chim Acta.* 2021;520:63–66.
6. Geoghegan P, Koch CD, Wockenfus AM, et al. Agreement between whole blood and plasma sodium measurements in profound hyponatremia. *Clin Biochem.* 2015;48(7-8):525–528.
7. Tang J, Watts G, Chen Y. Interchangeability of electrolyte and metabolite testing on blood gas and core laboratory analyzers. *Clin Lab.* 2020;66(7). doi: 10.7754/Clin.Lab.2020.191255.
8. Fortgens P, Pillay TS. Pseudohyponatremia revisited: a modern-day pitfall. *Arch Pathol Lab Med.* 2011;135(4):516–519.

# A Simple and Applicable Method for Human Platelet Lysate Preparation Using Citrate Blood

Narin Khongjaroensakun, MD,<sup>1,\*</sup> Karan Paisooksantivatana, MD,<sup>1</sup> Suttikarn Santiwatana, MD, PhD,<sup>2,3</sup> Tulyapruet Tawonsawatruk, MD, PhD,<sup>4</sup> Kantarat Kusolthammarat, MD,<sup>1,5</sup> Praguaywan Kadegasem, BSc,<sup>2</sup> Noppawan Tangbubpha, MS,<sup>2</sup> Juthamard Chantaraamporn, MS,<sup>2</sup> and Ampaiwan Chuansumrit, MD<sup>2</sup>

<sup>1</sup>Department of Pathology, Faculty of Medicine Ramathibodi Hospital, Mahidol University, Bangkok, Thailand, <sup>2</sup>Department of Pediatrics, Faculty of Medicine Ramathibodi Hospital, Mahidol University, Bangkok, Thailand, <sup>3</sup>Vejthani Hospital, Bangkok, Thailand, <sup>4</sup>Department of Orthopedics, Faculty of Medicine Ramathibodi Hospital, Mahidol University, Thailand, <sup>5</sup>Department of Pathology, Prince of Songkla University, Songkhla, Thailand; \*To whom correspondence should be addressed. [narin.kho@mahidol.edu](mailto:narin.kho@mahidol.edu)

**Abbreviations:** PRP, platelet-rich plasma; PDGF, platelet-derived growth factor; TGF, transforming growth factor; VEGF, vascular endothelial growth factor; HPL, human platelet lysate; PCs, platelet concentrates; IRB, institutional review board; CBC, complete blood count; QC, quality control; OD, optical density; RBC, red blood cell; MCV, mean corpuscular volume; WBC, white blood cell; MPV, mean platelet volume; PDGF-AB, platelet-derived growth factor-AB; PDGF-BB, platelet-derived growth factor-BB; TGF- $\beta$ 1, transforming growth factor beta 1; TGF- $\beta$ 2, transforming growth factor beta 2

*Laboratory Medicine* 2022;53:e109–e112; <https://doi.org/10.1093/labmed/lmab116>

## ABSTRACT

**Objectives:** To determine and compare the platelet growth factors in human platelet lysate (HPL) prepared from citrated whole blood, with final centrifugations at 4°C and 25°C.

**Methods:** We collected specimens of citrated whole blood from 27 healthy volunteers. The platelet-rich plasma (PRP) was separated to prepare the HPL, which was further divided into 2 portions for the final centrifugation, at 4°C and 25°C, respectively. Platelet growth factors were measured and compared between the 2 groups.

**Results:** All platelet growth factors were higher than those in PRP prepared from citrated whole blood. Moreover, the final centrifugation at 25°C resulted in noninferiority of platelet-growth-factor level.

**Conclusion:** This study provided a simple method for small-volume of HPL preparation using only 10–15 mL of citrated whole blood. Further, the entire process of centrifugation can be performed at

room temperature of 25°C, which is more applicable than lower temperatures for other laboratories.

Platelet-rich plasma (PRP) is an often-favored method for curing many diseases.<sup>1–3</sup> The reason is that platelets contain a variety of growth factors related to the healing process, such as platelet-derived growth factor (PDGF), transforming growth factor (TGF), and vascular endothelial growth factor (VEGF).<sup>4,5</sup> Nevertheless, the drawbacks of using PRP are short stability and the requirement of specific storage conditions, such as a 22°C platelet incubator with agitation. Therefore, many studies<sup>4–9</sup> have used human platelet lysate (HPL) instead because of its more extended stability and easier storage conditions, compared with PRP. HPL was prepared by repetitively frozen and thawed PRP, resulting in platelet lysis and release of intracellular growth factors into plasma, which encourage the healing process by promoting mesenchymal stem cells and angiogenesis.

However, HPL from those previous studies was prepared from platelet concentrates (PCs), which might be unsuitable for some patients with conditions such as degenerative joint disease for the following reasons. First, the volume of HPL prepared from PC was too much for intra-articular injection, which required as much as 5 milliliters per episode. Second, platelet concentrates at the blood bank were scarce due to other more urgent indications, such as massive transfusion or active bleeding. Third, most patients with degenerative joint conditions might not be medically authorized for autologous plateletpheresis according to their status—for example, advanced age, underlying disease, and medication administration.<sup>10</sup> Thereby, autologous HPL preparation from whole blood in citrated buffer solution might be more appropriate for these patients. This study aimed to determine platelet growth factors in HPL prepared from citrated whole blood and to compare the stability of HPL prepared from final centrifugation at 4°C and 25°C.

## Materials and Methods

### Subjects

This study was approved by the local institutional review board (IRB). All volunteers gave written informed consent following the Declaration

of Helsinki. The volunteers met all inclusion criteria, including age range of 18–60 years old, having neither history nor clinical manifestation of bleeding disorders, and having reported they had no history of receiving antiplatelet agents within 14 days before blood collection. Any problems related to specimen collection—namely, underfilled tube, clotted specimen, and/or abnormal plasma color—meant that those specimens were excluded from the study. Each volunteer was identified with an alphanumeric code, to ensure privacy.

### Preparation of platelet lysate

Blood specimens of 20 mL were drawn from the antecubital vein of each participant, according to the procedure indicated in CLSI publication H21-A5,<sup>11</sup> to minimize ex vivo platelet activation. The collected blood was added to three 5 mL plastic tubes contained 3.2% sodium citrate in a 9:1 ratio for platelet preparation and a 5 mL plastic tube containing potassium EDTA for complete blood count (CBC), respectively. All specimens were processed under room-temperature conditions within 2 hours after blood collection.

All citrated-blood tubes were centrifuged at room temperature of 25°C, 180g for 10 minutes. The gathered PRP was pooled and aliquoted to determine platelet count. The remaining PRP was frozen at –80°C for 1 hour and further thawed in a 37°C water bath for another hour.<sup>8,12</sup> Then, the thawed PRP specimen was divided into 2 portions to be spun at 4°C and room temperature of 25°C, with the same speed of 3220g, for 20 minutes to separate the supernatants, which were finally filtered with a 0.22 µM filter to remove the remaining debris. The steps of HPL preparation are summarized in **FIGURE 1**. CBC and platelet counts in PRP were measured using the Unicel DxH 800 Coulter Cellular Analysis System (Beckman Coulter, Inc.).

### Platelet growth factor measurement

The studied platelet growth factors—namely, PDGF-AB, PDGF-BB, TGF-β1, and TGF-β2—were simultaneously determined using Quantikine ELISA kits (R&D Systems, Inc.). Quality-control (QC) testing was performed using Quantikine Immunoassay Control (R&D Systems, Inc.) and the kit-specific assay diluents as the positive and negative control materials, respectively. According to the package insert, all control materials must be in the acceptable range before measuring the level in HPL. One particular staff member (N.K., P.K., N.T., and J.C.) used each ELISA kit until the end of the experiment to eliminate interpersonal variation. All specimens were run in duplicate. The optical density (OD) was measured and converted to the concentration of platelet growth factors using Synergy HT (BioTek Instruments, Inc.).

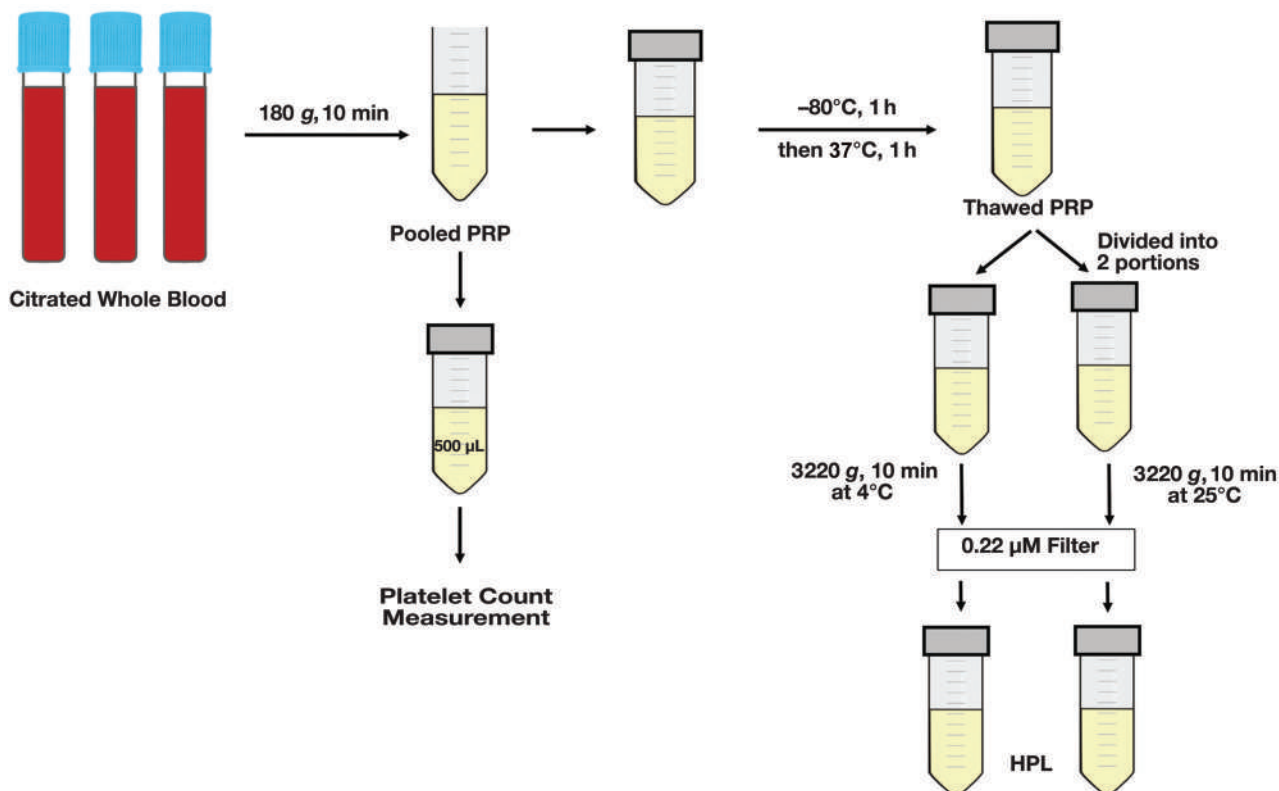
### Statistical analysis

The levels of platelet growth factors were reported as median (IQR). Each parameter was compared using the Mann-Whitney *U* test and Wilcoxon signed rank test. The correlation between platelet count in PRP and each platelet growth factor was analyzed using regression analysis. All statistical analysis was analyzed using MedCalc Statistical Software, version 19.2.1. A *P* value less than .05 was considered as statistical significance.

### Results

A total of 27 healthy volunteers (11 men and 16 women) were enrolled in this study. Their median age was 31.0 years, with an IQR of 27.2–40.0 years. Eight of the 27 subjects had blood group O; the others were non-blood-group O (6 in group A, 8 in group B, and 5 in group AB). All CBC parameters were within the normal range, as

**FIGURE 1.** Process of human platelet lysate preparation.



shown in **TABLE 1**. The median platelet count in PRP was 242,000/ $\mu\text{L}$ , with an IQR of 199,100–320,925/ $\mu\text{L}$ .

The QC result of all growth factors was within the acceptable range, as shown in the supplementary file. Most growth factors—namely, PDGF-AB, PDGF-BB, and TGF- $\beta$ 1—had higher levels when prepared by final spinning at room temperature of 25°C. In contrast, TGF- $\beta$ 2 prepared at 25°C had a slightly lower value than those specimens prepared by the last spinning at 4°C. All measured growth factors were demonstrated in **TABLE 2**. There was no statistically significant difference in growth factors to sex and ABO blood group (data not shown).

The correlation study revealed a significantly moderate correlation only between platelet count in PRP and PDGF-BB level measured from HPL prepared from final spinning at 4°C ( $r^2$ , 0.73,  $P < .01$ ) and room temperature of 25°C ( $r^2$ , 0.71,  $P < .01$ ). There was no statistically significant correlation between growth factors and age (data was not shown).

## Discussion

Platelets play an essential role in the healing process. They contain various growth factors, which promote the release of proinflammatory cytokines, leading to angiogenesis and tissue remodeling.<sup>15,16</sup> Recently, platelet-based products—namely, PC and PRP—have become popular in various medical specialties. Nevertheless, these products might not be applicable due to the shortage of PC in clinical practice and medical prohibition of autologous plateletpheresis procedures in some patients. Hence, this study aimed to measure platelet growth factors in HPL prepared from citrated whole blood.

The platelet growth factors in this study were higher than those measured in PRP from related published data,<sup>13,14,17</sup> as shown in **TABLE 2**. They were similar to those acquired from a previous study by some of us<sup>17</sup> using the same ELISA kits as in the current study. This finding

proved the efficacy of the procedure in the recent study using citrated whole blood. However, all growth factors measured in this study were lower than those in HPL prepared from PC.<sup>12,15,16</sup> The probable reasons are that platelet count in PC was higher than that obtained from PRP in this study, and that HPL from those previous studies was prepared from multiple freeze-thaw cycles, which might make more platelets deteriorate and result in the release of many more growth factors.

The HPL preparation using 4°C centrifugation at the final step may not be practical for many laboratories. Therefore, this study also assessed the effectiveness of the last spinning at room temperature of 25°C and demonstrated the noninferiority of growth-factor level. The higher yield at 25°C, compared to that at 4°C, was similar to the findings of a previous study from Du et al.<sup>14</sup> The possible reason could be cold denaturation, which requires more research for verification. Consequently, the method used in this study of centrifugation at room temperature of 25°C is more practical and applicable than other temperatures for other resource-limited laboratories.

Although platelets are the primary source of the measured growth factors, the results of this study found no correlation between the platelet count in PRP and all growth-factor levels. The variation in the cellular production of growth factors among subjects might be the cause of this circumstance. Nevertheless, the biological conditions influencing this variation remain unknown. Further study should be performed for more explanation.<sup>18–20</sup>

The advantages of HPL preparation using citrated whole blood in this study were that autologous HPL can be prepared from each patient individually, minimization of blood specimens of only 10–15 mL is more applicable for HPL preparation for intra-articular injection, and this method is applicable for other laboratories because the procedure is simple and no special instruments are required. In contrast, there were also some limitations inherent in the small sample size. For instance, the growth factor in PRP was not measured in this study, and some other growth factors related to the healing process (ie, VEGF and insulin-like growth factor-1 [IGF-1], a growth factor involved in cartilage hemostasis, balancing proteoglycan synthesis and breakdown, which stimulates collagen synthesis, together with PDGF) were omitted.<sup>21,22</sup> Further study is warranted.

## Conclusion

This study tested a simple method for HPL preparation using only 10–15 mL of citrated whole blood, which might be more suitable for procedures requiring only a small volume of HPL, such as intra-articular injection. Further, the entire process of centrifugation can be performed at room temperature of 25°C, which is more applicable than other temperatures for other laboratories.

**TABLE 1. Hematological Findings of the 27 Studied Subjects**

Parameters	Median (IQR)
Hemoglobin (g/ dL)	13.3 (13.0–15.2)
Hematocrit (%)	41.5 (40.1–45.9)
RBC count (cells/ $\text{mm}^3$ )	4,840,000 (4,322,500–5,227,500)
MCV (fL)	89.9 (86.7–93.5)
WBC count (cells/ $\mu\text{L}$ )	5800 (5077–7042)
Platelet count from initial EDTA blood ( $\mu\text{L}$ )	270,000 (224,250–297,000)
MPV (fL)	9.7 (8.5–10.3)
Platelet count from PRP ( $\mu\text{L}$ )	242,000 (199,100–320,925)

RBC, red blood cell; MCV, mean corpuscular volume; WBC, white blood cell; MPV, mean platelet volume; PRP, platelet-rich plasma.

**TABLE 2. Comparison of Platelet Growth Factors between the Final Centrifugation at 4°C and 25°C**

Platelet Growth Factor	Median (IQR)			Reference Range of Growth Factor in PRP <sup>13,14</sup>
	4°C	25°C	P Value	
PDGF-AB (pg/mL)	2144.5 (1808–2081.4)	2673.1 (2053, 3287.9)	.04	27.1–2400
PDGF-BB (pg/mL)	647.3 (570.3925)	698.1 (538.4847.6)	.27	225.5–800
TGF- $\beta$ 1 (pg/mL)	10,578.8 (8738.1–12,346.7)	11,010 (8528.9–12,191.3)	.75	400–3000
TGF- $\beta$ 2 (pg/mL)	50 (23.7–79.1)	44.8 (29.1–76.8)	.07	49.9

PDGF-AB, platelet-derived growth factor-AB; PDGF-BB, platelet-derived growth factor-BB; TGF- $\beta$ 1, transforming growth factor beta 1; TGF- $\beta$ 2, transforming growth factor beta 2; PRP, platelet-rich plasma.

## Acknowledgments

This research project is supported by the Faculty of Medicine Ramathibodi Hospital, Mahidol University, Bangkok, Thailand (grant no. RF\_63031 and no. RF\_64003). We thank Werarak Sasanakul, BSc, for his advice and assistance in this project, as well as Sornarong Poolsawat, BSc, and Roongrudee Singdong, MS, for specimen collection.

## Personal and Professional Conflicts of Interest

None reported.

## REFERENCES

1. Dohan Ehrenfest DM, Andia I, Zumstein MA, Zhang CQ, Pinto NR, Bielecki T. Classification of platelet concentrates (platelet-rich plasma-PRP, platelet-rich fibrin-PRF) for topical and infiltrative use in orthopedic and sports medicine: current consensus, clinical implications and perspectives. *Muscles Ligaments Tendons J.* 2014;4(1):3–9.
2. Zhu Y, Yuan M, Meng HY, et al. Basic science and clinical application of platelet-rich plasma for cartilage defects and osteoarthritis: a review. *Osteoarthr Cartil.* 2013;21(11):1627–1637.
3. O'Connell B, Wragg NM, Wilson SL. The use of PRP injections in the management of knee osteoarthritis. *Cell Tissue Res.* 2019;376(2):143–152.
4. Nurden AT, Nurden P, Sanchez M, Andia I, Anitua E. Platelets and wound healing. *Front Biosci.* 2008;13(9):3532–3548.
5. Tancharoen W, Aungsuchawan S, Pothacharoen P, et al. Human platelet lysate as an alternative to fetal bovine serum for culture and endothelial differentiation of human amniotic fluid mesenchymal stem cells. *Mol Med Rep.* 2019;19(6):5123–5132.
6. Dessels C, Durand C, Pepper MS. Comparison of human platelet lysate alternatives using expired and freshly isolated platelet concentrates for adipose-derived stromal cell expansion. *Platelets.* 2019;30(3):356–367.
7. Al-Ajlouni J, Awidi A, Samara O, et al. Safety and efficacy of autologous intra-articular platelet lysates in early and intermediate knee osteoarthritis in humans: a prospective open-label study. *Clin J Sport Med.* 2015;25(6):524–528.
8. Phetfong J, Tawonsawatruk T, Seenprachawong K, Srisarin A, Isarankura-Na-Ayudhya C, Supokawej A. Re-using blood products as an alternative supplement in the optimisation of clinical-grade adipose-derived mesenchymal stem cell culture. *Bone Joint Res.* 2017;6(7):414–422.
9. da Fonseca L, Santos GS, Huber SC, Setti TM, Setti T, Lana JF. Human platelet lysate - A potent (and overlooked) orthobiologic. *J Clin Orthop Trauma.* 2021;21:101534.
10. National Blood Center Thai Red Cross Society. Blood donor selection. In: Chiewsilp P, Charoonruangrit U, Jiwanuntavat W, eds. *Blood Donor Selection Guideline.* 6th ed. Thai Red Cross Society; 2017: 10–24.
11. Clinical & Laboratory Standards Institute (CLSI). *H21-A5: Collection, Transport, and Processing of Blood Specimens for Testing Plasma-Based Coagulation Assays and Molecular Hemostasis Assays; Approved Guideline.* 5<sup>th</sup> ed. Clinical and Laboratory Institute; 2008.
12. Notodihardjo SC, Morimoto N, Kakudo N, et al. Comparison of the efficacy of cryopreserved human platelet lysate and refrigerated lyophilized human platelet lysate for wound healing. *Regen Ther.* 2019;10:1–9.
13. Kobayashi E, Flückiger L, Fujioka-Kobayashi M, et al. Comparative release of growth factors from PRP, PRF, and advanced-PRF. *Clin Oral Investig.* 2016;20(9):2353–2360.
14. Du L, Miao Y, Li X, Shi P, Hu Z. A novel and convenient method for the preparation and activation of PRP without any additives: temperature controlled PRP. *Biomed Res Int.* 2018;2018:1–12.
15. Fekete N, Gadelorge M, Fürst D, et al. Platelet lysate from whole blood-derived pooled platelet concentrates and apheresis-derived platelet concentrates for the isolation and expansion of human bone marrow mesenchymal stromal cells: production process, content and identification of active components. *Cytotherapy.* 2012;14(5):540–554.
16. Klatte-Schulz F, Schmidt T, Uckert M, et al. Comparative analysis of different platelet lysates and platelet rich preparations to stimulate tendon cell biology: an in vitro study. *Int J Mol Sci.* 2018;19(1):1–18.
17. Santiwatana S, Sasanakul W, Kadegasem P, Chuansumrit A. The effect of adding platelet-rich plasma to fibrin glue on release of platelet growth factors and its stability. *J Hematol Transfus Med.* 2018;28:443–448.
18. Weibric G, Buch RS, Kleis WK, Hafner G, Hitzler WE, Wagner W. Quantification of thrombocyte growth factors in platelet concentrates produced by discontinuous cell separation. *Growth Factors.* 2002;20(2):93–97.
19. Mazzocca AD, McCarthy MB, Chowanec DM, et al. Platelet-rich plasma differs according to preparation method and human variability. *J Bone Joint Surg Am.* 2012;94(4):308–316.
20. Nugraha Y, Sari P, Purwoko RY, Luviah E, Pawitan JA. Effect of lysed platelet count in platelet concentrates on various growth factor levels after freeze thaw cycles. *Int J PharmTech Res.* 2014;6(7):2036–2042.
21. Schmidt MB, Chen EH, Lynch SE. A review of the effects of insulin-like growth factor and platelet derived growth factor on in vivo cartilage healing and repair. *Osteoarthritis Cartilage.* 2006;14(5):403–412.
22. Pavlovic V, Ciric M, Jovanovic V, Stojanovic P. Platelet rich plasma: a short overview of certain bioactive components. *Open Med (Wars).* 2016;11(1):242–247.

# Hospital and Laboratory Practice in an Integrated Medical System for HIV Infection Prevention Interventions at a Veteran Affairs Medical Center

Jeffrey M. Petersen, MD,<sup>1,2,\*</sup> Darshana N. Jhala, MD<sup>1,2</sup>

<sup>1</sup>Department of Pathology and Laboratory Medicine, Corporal Michael J. Crescenz VA Medical Center, Philadelphia, Pennsylvania, US, <sup>2</sup>Department of Pathology and Laboratory Medicine, University of Pennsylvania, Philadelphia, Pennsylvania, US; \*To whom correspondence should be addressed. [jeffrey.petersen@va.gov](mailto:jeffrey.petersen@va.gov)

**Keywords:** HIV, pre-exposure prophylaxis, evidence-based medicine, veteran population, quality assurance, sexually transmitted infection, quality improvement, laboratory result communication

**Abbreviations:** STI, sexually transmitted infection; PrEP, pre-exposure prophylaxis; QA, quality assurance; VAMC, Veteran Affairs Medical Center; RPR, rapid plasma reagin.

*Laboratory Medicine* 2022;53:e113–e116; <https://doi.org/10.1093/labmed/lmab108>

## ABSTRACT

**Objective:** The impact of sexually transmitted infection (STI) results on prompting clinicians to consider pre-exposure prophylaxis (PrEP) indication is sparse in the literature, particularly for veterans.

**Methods:** A retrospective search from June 2018 to February 2020 was performed to identify all patients who were HIV-negative at a regional Veteran Affairs Medical Center with a positive STI test result and review the medical chart of these patients.

**Results:** We identified 220 veterans who were HIV-negative with a positive STI test result. Of these 220 veterans, 51 unique patients were identified by the clinicians. In a provider-initiated discussion, PrEP was discussed with all 51 patients. In the end, 27 of these 51 patients started PrEP after discussion with their clinical providers.

**Conclusion:** Prior positive STI results successfully helped identify patients who may benefit from PrEP. Quality assurance studies on clinician reactions to test result reporting, particularly regarding highly effective preventive therapies, are important.

Patient-focused integrated health systems have been described in the literature as being more likely to enable positive health outcomes in their patient populations, including managing patients who are being treated using pre-exposure prophylaxis (PrEP).<sup>1-4</sup> These integrated systems have access to a wealth of patient information including positive test results for a recent bacterial sexually transmitted infection (STI) that would suggest an elevated risk for HIV.<sup>5-8</sup> One may therefore expect an integrated health system to be able to efficiently identify potential PrEP candidates.<sup>5-8</sup> The laboratory has a role in obtaining STI test results and communicating these results to the clinical teams. However, there are currently no published English literature articles on a quality assurance (QA) study by a laboratory within such an integrated health system, particularly the Veteran Affairs system, to verify that these results are acted upon by clinical teams to consider reducing long-term HIV infection risk with PrEP when/if appropriate. Although the consideration of PrEP requires a clinician to consider the entire clinical picture, the presence of a recent STI represents 1 significant risk factor that suggests an increased chance of contracting HIV; thus, systems to identify patients who may benefit from PrEP would benefit from considering recent bacterial STI history.<sup>9-13</sup>

## Methods

A laboratory retrospective search from June 2018 to February 2020 was performed to identify all patients with a positive STI test result at a regional Veteran Affairs Medical Center (VAMC), specifically by polymerase chain reaction testing for gonorrhea/chlamydia and rapid plasma reagin (RPR). In addition, we reviewed HIV test results to exclude all patients who were already HIV-positive. Among the patients who were not HIV-positive, the medical record was reviewed to obtain basic demographic information and to determine whether there was any documentation of PrEP being discussed with the patient by the clinical primary care team or the infectious disease consulting staff. The clinical team caring for the patient was notified of the positive STI test result through a view alert in the electronic medical record system; in addition, the infectious disease team received regular monthly reports of the STI test results to identify patients who might benefit from PrEP initiation. The clinical team provided the appropriate treatment for the STI as clinically indicated. Within the electronic health

record, documentation of the discussion with the patient was placed by the clinicians into their medical notes or consultation requests. Institutional review board approval at the VAMC was obtained before this study.

## Results

A total of 220 unique patients who were not HIV-positive but had tested positive for at least 1 STI infection (gonorrhea, chlamydia, or positive RPR) were identified in the search. Demographically, approximately two-thirds of the total patients (219 male patients and 1 female patient) were African American (149 out of 220 patients) with an age distribution as noted in **TABLE 1**. Of these 220 patients, 51 received clinician-initiated discussion of PrEP; slightly more than half (27 out of 51 patients, or 52.9%) were African American, and almost half (23 out of 51 patients, or 45%) were in their fourth decade of life (see **TABLE 1**). The selection of these 51 patients for discussion of PrEP relied on physician discretion. An additional 6 patients from the total of 220 patients were additionally reviewed by the infectious disease service team as part of their clinical care but did not have a documented PrEP discussion or a prescription in the medical chart.

After discussion of the benefits and risks, 27 patients out of the 51 who had the clinician-initiated PrEP discussion were prescribed PrEP. These patients were predominantly male (26 out of 27 patients, or 96%), approximately half were either African American (11 out of 27 patients, or 41%) or Caucasian (12 out of 27 patients, or 44%), and nearly half (13 out of 27 patients, or 48%) were in their fourth decade of life (see **TABLE 1**).

## Discussion

Although there have been a number of significant advances in the treatment and prevention of HIV over the past decades, HIV still remains a very important public health concern and a serious chronic medical condition.<sup>12-14</sup> One of these advances in prevention includes the availability of PrEP, which can significantly reduce the risk of HIV infection in those who are at elevated risk of HIV.<sup>5-7</sup> However, to take full advantage of this advance, patients who are at high risk of HIV need to be identified.<sup>8-13</sup> A number of identification strategies have been documented in the literature, including selection based on only proactive patients who self-advocate for PrEP, universal screening, clinical support tools based on diagnosis codes, or complex machine-learning algorithms.<sup>8-14</sup> Although a recent positive bacterial STI in the past 6 months is a risk factor for HIV acquisition per the U.S. Preventive Services Task Force, the literature is sparse on provider-initiated discussions of PrEP that use an screening system that includes recent positive bacterial STI test results.<sup>6</sup> Literature-documented methods of clinical identification such as universal screening may be excessively broad or, in the case of self-identification, excessively narrow and restricted.<sup>12-14</sup> It has often been observed in practice that the onus is generally on the patient, who often must not only advocate for PrEP from the provider but also navigate a number of highly restrictive roadblocks to access this preventive measure.<sup>12-14</sup> These roadblocks have been reported even within integrated medical systems.<sup>12-14</sup> Considering the useful role that PrEP may play in HIV prevention, the setting of these roadblocks is counterproductive to the goal of optimizing HIV prevention.<sup>6,7,12-14</sup> That roadblocks are commonly reported in the literature is also rather atypical considering that many other preventive medicine procedures such as a preventive colonoscopy

**TABLE 1. Demographics of Patients with History of STI (CT/NG or RPR testing) and Those with Whom Clinician Initiated PrEP Discussion**

All Patients		PrEP Discussed	Patients Started PrEP	PrEP Not Discussed
Sex				
Male	219	50	26	169
Female	1	1	1	0
Race/ethnicity				
African American	149	27	11	122
Asian <sup>5</sup>	2	2	2	0
Hispanic	1	0	0	1
Native Hawaiian or other Pacific Islander	3	1	1	2
Caucasian	57	20	12	37
Mixed	3	0	0	3
Declined to answer	5	1	1	4
Age (y)				
<30	24	8	5	16
30–39	59	23	13	36
40–49	24	5	3	19
50–59	30	7	1	23
>60	83	8	5	75
First positive STI test				
NG/CT PCR testing	137	41	20	96
RPR	83	10	7	73

CT, chlamydia; NG, gonorrhea; PCR, polymerase chain reaction; PrEP, pre-exposure prophylaxis; RPR, rapid plasma reagin for syphilis; STI, sexually transmitted infection.

or smoking cessation counseling tend to be provider-initiated instead of requiring extensive patient advocacy.<sup>12</sup> The benefits of providing PrEP to patients at elevated risk for HIV acquisition are clear: PrEP can reduce the risk of HIV infection in adults, and in the appropriate patient, considerations regarding the risk of treatment are part of the standard of preventive care.<sup>4,7</sup> However, the clinical decision of whether PrEP should be offered or initiated depends on clinical discretion after considering all clinical factors. This clinical judgment depends on the primary care physician and potentially on other consulting medical professionals such as an infectious disease consultant. Notably, in our study, there were 6 patients who were reviewed by the infectious disease service staff but likely because of clinical discretion after consideration of numerous factors did not have a documented discussion or prescription for PrEP.

In clinical care, the most important and basic role of the laboratory is to provide information to answer clinical questions about either the diagnosis or the care of patients.<sup>15,16</sup> Laboratory QA initiatives that review how physicians react to laboratory test results are just as important as internal QA within the laboratory.<sup>15,16</sup> The way that a test is utilized for the care of a patient is important not only for determining the amount of precision needed for the laboratory assay but also to both determine that laboratory resources are being used appropriately and identify processes for improvement.<sup>16</sup> The importance of laboratory QA programs to monitor and evaluate medical laboratory services to identify situations requiring improvement is widely noted and even codified in the Joint Commission on Accreditation of Healthcare Organizations regulatory requirements.<sup>15</sup> Therefore, the lack of any publication in the English literature of a QA study from a laboratory on how clinicians are utilizing STI test results is particularly noteworthy because such material would represent an important laboratory QA parameter. This parameter could not only indicate the usefulness of STI test results and the resources needed to carry out such testing but also help identify laboratory and clinical initiatives that may improve patient care. No laboratory test, including STI results, needs to be excluded from QA; indeed, QA for STI results has been reported for other aspects of QA, although not for clinical reactions to prompt consideration of PrEP.<sup>17</sup> Therefore, this study represents the very first published QA study on the monitoring and evaluation of clinical reactions to bacterial STI results that altered the treatment of some patients by leading to a consideration of PrEP.

The veteran population treated at a VAMC is known to represent a different population than the general population because of differences in rates of comorbidities, demographics, and other population characteristics that could be roughly generalized as patients being “sicker.”<sup>18-21</sup> These significant differences ensure that conclusions reached regarding the general population do not always apply to the veteran population. Hence, studies on the veteran population in addition to studies on the general population hold a prime importance in the literature to ensure a complete understanding of most population-based health care topics. Indeed, the veteran population treated at a VAMC has been documented to have high adherence when PrEP is indicated (>90% adherence), far greater than the adherence of other general nonveteran populations (some <25% adherence).<sup>22,23</sup> This documented high adherence among the veteran population as a whole compared to that among the nonveteran population is a potential population difference that may lead to better efficacy of HIV prevention using PrEP in veteran populations.<sup>22</sup>

In this study’s regional VAMC, a retrospective QA and improvement review of the medical records of all patients with positive STI results

seen by the clinical providers and infectious disease team showed that 51 patients of the 220 patients who were HIV-negative were identified as potential PrEP candidates by their clinician. Of these 51 patients, 27 patients began PrEP after consideration of the risks and benefits. Therefore, the standard communication regarding STI laboratory results at this regional VAMC is contributing to clinical reactions to discuss preventive measures such as PrEP in a minimum of 51 out of 220 patients, or 23% of patients. The actual initiation of PrEP occurred in 12% of patients, or 27 out of 220 patients. The communication of STI results was therefore efficacious in assisting the clinical teams in identifying the small proportion of patients with recent STI-positive results who may benefit significantly from PrEP and likely contributed to a significant reduction in HIV infection risk in the appropriate patients. This experience highlights a QA monitoring project that given the lack of any similar QA projects published in the English literature may serve as a model for the monitoring of clinical reactions to STI results for HIV prevention. Future potential directions based on this QA model include interdisciplinary approaches to optimize treatment-related decisions based on laboratory results and to further elucidate clinician reasons for pursuing or not pursuing PrEP discussions to identify areas of potential improvement. In addition, although bringing up the topic of PrEP to the appropriate patients in the clinical visit and even starting PrEP are good initial benchmarks, the continuation of PrEP in the setting of continued high-risk behavior is also another important clinical care quality parameter that is unrelated to the STI test results.

## Conclusion

The integrated medical system at the VAMC successfully screened and identified patients who may benefit from PrEP. This finding is a significant example of an integrated medical system successfully screening and providing quality care for identified patients who otherwise would not have this health-preserving intervention. It also highlights the first QA study to look at the efficacy of STI communication in leading to provider-initiated PrEP discussions.

## REFERENCES

1. Petersen JM, Jhala DN. Valuable hospital and laboratory practice in an integrated medical system for HIV infection prevention interventions at a Veteran Affairs Medical Center (VAMC). *Am J Clin Pathol*. 2020;154(1):S131.
2. Conrad DA, Shortell SM. Integrated health systems: promise and performance. *Front Health Serv Manage*. 1996;13(1):3–40.
3. Gröne O, Garcia-Barbero M; WHO European Office for Integrated Health Care Services. Integrated care: a position paper of the WHO European Office for Integrated Health Care Services. *Int J Integr Care*. 2001;1:e21.
4. Marcus JL, Hurley LB, Hare CB, et al. Preexposure prophylaxis for HIV prevention in a large integrated health care system: adherence, renal safety, and discontinuation. *J Acquir Immune Defic Syndr*. 2016;73(5):540–546.
5. U.S. Public Health Service. *Preexposure prophylaxis for the prevention of HIV infection in the United States—2017 update: a clinical practice guideline*. <https://www.cdc.gov/hiv/pdf/risk/prep/cdc-hivprepguidelines-2017.pdf>. Published March 2018. Accessed November 15, 2021.
6. U.S. Preventive Services Task Force; Owens DK, Davidson KW, Krist AH, et al. Preexposure prophylaxis for the prevention of HIV infection: US Preventive Services Task Force recommendation statement. *JAMA*. 2019;321(22):2203–2213.

7. Chou R, Evans C, Hoverman A, et al. Preexposure prophylaxis for the prevention of HIV infection: evidence report and systematic review for the U.S. Preventive Services Task Force. *JAMA*. 2019;321(22):2214–2230.
8. Marcus JL, Hurley LB, Krakower DS, Alexeeff S, Silverberg MJ, Volk JE. Use of electronic health record data and machine learning to identify candidates for HIV pre-exposure prophylaxis: a modelling study. *Lancet HIV*. 2019;6(10):e688–e695.
9. Silapaswan A, Krakower D, Mayer KH. Pre-exposure prophylaxis: a narrative review of provider behavior and interventions to increase PrEP implementation in primary care. *J Gen Intern Med*. 2017;32(2):192–198.
10. Krakower DS, Gruber S, Hsu K, et al. Development and validation of an automated HIV prediction algorithm to identify candidates for pre-exposure prophylaxis: a modelling study. *Lancet HIV*. 2019;6(10):e696–e704.
11. Smith DK, Pals SL, Herbst JH, Shinde S, Carey JW. Development of a clinical screening index predictive of incident HIV infection among men who have sex with men in the United States. *J Acquir Immune Defic Syndr*. 2012;60(4):421–427.
12. Skolnik AA, Bokhour BG, Gifford AL, Wilson BM, Van Epps P. Roadblocks to PrEP: what medical records reveal about access to HIV pre-exposure prophylaxis. *J Gen Intern Med*. 2020;35(3):832–838.
13. Chartier M, Gyls-Cowell I, Van Epps P, et al. Accessibility and uptake of pre-exposure prophylaxis for HIV prevention in the Veterans Health Administration. *Fed Pract*. 2018;35(Suppl 2):S42–S48.
14. Garner W, Wilson BM, Beste L, Maier M, Ohl ME, Van Epps P. Gaps in preexposure prophylaxis uptake for HIV prevention in the Veterans Health Administration. *Am J Public Health*. 2018;108(S4):S305–S310.
15. Wong ET, Nelson JM. Quality assurance and the clinical laboratory. *JAMA*. 1988;259(17):2584–2585.
16. Skendzel LP. How physicians use laboratory tests. *JAMA*. 1978;239(11):1077–1080.
17. Petersen JM, Patel S, Dalal S, Jhala D. Gonorrhea and chlamydia specimen positivity rate by polymerase chain reaction at a regional Veteran Affairs Medical Center. *Lab Med*. 2021;52(2):e23–e29.
18. Agha Z, Lofgren RP, VanRuiswyk JV, et al. Are patients at Veterans Affairs Medical Centers sicker? *Arch Intern Med*. 2000;160:3252–3257.
19. Eibner C, Krull H, Brown KM, et al. Current and projected characteristics and unique health care needs of the patient population served by the Department of Veterans Affairs. *Rand Health Q*. 2016;5(4):13.
20. Morgan RO, Teal CR, Reddy SG, Ford ME, Ashton CM. Measurement in Veterans Affairs health services research: veterans as a special population. *Health Serv Res*. 2005;40(5 Pt 2):1573–1583.
21. Pollard MS, Amaral EF, Mendelsohn J, Cefalu M, Kress A, Ross R. Current and future demographics of the veteran population, 2014–2024. In *2016 Annual Meeting*. Population Association of America; 2016.
22. Huang M, Liu W, Plomondon ME, Prochazka AV, Bessesen MT. High adherence to HIV pre-exposure prophylaxis among veterans. *J Gen Intern Med*. 2018;33(3):253–255.
23. Sidebottom D, Ekström AM, Strömdahl S. A systematic review of adherence to oral pre-exposure prophylaxis for HIV—how can we improve uptake and adherence? *BMC Infect Dis*. 2018;18(1):581.

# Chylomicronemia Due to the Rare Hyperlipoproteinemia Type 3 Complicated by a Circulating Monoclonal Protein

Hiba Basheer, MD, ECNU, CCD,<sup>1</sup> Beheshteh Nakhaee, MD,<sup>1</sup> Ishwarlal Jialal, MD, PhD, FRCPATH, DABCC, DABCL<sup>1,\*</sup>

<sup>1</sup>Veterans Affairs Medical Center, Mather, California, United States; \*To whom correspondence should be addressed. [kjialal@gmail.com](mailto:kjialal@gmail.com)

**Keywords:** hyperlipidemia, chylomicronemia, M-protein, pancreatitis, diabetes, dysbetalipoproteinemia

**Abbreviations:** HLP3, hyperlipoproteinemia type 3; TG, triglycerides; VLDL-C, very-low-density lipoprotein cholesterol; HTG, hypertriglyceridemia; T2DM, type 2 diabetes mellitus; TC, total cholesterol; RR, reference range; LDL-C, low-density lipoprotein cholesterol; apoB, apolipoprotein B; apoE, apolipoprotein E.

*Laboratory Medicine* 2022;53:e117–e119; <https://doi.org/10.1093/labmed/lmab127>

## ABSTRACT

The polygenic variety of chylomicronemia occurs in adults in whom factors such as obesity, diabetes, alcoholism, renal disease, and certain drugs can precipitate chylomicronemia. A rare cause of polygenic chylomicronemia is hyperlipoproteinemia type 3 (HLP3). We report on a 54-year-old male who presented with chylomicronemia with triglycerides (TG) >2000 mg/dL. From admission, the ratio of total cholesterol to total triglycerides was not below 0.2 but was closer to 0.5, suggesting that his condition was not classic chylomicronemia. We confirmed that the patient had HLP3 based on his very-low-density lipoprotein cholesterol (VLDL-C)/TG ratio, which was  $\geq 0.3$ , and lipoprotein electrophoresis showing a broad beta band. Because he was not responsive to initial therapy, we considered an interferent impairing lipolysis and TG reduction. The interferent was an M-protein that may also have falsely elevated both apolipoprotein-B and direct-LDL-C levels. In this case study, we report on a patient with chylomicronemia resulting from HLP3 complicated by a circulating M-protein.

Chylomicronemia is defined as hypertriglyceridemia (HTG), a triglycerides (TG) level >885 mg/dL (10 mmol/L), and it occurs in 1/600 persons.<sup>1–5</sup> It can be monogenic, resulting from rare primary genetic causes (5% of patients) such as homozygous mutations in lipoprotein lipase, and it has an early onset with clinical presentation by adolescence. More commonly chylomicronemia

is of the polygenic variety (95%), which occurs in adults in whom secondary factors such as obesity, diabetes, alcoholism, renal disease, and certain drugs can precipitate chylomicronemia.<sup>1–5</sup> The most serious complication of this syndrome is acute pancreatitis, which occurs with TG >885 mg/dL (10 mmol/L) and is greatest with TG >1770 mg/dL (20 mmol/L).<sup>1–5</sup>

A rare cause of polygenic chylomicronemia is the very uncommon disorder referred to as hyperlipoproteinemia type 3 (HLP3), also known as dysbetalipoproteinemia or broad beta disease,<sup>6,7</sup> and it is not often mentioned in the literature.<sup>5</sup> We report on a patient with chylomicronemia caused by HLP3 who presented with an elevated TG level >2000 mg/dL that was precipitated by obesity, severely uncontrolled diabetes mellitus, and possible chronic excess alcohol intake.

## Report of Case

Our patient was a 54-year-old man with a past medical history significant for diabetes mellitus type 2 (T2DM), hypertension, obesity, and hyperlipidemia. His relevant family history was positive for T2DM (mother and father) and hyperlipidemia (father). His social history was positive for smoking cigarettes (2–3 daily) for more than 10 years and drinking alcohol (4–8 drinks), especially on the weekends, for the last several years. Since 2012, the patient had shown elevated lipids and was placed on a lipid-lowering agent. He was diagnosed with T2DM in 2018 and was started on metformin 1.0 g/day and simvastatin 20 mg daily. The patient was non-compliant with his treatment and had stopped all medications at his initial presentation at our primary care clinic early in 2021. His complaints at this visit included muscle cramping, abdominal pain, and weight loss.

Laboratory tests revealed elevated total cholesterol (TC) >1000 mg/dL (reference range [RR], <200 mg/dL) and elevated total TG >2000 mg/dL (RR, <150 mg/dL) with a confirmed value with dilution of 2307 mg/dL. The patient was sent to the emergency department for admission, where his vitals were stable: temperature 98°F, heart rate 94 beats/minute, blood pressure 135/77 mm Hg, and respiratory rate 18/minute. Physical examination revealed a body mass index of 35.6 kg/m<sup>2</sup> (obesity) with no neuropathy, lipemia retinalis, hepatosplenomegaly, eruptive or palmar xanthoma, or abdominal tenderness. All pulses were palpable and there was no history of intermittent claudication. Additional laboratories revealed an elevated blood glucose of 365 mg/dL and an HbA1c of 14.5%, bicarbonate of 15 mmol/L (RR, 23–33 mmol/L), sodium 128 mmol/L (RR, 136–144 mmol/L), creatinine of 0.86 mg/dL (RR, 0.5–1 mg/dL), and thyrotropin of 2.1 microU/mL (RR, 0.34–5.6 microU/mL).

The patient was admitted to the hospital and started on subcutaneous insulin for uncontrolled hyperglycemia and a combination of

atorvastatin 40 mg/day, fenofibrate 145 mg/day, and a generic fish oil combination to lower the severe HTG of TG >2000 mg/dL. Although his glucose levels fell from admission within a week to 197 mg/dL on the subcutaneous insulin therapy, his TG level remained >2000 mg/dL and the endocrinology team was consulted. They recommended initiating icosapent ethyl 2 g twice daily and continuing with atorvastatin 40 mg/day and fenofibrate 145 mg/day. This treatment failed to lower his TG for another 3 days. The patient was transferred to the intensive care unit and was placed on an intravenous insulin drip, which successfully lowered both his TC and TG level to 567 mg/dL and 803 mg/dL, respectively. The patient improved clinically and was discharged home. His antidiabetic medications included lantus insulin 15 units/day, aspart insulin 5 units before each meal, and metformin 1.5 g/day.

The patient's 1-week postdischarge laboratories showed a TC of 421 mg/dL and TG of 611 mg/dL. During outpatient follow-up visits, his TG levels decreased to 187 mg/dL with a direct low-density lipoprotein cholesterol (LDL-C) of 155 mg/dL with a high apolipoprotein-B (apoB) level of 230 mg/dL. His therapies included fenofibrate 145 mg daily, atorvastatin 40 mg daily, and icosapent ethyl 2000 mg twice daily. Because his LDL-C level after discharge was >100 mg/dL, ezetimibe 10 mg/day was added to his regime. His most recent lipid profile 4 months after discharge revealed TC 167 mg/dL, TG 391 mg/dL, direct-LDL-C 61 mg/dL, and high-density lipoprotein cholesterol 31 mg/dL. In addition, his most recent antidiabetic medications included lantus insulin 22 units/day, empagliflozin 12.5 mg/day, metformin 1.5 g/day, and he showed an HbA1c of 6.9%.

From admission, the patient's TC/TG ratio was not below 0.2 but was closer to 0.5. In classic adult chylomicronemia (hyperlipoproteinemia type 5), because of the excessively elevated very-low-density lipoprotein cholesterol (VLDL-C) and chylomicron particles, which are predominantly TG-carrying lipoproteins, the TC/TG ratio is <0.2 because the TC level compared to the TG level is <20%.<sup>1-5,8</sup> Hence we considered that the patient had possible type 3 dyslipidemia because of his elevated TC/TG ratio. As shown in **TABLE 1**, his VLDL-C/TG ratio was  $\geq 0.3$  and his lipoprotein electrophoresis (**FIGURE 1, LANE 19**) showed a broad beta band confirming HLP3.<sup>6,7</sup> Apolipoprotein E (apoE) genotyping showed an E3/4 pattern consistent with HLP3.<sup>10</sup>

The M-protein can bind to TG-rich lipoproteins and interfere with their clearance.<sup>11</sup> Serum protein electrophoresis was conducted and revealed an M-protein in the gamma region, quantified as 0.45 g/dL and

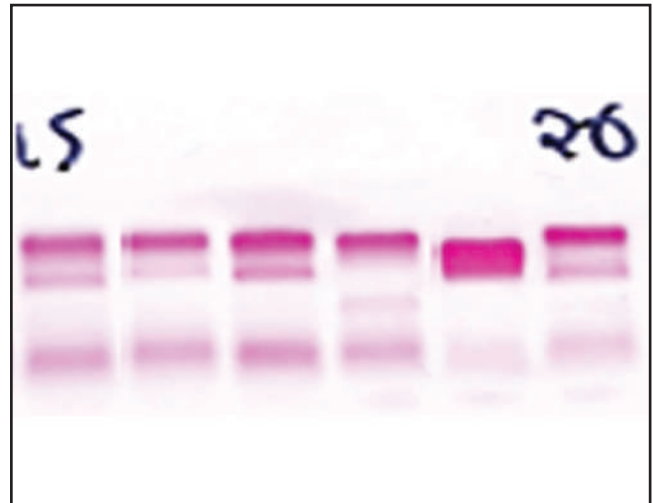
**TABLE 1. Representative Fasting Lipid and Lipoprotein Levels**

Lipid Levels	Date 1/21	Date 2/21
TC (mg/dL)	567	324
Total TG (mg/dL)	803	377
HDL-C (mg/dL)	14	21
Direct-LDL-C (mg/dL)	186	182
Non-HDL-C (mg/dL)	553	303
VLDL-C (mg/dL)	367	121
VLDL-C/TG ratio	0.46	0.32

HDL-C, high-density lipoprotein cholesterol; LDL-C, low-density lipoprotein cholesterol; TC, total cholesterol; TG, triglycerides; VLDL-C, very-low-density lipoprotein cholesterol.

LDL-C was quantified by a direct homogenous assay. VLDL-C was calculated as recommended by Nordestgaard et al.<sup>9</sup>

**FIGURE 1. Lipoprotein electrophoresis.** The gels of 6 patients—lanes 15–20—are shown. The 3 bands from top to bottom for each patient are beta-LDL, pre-beta-VLDL, and alpha-HDL. Our patient's specimen is in lane 19. It shows a broad beta band spanning both the beta (LDL) and pre-beta (VLDL) areas unlike that of the other patients showing discrete beta and pre-beta bands. This pattern is consistent with HLP3.<sup>6,7</sup> HLP3, hyperlipoproteinemia type 3; HDL, high-density lipoprotein; LDL, low-density lipoprotein; VLDL, very-low-density lipoprotein.



characterized by immunofixation as IgG lambda. A free light chain assay was performed to determine the patient's risk for myeloma and was normal (0.89 [RR, 0.26–1.65]).

## Discussion

Chylomicronemia in adults is usually of the polygenic variety.<sup>1-5</sup> In patients with familial HTG, familial combined hyperlipidemia and HLP3 secondary factors precipitate the severe HTG.<sup>1-7</sup> These secondary factors include diabetes, obesity, alcohol excess, chronic kidney diseases, hypothyroidism, high estrogen states, and certain drugs (eg, diuretics, corticosteroids, protease inhibitors, retinoids, atypical antipsychotics, L-asparaginase, bile acid sequestrants, immunosuppressants, propofol).<sup>1-6</sup> Patients can present with eruptive xanthoma, lipemia retinalis, and hepatosplenomegaly as part of the full chylomicronemia syndrome.<sup>1-6</sup> The greatest risk for these patients is acute pancreatitis; TG levels need to be lowered to <500 mg/dL to mitigate this major risk.<sup>1-7</sup> In addition to removing secondary causes, including alcohol intake and both fat and calorie intake, therapies that are efficacious in achieving this goal include fibrates, statins, icosapent ethyl, and insulin, especially in a patient with diabetes.<sup>1-6</sup>

We have presented a patient with chylomicronemia resulting from the rare HLP3 in which HTG was initially refractory to treatment and required insulin infusion rather than subcutaneous insulin. Factors that contributed to his HTG include uncontrolled T2DM (HbA1c 14.5%), excess alcohol intake, and obesity. Both T2DM and obesity are predisposing factors for the expression of HLP3. Most important, the patient had a VLDL-C/TG ratio  $\geq 0.3$  (which was diagnostic) and a broad beta band on lipoprotein electrophoresis.<sup>6,7</sup> The diagnosis of

HLP3 was also based on his apoE genotyping, which revealed a 3/4 genotype that is present in 21% of patients, according to Evans et al.<sup>10</sup> In their series, the classic apoE 2/2 genotype was present in only 16% of patients.

Because the patient did not respond to therapy for a week, we considered that he might have an M-protein that could interfere with lipolysis, which we subsequently confirmed.<sup>11</sup> In addition, this M-protein potentially interfered with the apoB measurement of 230 mg/dL by the Roche assay and direct-LDL-C, accounting for much higher values than what is seen in patients with classic HLP3 in whom both apoB and LDL-C are usually normal.<sup>6,7</sup> Measurement of apoB using the Beckman assay revealed a more realistic value of 124 mg/dL, suggesting lesser interference with this immunoturbidimetric assay by the M-protein. It is well known that M-proteins interfere with many assays, especially those for apoB and direct-LDL-C, as with our patient.<sup>12,13</sup> The product insert from both assay vendors mentions this potential interference. However, because we did not investigate this potential interference, we can only speculate about this scenario.

It is also possible that the patient had both a type 3 and type 2B pattern, accounting for the high LDL-C and apoB, but this prospect is unlikely and we suggest that both high levels resulted from potential interference from the M-protein.<sup>12,13</sup>

## Conclusion

Intensive therapy with a statin, fibrate, icosapent ethyl, and ezetimibe lowered our patient's TC (LDL-C, 61 mg/dL) and TG (<500 mg/dL) levels to threshold levels, minimizing his risk for pancreatitis and cardiovascular diseases. The greatest risk of severe HTG, chylomicronemia, is acute pancreatitis.

In a patient with chylomicronemia, if the TC/TG ratio is not <0.2, then one should consider HLP3 as a differential diagnosis. It can be diagnosed by clinical features coupled with an elevated VLDL-C/TG ratio  $\geq 0.3$  and a broad beta band on lipoprotein electrophoresis. In addition, apo-E genotyping can be useful.

If there is inadequate response to fibrate therapy combined with statins, icosapent ethyl, and subcutaneous insulin despite a reduction in hyperglycemia within 5 days, one should consider that there may be an interferent—as in our patient, the presence of an M-protein. This type of protein can also potentially interfere with certain assays such as those for apoB and direct-LDL-C, but this possibility was not tested directly. An insulin infusion usually reverses HTG, as happened with our patient.

## Acknowledgments

We thank the patient for consent to publish, Dr. Gail A. Wong for help in managing this patient, and Dr. R. Young at LabCorp for performing the lipoprotein electrophoresis. Both HB and BN produced the first few drafts. IJ edited all drafts and helped with developing the discussion. All authors contributed to all drafts and approved the final version.

## REFERENCES

1. Hegele RA, Ginsberg HN, Chapman MJ, et al.; European Atherosclerosis Society Consensus Panel. The polygenic nature of hypertriglyceridaemia: implications for definition, diagnosis, and management. *Lancet Diabetes Endocrinol.* 2014;2(8):655–666.
2. Brahm AJ, Hegele RA. Chylomicronemia—current diagnosis and future therapies. *Nat Rev Endocrinol.* 2015;11(6):352–362.
3. Chait A, Eckel RH. The chylomicronemia syndrome is most often multifactorial: a narrative review of causes and treatment. *Ann Intern Med.* 2019;170(9):626–634.
4. Kushner PA, Cobble ME. Hypertriglyceridemia: the importance of identifying patients at risk. *Postgrad Med.* 2016;128(8):848–858.
5. Goldberg RB, Chait A. A comprehensive update on the chylomicronemia syndrome. *Front Endocrinol (Lausanne).* 2020;11:593931.
6. Jialal I, Amess W, Kaur M. Management of hypertriglyceridemia in the diabetic patient. *Curr Diab Rep.* 2010;10(4):316–320.
7. Hopkins PN, Brinton EA, Nanjee MN. Hyperlipoproteinemia type 3: the forgotten phenotype. *Curr Atheroscler Rep.* 2014;16(9):440.
8. Stroes E, Moulin P, Parhofer KG, Rebours V, Löhner JM, Averna M. Diagnostic algorithm for familial chylomicronemia syndrome. *Atheroscler Suppl.* 2017;23:1–7.
9. Nordestgaard BG, Langlois MR, Langsted A, et al.; European Atherosclerosis Society (EAS) and the European Federation of Clinical Chemistry and Laboratory Medicine (EFLM) Joint Consensus Initiative. Quantifying atherogenic lipoproteins for lipid-lowering strategies: consensus-based recommendations from EAS and EFLM. *Atherosclerosis.* 2020;294:46–61.
10. Evans D, Beil FU, Aberle J. Resequencing the APOE gene reveals that rare mutations are not significant contributory factors in the development of type III hyperlipidemia. *J Clin Lipidol.* 2013;7(6):671–674.
11. Misselwitz B, Goede JS, Pestalozzi BC, Schanz U, Seebach JD. Hyperlipidemic myeloma: review of 53 cases. *Ann Hematol.* 2010;89(6):569–577.
12. Bakker AJ, Mücke M. Gammopathy interference in clinical chemistry assays: mechanisms, detection and prevention. *Clin Chem Lab Med.* 2007;45(9):1240–1243.
13. Jialal I, Remaley AT. Measurement of low-density lipoprotein cholesterol in assessment and management of cardiovascular disease risk. *Clin Pharmacol Ther.* 2014;96(1):20–22.

# Acquired FVII Deficiency and Acute Myeloid Leukemia: A Case Report and Literature Review

Emna Hammami, MD,<sup>1,\*</sup> Wijden El Borgi, MD,<sup>1,3</sup> Fatma Ben Lakhal, MD,<sup>1,3</sup> Sarra Fekih Salem, PhD,<sup>1,3</sup> Hend Ben Neji, MD,<sup>2,3</sup> and Emna Gouider, MD<sup>1,3</sup>

<sup>1</sup>Department of Biological Hematology, Aziza Othmana Hospital, Tunis, Tunisia; <sup>2</sup>Department of Clinical Hematology, Aziza Othmana Hospital, Tunis, Tunisia; and <sup>3</sup>UR14ES1 University of Tunis El Manar, Tunisia; \*To whom correspondence should be addressed. emnahammami1993@gmail.com

**Abbreviations:** FVII, Factor VII; aFVIIID, acquired FVII deficiency; AML, acute myeloid leukemia; CBC, complete blood count; CRP, C-reactive protein; PT, prolonged prothrombin time; aPTT, activated partial thromboplastin time; PCCFD, prothrombin complex coagulation factors dosing; CFDs, coagulation factor deficiencies; TF, tissue factor; M, male; F, female; NM, value not mentioned; rFVIIa, activated recombinant factor VII; CR, complete remission; ALL, acute lymphoblastic leukemia; ND, not done, FFP, fresh frozen plasma

*Laboratory Medicine* 2022;53:e120–e122; <https://doi.org/10.1093/labmed/lmab120>

## ABSTRACT

Factor VII (FVII) deficiency is the most common among all rare inherited bleeding disorders. However, acquired FVII deficiency (aFVIIID) is uncommon. Only few cases in the literature have been reported. Herein, we present a case of an aFVIIID associated with acute myeloid leukemia (AML), along with a literature review regarding this condition. A 50 year old Arab male patient was diagnosed with AML at the hematology department of our institution. At admission, coagulation tests showed a prolonged prothrombin time (PT) with a normal activated partial thromboplastin time (aPTT) and a slightly elevated fibrinogen level. Prothrombin complex coagulation factors dosing (PCCFD) revealed a decrease only in FVII levels. The patient, however, did not experience any bleeding. The evolution of the health of the patient was marked by a normalization of PT and FVII levels and complete remission.

Factor VII (FVII) deficiency is the most common among all rare inherited bleeding disorders.<sup>1</sup> However, acquired FVII deficiency (aFVIIID) is uncommon,<sup>2</sup> and aFVIIID associated with acute leukemia is even rarer—only a few cases of this latter type have been reported in the literature. Herein, we report the case of an aFVIIID associated with acute myeloid leukemia (AML), as well as providing a brief review of the current literature on this topic.

## Case Report

A 50 year old Arab man presented at the Aziza Othmana Hospital in Tunis, Tunisia, with acute abdominal pain; he was diagnosed with appendicitis. His preoperative complete blood count (CBC) showed anemia and thrombocytopenia. Hence, the patient was referred to the hematology department of our institution for further care. At admission, his CBC revealed pancytopenia: anemia, thrombocytopenia, and neutropenia. The results of his biochemistry panel tests are reported in **TABLE 1**. The blood film showed myeloblasts, and the diagnosis of acute myeloid leukemia (AML) with normal karyotype was confirmed in our hematology department. The patient had an infection with fever and C-reactive protein (CRP) of 203.9 mg/L.

Chemotherapy was started promptly, after diagnosis confirmation with bone marrow specimen collection and immunophenotyping. The patient received an AML 7 + 3 chemotherapy regimen as an induction. This regimen includes infusions of cytarabine 200 mg/m<sup>2</sup>/day continuously for 7 days and idarubicin 12 mg/m<sup>2</sup>/day for 3 days.

At diagnosis, coagulation tests showed prolonged prothrombin time (PT) (**TABLE 2**) with normal activated partial thromboplastin time (aPTT) and slightly elevated fibrinogen level. The patient had no known personal or family history of bleeding disorders. No coagulation testing history prior to AML diagnosis was reported. Vitamin K therapy was attempted because the patient had an infection and was at greater risk than usual for developing hypovitaminosis K. The patient did not respond to vitamin K therapy.

Meanwhile, we performed a mixing study with a pool of normal plasma specimens (1:1). The results showed a total correction of the PT. We also performed prothrombin complex coagulation factors dosing (PCCFD) (**TABLE 2**) using a chronometric method on an ACL TOP 350 instrument (Werfen). The results revealed a decrease only in FVII levels (23.1%). FVII testing was repeated on a different blood specimen to eliminate the effect of preanalytic conditions causing falsely low FVII levels.

The evolution was marked by a spontaneous normalization of PT and FVII levels. FVII-level normalization was confirmed at the second cycle of consolidation chemotherapy, 5 months after the diagnosis of FVII deficiency. Hence, the diagnosis of aFVIIID was established. In the meantime, the patient did not experience any bleeding symptoms.

## Discussion

Because we present, herein, a case of a rare aFVIIID associated with AML, we should emphasize the specific details of this case. Our patient had

**TABLE 1. Blood Test Results at Time of Leukemia Diagnosis<sup>a</sup>**

Variable	Value (Range)
Complete Blood Count, value (range)	
Hemoglobin, g/dL	9.6 (13–18)
Mean corpuscular volume (fl)	84.9 (78–98)
Mean corpuscular hemoglobin (pg), $\times 10^9/L$	30.9 (26–34)
Platelets	17 (15–40)
WBC	3.7 (4–11)
Neutrophils	0.49 (1.4–7.7)
Lymphocytes	1.05 (1–4.8)
Monocytes	0.21 (0.18–1)
Eosinophils	0 (0.02–0.63)
Biochemistry Panel Tests	
Alkaline phosphatase (IU/L)	63 (40–129)
Gamma glutamyltransferase (IU/L)	49 (7–64)
Alanine aminotransferase (IU/L)	4 (10–40)
Aspartate aminotransferase (IU/L)	7 (10–40)
Creatinine (mg/dL)	0.45 (0.84–1.24)

<sup>a</sup>Case individual is a 50 year old Arab man.

**TABLE 2. Coagulation Tests Results for Our Case Individual<sup>a</sup>**

Screening coagulation testing	PT (patient, no. (range) = 18.5 (11–13.5) s
	PT (normal, no. (range) = 11.5 (11–13.5) s
	Ratio = 1.6 (0.8–1.2)
	Activated partial thromboplastin time (patient) = 30.5 s
	Activated partial thromboplastin time (normal) = 32 s
	Ratio, value (range) = 0.95 (0.8–1.2)
Mixing studies, value (range)	Fibrinogen, value (range) = 4.2 (2–4) g/L
	PT (patient + normal) = 13.1 (11–13.5) s
Prothrombin complex factors at diagnosis, % (range)	PT (normal) = 11.5 (11–13.5) s
	Ratio = 1.13 (0.8–1.2)
	Factor VII = 23.1% (70%–120%)
	Factor X = 107.5% (70%–120%)
PT after 5 mo	Factor V = 107.5% (70%–120%)
	Factor II = 64.9% (70%–120%)
	Patient = 11.3 s
Factor VII after 5 mo, % (range)	Normal = 11.5 s
	Ratio, no. (range) = 0.98 (0.8–1.2)
	Factor VII = 84.6% (70%–120%)

PT, prothrombin time.

<sup>a</sup>Case individual is a 50 year old Arab man.

isolated aFVIID with no proof of an anti-FVII and did not experience any bleeding; his condition did not respond to vitamin K therapy.

In most cases, aFVIID is associated with other coagulation factor deficiencies (CFDs), such as the majority of acquired CFD.<sup>3</sup> The most common cause of aFVIID is hypovitaminosis K due to insufficient intake, malabsorption, or anti-vitamin K drugs such as warfarin. This condition manifests as a deficiency in FVII, FIX, FII, and FX. Intravascular disseminated coagulopathy and hepatic dysfunction can also cause a decrease in FVII levels, which can

be associated with other CFDs. Because FVII has the shortest lifespan, those conditions may initially manifest as an isolated FVII deficiency and lead to a prolongation of PT.

Persistently isolated aFVIID, however, is extremely rare, and it appears to be underdiagnosed.<sup>4</sup> Herein, we present a case of aFVIID in association with acute leukemia. This association has only been mentioned in a few cases in the literature<sup>4–7</sup> (TABLE 3).

Patients with acute leukemia have increased bleeding risk due to common thrombocytopenia.<sup>8</sup> This risk may also be due to sepsis and disseminated intravascular coagulopathy.<sup>9</sup> Hence, vigorous and early monitoring of coagulation test results is crucial.

Developing a CFD, such as FVII, significantly increases the risk of bleeding in those patients. The underlying mechanisms of this aFVIID are probably entangled, likely due to:

- An excessive consumption due to the binding of FVII to tissue factor (TF). Because intensive chemotherapy used in acute leukemia is known to alter the endothelium, it leads to increased TF exposure.
- Protein degradation of FVII due to the release of proteolytic enzymes by leukocytes, as observed in patients with sepsis.
- A neutralizing antibody directed against FVII (anti-FVII).<sup>10</sup>

Isolated aFVIID was reported in association with infection and tumors.<sup>4,11,12</sup> Also, anti-FVII was present in nearly half of the few previously described cases in the literature.<sup>13–16</sup> In aFVIID associated with acute leukemia, anti-FVII was identified in vitro only in 1 case.<sup>5</sup> In our case, the results of mixing studies were not in favor of an inhibitor. Our patient was, however, receiving intensive chemotherapy and had an infection by the time of his aFVIID diagnosis.

Also, our patient did not experience any bleeding, which was inconsistent with the reported cases of aFVIID in the literature. According to a review by Mulliez and Devrees,<sup>2</sup> bleeding occurred in 48% of the studied cases. Despite Anoun et al and White et al<sup>5,6</sup> reporting a higher level of FVII, their patients experienced severe bleeding symptoms.

In fact, the level of FVII is unrelated to the phenotype of bleeding. It may be associated with a broad variety of clinical symptoms, varying from no or minimal bleeding to life-threatening situations. Some authors set the 30% level of FVII as a hemostatic level.<sup>17</sup> However, this cut-off should be approached with caution because measurement variability differs depending on the couple of automated reagent used for clotting-factor dosing.<sup>18</sup> The impact of entangled aFVIID physiopathological mechanisms on the bleeding phenotype is also worth considering. Further studies could seek a better understanding of these acquired CFD mechanisms, along with assessing a possible correlation to the occurrence of bleedings.

The presence of aFVIID in patients with acute leukemia appears to be associated with poor outcomes (TABLE 3). However, the deaths observed in those cases were most likely caused by the underlying disease. Still, in the cases reported by Toor et al and Anoun et al,<sup>4,5</sup> the deaths reported were directly due to hemorrhage. Our patient, however, experienced complete remission.

## Conclusion

This case emphasizes the importance of carefully assessing bleeding risk and interpreting coagulation panels in patients with acute leukemia. Because coagulation disorders can be life-threatening, physicians

**TABLE 3. Acquired Factor VII Deficiency Associated with Acute Leukemia in the Literature: Clinical and Laboratory Data**

Reference	Sex	Age, y	Diagnosis	Bleeding	PT (s)	FVII Level (%)	Inhibitor Antibody <sup>a</sup>	Treatment	Outcome
White et al (1999) <sup>6</sup>	M	NM	AML	Hemoptysis	19	35	NM	rFVIIa	CR
Toor et al (2002) <sup>4</sup>	M for AML and F for ALL		AML (n = 1) ALL (n = 1) Other diagnosis (n = 6)	Oral mucosal hemorrhage, gastrointestinal, pituitary subarachnoid	NM	Mean (range), 22 (8–35)	ND	Platelet FFP	Death
Anoun et al (2015) <sup>5</sup>	M	50	AML	Nasal and sinus hematoma	NM	35	Yes	FFP	Death
Moosavi et al (2019) <sup>7</sup>	F	41	AML	Mucocutaneous bleeding	16.5	49	No	No	CR, PT back to normal
This case study (2021)	M	50	AML	No	18.5	23.1	No	No	CR, PT back to normal

M, male; F, female; NM, value not mentioned; AML, acute myeloid leukemia; rFVIIa, activated recombinant factor VII; CR, complete remission; ALL, acute lymphoblastic leukemia; ND, not done; FFP, fresh frozen plasma; PT, prothrombin time.

<sup>a</sup>Suspected given the absence of PT correction in the mixing studies.

should watch out for those disorders in patients with acute leukemia. In fact, diagnosing an FVII deficiency is not likely to be challenging— for instance, it could be easily suspected in cases involving isolated prolonged PT.

### Personal and Professional Conflict of Interest

None reported.

### REFERENCE

- da Silva VA, Silva SS, Martins FF. Acquired deficiency of coagulation factor VII. *Rev Bras Hematol Hemoter.* 2015;37(4):269–271.
- Mulliez SM, Devreese KM. Isolated acquired factor VII deficiency: review of the literature. *Acta Clin Belg.* 2016;71(2):63–70.
- Girolami A, Santarossa C, Cosi E, Ferrari S, Lombardi AM. Acquired isolated FVII deficiency: an underestimated and potentially important laboratory finding. *Clin Appl Thromb Hemost.* 2016;22(8):705–711.
- Toor AA, Slungaard A, Hedner U, Weisdorf DJ, Key NS. Acquired factor VII deficiency in hematopoietic stem cell transplant recipients. *Bone Marrow Transplant.* 2002;29(5):403–408.
- Anoun S, Lamchahab M, Oukkache B, Qachouh M, Benchekroun S, Quessar A. Acquired factor VII deficiency associated with acute myeloid leukemia. *Blood Coagul Fibrinolysis.* 2015;26(3):331–333.
- White B, Martin M, Kelleher S, Browne P, McCann SR, Smith OP. Successful use of recombinant FVIIa (Novoseven) in the management of pulmonary haemorrhage secondary to Aspergillus infection in a patient with leukaemia and acquired FVII deficiency. *Br J Haematol.* 1999;106(1):254–255.
- Moosavi L, Bowen J, Coleman J, Heidari A, Cobos E. Acute myelogenous leukemia with trisomy 8 and concomitant acquired factor VII deficiency. *J Investig Med High Impact Case Rep.* 2019;7:2324709619872657.
- Webert K, Cook RJ, Sigouin CS, Rebullia P, Heddle NM. The risk of bleeding in thrombocytopenic patients with acute myeloid leukemia. *Haematologica.* 2006;91(11):1530–1537.
- Uchiumi H, Matsushima T, Yamane A, et al. Prevalence and clinical characteristics of acute myeloid leukemia associated with disseminated intravascular coagulation. *Int J Hematol.* 2007;86(2):137–142.
- Franchini M, Lippi G, Favaloro EJ. Acquired inhibitors of coagulation factors: part II. *Semin Thromb Hemost.* 2012;38(5):447–453.
- Anand M, Babbar N. Acquired factor VII deficiency in association with pyelonephritis. *J Assoc Physicians India.* 2018;66(5):95–96.
- Granger J, Gidvani VK. Acquired factor VII deficiency associated with Wilms tumor. *Pediatr Blood Cancer.* 2009;52(3):394–395.
- Delmer A, Horellou M-H, Andreu G, et al. Life-threatening intracranial bleeding associated with the presence of an antifactor VII autoantibody. *Blood.* 1989;74(1):229–232.
- Okajima K, Ishii M. Life-threatening bleeding in a case of autoantibody-induced factor VII deficiency. *Int J Hematol.* 1999;69(2):129–132.
- Aguilar C, Lucía JF, Hernández P. A case of an inhibitor autoantibody to coagulation factor VII. *Haemophilia.* 2003;9(1):119–120.
- Kamikubo Y, Miyamoto S, Iwasa A, Ishii M, Okajima K. Purification and characterization of factor VII inhibitor found in a patient with life threatening bleeding. *Thromb Haemost.* 2000;83(1):60–64.
- Giansily-Blaizot M, Verdier R, Biron-Adréani C, et al; Study Group of FVII Deficiency. Analysis of biological phenotypes from 42 patients with inherited factor VII deficiency: can biological tests predict the bleeding risk? *Haematologica.* 2004;89(6):704–709.
- Takamiya O, Ishikawa S, Ohnuma O, et al. Japanese collaborative study to assess inter-laboratory variation in factor VII activity assays. *J Thromb Haemost.* 2007;5(8):1686–1692.

# Multisite *Pseudomonas aeruginosa* Infections Detected by Metagenomic Next-Generation Sequencing in a Child with Aplastic Anemia: A Case Report

Shu-yu Lai, MD, Fang Liu, MD, Li Chang, MD, Guang-lu Che, MD, Qiu-xia Yang, MD, Yong-mei Jiang, PhD, Jie Teng, MD\*

Department of Laboratory Medicine, West China Second University Hospital, and Key Laboratory of Obstetric and Gynecologic and Pediatric Diseases and Birth Defects of Ministry of Education, Sichuan University, Chengdu, China;  
\*To whom correspondence should be addressed. [854560484@qq.com](mailto:854560484@qq.com)

**Keywords:** metagenomic next-generation sequencing, aplastic anemia, infection, *Pseudomonas aeruginosa*, bacterial culture, pathogen detection

**Abbreviations:** AA, aplastic anemia; mNGS, metagenomic next-generation sequencing; VSAA, very severe aplastic anemia; BALF, bronchoalveolar lavage fluid; CSF, cerebrospinal fluid.

*Laboratory Medicine* 2022;53:e123–e125; <https://doi.org/10.1093/labmed/lmab123>

## ABSTRACT

Microbial cultivation is the current gold standard for the clinical diagnosis of bacterial infections. However, this method sometimes produces false negative results. We present a case study of multisite *Pseudomonas aeruginosa* infections detected by metagenomic next-generation sequencing in a child with aplastic anemia, highlighting the rapid and accurate advantages of this technique.

Aplastic anemia (AA) is characterized by decreased proliferation of bone marrow hematopoietic cells and peripheral blood pancytopenia. Infection is the leading cause of death in patients with severe AA.<sup>1</sup> *Pseudomonas aeruginosa* (*P. aeruginosa*) is a gram negative bacterium, which has been determined to be one of the most common and important pathogens during the past few decades,<sup>2</sup> especially in patients with hematologic diseases. The detection of *P. aeruginosa* by the traditional culture method generally takes approximately 2 to 4 days; however, false negative results sometimes occur because of the use of antibiotics or low bacterial load in some kinds of specimens. When the pathogenic type of the infection is not clear, the use of broad-spectrum antibiotics will increase the pathogen's resistance to antibiotics.<sup>3,4</sup> Research has shown that *P. aeruginosa* has a high intrinsic and acquired antibiotic resistance that makes its treatment challenging. Therefore, it is crucial to rapidly

and accurately identify the infectious pathogens and then optimize clinical anti-infective treatment.

Metagenomic next-generation sequencing (mNGS) is an emerging detection technique for supporting pathogen diagnosis without the requirement of preclinical prediction or culture.<sup>5</sup> Studies have shown that mNGS is capable of identifying novel or rare pathogens by determining all sequences of microbial genomes in clinical specimens within 24 to 48 hours,<sup>6</sup> which is conducive to the diagnosis of infectious diseases.

Herein, we report the application of mNGS to identify pathogens in a patient with very severe aplastic anemia (VSAA) whose blood bacterial cultures were negative. In this patient, *P. aeruginosa* was detected in blood, bronchoalveolar lavage fluid (BALF), and cerebrospinal fluid (CSF), respectively.

## Case Report

A 10-year-old boy with VSAA (meeting the criteria for severe disease and absolute neutrophil count  $<0.2 \times 10^9/L$ ) was admitted to our hospital because of cellulitis with fever for 1 month. During hospitalization, the patient received a transfusion of irradiated red blood cell suspension and irradiated apheresis platelets to alleviate the symptoms of hypoxia and bleeding caused by AA. In the early stage of the disease before he was hospitalized, a 3 cm  $\times$  3 cm lesion was seen on the right chest wall of the child without oozing pus or blood. Routine skin care was given and antibiotics such as vancomycin, imipenem, and micafungin were empirically used for anti-infection treatment but with little effect. Subsequently, as the disease progressed rapidly, the area of the lesion increased to 5 cm  $\times$  5 cm and an ulcer with a diameter of approximately 5 mm was seen in the middle of the lesion. The skin at the lesion was damaged and pus was flowing out. Because of obvious tenderness and swelling, incision drainage and pus culture were performed. Hospital staff successfully cultured *P. aeruginosa*, and piperacillin-tazobactam was selected for treatment according to a drug sensitivity test.

Unfortunately, the child did not show any improvement after being treated with periodic antibiotics. Given his worsening fever and high-sensitivity protein C levels (202.1 mg/L), the occurrence of sepsis was highly suspected. Blood specimens were collected twice for microbial culture. Both aerobic and anaerobic bacterial cultures in the blood were negative after 5 days' culture. Because of inconsistencies between the results and clinical manifestations, mNGS was chosen to identify the pathogens, and *P. aeruginosa* was detected within 24 hours (TABLE 1).

**TABLE 1. Results of mNGS in Blood, BALF, and CSF**

Sample	Pathogen Type	Species	Abundance	Reads	Coverage, %
Blood	Prokaryotes	<i>P. aeruginosa</i>	High	53,077	44.78
	Eukaryotes	...	...	...	...
	Virus	...	...	...	...
BALF	Prokaryotes	<i>P. aeruginosa</i>	High	2,450,881	95.04
	Eukaryotes	...	...	...	...
	Virus	...	...	...	...
CSF	Prokaryotes	<i>P. aeruginosa</i>	High	4,868,366	95.06
	Eukaryotes	...	...	...	...
	Virus	...	...	...	...

BALF, bronchoalveolar lavage fluid; CSF, cerebrospinal fluid; mNGS, metagenomic next-generation sequencing.

Because the *OXA-50*-encoding genes were detected (*OXA-50* is the only class D carbapenemase found in *P. aeruginosa*), carbapenem antibiotics were avoided, and amikacin in combination with piperacillin-tazobactam was used to fight the bacterial infection.

Soon the patient had cough, and computed tomography showed patchy shadows of the left upper lobe of the lung. Subsequently, the patient reported headache and showed a positive Kernig sign and neck stiffness. The patient was immediately transferred to the pediatric intensive care unit and later needed to rely on an invasive ventilator to maintain blood oxygen saturation. To master the progress of the disease as soon as possible, the clinicians sent BALF and CSF at the same time for mNGS and traditional culture. The results of mNGS were returned within 24 hours. The sequences of *P. aeruginosa* and associated drug resistance genes were detected in both BALF and CSF (TABLE 1). Three days later, carbapenem-resistant *P. aeruginosa* was successfully cultured in BALF, but the culture result in the CSF specimen was still negative. The doctors decided to maintain the anti-infective regimen and adjust the antibiotic dosage in time by monitoring the metabolic concentration of related antibiotics in the blood. After the periodic antibiotic treatment, the child's symptoms were gradually controlled.

On the 54th day of treatment, the child's guardians requested that he be discharged. Unfortunately, we were informed during follow-up that the child died several days after discharge because of his poor physical condition and repeated infections.

## Discussion

Opportunistic infections are a major cause of morbidity and mortality in patients with AA, and neutropenia is one of the major risk factors.<sup>7,8</sup> The organisms involved in patients with AA are more diverse than in patients without AA and are more likely to be resistant to first-line antibiotics.<sup>9</sup> We report a fatal case of a pediatric patient with VSAA with multisite *P. aeruginosa* infection.

In this case, the child was initially admitted with fever and cutaneous cellulitis of the right chest wall. The infection progressed rapidly and the child soon developed cough, dyspnea, and headache symptoms. Hospital staff detected *P. aeruginosa* and its drug resistance gene (*OXA-50*) in the patient's blood, CSF, and BALF through mNGS.

Persistent infections caused by the superbug *P. aeruginosa* and its resistance to multiple antimicrobial agents are huge threats to pub-

lic health.<sup>10</sup> Conventional antibiotics and treatments have limited efficacy against multidrug-resistant *P. aeruginosa* and can cause serious adverse effects.<sup>11</sup> In vitro studies, case reports, and retrospective analyses show promising effects of combination treatments.<sup>12</sup> In this case, the child was initially given piperacillin-tazobactam to fight the infection. As the infection continued to worsen, amikacin was added.

Although traditional culture is still considered the gold standard for pathogen detection, with the rapid development of molecular biology technologies, mNGS has an increasingly broad application prospect in the field of rapid diagnosis of pathogenic infection.<sup>13</sup> In this patient, both aerobic and anaerobic bacterial cultures in the peripheral blood were negative after 5 days' culture. This result could have occurred because of a low pathogenic bacteria load or antibiotic use. Research has shown that mNGS can be used to determine a broad range of pathogens in patients who have been treated with antibiotics or antivirals because the technique directly sequences all DNA and/or RNA from clinical specimens.<sup>14</sup> The turnaround time for mNGS is 24 to 36 hours at our hospital. In contrast, the average feedback time of a pathogen culture is  $\geq 3$  days for bacteria, 5 days for fungi, and 45 days for mycobacteria. Studies have indicated that mNGS is especially suitable for the identification of viruses and fastidious organisms; in this patient, the traditional culture method was not a wise choice.<sup>5,13</sup>

There are also limitations to the efficacy of mNGS. For example, the technique is relatively complicated, requiring the appropriate environment, professional equipment, and personnel. In China, the cost of mNGS is between \$500 and \$800, which is higher than conventional testing methods (\$15–\$100 for culture testing and approximately \$15 for nucleic acid testing of a single pathogen). However, controlling the further deterioration of infection and shortening the course of disease are fundamental ways to alleviate patients' pain and save costs, which means that the rapid and accurate diagnosis of a causative pathogen at the early clinical stage is crucial. Scientists are dedicated to reducing the cost of mNGS to expand its range of applications. Approaches to further reduce mNGS costs include reducing host sequences before sequencing<sup>15</sup> and testing specimens on a large scale.<sup>16</sup>

## Conclusion

In brief, mNGS can be a more cost-effective pathogen detection tool when traditional methods cannot meet clinical needs. We hope that mNGS will develop into a more rapid and universal technique to benefit the diagnosis and treatment of clinical infectious diseases.

## Acknowledgments

This work was supported by the Sichuan Province Science and Technology Department (2020YFS0100) and the Chengdu Science and Technology Bureau (2019-YF05-01178-SN). The funders had no role in the study design, data collection and analysis, decision to publish, or preparation of the manuscript.

## Conflict of interest

The authors declare that they have no competing interests.

## REFERENCES

1. Valdez JM, Scheinberg P, Young NS, Walsh TJ. Infections in patients with aplastic anemia. *Semin Hematol*. 2009;46(3):269–276.
2. Lertpongpiroon R, Rattarittamrong E, Rattanathammethee T, et al. Infections in patients with aplastic anemia in Chiang Mai University. *BMC Hematol*. 2018;18:35.
3. Breijyeh Z, Jubeh B, Karaman R. Resistance of Gram-negative bacteria to current antibacterial agents and approaches to resolve it. *Molecules*. 2020;25:1340.
4. Li M, Yang F, Lu Y, Huang W. Identification of *Enterococcus faecalis* in a patient with urinary-tract infection based on metagenomic next-generation sequencing: a case report. *BMC Infect Dis*. 2020;20(1):467.
5. Gu W, Miller S, Chiu CY. Clinical metagenomic next-generation sequencing for pathogen detection. *Annu Rev Pathol*. 2019;14:319–338.
6. Goldberg B, Sichtig H, Geyer C, Ledebner N, Weinstock GM. Making the leap from research laboratory to clinic: challenges and opportunities for next-generation sequencing in infectious disease diagnostics. *mBio*. 2015;6(6):e01888-15.
7. Furlong E, Carter T. Aplastic anaemia: current concepts in diagnosis and management. *J Paediatr Child Health*. 2020;56(7):1023–1028.
8. Chandar R, Chandrasekaran V, Jagadisan B, Kumar D, Biswal N. Hemophagocytic lymphohistiocytosis in a child with very severe aplastic anemia: double jeopardy resulting in fatality. *J Pediatr Hematol Oncol*. 2017;39(1):e43–e45.
9. José RJ, Brown JS. Opportunistic bacterial, viral and fungal infections of the lung. *Medicine (Abingdon)*. 2016;44(6):378–383.
10. Potron A, Poirel L, Nordmann P. Emerging broad-spectrum resistance in *Pseudomonas aeruginosa* and *Acinetobacter baumannii*: mechanisms and epidemiology. *Int J Antimicrob Agents*. 2015;45(6):568–585.
11. Shao X, Xie Y, Zhang Y, et al. Novel therapeutic strategies for treating *Pseudomonas aeruginosa* infection. *Expert Opin Drug Discov*. 2020;15(12):1403–1423.
12. Fritzenwanker M, Imirzalioglu C, Herold S, Wagenlehner FM, Zimmer KP, Chakraborty T. Treatment options for carbapenem-resistant Gram-negative infections. *Dtsch Arztebl Int*. 2018;115(20–21):345–352.
13. Miao Q, Ma Y, Wang Q, et al. Microbiological diagnostic performance of metagenomic next-generation sequencing when applied to clinical practice. *Clin Infect Dis*. 2018;67(suppl\_2):S231–S240.
14. Han D, Li Z, Li R, Tan P, Zhang R, Li J. mNGS in clinical microbiology laboratories: on the road to maturity. *Crit Rev Microbiol*. 2019;45(5–6):668–685.
15. Marotz CA, Sanders JG, Zuniga C, Zaramela LS, Knight R, Zengler K. Improving saliva shotgun metagenomics by chemical host DNA depletion. *Microbiome*. 2018;6(1):42.
16. Yohe S, Thyagarajan B. Review of clinical next-generation sequencing. *Arch Pathol Lab Med*. 2017;141(11):1544–1557.

# Acquired Factor VIII Inhibitors: A Case Study

Eric A. Walradth, MA, BS, MLS (ASCP)<sup>CM</sup>SH<sup>CM\*</sup>

Hematology Oncology Associates of Central Syracuse, New York, New York, United States; \*To whom correspondence should be addressed. [ewalradth@hoacny.com](mailto:ewalradth@hoacny.com)

**Keywords:** factor VIII, FVIII, coagulation, factor VIII inhibitor, FVIII inhibitor, mixing study, aPTT, activated partial thromboplastin time

**Abbreviations:** aPTT, activated partial thromboplastin time; FVIII, factor VIII; BU, Bethesda unit; FEIBA, factor eight inhibitor bypassing activity; NPP, normal pooled plasma; FIXa, factor IXa; rFVIIa, recombinant activated factor VII; aPCC, activated prothrombin complex concentrate.

*Laboratory Medicine* 2022;53:e126–e128; <https://doi.org/10.1093/labmed/lmab125>

## ABSTRACT

The physiology of hemostasis is one of high complexity that involves the initiation, amplification, and propagation of the many moving parts of the hemostatic system and its regulatory mechanisms. It is imperative that clinical laboratory professionals have a strong understanding of the many intricacies of the physiology of coagulation and its in vitro testing. An elongated activated partial thromboplastin time can have several causes, and the correct cause must be elucidated in a timely manner for proper treatment. A mixing study with normal pooled plasma should be performed to evaluate for the presence of an inhibitor vs factor deficiency. Factor inhibitors, specifically factor VIII in this case study, should be titered so that the clinician can decide which treatment may work best for the patient. Continued monitoring of factor levels and inhibitor titers should be conducted to follow the resolution or progression of inhibitor presence.

## Case

A 65 year old White male with a history of type 2 diabetes mellitus, hypertension, and hyperlipidemia presented to his primary care physician with hematomas after having noticed stiffness and swelling in his left lower leg approximately 2 to 3 weeks earlier. An ultrasound was performed and deep vein thrombosis was ruled out. A prolonged activated partial thromboplastin time (aPTT) was noted at 60 seconds (reference range, 22–35 seconds). The patient was started on Celebrex (celecoxib) for his discomfort. He later presented with new extensive areas of ecchymosis and hematomas and was admitted to the hospital. A prolonged aPTT was still present along with an undetectable factor

VIII (FVIII) level. He denied any familial history of bleeding disorders but had a history of hematuria post-cystoscopy 3 months earlier.

The presence of a FVIII inhibitor was confirmed by Bethesda testing at 47.4 Bethesda units (<0.6 Bethesda units [BUs]). Bethesda units are the quantification given to an inhibitor that is needed to neutralize half of the factor VIII when incubated for a specified time. The patient was started on factor eight inhibitor bypassing activity (FEIBA) treatment 1 day after his admission followed by prednisone 1 mg/kg daily and cytoxan (cyclophosphamide) 2 mg/kg/day. His dose at discharge was prednisone 40 mg in the morning and at lunch and cytoxan (cyclophosphamide) 200 mg alternating with 150 mg daily. Peripheral flow cytometry was obtained and showed a small clonal B-cell population.

## Laboratory Workup and Treatment of FVIII Inhibitors

A prolonged aPTT is a common screening abnormality seen in laboratory testing. A common way to investigate a prolonged aPTT is by performing a mixing study, which will determine whether a factor deficiency or factor-inhibiting antibody is the culprit.<sup>1-3</sup> There is no standard procedure for performing mixing studies, but the general practice involves making a 1:1 mixture of the patient's plasma with normal pooled plasma (NPP) and performing an aPTT.<sup>1-3</sup> Some laboratories perform mixing studies immediately upon mixing; others incubate the specimen for 1 hour at 37°C; others will incubate the specimen for 2 hours at 37°C.<sup>1-3</sup> If inhibitors are suspected, then incubation should be considered because FVIII inhibitors are time- and temperature-dependent.<sup>2</sup> Furthermore, a strong inhibitor may only take minutes to resolve, whereas a weak inhibitor may take up to 2 hours.<sup>2</sup>

If the patient has a factor deficiency, then the aPTT will correct because of the addition of the deficient factor that is being replaced by the NPP.<sup>1-3</sup> If there is a lack of correction in the aPTT, then there are likely to be inhibitors present.<sup>1-3</sup> Inhibitors come in many forms, including auto- or alloantibodies directed at specific coagulation factors, heparin, direct-oral anticoagulants, or antiphospholipid antibodies.<sup>3</sup> Deciding whether or not the aPTT has been corrected is another area where the mixing study procedure is not standardized. There have been a few helpful guides to help determine whether or not the aPTT has been corrected, such as the Rosner index or the Chang percent correction formula.<sup>1,4-8</sup> Adherence to the selected method of determination by each individual laboratory should be maintained.

$$\text{Rosner index} = \frac{1 : 1 \text{ mix aPTT} - \text{NPP aPTT}}{\text{patient aPTT}} \times 100$$

Inhibitor  $\geq 11$

Correction  $< 11$

$$\text{Chang's percent correction} = \frac{\text{patient aPTT} - 1 : 1 \text{ mix aPTT}}{\text{patient aPTT} - \text{NPP aPTT}} \times 100$$

Factor deficiency  $\geq$  75%

Inhibitor  $<$  75%

The main function of FVIII is as a cofactor to factor IXa (FIXa). Research has shown that FVIII has a molecular weight of 330,000 Da with a domain structure of A<sub>1</sub>-a<sub>1</sub>-A<sub>2</sub>-a<sub>2</sub>-B-a<sub>3</sub>-A<sub>3</sub>-C<sub>1</sub>-C<sub>2</sub>.<sup>2,6,7</sup> The A<sub>2</sub>, A<sub>3</sub>, and C<sub>2</sub> domains are found to have acquired FVIII inhibitors directed at them more frequently than the other domains.<sup>2,8,9</sup> These domains have different binding targets within the physiology of the hemostasis system. The C<sub>2</sub> domain binding targets are to phospholipids and von Willebrand factor, and the A<sub>2</sub> and A<sub>3</sub> domains binding targets are to factor X and FIXa.<sup>2,7,8</sup>

Acquired FVIII inhibitors occur in less than 1 patient per million per year.<sup>2,10,11</sup> Because there is no known genetic inheritance pattern, FVIII autoantibodies are spread equally among male and female patients.<sup>2,3,10</sup> The presence of circulating FVIII autoantibodies in adults is more common than in children, with the average presenting age between ages 60 and 80 years.<sup>2,10</sup> There are a few common associated illnesses with FVIII autoantibodies, including autoimmune disorders, solid tumor and hematologic malignancies, infections, adverse effects from medications, and skin disorders.<sup>2,3,10</sup> Autoantibodies to FVIII may spontaneously disappear or persist for years.<sup>12</sup>

Studies have shown that FVIII inhibitors are classified into 2 types based on the type of kinetics they display and the extent to which they inhibit FVIII.<sup>2,9</sup> In patients with congenital hemophilia A who have been treated with FVIII, alloantibodies are formed. These alloantibodies target the A<sub>2</sub> or C<sub>2</sub> domains of FVIII.<sup>2,8,9</sup> In patients with acquired hemophilia A, autoantibodies are formed and target the C<sub>2</sub> domain of FVIII.<sup>2,3,8,9</sup> Alloantibodies to FVIII typically follow first-order kinetics and have the nomenclature of type 1 inhibitors.<sup>2,9</sup> Autoantibodies to FVIII typically follow second-order kinetics and have the nomenclature of type 2 inhibitors.<sup>2,9</sup>

It is imperative to quantify the titer of the FVIII inhibitor to monitor treatment. There are 2 methodologies with which to test FVIII for the presence of inhibitors: clot-based assays or enzyme-linked immunosorbent assays.<sup>12</sup> The most commonly used FVIII inhibitor methodology is the Bethesda assay or the Nijmegen-modified Bethesda assay.<sup>2,3,9,10,12</sup> The Bethesda assay is performed by using serial dilutions of the patient's plasma and equal parts of NPP and incubating them at 37°C for 2 hours.<sup>2,3,9,12</sup> The residual FVIII level is then measured in both the patient specimen and a control specimen and an inhibitor titer is calculated using linear regression analysis.<sup>6,9,12</sup> The result is reported in BUs. One BU is the quantity of the inhibitor that is needed to neutralize 50% of the FVIII from the NPP after its 2-hour incubation at 37°C.<sup>3,6,9</sup> Although the Bethesda assay is standardized, there is a high level of interlaboratory variation that can be attributed to differences in aPTT reagents, lack of reference antibody standards, sources of phospholipids, and activating agents.<sup>6,9</sup>

Research has shown that FVIII inhibitors are categorized by the level of their titer. Inhibitors with a titer of 5 BUs or less are considered low-responding, whereas inhibitors with a titer greater than 5 BUs are considered high-responding, as per the recommendation of the International Society on Thrombosis and Hemostasis Scientific and Standardization Committee.<sup>6,9,12</sup> Patients with low-responding inhibitors

generally have a low immunologic response to FVIII replacement therapy that may be overcome by higher doses of FVIII.<sup>3,9,10,12</sup> Conversely, patients with high-responding inhibitors generally have high immunologic response and are found to generally be refractory to FVIII replacement therapy.<sup>3,9,10,12</sup>

Patients who have high-responding inhibitors are treated using bypassing agents as first-line treatment options, including recombinant activated factor VII (rFVIIa) and the activated prothrombin complex concentrate (aPCC) FEIBA in the United States.<sup>2,3,9,10</sup> Studies have shown that FEIBA can achieve an overall complete response rate of 86%, and rFVIIa has shown an overall complete response rate of 75% and a partial response in an additional 17%.<sup>2</sup> Along with achieving hemostasis using rFVIIa and aPCC therapy, another goal of acquired FVIII hemophilia treatment is the elimination of the inhibitor. This goal can be achieved using several methods as either standalone agents or in various combinations, including plasmapheresis or immunoadsorption, intravenous immunoglobulin, immunosuppressive agents, biologic therapy, and immune tolerance.<sup>2,10,11</sup>

## Case Conclusion

Repeat testing for FVIII activity and FVIII inhibitor continued several times a week for a few weeks followed by continued FVIII activity levels to monitor improvement. Within 2 weeks of initiating treatment, the patient's FVIII inhibitor level had decreased to 23.7 BUs and his FVIII activity levels rose from undetectable to 4% (reference range, 50%–150%). The FVIII activity level continued to rise over the next 6 weeks and remained stable at 60%. Because of these results, the treatment plan was altered to be slowly tapered.

The patient was supposed to follow up 1 week after the tapered dose for more bloodwork to monitor FVIII levels. However, during this time period the patient was directly exposed to SARS-CoV-2 and, although he tested negative, he was told to quarantine by the local department of health for 14 days. His scheduled appointments were pushed back to accommodate his quarantine. During his quarantine, he developed shortness of breath and was taken by ambulance to the local hospital.

Upon arrival he was found to be hypoxic on room air and delirious. He was placed on a nonbreather mask. An electrocardiogram revealed sinus tachycardia with a right branch bundle block. Chest X-ray showed resolving pneumonia. Laboratory studies showed markedly increased glucose and lactic acid levels and a troponin level within normal limits. The patient was also found to be positive for SARS-CoV-2, and his blood culture grew gram-negative rods. Zosyn (piperacillin/tazobactam) and vancomycin treatment was initiated. His respiratory status declined quickly and he was intubated. Laboratory studies were repeated and showed severe hypokalemia, renal failure, hypomagnesemia, hypophosphatemia, and continued diabetic ketoacidosis and lactic acidosis. After intubation, the patient developed hypotension and was placed on multiple vasopressors but his hypotension continued to worsen. Cardiopulmonary resuscitation was initiated; unfortunately, it was to no avail.

## REFERENCES

1. Castellone D. Inhibitor identification in the coagulation laboratory. *Lab Med*. 2013;44(4):e118–e120.
2. Ma A, Carrizosa D. Acquired factor VIII inhibitors: pathophysiology and treatment. *Hematology*. 2006;1:432–437.

3. Winter WE, Flax SD, Harris NS. Coagulation testing in the core laboratory. *Lab Med*. 2017;48(4):295–313.
4. Chang SH, Tillema V, Scherr D. A “percent correction” formula for evaluation of mixing studies. *Am J Clin Pathol*. 2002;117(1):62–73.
5. Baig M, Iqbal M, Tabassum A. Evaluation of Rosners index vs Brandt correction and Chang's %, in the interpretation of mixing studies at varying dilutions. *Int J Adv Med*. 2019;6(6):1750–1754.
6. Kottke-Marchant K. *An Algorithmic Approach to Hemostasis Testing*. Northfield, IL: College of American Pathologists Press; 2016.
7. Al-Huniti A, Sharathkumar A, Krantz M, Watkinson K, Bhagavathi S. Discrepant hemophilia a: an underdiagnosed disease entity. *Am J Clin Pathol*. 2020;154(1):78–87.
8. Green D. *Factor VIII inhibitors: a 50-year perspective*. *Haemophilia*. 2011;17(6):831–838.
9. Witmer C, Young G. Factor VIII inhibitors in hemophilia. A: rationale and latest evidence. *Ther Adv Hematol*. 2013;4(1):59–72.
10. Franchini M, Lippi G. Acquired factor VIII inhibitors. *Blood*. 2008;112(2):250–255.
11. Wiestner A, Cho HJ, Asch AS, et al. Rituximab in the treatment of acquired factor VIII inhibitors. *Blood*. 2002;100(9):3426–3428.
12. Peerschke EI, Castellone DD, Ledford-Kraemer M, Van Cott EM, Meijer P; NASCOLA Proficiency Testing Committee. Laboratory assessment of factor VIII inhibitor titer: the North American Specialized Coagulation Laboratory Association experience. *Am J Clin Pathol*. 2009;131(4):552–558.

# Evaluation of RNA Isolation Methods in Human Adipose Tissue

Bipasha Nandi Jui, MBBS, MMedSci,<sup>1</sup> Assel Sarsenbayeva, PhD,<sup>1</sup> Henning Jernow, MD,<sup>1</sup> Susanne Hetty, PhD,<sup>1</sup> Maria J. Pereira, PhD<sup>1</sup>

<sup>1</sup>Clinical Diabetes and Metabolism, Department of Medical Sciences, Uppsala University, Uppsala, Sweden; \*To whom correspondence should be addressed. maria.pereira@medsci.uu.se

**Keywords:** RNA isolation, adipose tissue, RNA quantity, RNA purity, traditional phenol-chloroform method, column-based methods

**Abbreviations:** AT, adipose tissue; RT, room temperature; RIN, RNA integrity number; cDNA, complementary DNA.

*Laboratory Medicine* 2022;53:e129–e133; <https://doi.org/10.1093/labmed/lmab126>

## ABSTRACT

**Objective:** Research has shown that RNA extraction from adipose tissue (AT) is challenging because of high lipid content and low RNA quantity. We compared a traditional RNA extraction with a column-based method in human AT to evaluate RNA quantity and quality.

**Materials and Methods:** Human subcutaneous AT (n = 9) was collected through needle biopsy, and RNA was extracted using the phenol-chloroform traditional method and the RNeasy Lipid Tissue Mini Kit column-based method. The RNA quantity, quality, integrity, and expression of key AT genes were assessed.

**Results:** We found that the RNA quantity and integrity were reduced by 40% and 15–20%, respectively, using the column-based method compared to the traditional method, but the findings were not statistically significant. The column-based method showed a higher 260/280 ratio (~2.0) compared to the traditional method (~1.8) ( $P < .05$ ), suggesting lower amounts of contaminants. The expression of AT genes was comparable between methods.

**Conclusion:** The traditional extraction method provides adequate RNA yield and integrity compared to the column-based method, which is an advantage when AT specimens are small.

Adipose tissue (AT) is a fat depot specializing in storing energy as triglycerides. The AT is made up of adipocytes, but it also contains other cells like preadipocytes, fibroblasts, and immune cells.<sup>1</sup> In addition, it contains a connective tissue matrix and neural and vascular cells. In recent years, AT has been categorized as a major endocrine organ because it produces many hormones and regulates different metabolic activities, hence making it very important in diabetes, obesity, and metabolic research.<sup>2</sup>

The isolation of RNA with high quality is pivotal in performing RNA-based analyses, such as transcriptomic and microarray analyses and reverse transcription-quantitative polymerase chain reaction. However, the extraction of good-quality RNA from AT is complex because of its high fatty acid content and low nucleic acid number.<sup>2,3</sup> Standard RNA isolation techniques for AT are the traditional and the spin column-based isolation methods.<sup>2–5</sup> Different RNA isolation protocols provide mixed results regarding protein and organic compound contamination and low RNA content. For example, Hemmrich and colleagues<sup>6</sup> compared 3 column-based RNA isolation methods after stabilizing varying amounts of human AT with RNA<sub>later</sub> reagent, and among the other column-based methods they used, the RNeasy Lipid Tissue Mini Kit yielded a greater amount of RNA. Studies have also compared a traditional and a column-based method with their own modified protocol in human and porcine AT, respectively, and found that neither methods obtained high-quality RNA compared to their own modified protocol.<sup>2,3</sup> Meanwhile, some studies have shown that good RNA quantity and quality were achieved by using an optimized traditional method from mouse and human AT, respectively.<sup>5,7</sup>

Although the above-mentioned studies showed improved RNA isolation methods, there have been very few direct comparisons between traditional with column-based method to isolate RNA from human AT specimens.<sup>2</sup> Human AT specimen size is usually small, resulting in low RNA yield, limiting the subsequent analyses that can be performed.<sup>6</sup> Furthermore, RNA degrades more rapidly than DNA, and human AT is obtained either from a needle biopsy or by following operative procedures; hence it can often not be processed immediately, thus making it more vulnerable to further degradation of its RNA.<sup>6</sup>

This work aimed to evaluate the traditional phenol-chloroform method and a column-based method, the RNeasy Lipid Tissue Mini Kit, in human AT for RNA yield, quality, and integrity using the 2 reagents

Qiazol and TRIzol. These 2 methods have not been compared before in the same specimens of human AT.

## Materials and Methods

### Patients

Abdominal subcutaneous AT was collected from 9 healthy volunteers (7 women, 2 men, body mass index 22.2–48.7 kg/m<sup>2</sup>) through needle biopsy under local anesthesia with lidocaine (xylocaine; AstraZeneca, Sweden). Biopsies were performed at the Uppsala University Hospital, Uppsala, Sweden, and patients with type 2 diabetes and other major endocrine disorders, cancer, and other major illnesses were excluded from this study. All patients gave their informed written consent, and the study was approved by the Regional Ethics Review Board in Uppsala.

### AT Processing

After the biopsy, the AT was cleaned immediately in normal saline (B. Braun Melsungen AG 34209, Melsungen, Germany), and 4 specimens of 100 mg each were prepared from each patient by dissecting and weighing the tissue pieces. The tissue pieces were subsequently placed in RNase-free tubes, snap-frozen in liquid nitrogen, and stored at –80°C until the day of RNA extraction. Tissues were processed and frozen within 2 to 3 minutes of the biopsy.

### Isolation of RNA

To compare different RNA isolation techniques, we chose 2 reagents; Qiazol Lysis Reagent (Qiagen Sciences, Germantown, MD) and TRIzol Reagent (Thermo Fisher, Carlsbad, CA), and compared the traditional phenol-chloroform method with the RNeasy Lipid Tissue Mini Kit method (Qiagen, Hilden, Germany). We divided the RNA extraction from the 100 mg AT specimens from each patient into the following 4 groups: (i) traditional method with Qiazol (n = 9), (ii) traditional method with TRIzol (n = 9), (iii) column-based method with Qiazol (n = 8), and (iv) column-based method with TRIzol (n = 9). The 100 mg AT was homogenized in 1 mL Qiazol or TRIzol with 0.5 mm RNase-free zirconium oxide beads (Next Advance, Inc., New York) using a TissueRuptor (Next Advance, Inc., New York) for 5 minutes followed by another 5 minutes of incubation at room temperature (RT). Then 200 µL chloroform was added to each specimen and mixed vigorously for 15 seconds followed by 3 minutes incubation at RT. Specimens were centrifuged at 12,000 g for 15 minutes at 4°C.

### Traditional Phenol-Chloroform Method

This method was performed as described previously.<sup>8,9</sup> After centrifugation, 500 to 600 µL of the upper aqueous phase was transferred to a new 1.5 mL Eppendorf tube, carefully avoiding the interphase. For better visualization of the pellet, 1–1.2 µL (1:1000) of GlycoBlue reagent (Thermo Fisher Scientific, Waltham, MA) was added to each specimen, followed by 500 to 600 µL isopropanol (Sigma). All specimens were vortexed and left overnight at –20°C. The following day, specimens were centrifuged at 4°C for 30 minutes at 18,000 g to precipitate the RNA as a blue pellet. The supernatant was discarded, and the pellet was washed with 1 mL 70% ethanol. After thoroughly mixing the content by vortexing, we centrifuged the specimens at 4°C for 15 minutes at 18,000 g. Pellets were washed 3 times the same way and left to air-dry

for 10 to 15 minutes at RT. The RNA pellets were then dissolved in 40 µL RNase-free water.

### RNeasy Lipid Tissue Mini Kit Method

We extracted the RNA following the manufacturer's protocol. In brief, the tissue was homogenized with Qiazol/TRIzol reagent as described above and centrifuged for 15 minutes after the addition of chloroform. We then added 500–600 µL of the clear phase to a new Eppendorf tube. Then an equal volume of 70% ethanol was added to each tube and mixed well. Next, we transferred 700 µL of the specimens to the respective RNeasy Mini spin column in a 2 mL collection tube (supplied) and centrifuged at RT for 15 seconds at 9000 g, and the flow-through was discarded. The same step was repeated with the remainder of the specimens. Then the specimens were washed 2 times with 700 µL RW1 buffer (Qiagen, Hilden, Germany) by centrifuging at RT for 15 seconds at 9000 g, and the flow-through was discarded. Again the specimens were washed twice with 500 µL of RPE buffer (Qiagen, Hilden, Germany) and centrifuged for 15 seconds and 2 minutes, respectively. To dry the membrane further, the spin columns were placed in a new set of collection tubes and centrifuged at full speed for 1 minute. Then the RNeasy columns were placed in new 1.5 mL Eppendorf tubes, 40 µL RNase-free water was added, and the specimens were centrifuged for 1 minute at 9000 g.

### RNA Quantity, Quality, and Integrity Analysis

The RNA quantity was obtained using the NanoDrop 2000 spectrophotometer (Thermo Fisher Scientific, Rockford, IL), by measuring absorbance at 260 nm. The RNA quality was measured by assessing the absorbance ratio at 260 vs 280 nm ( $A_{260/280}$ ) and 260 vs 230 nm ( $A_{260/230}$ ) because protein absorbs light at 280 nm, phenol at both 280 nm and 230 nm, and guanidine at <230 nm. An  $A_{260/280}$  ratio of ~2 is considered as pure RNA without protein or phenol contamination.<sup>10</sup>

The integrity of the extracted RNA was assessed by calculating the RNA integrity numbers (RINs) using the RNA 6000 Pico kit (chip lot number ZG14BK30, reagent kit lot number 2106) in an Agilent 2100 bioanalyzer (Agilent Technologies, Santa Clara, CA). The RIN range from 1 to 10 was determined by measuring the 28S to 18S rRNA ratio in each specimen.<sup>11</sup> The specimens had thawed 3 times before performing the RIN analysis.

### Gene Expression Analysis

We reverse-transcribed 400 ng total RNA from each specimen to complementary DNA (cDNA) using the High-Capacity cDNA Reverse Transcription Kit (Applied Biosystems, Thermo Fisher Scientific, Foster City, CA) according to the manufacturer's guidelines. The cDNA was diluted 1:10 in nuclease-free water. TaqMan probes (Thermo Fisher Scientific, Waltham, MA) listed in **TABLE 1** were used for *ADIPOQ*, *LEP*, *PPARG*, and *SLC24A4* gene expression analyses by quantitative polymerase chain reaction. The gene expression analysis was performed using the QuantStudio 3 System (Applied Biosystems, Thermo Fisher Scientific, Waltham, MA). The relative gene expression was normalized to the housekeeping gene *GUSB*.<sup>12</sup> Specimens were run in duplicate, and data were calculated as  $2^{-\Delta\Delta C_t}$ .

### Statistical Analysis

Data are presented as mean ± standard error of the mean. All data were analyzed using GraphPad Prism, and mixed-model repeated-measures

1-way analysis of variance was used to analyze the differences in RNA concentration, absorbance ratios, integrity number, and gene expression between different isolation methods. Nonnormally distributed data were log-transformed. Multiple comparisons were corrected by controlling the false discovery rate with the 2-stage step-up method of Benjamini, Krieger, and Yekutieli.<sup>13</sup> A  $P$  value  $< .05$  was considered statistically significant.

## Results

### Effect of Different RNA Isolation Techniques on RNA Quantity

With the traditional method using Qiazol and TRIzol, the amount of RNA isolated from 100 mg human AT was  $117.9 \pm 25.1$  ng/ $\mu$ L and  $115.8 \pm 20.7$  ng/ $\mu$ L, respectively. The column-based method resulted in an RNA yield of  $78.1 \pm 14.7$  with Qiazol and  $64.3 \pm 10.1$  with TRIzol from the same amount of tissue (FIGURE 1A). In total, from 100 mg AT, we obtained 4.64  $\mu$ g RNA using the traditional method whereas the column-based method yielded 40% less (2.83  $\mu$ g) regardless of lysis reagent.

### Effect of Different RNA Isolation Techniques on RNA Quality

The traditional isolation method had a 260/280 ratio of  $\approx 1.8$ , whereas the column-based method was  $\approx 2.0$  ( $P < .01$ ; FIGURE 1B). Regarding

the 260/230 ratio, the traditional method was approximately 1.6–1.7, and the column-based method was lower (0.8; ( $P < .05$ ; FIGURE 1C). No significant differences were observed between isolation with Qiazol or TRIzol for either isolation method.

### Effect of Different RNA Isolation Techniques on RNA Integrity

The RNA integrity numbers tended to be higher using the traditional method compared to the column-based method, but the difference did not reach statistical significance: traditional with Qiazol (integrity =  $7.3 \pm 0.4$ ), traditional with TRIzol (integrity =  $7.4 \pm 0.3$ ), column-based with Qiazol (integrity =  $6.0 \pm 0.4$ ), and column-based with TRIzol (integrity =  $6.5 \pm 0.2$ ; FIGURE 2).

### Effect of Different RNA Isolation Techniques on Gene Expression

Our results showed no differences in the expression of the 4 genes (*PPARG*, *SLC2A4*, *ADIPOQ*, and *LEP*) related to adipocyte function and normalized to *GUSB* (FIGURE 3).

## Discussion

Gene expression profiling of AT is essential in metabolic research. Successful gene expression analysis requires a reliable RNA isolation technique that ensures adequate RNA yield and quality even from a small amount of specimen. The optimized RNeasy Lipid Tissue Mini Kit for use with fatty tissues such as AT offers a rapid and validated method for RNA extraction.<sup>6</sup> However, this is the first study comparing the RNeasy Lipid Tissue Mini Kit protocol with the traditional phenol-chloroform technique in terms of RNA yield, quality, and integrity in paired specimens of human AT.

Our study showed better RNA yield (4.64  $\mu$ g/100 mg) using the traditional extraction method compared to the column-based method (2.83  $\mu$ g/100 mg). This finding is in agreement with previous publications showing better RNA yield using a traditional method than using a column-based method in human and porcine AT, respectively.<sup>2,3</sup>

**TABLE 1. List of Genes Used in Study**

Gene Name	Gene Symbol	TaqMan Probes
Peroxisome proliferator-activated receptor gamma	<i>PPARG</i>	Hs01115513_m1
Solute carrier family 2 member 4/glucose transporter 4 ( <i>GLUT4</i> )	<i>SLC2A4</i>	Hs00168966_m1
Adiponectin	<i>ADIPOQ</i>	Hs00605917_m1
Leptin	<i>LEP</i>	Hs00174877_m1
Glucuronidasebeta	<i>GUSB</i>	Hs99999908_m1
18S ribosomal RNA	<i>18S</i>	Hs99999901_s1

**FIGURE 1. Differences in (A) RNA concentration (ng/ $\mu$ L), (B) 260/280 ratio, and (C) 260/230 ratio of isolated RNA from human AT using 4 isolation techniques: traditional with Qiazol (n = 9), traditional with TRIzol (n = 9), column-based with Qiazol (n = 8), and column-based with TRIzol (n = 9). \* $P < .05$ , \*\* $P < .01$ , \*\*\* $P < .001$ . AT, adipose tissue.**

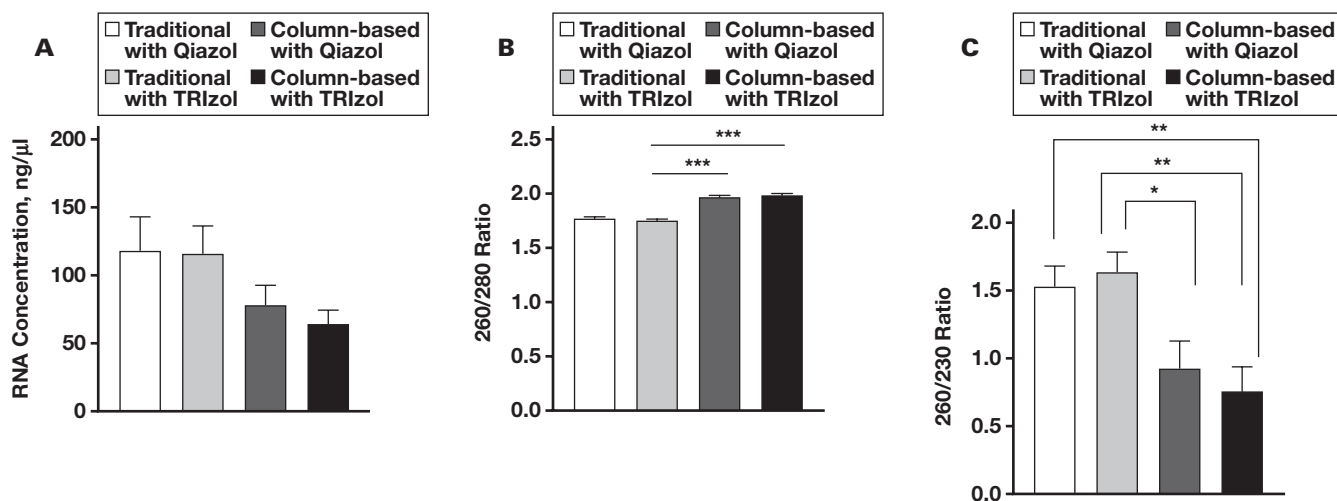


**FIGURE 2.** Analysis of RIN in 100 mg human AT extracted using 4 isolation methods: traditional with Qiazol (n = 6), traditional with TRIzol (n = 7), column-based with Qiazol (n = 7), and column-based with TRIzol (n = 8). AT, adipose tissue; RIN, RNA integrity number.

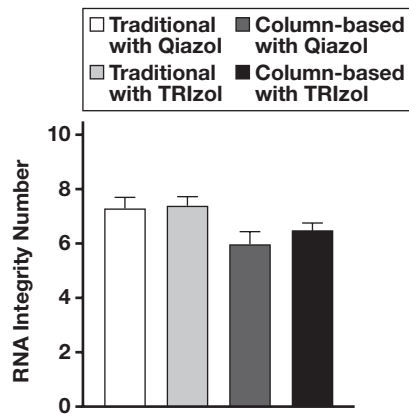
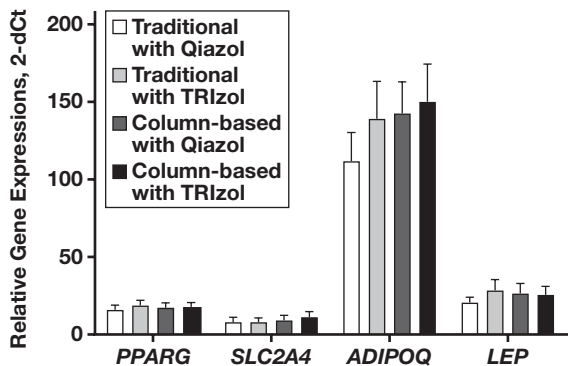


**FIGURE 3.** Messenger RNA (mRNA) expression in human subcutaneous AT. Relative comparison of gene expression of *PPARG*, *SLC2A4*, *ADIPOQ*, and *LEP* normalized to *GUSB* using 4 isolation methods: traditional with Qiazol (n = 8), traditional with TRIzol (n = 9), column-based with Qiazol (n = 8), and column-based with TRIzol (n = 9). \**P* < .05. AT, adipose tissue.



Because the column-based method enriches for messenger RNA (mRNA) and other RNA species >200 nucleotides, and the total RNA yield does not include 5S ribosomal RNA (rRNA), transfer (RNA), and other low-molecular-weight RNAs, we found a 15% to 20% less RNA yield using the column-based method compared to the traditional method.<sup>3,14</sup> Thus, the traditional extraction method is an advantage when small amounts of AT are available for RNA extraction. Hemmrich and colleagues<sup>6</sup> showed that better RNA yield and quality were achieved using the RNeasy Lipid Tissue Mini Kit method compared to another column-based method, but their comparisons were between two column-based methods. The current work highlights that non-column based methods may provide different results.

Our data indicate that column-based methods are more efficient in removing protein contamination, because the 260/280 ratio was significantly better with the column-based method (2.0) than with the traditional method (1.8). However, a 260/280 ratio of between 1.8 and 2.0 is generally accepted as pure RNA.<sup>2,3</sup>

Although a 260/230 ratio should ideally be 1.8 or higher, it was consistently low when we used both methods; the traditional method showed a 1.6 ratio, and the column-based method showed a 0.8 ratio. This finding suggests that unwanted organic compounds such as phenol/chloroform or chaotropic salts (guanidine thiocyanate) are present in the RNA solution and are removed less efficiently using the column-based method as reflected in the lower 260/230 value. This theory corresponds with previous publications showing the presence of organic compounds (TRIzol/phenol) using the traditional and the column-based methods.<sup>2,3</sup> Note that we included 3 ethanol wash steps when we used the phenol-chloroform method, which could have improved the 260/230 ratio but reduced the RNA yield. Roy and colleagues<sup>7</sup> showed that decreasing the volume of the TRIzol reagent and 2 ethanol washes improved the 260/230 ratio in RNA extracted using the manual phenol-chloroform method from visceral AT.

The RIN values were better (>7) in the specimens extracted using the traditional method than in those extracted using the column-based method (<7). A RIN value >7 is generally considered sufficient for gene expression analyses, which was assessed by the 28S and 18S ratio in the electropherogram result from the bioanalyzer.<sup>15</sup> Notably, the RIN analyses were performed after 3 cycles of thawing and freezing, which reduces the RNA quality by approximately 20%.<sup>16</sup> However, the specimens went through the same thawing and freezing cycles, so the results should have been comparable between methods. Moreover, with the traditional method, the quality of the specimens was still good enough to perform subsequent downstream gene expression analysis despite being defrosted 3 times.

Note that the expression of prominent AT genes, along with the reference gene *GUSB*, showed consistent cycle threshold values across the different RNA extraction methods. This finding suggests that all 4 different techniques are of acceptable and standard quality.

TRIzol or Qiazol reagents are equally used in RNA isolation from AT,<sup>17,18</sup> and no differences were observed between them for both RNA extraction methods in terms of RNA yield, quality, or integrity.

There are advantages and disadvantages of each method. The traditional extraction method is less expensive and gives a higher RNA yield, but the chances of protein contamination are higher and the protocol requires a longer time.<sup>2,5</sup> Column-based methods provide good-quality RNA; however, they are more expensive and based on our findings and those of others, they result in a lower concentration of RNA than traditional extraction methods.<sup>2</sup> Furthermore, kit-based methods are less environmentally friendly because they require the use of more plastics.

Our study has limitations, including a small sample size, variable specimen numbers between different extraction groups, and repeated thawing before RIN analysis. In addition, the biopsies were taken from healthy patients, so the results may not adequately generalize to different populations. However, the successful use of the conventional phenol-chloroform RNA isolation technique with desired results from both AT and adipocytes has been shown before.<sup>5,7,8,17</sup>

To conclude, the conventional traditional protocol for total RNA isolation from human AT yields a higher total RNA than a column-based method, with good RNA quality and integrity.

## Acknowledgments

We gratefully acknowledge the valuable technical, administrative, and analytical contributions and expert advice from coworkers at Clinical

Diabetes and Metabolism, Uppsala University. This work was supported by research grants from the Excellence of Diabetes Research in Sweden (EXODIAB), the European Commission via the Marie Skłodowska Curie Innovative Training Network Treatment (H2020-MSCA-ITN-721236), the Uppsala University Hospital Avtal om Läkarutbildning och Forskning (ALF) grants, the Stiftelsen Familjen Ernfors Foundation, and the P. O. Zetterlings stiftelse.

## REFERENCES

1. Luo L, Liu M. Adipose tissue in control of metabolism. *J Endocrinol*. 2016;231(3):R77–R99.
2. Sinitsky MY, Matveeva VG, Asanov MA, Ponasenko AV. Modifications in routine protocol of RNA isolation can improve quality of RNA purified from adipocytes. *Anal Biochem*. 2018;543:128–131.
3. Cirera S. Highly efficient method for isolation of total RNA from adipose tissue. *BMC Res Notes*. 2013;6:472.
4. Pereira MJ, Thombare K, Sarsenbayeva A, et al. Direct effects of glucagon on glucose uptake and lipolysis in human adipocytes. *Mol Cell Endocrinol*. 2020;503:110696.
5. Tan P, Pepin É, Lavoie JL. Mouse adipose tissue collection and processing for RNA analysis. *J Vis Exp*. 2018;131:57026.
6. Hemmrich K, Denecke B, Paul NE, et al. RNA isolation from adipose tissue: an optimized procedure for high RNA yield and integrity. *Lab Med*. 2010;41(2):104–106.
7. Roy D, Tomo S, Modi A, Purohit P, Sharma P. Optimising total RNA quality and quantity by phenol-chloroform extraction method from human visceral adipose tissue: a standardisation study. *MethodsX*. 2020;7:101113.
8. Chomczynski P, Sacchi N. Single-step method of RNA isolation by acid guanidinium thiocyanate-phenol-chloroform extraction. *Anal Biochem*. 1987;162(1):156–159.
9. Toni LS, Garcia AM, Jeffrey DA, et al. Optimization of phenol-chloroform RNA extraction. *MethodsX*. 2018;5:599–608.
10. Thermo Fisher Scientific. NanoDrop microvolume spectrophotometers and fluorometer. <https://www.thermofisher.com/us/en/home/industrial/spectroscopy-elemental-isotope-analysis/molecular-spectroscopy/ultraviolet-visible-visible-spectrophotometry-uv-vis-vis-uv-vis-vis-instruments/nanodrop-microvolume-spectrophotometers.html>. Accessed January 11, 2022.
11. Schroeder A, Mueller O, Stocker S, et al. The RIN: an RNA integrity number for assigning integrity values to RNA measurements. *BMC Mol Biol*. 2006;7:3.
12. Fink T, Lund P, Pilgaard L, Rasmussen JG, Duroux M, Zachar V. Instability of standard PCR reference genes in adipose-derived stem cells during propagation, differentiation and hypoxic exposure. *BMC Mol Biol*. 2008;9:98.
13. Benjamini Y, Krieger AM, Yekutieli D. Adaptive linear step-up procedures that control the false discovery rate. *Biometrika*. 2006;93(3):491–507. <http://www.jstor.org/stable/20441303>.
14. Qiagen. RNeasy lipid tissue mini handbook. 2018. <https://www.qiagen.com/ca/resources/download.aspx?id=7f13ac1a-841d-4e9b-b39d-42fe71b3d585&lang=en>. Accessed January 11, 2022.
15. Cashion AK, Umberger RA, Goodwin SB, Sutter TR. Collection and storage of human blood and adipose for genomic analysis of clinical samples. *Res Nurs Health*. 2011;34(5):408–418.
16. Yu K, Xing J, Zhang J, Zhao R, Zhang Y, Zhao L. Effect of multiple cycles of freeze-thawing on the RNA quality of lung cancer tissues. *Cell Tissue Bank*. 2017;18(3):433–440.
17. Sarsenbayeva A, Jui BN, Fanni G, et al. Impaired HMG-CoA reductase activity caused by genetic variants or statin exposure: impact on human adipose tissue,  $\beta$ -cells and metabolome. *Metabolites*. 2021;11(9):574.
18. Qiagen. User-developed protocol: purification of total RNA from plant tissue using the RNeasy Lipid Tissue Mini Kit. <https://www.qiagen.com/ch/resources/download.aspx?id=2248d99e-5fe4-490e-b710-115d51e5ea8a&lang=en>. Accessed January 11, 2022.

# A Novel *USP25::PDGFRA* Gene Fusion in a 78 Year Old Patient with a Myeloid Neoplasm

Joanna C. Dalland, MD,<sup>1,\*</sup> Patrick R. Blackburn, PhD,<sup>2</sup> Kaaren K. Reichard, MD,<sup>1</sup> Sarah H. Johnson, MS,<sup>3</sup> James B. Smadbeck, PhD,<sup>3</sup> George Vasmatazis, PhD,<sup>3</sup> Nicole L. Hoppman, PhD,<sup>4</sup> Xinjie Xu, PhD,<sup>1</sup> Patricia T. Greipp, DO,<sup>1</sup> Linda B. Baughn, PhD,<sup>1</sup> Jess F. Peterson, MD<sup>1,\*</sup>

<sup>1</sup>Division of Hematopathology, Department of Laboratory Medicine and Pathology, Mayo Clinic, Rochester, Minnesota, United States, <sup>2</sup>Department of Pathology, St. Jude Children's Research Hospital, Memphis, Tennessee, United States, <sup>3</sup>Center for Individualized Medicine-Biomarker Discovery, Mayo Clinic, Rochester, Minnesota, United States, <sup>4</sup>Division of Laboratory Genetics and Genomics, Department of Laboratory Medicine and Pathology, Mayo Clinic, Rochester, Minnesota, United States; \*To whom correspondence should be addressed. [peterjohn.jess@mayo.edu](mailto:peterjohn.jess@mayo.edu)

**Keywords:** *PDGFRA*, *USP25*, eosinophilia, mate-pair sequencing, next-generation sequencing

**Abbreviations:** MLN-*PDGFRA*, myeloid/lymphoid neoplasm with *PDGFRA* rearrangement; AML, acute myeloid leukemia; ABMGG, American Board of Medical Genetics and Genomics; BAP, break-apart probe; FISH, fluorescence in situ hybridization; NGS, next-generation sequencing; CHIP, clonal hematopoiesis of indeterminate potential.

*Laboratory Medicine* 2022;53:e134–e138; <https://doi.org/10.1093/labmed/lmac010>

## ABSTRACT

The World Health Organization category of myeloid/lymphoid neoplasms with eosinophilia and *PDGFRA* rearrangements is composed of a heterogeneous group of neoplasms that can present as a myeloproliferative neoplasm, acute myeloid leukemia, myeloid sarcoma, or lymphoblastic leukemia/lymphoma. The overall outcome of these neoplasms is favorable with imatinib therapy. Herein, we describe an adult female patient with a myeloid neoplasm accompanied by eosinophilia and a novel *USP25::PDGFRA* gene fusion.

The category of myeloid/lymphoid neoplasms with *PDGFRA* rearrangement (MLN-*PDGFRA*) is an uncommon entity, defined as a myeloid or lymphoid neoplasm, usually with prominent eosinophilia, and the presence of a *FIP1L1::PDGFRA* fusion, a variant fusion gene with rearrangement of *PDGFRA* or an activating mutation of *PDGFRA*.<sup>1</sup> At presentation, patients with MLN-*PDGFRA* rearrangement can show features of a myeloproliferative neoplasm, acute myeloid leukemia (AML), myeloid sarcoma, or lymphoblastic leukemia/lymphoma.<sup>1–3</sup> The

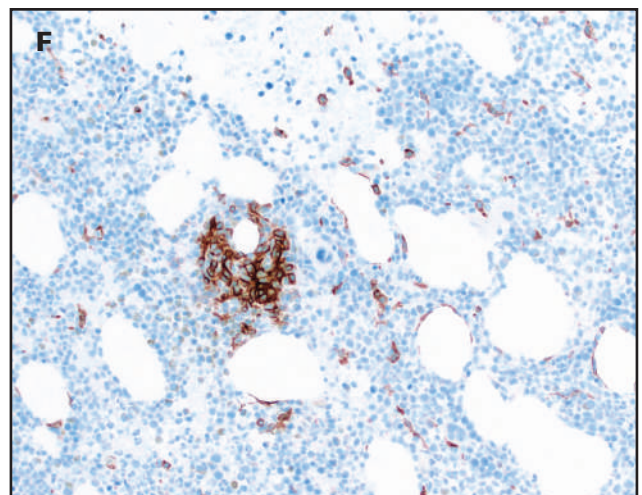
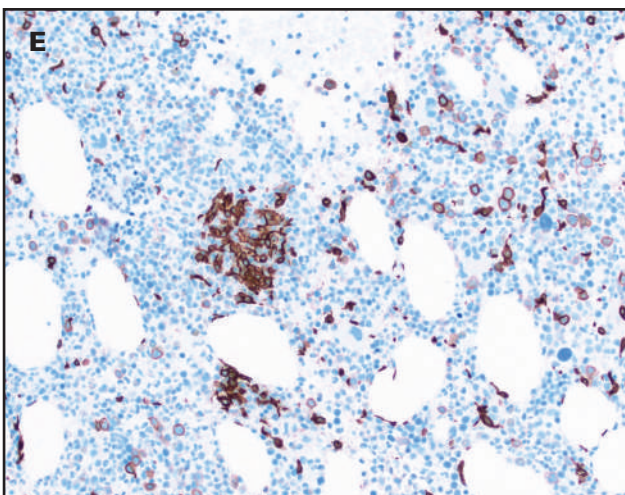
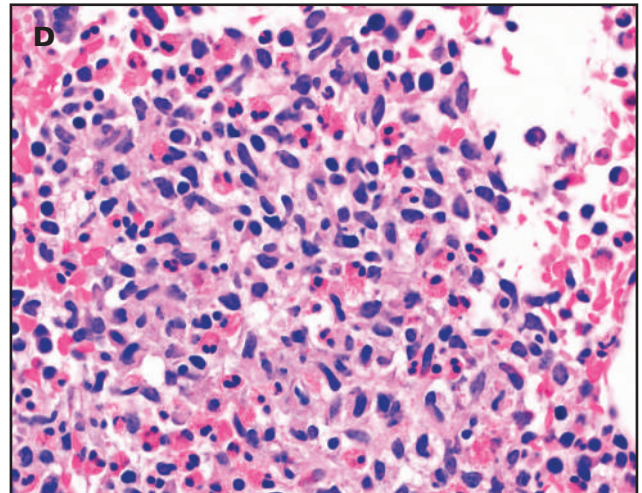
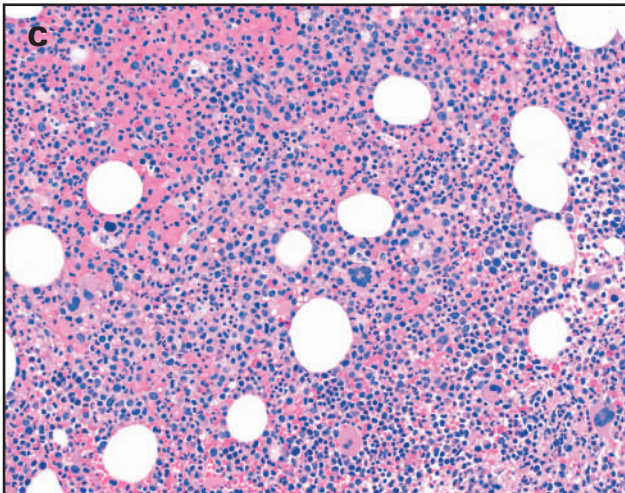
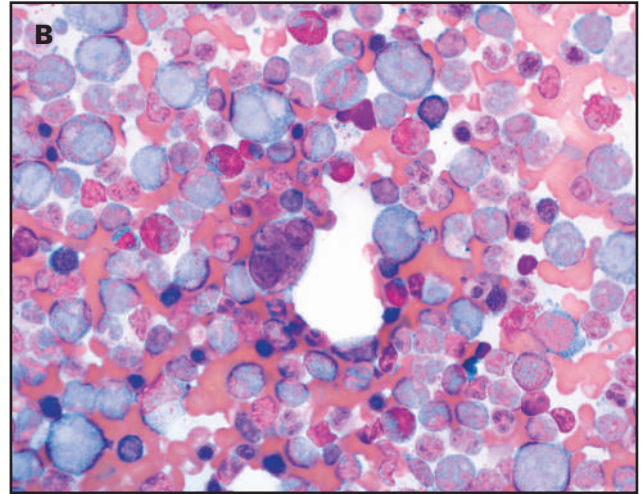
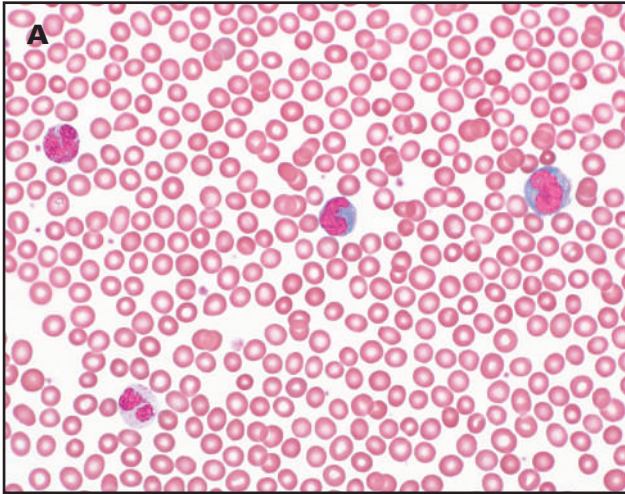
*FIP1L1::PDGFRA* fusion is caused by a cryptic deletion at 4q12 and is the most common rearrangement seen in these patients.<sup>1,2</sup> However, several other *PDGFRA* gene fusion partners have been reported, many of which result from a cryptic deletion.<sup>1</sup> In the setting of a patient presenting with eosinophilia and a myeloid or lymphoid neoplasm, identifying *PDGFRA* rearrangements is important because these patients show a favorable prognosis with imatinib therapy.<sup>1</sup> Herein, we report a patient with a myeloid neoplasm with eosinophilia and a novel gene fusion between the *USP25* and *PDGFRA* genes.

## Clinical History and Hematopathologic Evaluation

A 78 year old female patient presented for evaluation of persistent monocytosis and thrombocytopenia. Her past medical history was significant for follicular lymphoma and status post 5 cycles of rituximab, cyclophosphamide, doxorubicin hydrochloride, vincristine sulfate, and prednisone followed by maintenance rituximab completed 6 years earlier. Computed tomography imaging of the chest, abdomen, and pelvis showed no evidence of recurrence of lymphoma. To further evaluate for the underlying cause of persistent monocytosis and thrombocytopenia, a bone marrow biopsy was performed and was referred to our institution with concerns for a myeloid neoplasm.

A complete blood cell count showed an elevated white blood cell count ( $13.6 \times 10^9/L$ ; reference range,  $3.7\text{--}12.1 \times 10^9/L$ ) with the differential count notable for absolute eosinophilia ( $2.4 \times 10^9/L$ ) and absolute monocytosis ( $2.6 \times 10^9/L$ ). This finding was associated with slight thrombocytopenia (platelets:  $113 \times 10^9/L$ ; reference range,  $179\text{--}450 \times 10^9/L$ ) and a normal hemoglobin ( $14.5\text{ g/dL}$ ; reference range,  $11.2\text{--}15.8\text{ g/dL}$ ). The peripheral blood smear was notable for increased numbers of mature-appearing eosinophils, mature-appearing monocytes, and occasional hypogranular and hyposegmented neutrophils (FIGURE 1A). Rare circulating blasts were also observed. The bone marrow aspirate and touch preparations showed occasional small hypolobated megakaryocytes (FIGURE 1B). The bone marrow core biopsy and clot sections were markedly hypercellular (90% cellularity) with marked panhyperplasia and occasional clusters of spindled cells associated with eosinophils (FIGURE 1C, 1D). Immunohistochemical stains showed that the clusters of spindled cells were tryptase- and CD117-positive mast cells with aberrant coexpression of CD25 (FIGURE 1E, 1F). No morphologic or immunophenotypic features of lymphoma were seen. The overall findings were diagnostic of a myeloid

**FIGURE 1.** Peripheral blood, bone marrow aspirate, and biopsy. (A) The peripheral blood smear shows mature eosinophils, mature monocytes, and occasional hypogranular and hyposegmented neutrophils (Wright-Giemsa, 60× oil immersion magnification). (B) The bone marrow touch preparation shows a small hyplobated megakaryocyte with discrete separation of nuclear lobes (Wright-Giemsa, 60× oil immersion magnification). (C) The bone marrow biopsy is hypercellular with panhyperplasia and occasional hyperchromatic megakaryocytes (H&E, 20× magnification). (D) The bone marrow clot section shows occasional clusters of spindled mast cells associated with eosinophils (H&E, 60× oil immersion magnification). (E, F) The clusters of mast cells are positive for CD117 (E) and show aberrant CD25 expression (F) (20× magnification). H&E, hematoxylin and eosin.



neoplasm associated with eosinophilia. Additional cytogenetic studies were performed for further subclassification.

## Materials and Methods

### Conventional Chromosome Analysis

Cells from a bone marrow aspirate specimen were cultured, harvested, and banded utilizing standard cytogenetic techniques according to specimen-specific protocols. Twenty metaphases were analyzed by 2 qualified clinical cytogenetic technologists and were interpreted by a certified American Board of Medical Genetics and Genomics (ABMGG) clinical cytogeneticist.

### Fluorescence in Situ Hybridization

A *PDGFRA* break-apart probe (BAP; laboratory-developed test) was performed on the bone marrow aspirate. The specimen was subjected to standard fluorescence in situ hybridization (FISH) pretreatment, hybridization, and fluorescence microscopy according to specimen-specific protocols. Two hundred total interphase nuclei were analyzed by 2 qualified clinical cytogenetic technologists and were interpreted by an ABMGG-certified clinical cytogeneticist.

### Mate-Pair Sequencing

We processed DNA from the bone marrow aspirate using the Illumina Nextera Mate Pair library kit (Illumina, San Diego, CA) and sequenced it on the Illumina NovaSeqS4 for a bridged coverage of 136×. Data were aligned to the reference genome (GRCh38) using BIMA, and abnormalities were identified and visualized using SVAtools and Genome Explorer, all three of which are Mayo Clinic–developed bioinformatics tools.<sup>4,5</sup>

### Molecular Analysis

Next-generation sequencing (NGS) testing was performed using a targeted, myeloid neoplasm–focused OncoHeme panel that interrogates 42 genes (Supplemental Table 1). The DNA was extracted from the bone marrow aspirate using the Qiagen EZ1 (Germantown, MD). The 200 ng sheared DNA was target-enriched with a custom hybridization-capture reagent (SureSelectXT; Agilent) and was sequenced on the MiSeq platform (Illumina, San Diego, CA) at the Mayo Clinic Clinical Genome Sequencing Laboratory. The read length was 151 bp. Sequencing data were processed using a custom bioinformatics pipeline, Mayo NGS Workbench, using the CLC Bio Genomics Server v6.0 (Qiagen) for alignment and variant calling. The aligned BAM files were further processed through a breakpoint search tool developed in-house for large insertion and deletion detection. The BAM files of all variant calls were manually reviewed in the genome browser Alamut Visual (Interactive Biosoftware) for confirmation. The limit of detection of the NGS assay was 5% with a minimum 250× depth of coverage. More than 95% of tested regions had a >1000× depth of coverage in the clinical assay. Genetic variants were curated and annotated in the molecular hematopathology laboratory following the American College of Medical Genetics and Genomics 5-tier system.<sup>6</sup>

## Results and Discussion

All 20 metaphases analyzed had monosomy X. In addition, 8 of 20 metaphases with monosomy X also had an apparently balanced t(4;21)(q12;q21) (FIGURE 2A). The *PDGFRA* BAP FISH identified an apparently balanced *PDGFRA* rearrangement in 44% of 200 analyzed inter-

phase nuclei, indicated by a single fusion signal and separated green and red probe signals (FIGURE 2B). To further characterize the *PDGFRA* rearrangement, mate-pair sequencing was performed and revealed a balanced translocation between the *PDGFRA* gene (exon 12, NM\_006206) at 4q12 and the *USP25* gene (intron 20, NM\_001283041) at 21q21.1 (FIGURE 2C). This translocation was predicted to create an in-frame chimeric gene fusion consisting of exons 1 to 20 of *USP25* and exons 12 to 28 of *PDGFRA* (FIGURE 2D). Although not confirmed, the monosomy X observed in all 20 metaphases likely represented a constitutional abnormality (Turner syndrome). Alternatively, this finding could represent age-related loss.

MLN-*PDGFRA* can present as a heterogeneous number of diseases, and the most common gene fusion involves *FIP1L1::PDGFRA*, accounting for approximately 85% of patients with this rearrangement.<sup>2</sup> Additional variant gene fusion partners have been described, including *BCR*, *ETV6*, *KIF5B*, *CDK5RAP2*, *STRN*, *TNKS2*, and *FOXP1*.<sup>1</sup> The *USP25::PDGFRA* gene fusion has not been reported in the literature. The *USP25* gene encodes a deubiquitinating enzyme that catalyzes the hydrolysis and removal of ubiquitin chains from target proteins.<sup>7</sup> Notably, disruptions of the proteasome system, including alterations of *USP25* activity, have been associated with various human malignancies.<sup>7</sup> Similar to previously reported *FIP1L1::PDGFRA* gene fusions, the *PDGFRA* breakpoint in our patient was located within exon 12 and likely resulted in constitutively increased tyrosine kinase activity of the fusion protein.<sup>8</sup>

In our patient, the morphologic findings including peripheral eosinophilia and a hypercellular bone marrow with cytologic atypia prompted additional evaluation for cytogenetic abnormalities that can be seen in the setting of eosinophilia. Furthermore, the bone marrow also showed loose clusters of atypical spindled mast cells with aberrant CD25 expression, which has been previously reported in MLN-*PDGFRA* and lacks a *KIT D816V* mutation.<sup>2</sup> Previous studies evaluating NGS in MLN-*PDGFRA* have reported gene mutations involving *ASXL1*, *BCOR*, *CSF3R*, *DNMT3A*, *ETV6*, *KIT*, *PAK7*, *RUNX1*, *SRSF2*, and *TET2*.<sup>2,9,10</sup> In this patient, a targeted NGS panel for mutations commonly seen in myeloid neoplasms revealed 3 pathogenic mutations involving *KRAS* (VAF 9%), *NRAS* (VAF 10%), and *TET2* (VAF 45%), along with a *TET2* variant of uncertain significance (VAF 46%). It has been suggested that the disease is driven by the *PDGFRA* rearrangement and that the additional mutations may represent passenger mutations; however, only a small subset of patients with MLN-*PDGFRA* have had NGS testing performed.<sup>10</sup> In our patient, we determined that the 2 low-level *KRAS* and *NRAS* mutations likely represented emerging subclones, given that clonal hematopoiesis of indeterminate potential (CHIP) typically only harbors 1 genetic mutation.<sup>11,12</sup> Furthermore, *KRAS* and *NRAS* mutations are much less commonly reported as genes underlying CHIP.<sup>11,12</sup>

Considering MLN-*PDGFRA* in a patient with prior cytotoxic chemotherapy is also important because these neoplasms have been reported in the posttherapy setting.<sup>13-15</sup> In this setting, the emergence of a *PDGFRA* rearrangement may represent a therapy-related process vs a de novo hematologic neoplasm; therefore, disease classification in this setting could pose a challenge. A previously reported case of a patient with AML with eosinophilia and *PDGFRA* rearrangement with a complex karyotype was described in a patient status posttreatment for B-lymphoblastic leukemia/lymphoma.<sup>15</sup> The MLN-*PDGFRA* rearrangement typically shows a normal or noncomplex karyotype; thus, when clinicians are faced with a complex karyotype, they may best classify it as a therapy-related myeloid neoplasm.<sup>2</sup> In our patient, given the

**FIGURE 2.** Cytogenomic evaluation of a novel *USP25::PDGFRA* gene fusion observed in an adult patient with a myeloid neoplasm and eosinophilia. (A) Representative karyogram showing t(4;21)(q12;q21) (arrows) and monosomy X. The t(4;21) was observed in 8 of 20 metaphases whereas monosomy X was observed in all 20 metaphases. (B) Representative interphase nucleus showing a balanced *PDGFRA* rearrangement (BAP), indicated by separated green (5'*PDGFRA*) and red (3'*PDGFRA*) signals (arrows) that flank the *PDGFRA* gene region (4q12). (C) Junction plot showing a balanced translocation between the *PDGFRA* gene (exon 12, NM\_006206) at 4q12 and the *USP25* gene (intron 20, NM\_001283041) at 21q21.1. This translocation was predicted to create an in-frame chimeric gene consisting of exons 1–20 of *USP25* and exons 12–28 of *PDGFRA*. (D) Schematic diagram showing *USP25::PDGFRA* chimeric protein structure generated by ProteinPaint.<sup>19</sup> BAP, break-apart probe.

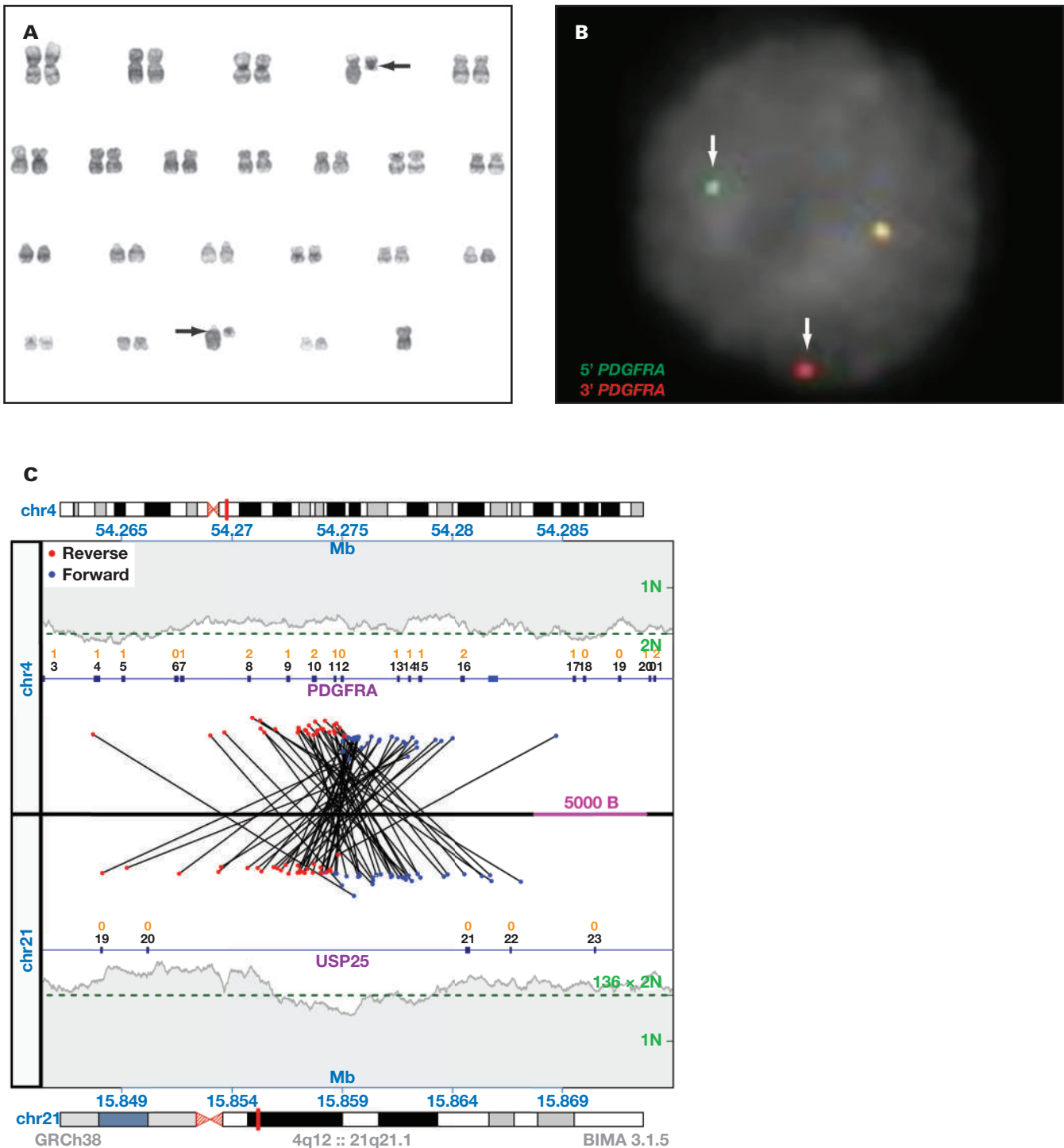
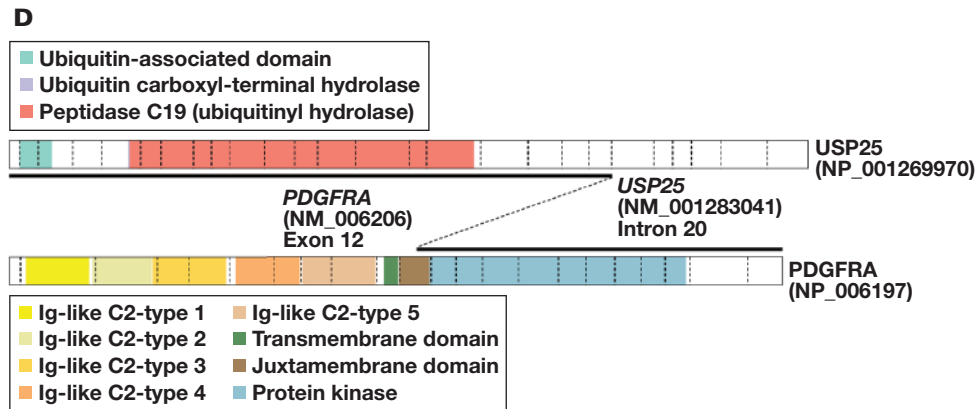


FIGURE 2. Continued



noncomplex karyotype, we classified the current case as MLN-*PDGFRA*. Identifying patients with MLN-*PDGFRA* is crucial because this condition has been reported to be particularly imatinib-responsive, with most patients achieving molecular remission.<sup>2,3,16,17</sup> As a result, imatinib is the first-line therapy for patients with MLN-*PDGFRA* presenting in a chronic phase and should be given in the absence of organ dysfunction.<sup>18</sup> Discontinuation of imatinib therapy can lead to relapse, and therefore ongoing maintenance therapy is generally recommended.<sup>2,16,18</sup>

This case study highlights the importance of evaluating patients presenting with a myeloid/lymphoid neoplasm with eosinophilia for recurrent cytogenetic abnormalities, including *PDGFRA* rearrangements.

### Supplementary Data

Supplemental figures and tables can be found in the online version of this article at [www.labmedicine.com](http://www.labmedicine.com).

### REFERENCES

1. Swerdlow SH, Campo E, Harris NL, et al. *WHO Classification of Tumours of Haematopoietic and Lymphoid Tissues*. 4th ed. Lyon, France: IARC; 2017.
2. Pozdnyakova O, Orazi A, Kelemen K, et al. Myeloid/lymphoid neoplasms associated with eosinophilia and rearrangements of *PDGFRA*, *PDGFRB*, or *FGFR1* or with *PCM1-JAK2*. *Am J Clin Pathol*. 2021;155:160–178.
3. Vega F, Medeiros LJ, Bueso-Ramos CE, et al. Hematolymphoid neoplasms associated with rearrangements of *PDGFRA*, *PDGFRB*, and *FGFR1*. *Am J Clin Pathol*. 2015;144:377–392.
4. Drucker TM, Johnson SH, Murphy SJ, et al. BIMA V3: an aligner customized for mate pair library sequencing. *Bioinformatics*. 2014;30:1627–1629.
5. Johnson SH, Smadbeck JB, Smoley SA, et al. SVAtools for junction detection of genome-wide chromosomal rearrangements by mate-pair sequencing (MPseq). *Cancer Genet*. 2018;221:1–18.
6. Richards S, Aziz N, Bale S, et al. Standards and guidelines for the interpretation of sequence variants: a joint consensus recommendation of the American College of Medical Genetics and Genomics and the Association for Molecular Pathology. *Genet Med*. 2015;17:405–424.
7. Zhu W, Zheng D, Wang D, et al. Emerging roles of ubiquitin-specific protease 25 in diseases. *Front Cell Dev Biol*. 2021;9:698751.
8. Walz C, Score J, Mix J, et al. The molecular anatomy of the FIP1L1-*PDGFRA* fusion gene. *Leukemia*. 2009;23:271–278.
9. Baer C, Muehlbacher V, Kern W, et al. Molecular genetic characterization of myeloid/lymphoid neoplasms associated with eosinophilia and rearrangement of *PDGFRA*, *PDGFRB*, *FGFR1* or *PCM1-JAK2*. *Haematologica*. 2018;103:e348–e350.
10. Pardanani A, Lasho T, Barraco D, et al. Next generation sequencing of myeloid neoplasms with eosinophilia harboring the FIP1L1-*PDGFRA* mutation. *Am J Hematol*. 2016;91:E10–E11.
11. Steensma DP, Bejar R, Jaiswal S, et al. Clonal hematopoiesis of indeterminate potential and its distinction from myelodysplastic syndromes. *Blood*. 2015;126:9–16.
12. Jaiswal S, Fontanillas P, Flannick J, et al. Age-related clonal hematopoiesis associated with adverse outcomes. *N Engl J Med*. 2014;371:2488–2498.
13. Tanaka Y, Kurata M, Togami K, et al. Chronic eosinophilic leukemia with the FIP1L1-*PDGFRA* fusion gene in a patient with a history of combination chemotherapy. *Int J Hematol*. 2006;83:152–155.
14. Safley AM, Sebastian S, Collins TS, et al. Molecular and cytogenetic characterization of a novel translocation t(4;22) involving the breakpoint cluster region and platelet-derived growth factor receptor-alpha genes in a patient with atypical chronic myeloid leukemia. *Genes Chromosomes Cancer*. 2004;40:44–50.
15. Zhou J, Papenhausen P, Shao H. Therapy-related acute myeloid leukemia with eosinophilia, basophilia, t(4;14)(q12;q24) and *PDGFRA* rearrangement: a case report and review of the literature. *Int J Clin Exp Pathol*. 2015;8:5812–5820.
16. Pardanani A, D'Souza A, Knudson RA, et al. Long-term follow-up of FIP1L1-*PDGFRA*-mutated patients with eosinophilia: survival and clinical outcome. *Leukemia*. 2012;26:2439–2441.
17. Pardanani A, Ketterling RP, Li CY, et al. FIP1L1-*PDGFRA* in eosinophilic disorders: prevalence in routine clinical practice, long-term experience with imatinib therapy, and a critical review of the literature. *Leuk Res*. 2006;30:965–970.
18. Shomali W, Gotlib J. World Health Organization-defined eosinophilic disorders: 2021 update on diagnosis, risk stratification, and management. *Am J Hematol*. 2022;97:129–148.
19. Zhou X, Edmonson MN, Wilkinson MR, et al. Exploring genomic alteration in pediatric cancer using ProteinPaint. *Nat Genet*. 2016;48:4–6.

# Corrigendum to: A Simple and Applicable Method for Human Platelet Lysate Preparation Using Citrate Blood

Narin Khongjaroensakun, MD,<sup>1,\*</sup> Karan Paisooksantivatana, MD,<sup>1</sup> Suttikarn Santiwatana, MD, PhD,<sup>2,3</sup>  
Tulyaprupek Tawonsawatruk, MD, PhD,<sup>4</sup> Kantarat Kusolthammarat, MD,<sup>1,5</sup> Pragyuan Kadegasem, BSc,<sup>2</sup>  
Noppawan Tangbubpha, MS,<sup>2</sup> Juthamard Chantaraamporn, MS,<sup>2</sup> and Ampaiwan Chuansumrit, MD<sup>2</sup>

<sup>1</sup>Department of Pathology, Faculty of Medicine Ramathibodi Hospital, Mahidol University, Bangkok, Thailand, <sup>2</sup>Department of Pediatrics, Faculty of Medicine Ramathibodi Hospital, Mahidol University, Bangkok, Thailand, <sup>3</sup>Vejthani Hospital, Bangkok, Thailand, <sup>4</sup>Department of Orthopedics, Faculty of Medicine Ramathibodi Hospital, Mahidol University, Thailand, <sup>5</sup>Department of Pathology, Prince of Songkla University, Songkhla, Thailand; \*To whom correspondence should be addressed. [narin.kho@mahidol.edu](mailto:narin.kho@mahidol.edu)

In “A Simple and Applicable Method for Human Platelet Lysate Preparation Using Citrate Blood (<https://doi.org/10.1093/labmed/lmab116>)”, there were errors in the first two affiliations which should read “Department of Pathology, Faculty of Medicine Ramathibodi Hospital, Mahidol University, Bangkok, Thailand” and “Department of Pediatrics, Faculty of Medicine Ramathibodi Hospital, Mahidol University, Bangkok, Thailand”, respectively. These errors have been corrected online.

# On labmedicine.com

---

Several articles featuring practical information are now available on labmedicine.com.

This month, the website features a paper by Petersen et al about HIV infection interventions at a Veteran Affairs Medical Center. In “Acquired FVII Deficiency and Acute Myeloid Leukemia: A Case Report and Literature Review,” Hammami et al present a case study of a man with factor VII deficiency acquired secondary to AML. And finally, “Acquired Factor VIII Inhibitors: A Case Study” highlights how technologists can distinguish between factor inhibitors and factor deficiencies.

Check out these articles and more on labmedicine.com.

## **Lablogatory**

Recent contributions to the blog for medical laboratory professionals include the latest in cancer diagnostics, microbiology case studies, and laboratory safety. To see why over half a million readers visited Lablogatory in 2021, visit [labmedicineblog.com](http://labmedicineblog.com).